

Notebook 2018-03-13 Mikhail Korchelev

Ray Tracing and Raymarching

1

Ray Tracing.

Features to consider when writing a ray tracer.

- Camera: how, and where the perspective is rendered.
The camera generates rays from the viewing point on screen.
- Ray tracing intersections: we must be able to tell precisely where a given ray pieces on object, we need to determine certain geometric properties of the object at the intersection point, such as the surface normal or material.
- Light distribution: we must have a pdf for the light in the scene (probabilistic distribution for not only location directly in model)
light, but also diffuse light energy.
- Visibility: we must know if light is only being rendered where we can see it.
- Surface scattering: each object has a description of its appearance and how light interacts with it, specifically the materials surface, and
There is also reradiated light (scattered.)
- Recursive Ray tracing.
Light bounces off multiple surfaces before it reaches its result.
- Ray propagation: we need to know what happens to light traveling alone as a ray as it passes thru space.
Vacuum, fog, smoke, atmosphere have different results.

Convens : Orthographic, normal probe.

Ray object intersections and Radiometry.

Radiometry is the Measurements of light distribution in space-time.

Radiant energy $\Delta e [J] \rightarrow$ Energy of light.

Radiant flux / Radiant Power $\rightarrow \Phi_e [W = Js^{-1}]$

Energy per unit time.

Flux is too generic as it contains no spatial or directional information.

↓
Radiant Intensity $I_e (\omega) [Wsr^{-1}] \rightarrow$
Solid angle Emanated flux per solid angle of a point source.

$$I_e (\omega) = \frac{d\Phi_e}{d\omega}$$

$$d\omega = \frac{1}{r^2} dA$$



Steradian.

$$d\omega = \frac{1}{r^2} dA = \frac{1}{r^2} (r d\theta)(r \sin\theta d\phi) = \sin\theta d\phi d\theta$$

$$\text{Isotropic point source } \Phi_e = \int_{\text{sphere}} I_e(\omega) d\omega$$

$$\Phi_e = I \int_{\text{sphere}} d\omega = I \int_0^{2\pi} \int_0^\pi \sin\theta d\phi d\theta$$

$$\Phi_e = 4\pi I$$

~~Radiant~~ Irradiance $E_e(x) [W m^{-2}]$
Flux per unit area incident on a surface
 $E_e(x) = \frac{d\Phi_{e,i}}{dA}$

Radiant exitance $M_e(x) [W m^{-2}]$

$\rightarrow M_e(x) = \frac{d\Phi_{e,e}}{dA}$ Flux per unit area
incident on a surface.

Radiosity $J_e(x)$ Flux per unit area emitted
plus reflected from surface.

$$J_e(x) = \frac{d\Phi_{e,er}}{dA}$$

Radiant Flux (or Power) : Total amount of Energy passing through surface

$$\Phi [W] \text{ or } [J/s]$$

Not descriptive enough for simulations



We have square loss.

So, we compute Radiant Flux per Area.

Irradiance $E [W/m^2]$ (flux normalized per square meter)
This is still ambiguous. We have not considered the angle coming into object.

A lot of energy in small angle or large angle etc.

Radiance: $L [W/(m^2 \cdot sr)]$ (flux normalized per area (m^2) and solid angle (sr))

From Maxwell equations, how light waves behave

400 - 730nm

$$\nabla \cdot E = 0$$

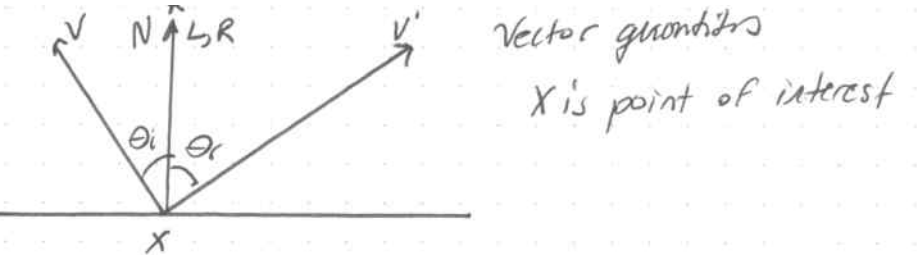
$$\nabla \cdot B = 0$$

$$\nabla \times E = -\frac{\partial B}{\partial t}$$

$$\nabla \times B = \mu_0 \epsilon_0 \frac{\partial E}{\partial t}$$

Scalar Product $\vec{a} \cdot \vec{b} = \|\vec{a}\| \|\vec{b}\| \cos \theta$
in rendering all vectors are length 1.

$$\Rightarrow \vec{a} \cdot \vec{b} = \cos \theta$$



$V \rightarrow$ direction toward viewer.

$N \rightarrow$ surface normal

$L \rightarrow$ vector toward light source

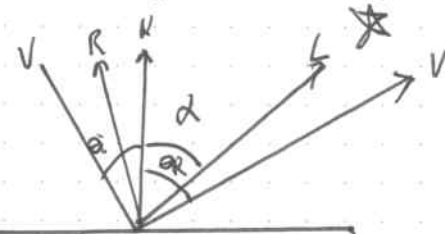
$R \rightarrow$ reflected Ray

$\theta_i, \theta_r \rightarrow$ incident and reflected angles.

$$R = L - 2N(L \cdot N)$$

Diffuse shading

$$(L \cdot N) \Phi = (\cos \alpha | \alpha=90^\circ) \Phi = (1) \Phi = \Phi$$

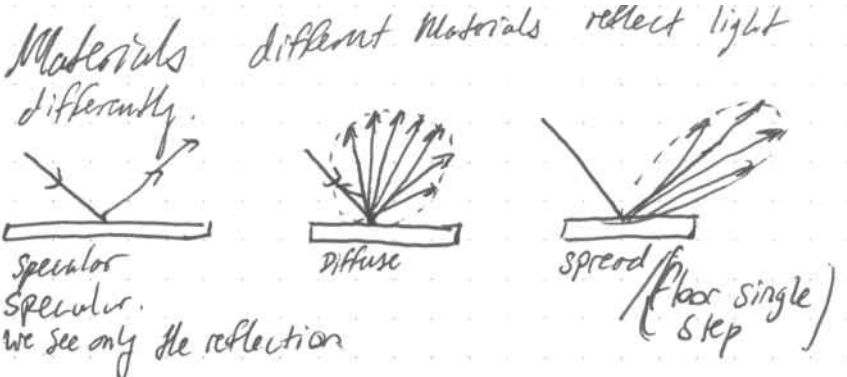


What if the light points at an angle α

$\alpha = 45^\circ \quad (L \cdot N) \Phi = (\cos \alpha | \alpha=45^\circ) \Phi = 0,7 \Phi$

only about 0,7 of power is received.

$\alpha \approx 90^\circ \quad (L \cdot N) \Phi = (\cos \alpha | \alpha \approx 90^\circ) \Phi \approx 0$



Diffuse, many possible outcomes

Floor single step (combination of specular diffuse)

Let's make a PDF with two parameters.

- Incident light direction
- Surface point.

f_r (incoming direction, a point, outgoing direction)

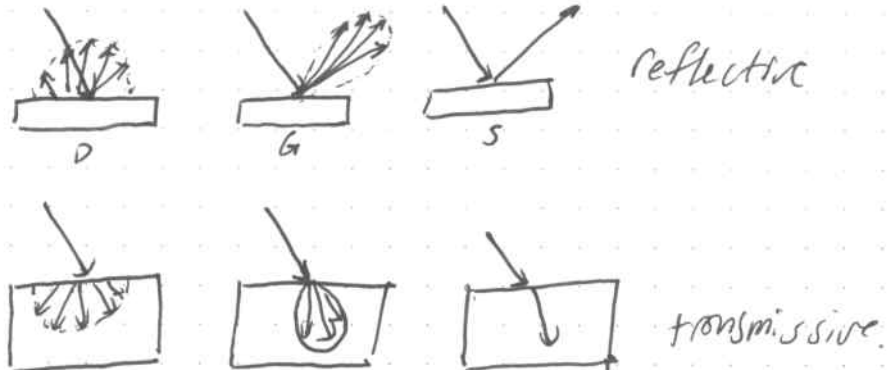
$$f_r(\vec{\omega}, x, \vec{\omega}')$$

This is called the Bidirectional Reflectance Distribution function (BRDF)

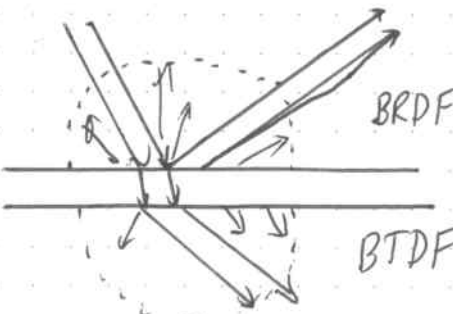
Bidirectional Reflectance Distribution function (BRDF)

$$f_r(\vec{\omega}, x, \vec{\omega}')$$

What about Transmissive materials ?



These Two are combined into the Bidirectional transmittance distribution function (BTDF)



The generic umbrella term is BSDF
Bidirectional Scattering distribution function.

$$BSDF = BRDF \cup BTDF$$

1 Helmholtz-reciprocity → The direction of the ray of light can be reversed.

$$\forall \vec{\omega}, \vec{\omega}': f_r(\vec{\omega}, x \vec{\omega}') = f_r(\vec{\omega}', x \vec{\omega})$$

2. Positivity: It is an impossibility for an exit direction to have a negative probability.

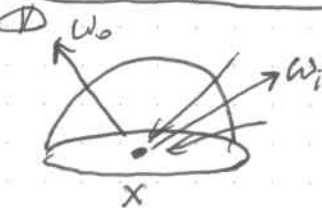
$$\forall \vec{\omega}, \vec{\omega}': f_r(\vec{\omega}, x \vec{\omega}') \geq 0$$

3. Energy conservation: An object may only absorb or reflect light, but not more than incoming amount.
(strictly material models)

Then

$$\int_{\Omega} f_r(\vec{\omega}, x \vec{\omega}') \cos \theta d\vec{\omega}' \leq 1$$

- If it equals 1 → all light reflected
- if less than 1, some light absorbed



Sum up all the incoming light, and see what reaches our viewpoint.

objects can emit light themselves.

Light exiting surface = Self emitted light + reflected incoming light

$$L_o(x, \vec{\omega}) = \underbrace{L_e(x, \vec{\omega})}_{\text{emitted}} + \underbrace{\int_{\Omega} L_i(x, \vec{\omega}') f_r(\vec{\omega}', x, \vec{\omega}) \cos \theta d\vec{\omega}'}_{\text{reflected incoming light.}}$$

$$\text{Light exiting} = \text{Emitted light} + \text{reflected incoming light}$$

$$L_o(x, \vec{\omega}) = L_e(x, \vec{\omega}) + \underbrace{\int_{\Omega} L_i(x, \vec{\omega}') f_r(\vec{\omega}, x, \vec{\omega}') \cos \theta d\vec{\omega}'}_{\substack{\text{emitted light} \\ \text{reflected incoming light}}}$$

$L_o(x, \vec{\omega}) \rightarrow$ exiting radiance at point x toward direction $\vec{\omega}$

$L_e(x, \vec{\omega}) \rightarrow$ emitted radiance at point x toward direction $\vec{\omega}$

$\int_{\Omega} \dots d\vec{\omega}' \rightarrow$ integral summation of all incoming radiance from all $\vec{\omega}'$ directions over area $\Omega \rightarrow$ ~~2π~~ radians.

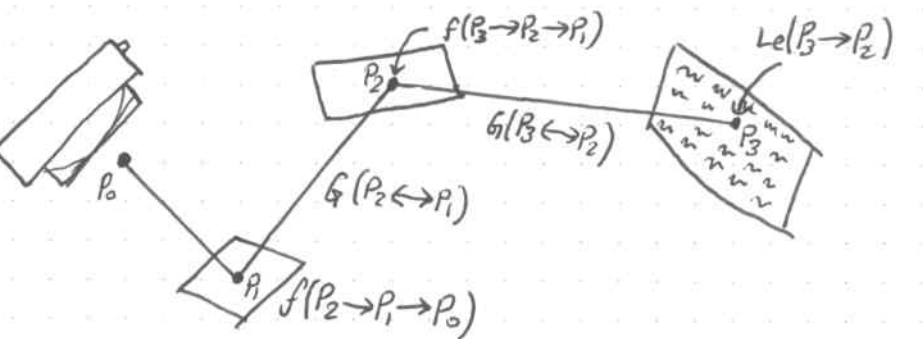
Ω is integrated over a hemisphere

$L_i(x, \vec{\omega}') \rightarrow$ incoming radiance from direction $\vec{\omega}'$ to point x

$f_r(\vec{\omega}, x, \vec{\omega}') \rightarrow$ BRDF

This problem is very difficult to solve. Impossible analytically.

- The exitant radiance of a point x depends on the incoming radiance of every other point, which also depend on x .
- Cannot be computed in closed form Integral.
- Integral is infinite dimensional.
- Singular



An example light path.

light source P_3 , light sink P_o

We compute one light path, how much light is going through
then we disturb P_2 , and see how much it changes.

Then we add up all the contributions to the sensor
from the light source.

Surface Integral Formulation:

$$L_o(p' \rightarrow p) = L_e(p' \rightarrow p) + \int_A L_i(p'' \rightarrow p') f_r(p'' \rightarrow p' \rightarrow p) G(p'' \rightarrow p') dA(p'')$$

$L_o(p' \rightarrow p)$ → outgoing radiance from point p' to p

$L_e(p' \rightarrow p)$ → emitted radiance from point p' to p

$\int_A \dots dA(p'')$ → sum of all possible p'' surface points.

$L_i(p'' \rightarrow p')$ → incoming radiance from point p'' to p'

$f_r(p'' \rightarrow p' \rightarrow p)$ → probability of $p'' \rightarrow p' \rightarrow p$ transfer.

Simplified BRDF Models. A compilation of hacks.

Ambient BRDF

$$I = k_a I_a$$

$I \rightarrow$ intensity

$k_a \rightarrow$ ambient coefficient of object (color, ·)

$I_a \rightarrow$ ambient intensity of the scene/light source



color, intensity 1
color intensity 2,
ambient

Ambient shading just takes the color and intensity

Diffuse BRDF

$$I = k_d (\vec{L} \cdot \vec{N})$$

$k_d \rightarrow$ diffuse albedo of object

$\vec{L} \rightarrow$ vector pointing to light source

$\vec{N} \rightarrow$ Surface Normal vector

How much light is not absorbed at every wavelength,
able to see the light source.

Specular BRDF

$$I = k_s (\vec{V} \cdot \vec{R})^n$$

$k_s \rightarrow$ specular coefficient of object

$\vec{V} \rightarrow$ vector pointing at viewport

$\vec{R} \rightarrow$ reflected direction of light ray.

$(\cdot)^n \rightarrow$ "shininess" factor.

Phong Shading is the summation of these three.

$$I = K_a I_a + I_l \left(K_d (\vec{L} \cdot \vec{N}) + K_s (\vec{V} \cdot \vec{R})^n \right)$$

The Illumination equation

$I_l \rightarrow$ incoming light (0 - 1)

- This only accounts for direct illumination
- The indirect illumination is neglected, the ambient term helps to remedy this by re-injecting lost energy from the discrepancy back into system.

Crude approximation, Simple but easy.

If there are multiple light sources, it is a summation of all light sources.

Ray Tracing Algorithm.



1. Construction of camera
2. Intersection with scene
3. Shading
4. reflection/refraction

Instead of originating rays at light source we originate rays at light sink. This way we guarantee we only render what we see.

Ray tracing algorithm.

There is a camera plane, and we project the 3D-world onto that plane.

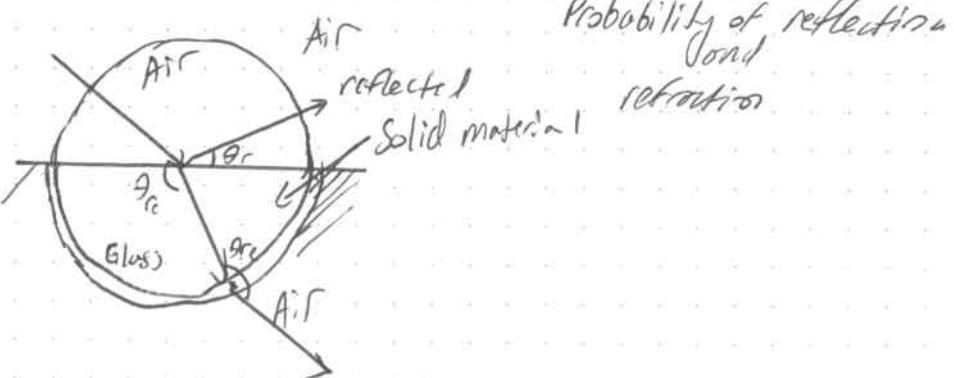
We shoot the rays out, and intersect them with objects in scene. Then we compute all the shading terms like ambient, diffuse, and rest, and then we add recursion.

Recursion: We stop at first point.

then we imagine this is the starting point of a ray.

We shoot the ray outwards and start ray tracing again.

Reflection and Refraction.



Schlick's approximation:

$$R(\theta) = R_0 + (1-R_0)(1-\cos\theta)^5$$

$R(\theta)$ → Probability of reflection when incident ray is θ

R_0 probability of reflection on normal incidence

R_0 can be given by:

$$R_0 = \left(\frac{n_1 - n_2}{n_1 + n_2} \right)^2$$

$n_1, n_2 \rightarrow$ indices of refraction

Schlick's approximation

$$R(\theta) = R_0 + (1-R_0)(1-\cos\theta)^5 \text{ where } R_0 = \left(\frac{n_1 - n_2}{n_1 + n_2} \right)^2$$

Refraction index of air is 1.

⇒ Air / vacuum - medium interaction approximation

$$R_0 = \left(\frac{n_1 - 1}{n_1 + 1} \right)^2 \quad n_1 \rightarrow \text{index of refraction of new medium.}$$

T is probability of transmission

$$T(\theta) = 1 - R(\theta)$$

examples.

$$R(0^\circ) = R_0$$

$$R(90^\circ) = R_0 + (1-R_0) = 1$$

We can think of this function as the interpolation between these two states.

Air-glass interaction

$$R(\theta) = R_0 + (1-R_0)(1-\cos\theta)^5$$

$$R_0 = \left(\frac{n_{\text{glass}} - 1}{n_{\text{glass}} + 1} \right)^2 \quad n_{\text{glass}} = 1.5$$

$$\Rightarrow R(\theta) \approx \left(\frac{0.5}{2.5} \right)^2 + \left(1 - \left(\frac{0.5}{2.5} \right)^2 \right) (1-\cos\theta)^5$$

artifact
of Taylor series.

its only approximation

There is a high probability of refraction when the light ray comes from the direction of the normal ($\theta=0$).

High probability of refraction means low reflection

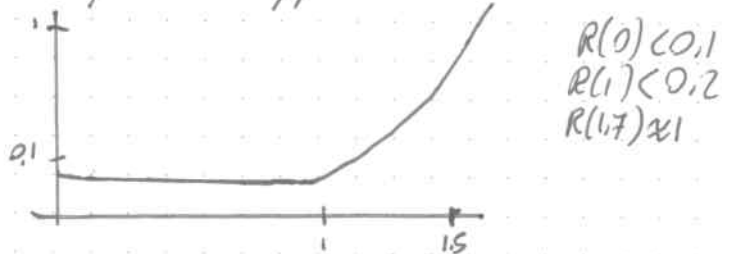
$R(0) < 0.1 \rightarrow 10\% \text{ reflected}, 90\% \text{ refracted}$.

What if we choose 60 degrees.

$$\frac{60^\circ \cdot \pi}{180^\circ} = 1 \text{ rad}$$

$R(1) < 0.2 \rightarrow 20\% \text{ reflection}, 80\% \text{ refraction}$.

Let's plot the approximation pdf.



This approximation does not work for vacuum-vacuum interactions.

$$R(\theta) = R_0 + (1-R_0)(1-\cos\theta)^5$$

$$R_0 = \left(\frac{n_{vac}-1}{n_{vac}+1} \right)^2 \quad n_{vac} = 1$$

$$R(\theta) = 0 + (1-0)(1-\cos\theta)^5 = (1-\cos\theta)^5$$

which is not correct.

Vacuum-Vacuum has full transmission.

The Schlick approximation is an approximation of the Fresnel equation:

$$R_s(\theta) = \left| \frac{n_1 \cos \theta - n_2 \sqrt{1 - \left(\frac{n_1}{n_2} \sin \theta \right)^2}}{n_1 \cos \theta + n_2 \sqrt{1 - \left(\frac{n_1}{n_2} \sin \theta \right)^2}} \right|^2$$

it is more computationally expensive.

Snell's law light slows down through mediums.

$$n_{\text{medium}} = \frac{\text{Speed of light in vacuum}}{\text{Speed of light in medium}} = \frac{c}{v_{\text{medium}}}$$

\Rightarrow Speed of light in glass $\approx 1.5 = \frac{3e8}{v_{\text{medium}}}$

Snell's law $n_2 \sin \theta_1 = n_1 \sin \theta_2$

$$\Rightarrow \frac{\sin \theta_1}{\sin \theta_2} = \frac{n_1}{n_2}$$

There is a critical angle at which only reflection will happen.

Air-glass interaction

$$\sin \theta_2 = \frac{n_1}{n_2} \sin \theta_1 = \frac{1.5}{1} \cdot \sin(50^\circ) = 1.149 \quad \text{No reflection}$$

There is no such angle, so we find a critical angle

$$\sin \theta_1 = \left(\frac{n_2}{n_1} \sin \theta_2 \right) \Big|_{\theta_2=90^\circ}$$

$$\theta_{\text{crit}} = \arcsin\left(\frac{n_2}{n_1}\right) = \arcsin\left(\frac{1}{1.5}\right) = 41.8^\circ$$

Beginning of Ray tracing.

What is a ray, or vector.

~~$$\vec{r}(t) = \vec{o} + t \vec{d}$$~~

Parametric ray equation

\vec{o} origin

\vec{d} direction

t - time duration distance.

$$\|\vec{d}\|=1$$

$$\vec{r}(t) = \vec{o} + t\vec{d} \quad \vec{o} \rightarrow \text{origin}, \vec{d} \rightarrow \text{direction}, t \rightarrow \text{distance}$$

The direction vector is always a unit vector

$$\|\vec{d}\| = 1$$

$$\begin{aligned} x &= x(t) \\ y &= y(t) \end{aligned}$$

parametric

as opposed
to implicit

$$\text{implicit } \left[f(x,y) = (x-a)^2 + (y-b)^2 + \dots - r^2 = 0 \right]$$

Ray sphere intersection

Expectation :

Sphere equation :

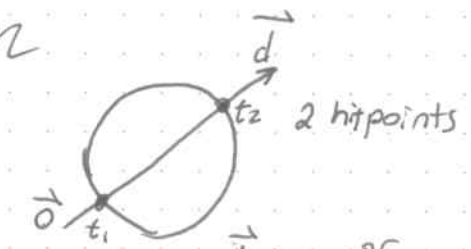
$$(\vec{p} - \vec{c}) \cdot (\vec{p} - \vec{c}) = r^2$$

\vec{p} = point on Sphere
surface

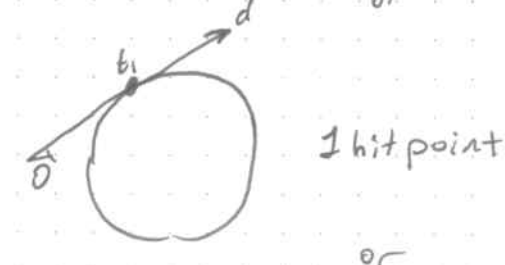
\vec{c} = center

Ray equation

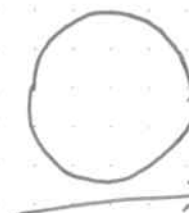
$$\vec{r}(t) = \vec{o} + t\vec{d}$$



2 hitpoints



or



0 hitpoints

Substitute $\vec{r}(t)$ in place
of \vec{p}

$$(\vec{o} + t\vec{d} - \vec{c}) \cdot (\vec{o} + t\vec{d} - \vec{c}) = r^2$$

$$t^2(\vec{d} \cdot \vec{d}) + 2(\vec{o} - \vec{c}) \cdot t\vec{d} + (\vec{o} - \vec{c}) \cdot (\vec{o} - \vec{c}) - r^2 = 0$$

$$t^2(\vec{d} \cdot \vec{d}) + 2(\vec{d} \cdot \vec{c})t + (\vec{c} \cdot \vec{c}) - r^2 = 0$$

$$At^2 + Bt + C = 0$$

Two hits if $B^2 - 4AC > 0$

$$A = \vec{d} \cdot \vec{d}$$

One hit if $B^2 - 4AC = 0$

$$B = 2\vec{d} \cdot (\vec{c} - \vec{d})$$

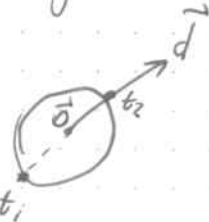
No hits if $B^2 - 4AC < 0$

$$C = (\vec{c} \cdot \vec{c}) - (\vec{c} \cdot \vec{d}) - r^2$$

two solutions:

$$t_{1,2} = \frac{-B \pm \sqrt{-4AC}}{2A}$$

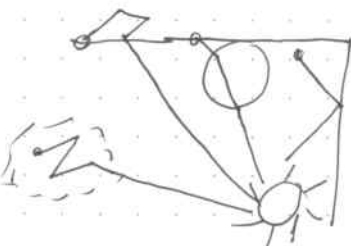
However, if we have two solutions, t can be a negative value if we are inside object.



Surface Normals

For an implicit equation $f(x, y) = 0$, the surface Normal is the gradient $\nabla f(x, y)$

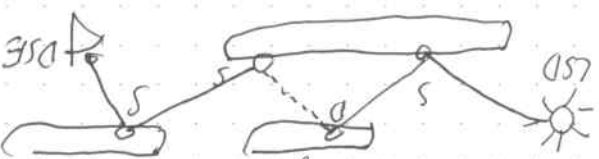
$$\nabla f(x, y, z) = \left(\frac{\partial f}{\partial x}, \frac{\partial f}{\partial y}, \frac{\partial f}{\partial z} \right)$$



Hey idea: therefore happens all parallel light path, but make an approximation by shadowing planar, but and compare the four rays by interpolation
light source need often with a planar map

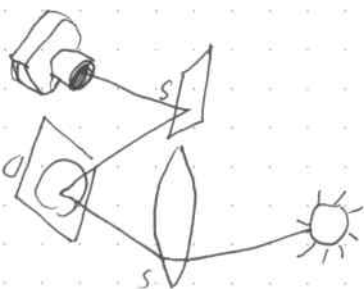
Therefore happens all parallel light path, but

the x, y of left ray surface need to be
done in parallel



Note that if no rays hit the surface
it is called a missed ray.

It is very unlikely that
it will hit the surface
because it is far away.
The surface is curved
and the rays are straight.
So it is very unlikely that
it will hit the surface.



ray starts at the origin
of the coordinate system.

MLT is when the ray
intersects the object's
surface. It is the first
intersection point of the
ray with the object's
surface.

If it is a transparent
object, we can
choose to ignore it.

Intersection
number

It is the first
intersection point of the
ray with the object's
surface.

We call it the
intersection of the
ray with the object's
surface.

Vector style intersection
is different from
ray-ray intersection.

$$\text{Example: } f(x, y, z) = \frac{x^2}{a^2} + \frac{y^2}{b^2} - 1$$

a, b are curvatures of the
elliptical paraboloid.



Let's compute the surface normal

$$\nabla f(x, y, z) = \left(\frac{\partial f}{\partial x}, \frac{\partial f}{\partial y}, \frac{\partial f}{\partial z} \right)$$

$$\frac{\partial f}{\partial x} = \frac{2}{a^2} x, \quad \frac{\partial f}{\partial y} = \frac{2}{b^2} y, \quad \frac{\partial f}{\partial z} = -1$$

$$\nabla f(x, y, z) = \left(\frac{2}{a^2} x, \frac{2}{b^2} y, -1 \right)$$

Intersection Routine

Intersect the ray to hit all objects in scene.
What is the first object the ray hits?

If the object is not transparent we will only
need to take the first intersection.

We have a list of time coordinates

we only pick the smallest positive t .

Can we take $t = 0$?

Means we are exactly on the object surface.
There is a trivial intersection
we substitute it with a small ϵ .

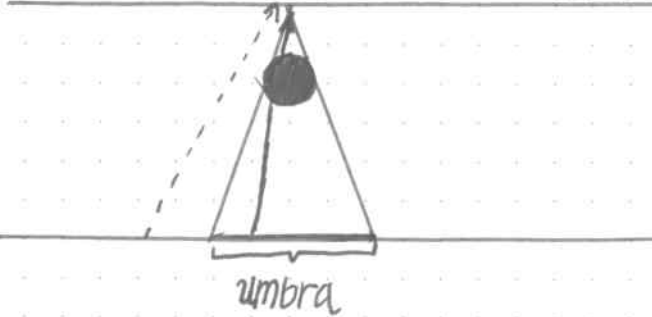
Shadows

Occluded regions from light source.

Simple point source

obstructed

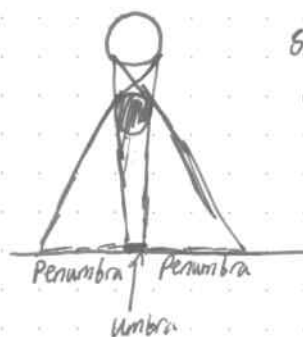
unobstructed



There is a visibility term along with the ambient and illuminance.

We set $I \leftarrow 0$ when there is a complete obstruction.

In real life, point light sources do not exist.



Since we cannot have a point source, we have a light source with area.

This visibility is continuous.

It is incredibly difficult to implement, published in 1997

because it's very difficult to take into account all the different types of objects in the scene, which makes it even more difficult to implement.

over multiple bounces

outwardly;

solution: If walls as a mirror then process, which, in this strategy, provides an opportunity to work with parallel rays.

we do transformations of the camera, and update

$$\text{random variables} \quad \phi = 2\pi \cdot \frac{\theta}{\pi} \quad P(\theta) = \int_{-\pi/2}^{\pi/2} p(\phi) d\phi$$

$$\frac{dI}{I} = \frac{P(\theta)}{P(\phi)} d\phi = (\phi/\theta) d\phi$$

$$P(\theta, \phi) d\theta d\phi = (n+1) \cos \theta \sin \theta$$

$$\frac{dI}{I} = \frac{\int_{-\pi/2}^{\pi/2} P(\theta, \phi) d\phi}{n+1} \cos \theta \sin \theta$$

$$P(\theta, \phi) = \cos \theta \sin \theta$$

$$L(w_0, x) = \int_{-\pi/2}^{\pi/2} L(w_0, x) \cos \theta \sin \theta d\theta$$

possible to use.

if it is done through a technique called direct rendering it is possible to do better than ray tracing - this takes quite a lot of work, even for simple cases, and it's not always

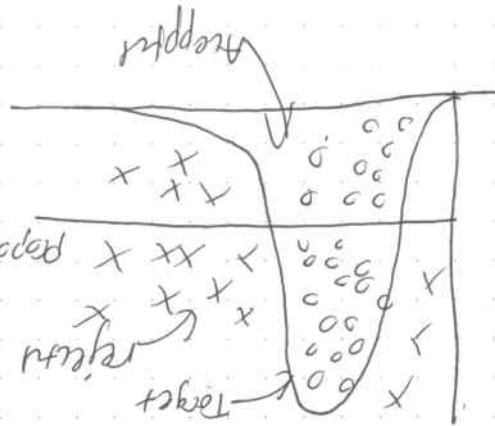
we construct a reflection similar to $f(x)$, and we draw surfaces depending on the shape of function, we can sample of it by rejection sampling - this is inefficient.

in many ways
makes it hard to
see what's going on

box is a box
with many flaps

we can't see what's
inside from here.

we draw samples of it with
we construct a function very similar to $f(x)$ and
then fit that to $f(x)$.



importance sampling

$$\frac{f(x)}{\int f(x) dx} \sum_{i=1}^N x_i p(x_i) = \left[\frac{f(x)}{\int f(x) dx} \right]$$

we find, if adds small perturbations to the
first of remember the successful path

we finally randomly found a light path that escape the
about this first and then escape the scene
room and it would be a case of just random

light is in the other room.
Hey idea! Imagine a dark room with a door open, and

more sophisticated decisions if it will be a bright light
it is "neighboring" importance sampling. If we initially
make a bright point if it is on the first few steps

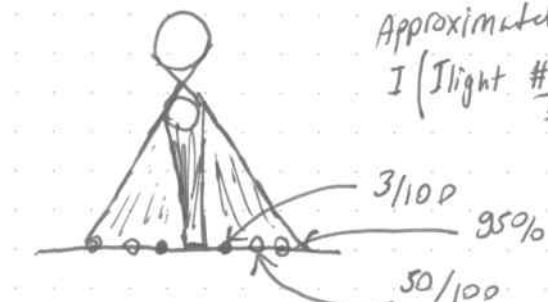
this sounds like classical importance sampling, but it is not!
Traditional importance sampling is used to determine
whether the bright point is on the first few steps

new idea! "see the light" - by some brighter parts more often
represents light rays

The Brightness of the point Would Be

$$I \leftarrow \left(I_{\text{light}} \frac{\text{Area of light that is visible}}{\text{Area of light source}} \right) \cdot I$$

Approximated by
 $I \left(I_{\text{light}} \frac{\# \text{visible shadows rays}}{\# \text{all shadow rays}} \right)$



This is monte carlo integration

This cannot be physically correct however,
The block umbra should continuously
fade to partial shadows.

We never see perfectly block shadows.

We are only accounting for direct light
source.

There are also light bounces.

This is why we have an ambient term to
warm up the images of Direct illumination.

This is still the most method that is doing an encoder
and it's difficult to do without bidirectional path tracing.

+ Better convergence speed, especially in indoor scenes
+ Getting the path weighting and this perfectly parallel
+ Another consequence for cosines.

Convergence speed improvement with paper multiple passes sampling.

Look for Multiplane importance sampling, and Balance Heuristics
EBC Leach's Thesis, Chapter 9

We call this technique Multiplane importance sampling (MIS)
These are techniques that are probably good both in a theoretical and practical sense.

The ~~one~~ variable is additive, therefore averaging will give better result.
The ~~one~~ variable is additive, therefore average rate.

If it is a non-trivial matter, because the separate path

We have two different sampling strategies (BSDF and Light source sampling) for the same target - we need to sample them for best result.

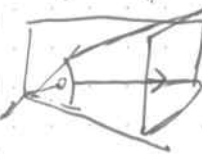
• take light path more often.
• when we start from eye and hit diffuse or glossy object, then we start importance sampling the BSDF.

• The light source samples the distribution of the light source
• This is actually two Monte Carlo processes.
• Path is and we cannot do this in all possible different ways.
• What is difficult about bidirectional path tracing is that are two light distributions both coming from

Camera Models



Pinhole



Perspective

The starting point are fixed in the edges of the viewer.

Every pixel has an (x, y) pair coordinate.

n, w, fov_x are given and the desired pixel positions are x_p, y_p

$$\begin{aligned} x_p &\in (0, w) \\ y_p &\in (0, h) \\ \text{fov}_x &\in (0, \pi) \end{aligned} \Rightarrow x = \frac{2x_p - w}{w} \tan(\text{fov}_x)$$

$$y = \frac{2y_p - h}{h} \tan(h/w \cdot \text{fov}_x)$$

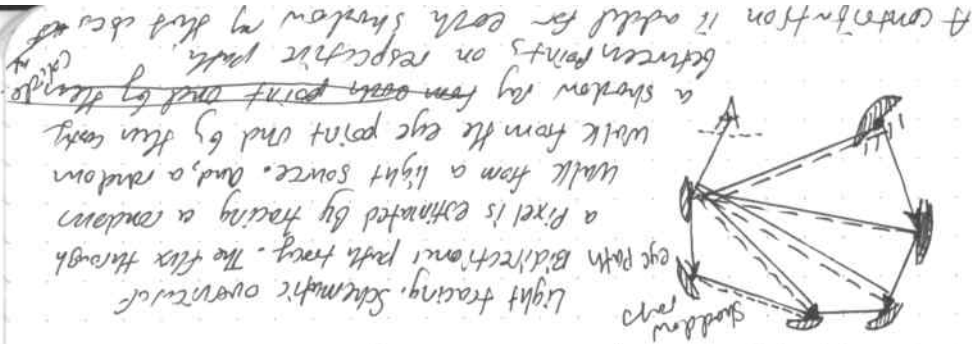
$z = -1$

Mapping of a polar rectangle onto a raster.

Orthographic camera



The Camera rays are parallel to each other.



and connect the end points of those paths.

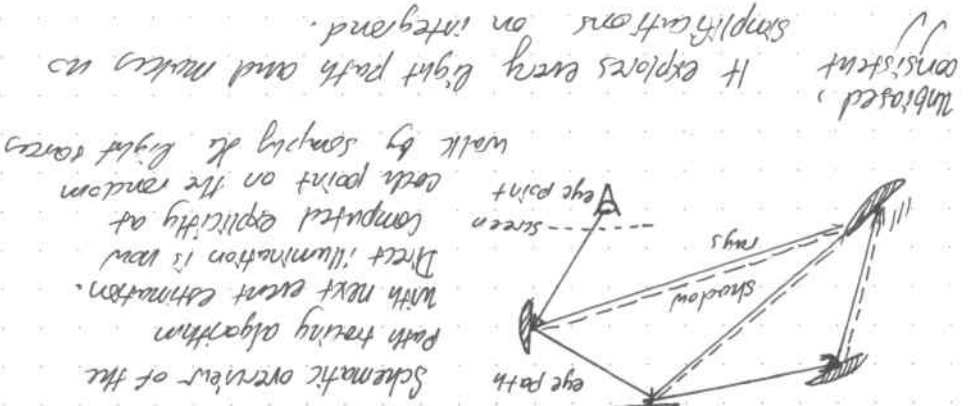
Solution: Short rays from both the light source and camera. Even with next event detection, most computations are expensive. The camera is not too likely to hit the light source, but it is possible. Use these more robust.

With a path from the camera, can handle situations with the light scattered from the light and is connected. Path is scattered from the light. Bidirectional methods, where a ray from the light hits a material will be able to find illuminations in the area. Illumination will be able to find a second-to-last vertex coloring such that only path with a second-to-last vertex. A light source is illuminating a small area on the camera is not difficult case for Path Tracing starting from camera.

Bidirectional Path Tracing [1993]

+ surfaces converge slowly
+ parallelize well
+ easy to implement

* This are our cases but it's out of scope for now.
+ explores every light path and makes no mistakes



We have discussed this one before.

Ray Tracing is a simplification. It assumes every angle has the same probability of reflection.

The illumination Equation with recursion

$$I = \underbrace{k_a I_a + I_i}_{\text{ambient}} \left(\underbrace{k_d (\vec{L} \cdot \vec{n}) + k_s (\vec{V} \cdot \vec{R})^n}_{\text{diffuse, specular}} \right) + \underbrace{k_t I_t}_{\text{material properties}} + \underbrace{k_r I_r}_{\text{recursion}}$$

Ambient is a hook, to warm up block shadows.

$I_i \rightarrow$ incoming light

$k_t \rightarrow$ Fresnel transmission coefficient.

$I_t \rightarrow$ intensity from flat direction.

$k_r \rightarrow$ Fresnel transmission coefficient

$I_r \rightarrow$ Intensity of light.

Heckbert's notation for light path

$L \rightarrow$ light source

$D \rightarrow$ diffuse light path

$S \rightarrow$ specular light path

$E \rightarrow$ eye / camera

$[D]^*$ → any amount of diffuse bounces (or zero)

$[S|D]$ → specular or diffuse

Ray Casting: $L[D]E$

Radiosity: $L[D^*]E$

Recursive ray tracing: $L[D]S^*E$

Global illumination:

$L[DIS]^*E$

Global illumination algorithm classes
Intuition: A consistent algorithm
solution after an infinite
number of samples.
Soon - or later if will converge.

Intuition: The expectation over
unbiased samples of the samples.
with an unbiased algorithm, if we had two noisy images, combining
them would give a more accurate solution.

$$E_N[F - \int f(x)dx] = 0$$

unbiased

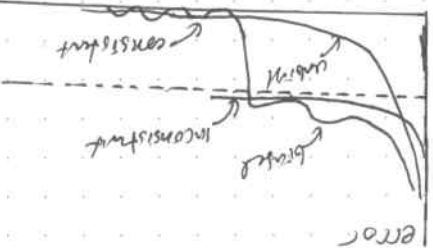
Intuition: A consistent algorithm
will converge to the right
solution after an infinite
number of samples.

$$\lim_{N \rightarrow \infty} E_N[F] = \int f(x)dx$$

Global illumination algorithm classes

State of the art algorithms:
If I calculate a new approximation, it will have to be passed
to the other threads.

Time



Corollary: If mathematical terms are correct, it should be possible
to do rendering without a raytrace!

That is no systematic error in the algorithm, the derivation is correct.
The algorithm has the same chance of over and underestimating
the intensity.

2018-03-14
Lambertian Model Oren-Nayar model
Oren-Nayar model takes into consideration microscopic imperfections

An alternative specular model is Phong-Blinn model

$$I = ks (\vec{N} \cdot \vec{H})^n \quad \text{where} \quad \vec{H} = \frac{\vec{L} + \vec{V}}{\|\vec{L} + \vec{V}\|}$$

Cook-Torrance Model: Phong-Blinn + microscopic
roughness

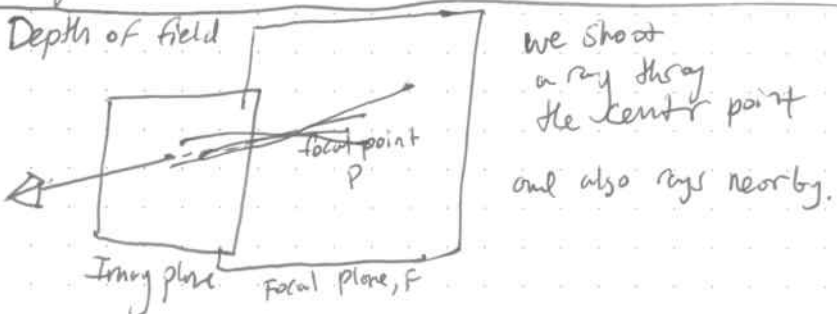
Ashikhmin-Shirley model: Anisotropic, specular only
on a diffuse substrate.

BRDF explorer by Disney

F-Stop On hand-held cameras, we can set
the size of the aperture

The higher the F-Stop, the smaller the aperture
lower F-Stop, more light let in, more regions out
of focus

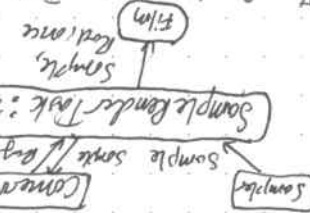
This gives us dof.



We shoot
a ray through
the center point

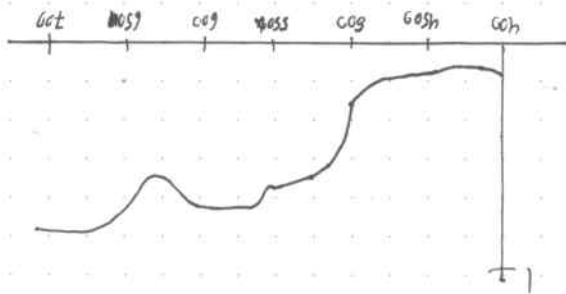
and also rays nearby.

We can sample indirect light in a similar way with this information on film.
 The samples are taken with the same camera as input, and contains all the necessary
 information about the scene if back
 of the next pixel. The camera contains a field of view.
 The samples render full also the camera for the reflection
 of the environment, etc.
 This is done by direct sampling or
 Global sampling, which
 uses some of pixels
 as samples to provide
 the samples for
 the samples.
 PBR architecture
 also render on per
 sample basis.



More on this in PBR Chapter 5 - Color and Light.

And take the ray of light.
 And take the second the direct light.
 And take the direct light.



Spectral Power Distribution (SPD)

First we introduce a function that describes how much light is
 carried at different wavelengths.

How to carry out a simulation for the whole visible wavelength?

We know Recursive Ray Tracing

$$I = K_a I_a + I_i \left(K_d (\vec{L} \cdot \vec{N}) + K_s (\vec{V} \cdot \vec{R})^n \right) + K_t I_t + K_r I_r$$

Illumination vs.

$$L_o(x, \vec{\omega}) = L_e(x, \vec{\omega}) + \int_{\Omega} L_i(x, \vec{\omega}) f_r(\vec{\omega}, x, \vec{\omega}') \cos \theta \vec{\omega}' \text{ Rendering}$$

The Rendering equation is very difficult to solve.

We get indirect illumination.

Caustics LSSDE

Shadow computation

What is the definition of shadows?

The absence of light

In global illumination there are no shadows.

Shadows are not computed explicitly anymore

Global illumination

Recursive Ray Tracing ($L[D]S^*E$) are unable to compute indirect illumination:

- $LDD[D^*]E$ (indirect illumination / color bleeding)

- $LS[S^*]DE$

In recursive ray tracing, we only approximate the diffuse BRDF locally, which in reality we would have to collect all incoming light from the illumination hemisphere. We don't take into account the neighborhood of points.



To account the neighborhood of points,

$$I = k_a I_a + \int_i (k_d (\vec{L} \cdot \vec{n}) + k_s (\vec{V} \cdot \vec{R}))^n + k_t I_t + k_r I_r$$

If we switch to global illumination

$$L(x, \vec{w}) = L_e(x, \vec{w}) + \int_{\Omega} \int_i L_i(x, \vec{w}') f_r(\vec{w}, x, \vec{w}') \cos \omega_i$$

Incoming Radiance integration



Sends samples out in every direction

BRDF (The Real Thing)

It collects the radiance from all directions on a hemisphere. If we shoot a ray in, every outgoing direction has the same probability.

$$f_r(\vec{w}, x, \vec{w}') = \frac{1}{\pi}$$

But does not have to reflect all the incoming light.

$$f_r(\vec{w}, x, \vec{w}') = \frac{P}{\pi} P_E(0, 1)$$

so we scale it with albedo.

```

FILE *f = fopen("ray.ppm", "w");
fputchar(f, '\n');
fputchar(f, '\n');
fputchar(f, '\n');

FILE *fr = fopen("ray.ppm", "r");
fscanf(fr, "%d %d %d", &W, &H, &P);
fscanf(fr, "%f %f %f", &Lx, &Ly, &Lz);

float f = 0;
for (int i = 0; i < W; i++) {
    for (int j = 0; j < H; j++) {
        float R = 0.0;
        float G = 0.0;
        float B = 0.0;
        for (int k = 0; k < P; k++) {
            float u = (rand() / (float) RAND_MAX) * 2 * M_PI;
            float v = (atan((sqrt(1 - (u * u))) / (sqrt(1 - (v * v))))) / PI;
            float w = sqrt(1 - u * u - v * v);
            float NdotL = max(0, dot(N, L));
            float NdotR = max(0, dot(N, R));
            float NdotV = max(0, dot(N, V));
            float F = max(0, pow(2, dot(R, V)) / 4);
            float D = max(0, 0.5 * (1 + cos(v)));
            float S = max(0, 0.5 * (1 + cos(v)));
            float Kd = NdotL * D;
            float Ks = NdotR * S;
            float Kt = 0.0;
            float Kr = 0.0;
            float Ia = 0.2;
            float Id = 0.0;
            float Ir = 0.0;
            float Ie = 0.0;
            float I = Kd * Ia + Id * (Kd * (L.x + L.y + L.z)) + Kr * Ir + Ie;
            R += I;
            G += I;
            B += I;
        }
        R /= P;
        G /= P;
        B /= P;
        printf("%c", char(R));
        printf("%c", char(G));
        printf("%c", char(B));
    }
}

```


What is the dimensionality of global illumination.

$$L_o(x, \vec{\omega}) = L_c(x, \vec{\omega}) + \int_s L_i(y, \vec{\omega}') f_r(\vec{\omega}, \vec{\omega}') \cos\theta d\vec{\omega}'$$

$L_i(y, \vec{\omega}')$ would be another rendering equation inside.
⇒ infinitely large

It is also singular because of the possibility of - - - specular BRDF.

$$f_r(\vec{\omega}, x, \vec{\omega}') = \delta(\cdot) = \begin{cases} 1 & \text{reflection direction} \\ 0 & \text{elsewhere} \end{cases}$$

The solution is to handle this BRDF explicitly: We get an input direction where we automatically sample the reflection direction (and only that.)

Monte Carlo integration.

Simple method to approximate integrals.

It is one of the most powerful techniques created during second world war. during Manhattan project.

The goal is to compute $\int_a^b f(x) dx$

Samples are either taken into consideration as:

- hit/miss

- simple mean.

Hit/Miss

- Draw a function on paper

- Close it in a box of size A.

- Throw random points on paper

- for every point, determine if it's above or below function.

$$\int_a^b f(x) dx / A \approx \frac{\text{hit}}{\text{hit/miss}}$$

to reverse its law
approximate
scattering

Sample mean monte carlo integration.

Instead of hit/miss, we get information from the function:
 $f(2), f(15), f(273), f(2)$

$$\int_a^b f(x) dx$$

Sample the function at multiple points over the interval.

The over estimations and under estimations occur, but the error is less and less.

This leads to stochastic convergence.

Space optimizations.

We can use kd-trees and well organized data to logarithmic time.

We will be able to compute 1 million objects with 4-5 intersections.

We have to convert radiance into colorspace with tone mapping.

Filtering: With global illumination, we shoot lots of rays through a pixel. We could send them all through the same point, but if we integrate the surface of the pixel, we obtain anti-aliasing and other effects free.

Anti-aliasing with supersampling is expensive.

Participating media.

Light can also go through volumes.

Constituents and shadows are volumetric.

and compute intersection distances with vector form of results.
We iterate to reduce effect of reflection upon medium change.

Intersection BSP tree

the hubris of the light, and the end of subsurface scattering. We also have to compute diffuse. We can do this by performing a convolution of the previous step with a kernel that has a different distribution. It will be set to zero during rendering with a threshold.

```

    clr = clamp(
        face (ray, scene, depth+1, tmap, process, ha1, ha2),
        vec3(0,0,0));
    ray.d = ray.d - N * (cosf * 2) / (2 * pi);
    if (double cosf < ray.d + (N / 2))
        if (scene[Ld] < tmap)
            smaller_tmap;
    else
        larger_tmap;
}

```

we can do this by doing a convolution of the previous step with a random sample. This random sample is added to the result. We compute the low discrepancy shift. For example, then construct a random sample, and add it to the convolution on the hemisphere with uniform distribution. The result is added to the current result. This is a good way to do subsurface scattering. We can do this by doing a convolution of the previous step with a random sample, and add it to the current result. This is a good way to do subsurface scattering.

```

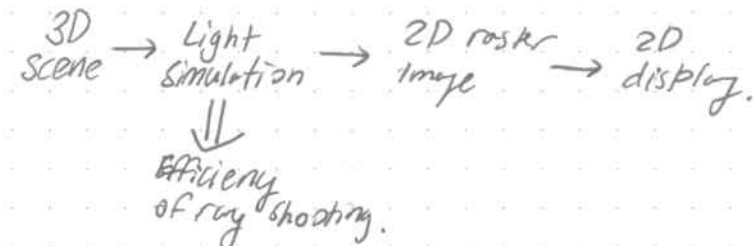
    cln.z += cosf * (tmap.z * scene[Ld] - Ld.z);
    cln.y += cosf * (tmap.y * scene[Ld] - Ld.y);
    cln.x += cosf * (tmap.x * scene[Ld] - Ld.x);
    face (ray, scene, depth+1, tmap, process, ha1, ha2);
    vec3 tmap = clamp(
        face (ray, scene, depth+1, tmap, process, ha1, ha2),
        vec3(0,0,0));
    ray.d = (N + hemi) * tmap * (horig + (ha12 * gct1));
    ha12 *= tmap;
    ha1, ha2 += (1 - ha12) * tmap;
    if (scene[Ld] < tmap)
        smaller_tmap;
    else
        larger_tmap;
}

```

Subsurface Scattering is volumetric.

Spatial acceleration structures.

Rendering pipeline



Spatial acceleration makes ray shooting more efficient.

Problems

- Generally, Monte-Carlo Methods uses ray shooting to sample the integrand of the rendering equation.
- Computing the closest intersection with the scene is equivalent to computing the local visibility.
- This is expensive for large amount of scene options.

• Naive approach:

Intersect Ray with all objects to determine the closest intersection ($O(n)$ for n objects)

• Better approach:

Reorganize the objects into a spatial hierarchy to skip large parts of the scene.

$O(n \log n)$ for n objects.

Linear vs. Sublinear



o K-d tree
Subdivide space and store the objects in overlapping nodes.

o Bounding Volume hierarchy (BVH)

group objects recursively into a tree structure.

By creating tree structures we can quickly check if a query falls into a subspace.

o KD-Tree

- + faster traversal on CPU
- larger amount of nodes

o Bounding Volume Hierarchy (BVH)

- + faster traversal on the GPU
- + easier to update
- + every object has only one leaf
- Spatial overlaps

Bounding Volume Hierarchies

Object grouping can be done in many ways -
optimally is usually scene dependent but heuristics exist

Surface Area Heuristic (SAH)

$$SAH = C_{inner} \sum_i \frac{A_n}{A_{root}} + C_{leaf} \sum_l \frac{A_l}{A_{root}}$$

$I \rightarrow$ inner nodes, $L \dots$ leaf nodes

$A_n \dots$ Surface area of node n

$A_{root} \rightarrow$ Surface area of its root.

group triangles together.

We want to minimize leaf box volume

weights = $1.0 / ((1.0 - weight) * 0.66666667)$

{ return }
if (BUDS <= maxDepth) { pfs = min((1.0, 0.0625 * depth)); }

const double maxDepth = 1.0; min((1.0, 0.0625 * depth)); }
else (depth < 5) {
double mfp = 1.0; }
else (depth <= maxDepth) { pfs = min((1.0, 0.0625 * depth)); }

Scene[id] = emission;

vec N = scene[id] - normal(ray);
vec Np = ray.o + ray.d * max(0.0, dot(N, ray.d));
if (Np == 1.0) return; }
else (Np >= 0.0) {

{ if (t > ps && t < min(t, max(t, t - hitResc + ray)));
t = scene[x] - hitResc + ray); }
++x; } x = 0; x < 32; } for (unsigned int i = 0; i < 32;) {

const unsigned int slice = scene[slice];
double mfp = inf;

if (depth <= 20) return;
The tree function

} return vec (cos(phi) * c, sin(phi) * b, u1);

const double phi = 2 * PI * u2;

const double r = sqrt(1.0 - u1 * u1);
vec hemisphere (double u3, double u4); }
with inner shading

```

        float fovy = PI / 4;
        double h = height;
        double w = width;
        Vec camera(const double x, const double y);

        Vec normal(const Vec& p) const {
            return Vec((p.x - c.x) / h,
                       (p.y - c.y) / w,
                       0);
        }

        Vec normal(Vec p) const {
            return Vec((p.x - c.x) / h,
                       (p.y - c.y) / w,
                       0);
        }

        void setMat4(Vec CL = 0, double emission = 0, int type = 0) {
            CL = CL; emission = emission; int type = type;
            world.setMat4(CL = 0, double emission = 0, int type = 0);
        }

        class Obj {
        public:
            double CL;
            Vec CL;
            double emission;
            int type;
        };
    };

    virtual Vec normal(const Vec& p) const = 0;
}

Sphere (double r = 0, Vec C = 0, double radius = 0, int type = 0) {
    double r;
    Vec C;
    double radius;
}
};

class Sphere : public Obj {
public:
    double radius;
    Vec C;
    double r;
    double radius;
    int type;
};

Sphere() {
    radius = 1;
    C = Vec(0, 0, 0);
    r = 1;
}
};

class Plane {
public:
    double A;
    double B;
    double C;
    double D;
    double radius;
    Vec N;
};

Plane::Plane(double A, double B, double C, double D, double radius) {
    this->A = A;
    this->B = B;
    this->C = C;
    this->D = D;
    this->radius = radius;
    N = Vec(-A, -B, -C).norm();
}

double Plane::hit(const Ray &r) const {
    double t = (-D - r.o.z * C) / (r.d.z * C + r.d.w);
    if (t < 0) return -1;
    if (t > radius) return -1;
    return t;
}

double Plane::reflect(const Ray &r) const {
    double t = hit(r);
    if (t < 0) return -1;
    double d = ((ray.o - C).dot(r.d)) * 2;
    double C = (ray.o - C).dot((ray.o - C)) - (r * r);
    double b = ((ray.o - C) * r).dot((ray.o - C));
    double disc = sqrt(d * d - b * b);
    if (disc < 0) return -1;
    double t1 = (-d - b - disc) / (r * r);
    double t2 = (-d - b + disc) / (r * r);
    if (t1 < 0) return t2;
    if (t2 < 0) return t1;
    return (t1 + t2) / 2;
}

double Plane::reflect(const Ray &r) const {
    double t = hit(r);
    if (t < 0) return -1;
    double d = ((ray.o - C).dot(r.d)) * 2;
    double C = (ray.o - C).dot((ray.o - C)) - (r * r);
    double b = ((ray.o - C) * r).dot((ray.o - C));
    double ddisc = sqrt(d * d - b * b);
    if (ddisc < 0) return -1;
    double t1 = (-d - b - ddisc) / (r * r);
    double t2 = (-d - b + ddisc) / (r * r);
    if (t1 < 0) return t2;
    if (t2 < 0) return t1;
    return (t1 + t2) / 2;
}

double Plane::reflect(const Ray &r) const {
    double t = hit(r);
    if (t < 0) return -1;
    double d = ((ray.o - C).dot(r.d)) * 2;
    double C = (ray.o - C).dot((ray.o - C)) - (r * r);
    double b = ((ray.o - C) * r).dot((ray.o - C));
    double ddisc = sqrt(d * d - b * b);
    if (ddisc < 0) return -1;
    double t1 = (-d - b - ddisc) / (r * r);
    double t2 = (-d - b + ddisc) / (r * r);
    if (t1 < 0) return t2;
    if (t2 < 0) return t1;
    return (t1 + t2) / 2;
}

double Plane::reflect(const Ray &r) const {
    double t = hit(r);
    if (t < 0) return -1;
    double d = ((ray.o - C).dot(r.d)) * 2;
    double C = (ray.o - C).dot((ray.o - C)) - (r * r);
    double b = ((ray.o - C) * r).dot((ray.o - C));
    double ddisc = sqrt(d * d - b * b);
    if (ddisc < 0) return -1;
    double t1 = (-d - b - ddisc) / (r * r);
    double t2 = (-d - b + ddisc) / (r * r);
    if (t1 < 0) return t2;
    if (t2 < 0) return t1;
    return (t1 + t2) / 2;
}
};

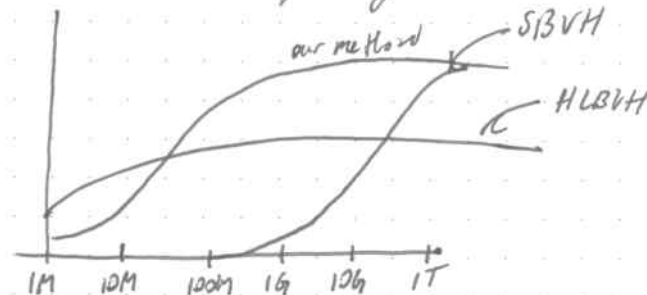
void Plane::reflect(Ray &r) const {
    double t = hit(r);
    if (t < 0) return;
    double d = ((ray.o - C).dot(r.d)) * 2;
    double C = (ray.o - C).dot((ray.o - C)) - (r * r);
    double b = ((ray.o - C) * r).dot((ray.o - C));
    double ddisc = sqrt(d * d - b * b);
    if (ddisc < 0) return;
    double t1 = (-d - b - ddisc) / (r * r);
    double t2 = (-d - b + ddisc) / (r * r);
    if (t1 < 0) return;
    if (t2 < 0) return;
    r.o = C + r.d * (t1 + t2) / 2;
}
};

Vec Plane::normal(const Ray &r) const {
    return Vec(-A, -B, -C).norm();
}

```

Constructing the tree with minimal SAD cost is expensive
→ usually approximations used.

This leads to a quality / speed trade off.



Tone Mapping.

3D scene → light simulation → ? \rightarrow 20 DNPJ
input RGB
output RGB

The radiance has to be mapped to RGB.

Dynamic Range huge difference between world and screens, one computer display, surface illumination sun/moon, distance white/black surface
 $800,000:1$
 $100:1$
 $90,000,000:1$ Expected real world dynamic range.

Human Vision $100:1$ Photo Receptors
 $10:1$ Pupil size
 $10,000:1$ Neural adaptation
 $100,000,000:1$ Dynamic human range.

Technology

$1000:1$ Display
 $256:1$ 8-bit image

Small part:
 Path tracing implementation & late wife rendering
 features:
 - Implementation in 250 lines of code.
 - Multi-threaded rendering thanks to the openMP library.
 - C++11 with SIMD.
 - quasi-random sampling by integrating over screen pixels
 - cosine importance sampling
 - soft shadows, antialiasing by integrating over screen pixels
 - with less than 4096 bytes.
 - compiled into a binary
 - refractions, color bleeding, caustics
 - with texture
 Vector class
 struct Vec {
 double x,y,z;
 Vec (double x,y,z) : double(x), double(y), double(z) {}
 Vec (double x,y=0, double z=0) : double(x,y), double(z) {}
 Vec (double x,y=0, double z=0, double w=1) : double(x,y), double(z), double(w) {}
 Vec (double x,y,z,w) : double(x), double(y), double(z), double(w) {}
 Vec operator+ (const Vec& b) const {return Vec(x+b.x,y+b.y,z+b.z,w+b.w);}
 Vec operator- (const Vec& b) const {return Vec(x-b.x,y-b.y,z-b.z,w-b.w);}
 Vec operator* (const Vec& b) const {return Vec(x*b.x,y*b.y,z*b.z,w*b.w);}
 Vec operator/ (double b) const {return Vec(x/b,y/b,z/b,w/b);}
 Vec operator* (double b) const {return Vec(x+b,y+b,z+b,w+b);}
 Vec operator/ (double b) const {return Vec(x/b,y/b,z/b,w/b);}
 Vec normal() const {return Vec((x+b.x)*(y+b.y)+(z+b.z)*(w+b.w))/4.0f;}
 Vec mult (const Vec& b) const {return Vec((x+b.x)*(y+b.y)+(z+b.z)*(w+b.w))/4.0f;}
 Vec operator* (double b) const {return Vec((x+b.x)*(y+b.y)+(z+b.z)*(w+b.w))/4.0f * b;}
 Vec operator/ (double b) const {return Vec((x+b.x)*(y+b.y)+(z+b.z)*(w+b.w))/4.0f / b;}
 Vec dot (const Vec& b) const {return (x*b.x)+(y*b.y)+(z*b.z)+(w*b.w);}
 Vec cross (const Vec& b) const {return Vec((y*z)-(w*x),(z*x)-(w*y),(x*y)-(z*w));}
 Vec operator* (const float s) const {return Vec(s*x,s*y,s*z,s*w);}
 Vec operator/ (const float s) const {return Vec(x/s,y/s,z/s,w/s);}
 Vec operator+= (const Vec& b) {x += b.x; y += b.y; z += b.z; w += b.w; return *this;};
 Vec operator-= (const Vec& b) {x -= b.x; y -= b.y; z -= b.z; w -= b.w; return *this;};
 Vec operator*= (const float s) {x *= s; y *= s; z *= s; w *= s; return *this;};
 Vec operator/= (const float s) {x /= s; y /= s; z /= s; w /= s; return *this;};
 Vec operator< (const Vec& b) const {return (x<b.x) || (y<b.y) || (z<b.z) || (w<b.w);}
 Vec operator> (const Vec& b) const {return (x>b.x) || (y>b.y) || (z>b.z) || (w>b.w);}
 Vec operator<= (const Vec& b) const {return (x<=b.x) || (y<=b.y) || (z<=b.z) || (w<=b.w);}
 Vec operator>= (const Vec& b) const {return (x>=b.x) || (y>=b.y) || (z>=b.z) || (w>=b.w);}
 Vec operator== (const Vec& b) const {return (x==b.x) && (y==b.y) && (z==b.z) && (w==b.w);}
 Vec operator!= (const Vec& b) const {return (x!=b.x) || (y!=b.y) || (z!=b.z) || (w!=b.w);}
 friend Vec operator* (const float s, const Vec& v) {return v*s;};
 friend Vec operator* (const Vec& v, const float s) {return v*s;};
 friend Vec operator/ (const float s, const Vec& v) {return v/s;};
 friend Vec operator/ (const Vec& v, const float s) {return v/s;};
 friend Vec operator< (const Vec& a, const Vec& b) {return a.x<b.x || a.y<b.y || a.z<b.z || a.w<b.w;};
 friend Vec operator> (const Vec& a, const Vec& b) {return a.x>b.x || a.y>b.y || a.z>b.z || a.w>b.w;};
 friend Vec operator<= (const Vec& a, const Vec& b) {return a.x<=b.x || a.y<=b.y || a.z<=b.z || a.w<=b.w;};
 friend Vec operator>= (const Vec& a, const Vec& b) {return a.x>=b.x || a.y>=b.y || a.z>=b.z || a.w>=b.w;};
 friend Vec operator== (const Vec& a, const Vec& b) {return a.x==b.x && a.y==b.y && a.z==b.z && a.w==b.w;};
 friend Vec operator!= (const Vec& a, const Vec& b) {return a.x!=b.x || a.y!=b.y || a.z!=b.z || a.w!=b.w;};
 friend Vec min (const Vec& a, const Vec& b) {return (a.x<b.x) ? a : b;};
 friend Vec max (const Vec& a, const Vec& b) {return (a.x>b.x) ? a : b;};
 friend Vec clamp (const Vec& v, const float min, const float max) {return (v.x<min) ? min : (v.x>max) ? max : v;};
 };

Tone Mapping is the method to combat the difference in ranges.

- Output of our simulation:
real world dynamic range or High dynamic range (HDR)
- Input of conventional display devices:
low dynamic range (LDR)
- Need to apply range compression. Referred to as
 - Tone Mapping
 - Tone reproduction

Two issues to resolve

1. Range Compression: Convert HDR Luminance to LDR luminance
2. Color space conversion: Convert LDR to desired color space.
(RGB, XYZ, CMYK)

(Noise HDR)

Take multiple images at separate exposures
then normalize by the maximum luminance

Clamp over and under parts.

Clamp.

exponential mapping: Assume the luminance values have an exponential distribution, bright values do not over dominate.

loring tone map

Reinhard tone mapping: one of most common tone mappers.

Misused Tone Mapping: combine multiple images for HDR photography.

Tone Mapping is supposed to be a physically valid technique

short exposure

long exposure
division by max

Tone Mapping Taxonomy

• Global

Mapping function is uniform on whole image.

• Local

Mapping function depends on the values of the pixels in the neighborhood of the currently mapped pixel.

Global

Map is uniform on image

+ Fast

- Loss of detail

Local

Mapping function depends on the values of pixels in neighborhood.

- Slow

+ Local contrast enhancement.

Reinhard Tone mapper

◦ Developed by Reinhard et al., Photographic tone reproduction for digital images, Siggraph 2002.

◦ Widely used

◦ Global and local variant,

Can have non-linear mapping

Processing Steps (global version)

◦ Compute log average (luminance space)

→ Reverses large weights first
on size.
average in log space.

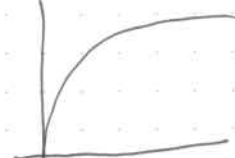
$$L_{avg} = \exp \left(\frac{1}{N} \sum_{x,y} \log (L_{input}(x,y)) \right) = \sqrt[N]{\prod_{x,y} L_{input}(x,y)}$$

◦ Map average value to middle-gray given a

$$L_{scaled}(x,y) = \frac{a}{L_{avg}} L_{input}(x,y)$$

◦ Compress high luminances

$$L_{output}(x,y) = \frac{L_{scaled}(x,y)}{1 + L_{scaled}(x,y)}$$



The most promising choice sample brighter path longer

is the consequence space
highlight is between 1/4 the, 6x, & the only distance
 $p_i = 1 \rightarrow$ never surface, impossible, never steps.
 $p_i = 0 \rightarrow$ always steps, accurate +
What choice for p_i ?

We want get out same expected
choose good instead of add
we can send out one old with good

$$P_i = p \cdot P_i + (1-p) \cdot 0 = E[P_i] \Leftrightarrow$$

$$\frac{P_i}{P} = (p) \text{ or } P_i \text{ from } p$$

$$P_i = \underbrace{p}_{\text{dots}} + \underbrace{(1-p)}_{\text{anywhere}} = E[P_i]$$

not with probability if there are dots am I

$$P_i = p \cdot P_i + q \cdot P_i = E[P_i]$$

What this means in terms of expected values:

If $\sum P_i$ terminate light path, also multiply it with
somebody else

If $\sum P_i < P_i$, continue the light path, but multiply
the solution with somebody else

choose a random variable $\sum P_i$

This is some as importance sampling.

Processing steps for local Reinhardt tone mapping.

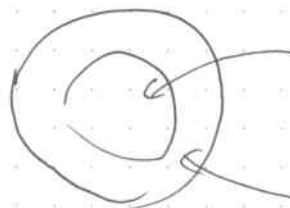
- Compute local average
- Map values to middle gray
- Compress luminances by spatially varying function

$$\text{Output } (x,y) = \frac{L_{\text{scaled}}(x,y)}{1 + V(x,y, S(x,y))}$$

- Local average $V(x,y,S)$ with scale S
(think Gaussian smoothing)
- Local scale $S(x,y)$ where $L_{\text{scaled}}(x,y)$ does not change

The scale is an estimation of the region where the brightness does not change too much.

It draws two circles



The inner surface texture should be uniform in brightness,

The outer should not be uniform in brightness.

The larger the scale the higher over you are able to enhance contrast.

Our approach:

Bilateral filter } reduce ranges only at
gradient polarity } extremes.

gradient polarity is first.

Reinhardt et al., high dynamic range

Lemmeber: The integral is infinite dimensional, therefore the three solutions would require an infinite resolution depth.
 Goal: we probabilities theory and make the estimator converge to the expected value of the integral.
 We can have multiple estimators, and we sort the one with the lowest variance.
 If by chance we continue, we multiply the collector's outcome if with a certain probability p :
 After the i th step, it's randomly determine the path or route with some depth.
 In parallel, we compute the probability of reflection and reflection.
 We can compute many samples and add them together.
 What we can do is that! don't want many samples and computation time is on 80% chance of reflection
 and reflection, and multiply by the relative probability of reflection.
 This conversion leads to the expected value of routes
 Russian roulette path elimination idea of some sort,
 just with an infinite number of outcomes
 and this factor for final example sort to the parallel.

Monte-Carlo integration
Scale by size of integral

$$\int_a^b x dx = \frac{x^2}{2} \Big|_a^b$$

Monte Carlo $\frac{(b-a)(x_1 + x_2 + x_3)}{3}$

What we have done:

$$P(x) = \frac{1}{\pi} \rightarrow \text{uniform distribution on } (0, \pi)$$

$$\int_0^\pi f(x) \cdot P(x) dx = \int_0^\pi f(x) \cdot \frac{1}{\pi} dx$$

so to get
the original
integral we
multiply by.

$$\frac{1}{\pi} \cdot 2 \int_0^\pi \sin^2(x) dx = 1$$

$$\pi \cdot \frac{1}{\pi} \cdot 2 \int_0^\pi \sin^2(x) dx = \pi$$

Let's examine this technique more deeply.
The expected value of a dice roll:

$$\sum \text{Value} \cdot \text{Probability} = 1 \cdot \frac{1}{6} + 2 \cdot \frac{1}{6} + \dots + 6 \cdot \frac{1}{6} = (1+2+3+4+5+6) \cdot \frac{1}{6} = 3.5$$

expected value 3.5

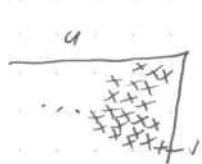
To guess the best value, it will be that to minimize error.

There is a technique that can compact an inexact amount of bytes.
This is a modified Huffman technique that gives a result as if you had all the data.
There is a technique that can compact an inexact amount of bytes.
as some bytes will be lost.
This is a fixed solution that does not give perfect results.

Question: When do we stop traversing a tree?
Answer: We do a cutoff after a certain amount of bytes.

A lot of the time bad cases end up with merges.
that or they end with merges.

Disadvantages: It is a non-simple task of source code.
It is deterministic, not random.
Access times.
Therefore when rendering animations, the noise will look coherent.
there is no randomness introduced in the synchronization of them,
Advantages: A big advantage of low discrepancy sampling is that
this is not trivial.



if it is not completely sorted +! unique hopefully same spot.

We get much better convergence our results.
number of dimensions.
algorithm solves that are generated to be "well-discretized", in an arbitrary instead of sampling with true random numbers, we could use low discrepancy seeds.

The expected value of "Something":

Discrete Case:

$$E[\text{Something}] = \sum_{i=1}^{\infty} \text{Something}_i \cdot P_i$$

Continuous Case:

$$E[\text{Something}] = \int_a^b \text{Something}(x) \cdot p(x) dx$$

We are sampling $f(x)$ with an N amount of random samples, denoted as x_i .

$$\begin{aligned} E_n[f(x)] &= \int_a^b f(x) p(x) dx \approx \frac{b-a}{N} \sum_{i=1}^N f(x_i) \\ &= \lim_{N \rightarrow \infty} \frac{b-a}{N} \sum_{i=1}^N f(x_i) \end{aligned}$$

Lets use different sampling distributions.

$$\int_a^b f(x) dx \cdot \frac{p(x)}{p(x)} = \int_a^b \frac{f(x)}{p(x)} \cdot p(x) dx = E\left[\frac{f(x)}{p(x)}\right] = \frac{1}{N} \sum_{i=1}^N \frac{f(x_i)}{p(x_i)}$$

Lets solve an actual problem

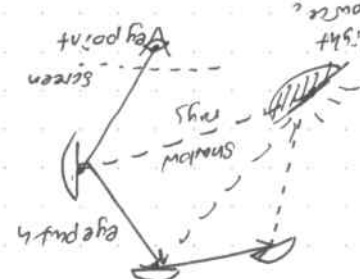
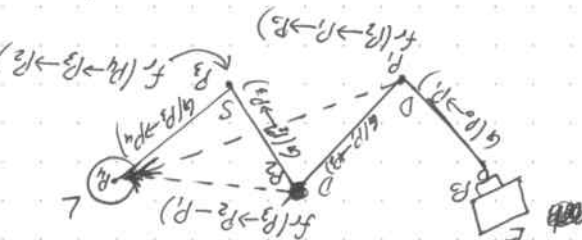
$$\begin{aligned} \int_0^{\pi} \frac{f(x)}{p(x)} \cdot p(x) dx &= \int_0^{\pi} \frac{2 \sin^2(x)}{\frac{1}{\pi}} \frac{1}{\pi} dx & f(x) = 2 \sin^2 x \\ &= \int_0^{\pi} 2 \sin^2(x) dx \approx \frac{1}{N} \sum_{i=1}^N \frac{f(x_i)}{p(x_i)} & p(x) = \frac{1}{\pi} \end{aligned}$$

If with Monte Carlo rendering algorithm, the variance of the estimation shows up as high frequency noise.

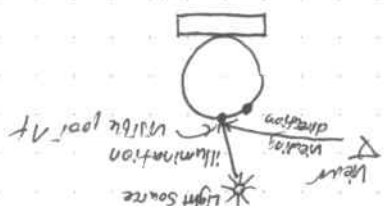
As we get more samples, we get a more coherent image as the estimation approaches the integral.

The metric is samples per pixel (SPP)

This is Path Tracing
Does Nonsense, as if random light
illuminating our scene and hitting the scene separately
since every bounce adds some distance, this is
as next about estimation how far the light can go in the way
when arriving at light source, we don't add the emission
rate of path segments, and strangely becomes path length in average
an explicit path to a light source is constructed. This allows
next event estimation in path tracing at each surface interaction,



Next Event Estimation Path

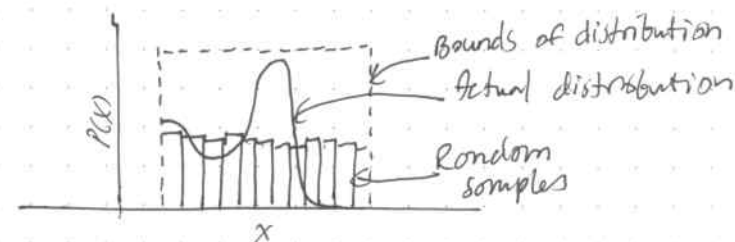


Every time we hit a non-light source, we calculate the direct effect of the light source on this point.
How do we overcome this?

Importance Sampling
it is usually not a great idea to sample any function with a uniform distribution.

So far we have used random sampling variables with uniform distributions to sample function.

The goal would be to minimize the error of the estimation using a given amount of samples.



The sampling probability has to represent the sample distribution for low error.

This way we can have less overall samples.

Importance Sampling:

$$E\left[\frac{f(x)}{p(x)}\right] = \int_a^b \frac{f(x)}{p(x)} p(x) dx \approx \frac{1}{N} \sum_{i=1}^N \frac{f(x_i)}{p(x_i)}$$

Optimal importance sampling (in terms of least variance)
is achieved when every element of the function
is sampled with a probability proportional to its value.

$$p(x_i) \propto f(x_i)$$

where there is more light, we put more samples.

The point does not have ω for $\omega \in \Omega$, it is impossible to trace a path if there is no point ω in the trajectory.

If we have a point light source, we should expect the light to travel in straight lines.

If we have small light sources, we should expect similar consequences.

- If we compute a light path from a point source, we get zero results.
- If we compute a light path from a light source, we get non-zero results.

• Only light path that hit a light source carry a contribution.

Therefore, if we calculate a long light path where no measure was done, we get zero results.

We always add the emittance, $L_e(x, \vec{\omega})$, of the end result to every

light source it hits, a contribution is added to the estimator. Each time a secondary scattering hits another surface, the sum corresponds to the sum of random walk through the scene corresponding to the emission for the flux.

The tracing of a primary ray from eye point to virtual eye point through a pixel.



The path between two surfaces can be estimated.

return emittance + (BDF * reflected);

color reflected = Trace Path (new Ray, depth + 1);
 $color_{reflect} = m.reflection * color_{reflectance} * (1 - reflectance)$

Monte Carlo integration in rendering equation

$$L_o(x, \vec{\omega}) = L_e(x, \vec{\omega}) + \int_{\Omega} L_i(x, \vec{\omega}') f_r(\vec{\omega}, x, \vec{\omega}') \cos \theta d\vec{\omega}'$$

emitted reflected incoming light

Intuition - The outgoing light is the emitted plus the reflected incoming light.

Let's evaluate integral with Monte Carlo integration!

$$\int_a^b f(x) dx \approx \frac{1}{N} \sum_{i=1}^N \frac{f(x_i)}{p(x_i)}$$

↓

$$\int_{\Omega} L_i(x, \vec{\omega}') f_r(\vec{\omega}, x, \vec{\omega}') \cos \theta d\vec{\omega}' \approx \frac{1}{N} \sum_{i=1}^N \frac{L_i(x, \vec{\omega}_i) f_r(\vec{\omega}, x, \vec{\omega}_i) \cos \theta}{P(\vec{\omega}_i)}$$

There is now a sampling probability for outgoing directions.

So we have to choose the outgoing direction.
 Note: the denominator in the sum is this means we sample one outgoing direction on the hemisphere.

Monte Carlo estimator

$$\int_{\Omega} L_i(x, \vec{\omega}') f_r(\vec{\omega}, x, \vec{\omega}') \cos \theta d\vec{\omega}' \approx \frac{1}{N} \sum_{i=1}^N \frac{L_i(x, \vec{\omega}_i) f_r(\vec{\omega}, x, \vec{\omega}_i) \cos \theta}{P(\vec{\omega}_i)}$$

$$Solve \ for \ diffuse \ case \\ f_r(\vec{\omega}, x, \vec{\omega}_i) = \frac{1}{\pi}$$

The perfect diffuse material means
every angle has the same probability.

The absorption is wavelength dependent.

$$\frac{1}{N} \sum_{i=1}^N \frac{L_i(x, \vec{\omega}_i) P / \pi \cos \theta}{P(\vec{\omega}_i)}$$

Know every Ray
but L_i

$$\text{Monte Carlo estimator}$$

$$\int_{\Omega} L_i(x, \vec{\omega}) f_r(\vec{\omega}, x, \vec{\omega}') \cos\theta d\vec{\omega}' \approx \frac{1}{N} \sum_{i=1}^N \frac{L_i(x, \vec{\omega}_i) f_r(\vec{\omega}_i, x, \vec{\omega}_i') \cos\theta}{P(\vec{\omega}_i')}$$

Diffuse case : $f_r(\vec{\omega}, x, \vec{\omega}_i') = \frac{\rho}{\pi}$ $\rho \rightarrow \text{albedo}$

$$\Rightarrow \frac{1}{N} \sum_{i=1}^N \frac{L_i(x, \vec{\omega}_i') \frac{\rho}{\pi} \cos\theta}{P(\vec{\omega}_i')}$$

We know everything but L_i .
 We do this by calculation by collecting
 the incoming radiance by sending
 out samples.



What would make a good sampling probability density function, $P(\vec{\omega}_i')$?

One that admits the performance sampling rule — a function that is proportional to the integrand

We cannot know this distribution once we do the sampling.

so let's try this: $P(\vec{\omega}_i') = \frac{\cos\theta}{\pi}$

$$\Rightarrow \frac{1}{N} \sum_{i=1}^N \frac{L_i(x, \vec{\omega}_i') \frac{\rho}{\pi} \cos\theta}{\frac{\cos\theta}{\pi}} = \frac{1}{N} \sum_{i=1}^N L_i(x, \vec{\omega}_i') \rho$$

Color TracePath(Ray r, depth){
 if(depth == Max Depth){

 return Black;} // bounced enough times

 r.FindNearestObject();

 if(r.hitSomething == false) {return Black;} // nothing hit

 Material m = r.hitMaterial;

 Color emittance = m.emittance;

// Pick a random direction and keep going.

Ray = NewRay; newRay.origin = r.pointWhereObjWasHit;

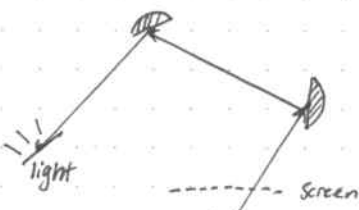
newRay.direction = RandomUnitVectorInHemisphereOf(r.normalWhereObjWasHit);

// Compute BRDF

float cos_theta = DotProduct(newRay.direction, r.normalWhereObjWasHit);

Color $BRDF = m_{reflectance} * \cos_{\theta}$
 Color reflected = Trace Path (new Ray, depth + 1);
 // Apply rendering equation here.

return emittance + (BRDF * reflected);



Schematic overview of the Path tracing algorithm.
 The radiant flux through a pixel has to be estimated.

The tracing of a primary ray from the eye point to the virtual eye point through a pixel corresponds to sampling the expression for the flux. The subsequent random walk through the scene corresponds to recursively estimating the radiance values. Each time a light source is hit, a contribution is added to the estimate.

We always add the emittance, $L_e(\vec{x}, \vec{w})$ to the end result at every recursion step.

Therefore, if we calculate a long light path where no material has emittance, we get zero radiance.

Corollary: • Only light path that hit a light source carry a contribution.

- * If we compute a light path that avoids all light sources, then the path will return zero radiance, which means, we are wasting our time and resources.

If we have small light sources, we should expect slower convergence.

If we have a point light source, we should expect the ray tracer to return nothing.

A point does not have area \Rightarrow hitting it is impossible. The probability of hitting a point, which has infinity little space is ... zero.

$$\text{Monte Carlo estimator}$$

$$f_s(\vec{x}, \vec{w}) = \frac{\sum_{i=1}^N L_i(\vec{x}, \vec{w})}{N}$$

The absorption is wavelength dependent.

The surface area of the material is πr^2 .

The surface density is ρ .

The surface reflectance is m .

The surface color is \vec{c} .

The surface normal is \vec{n} .

The surface position is \vec{p} .

The surface area is A .

The surface density is ρ .

The surface reflectance is m .

The surface color is \vec{c} .

The surface normal is \vec{n} .

The surface position is \vec{p} .

The surface area is A .

$$f_s(\vec{x}, \vec{w}) = \frac{\sum_{i=1}^N L_i(\vec{x}, \vec{w})}{N}$$

The is now a sampling problem for direct and indirect contributions.

of the primary sampling probability

$$f_s(\vec{x}, \vec{w}) = \int_{\Omega} f(\vec{x}, \vec{w}, \vec{y}, \vec{z}) d\Omega$$

Let's evaluate the integral with monte carlo integration.

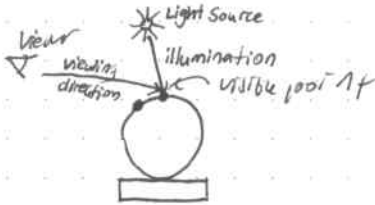
Integration - The outgoing light is the emitted plus the reflected incoming light.

$$L(\vec{x}, \vec{w}) = \int_{\Omega} f(\vec{x}, \vec{w}, \vec{y}, \vec{z}) + (m(\vec{x}))^2 = (m(\vec{x}))^2$$

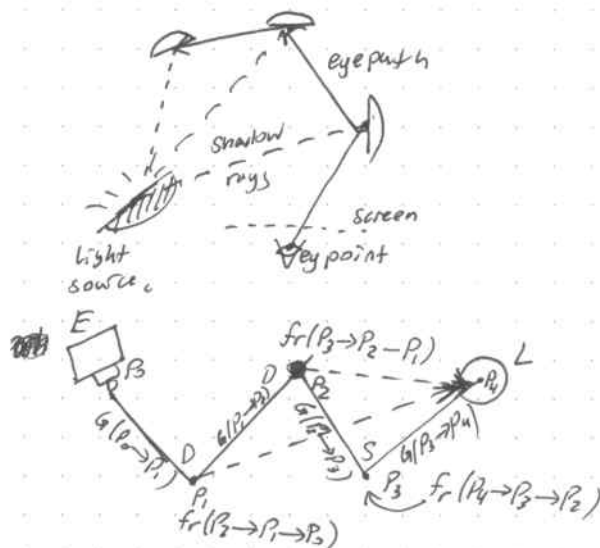
Monte Carlo integration in kernelization

How do we overcome this?

Every time we hit a non-light source, we calculate the direct effect of the light source on this point.



Next Event Estimation path tracing.



Next event estimation in path tracing at each surface interaction, an explicit path to a light source is constructed. This allows reuse of path segments, and strongly decreases path length on average.

When arriving at light source, we don't add the emission as next event estimation has taken care of it on the way. Since every bounces adds some radiance, this is a nice way to decouple the direct and indirect illumination and handle the cases separately.

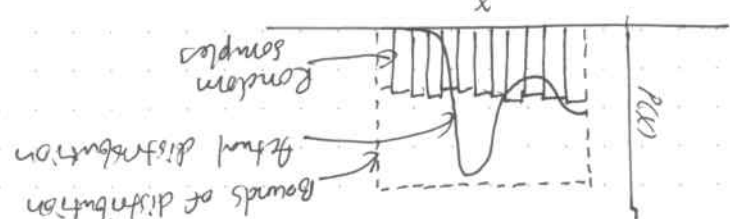
lower variance, so it renders faster

This is Path Tracing.

It's better not to have many sources of light, as it induces more artifacts

So far we have used random sampling with uniform distribution, which is not a good idea for sources of light, as it induces more artifacts

The goal would be to render the ear off the ear of the person with a higher quality of sampling instead of samples



The metric is samples per pixel (SSP)

more the number of samples per pixel is lower so the estimation error is less as we get more samples

so the variance of the samples is less if we have more samples. If we have more samples, the variance will be less.

$$\frac{1}{N} \int_{\Omega} f(x) p(x) dx = \frac{1}{N} \sum_{i=1}^N \frac{1}{T} \int_{\Omega} x_i p(x) dx = \frac{1}{T} \int_{\Omega} 2 \sin^2(x) dx = \frac{1}{T} \int_{\Omega} x p(x) d(p(x)) =$$

Let's see what's happening here

$$\frac{1}{N} \sum_{i=1}^N \frac{1}{T} \int_{\Omega} x_i p(x) dx = \left[\frac{p(x)}{f(x)} \right] = E[x] = \int_{\Omega} x p(x) d(p(x)) = \frac{1}{T} \int_{\Omega} x p(x) d(p(x))$$

Let's see what's happening here

$$(x_i) f \sum_{i=1}^N \frac{1}{N} = \frac{1}{N} \sum_{i=1}^N x_i =$$

$$E[x] = \int_{\Omega} x p(x) d(p(x))$$

We are sampling $f(x)$ with N amount of random samples, limited to Ω

$$E[\text{samples}] = \int_{\Omega} f(x) p(x) d(p(x))$$

Uniformly distributed

$$E[\text{samples}] = \sum_{i=1}^{\infty}$$

Discrete case;

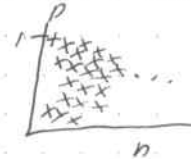
We applied this to some thing?

Low Discrepancy Series.

Instead of sampling with true random numbers, we could use artificial series that are guaranteed to be "well-distributed" in an arbitrary number of dimensions.

We get much better convergence and results.

it is not completely random it tries to fill the space reasonably.



Halton Sequence

Sobol

Vander Corput

This is not trivial.

Advantage: A big advantage of low discrepancy sampling is that there is no randomness included in the construction algorithm, therefore when rendering animations, the noise will look coherent across frames.

It is deterministic, not random.

Disadvantage: It is a non-simple task to generate these series.

A lot of the time bad series end up with craters.

that or they end with blurry images.

Question: When do we stop tracing a ray?

Answer: We do a cutoff after a certain amount of bounces.

This is a biased solution that does not give perfect results as some energy will be lost.

There is a technique that can compute an infinite amount of stuff.

death
There is a mathematical technique that gives a result as if you calculated on infinite amount of bounces.

Remember: The integral is infinite dimensional, therefore the true solution would require an infinite recursion depth.

Goal: use probability theory and make the estimator converge to the expected value of the integral.

We can have multiple estimators, and we select the one with the lowest variance.

After the i th step, let's randomly terminate the path or continue it with a carefully chosen probability p :

If by chance we continue, we multiply the collected radiance with something.

In Frenel's law, we compute the probability of reflection and refraction.

- We can compute many samples and add them together or
- What we can also do is that I don't want many samples and I compute here is an 80% chance of reflection and refraction, and multiply by the relative probability.

This converges ~~fast~~ to the expected value of Radiance.

Russian Roulette path termination does the same thing, but with an infinite number of bounces.

We will multiply the collected radiance with a factor and this factor for Frenel's example could be the probability.

Result of first 20 samples, it will be like this, to sum up to 1.

5's are expected values

$S' =$

$$\frac{1}{T} (7.9 + 6.8 + 2.7 + 1) = \frac{1}{T} \cdot 9 + \dots + \frac{1}{T} \cdot 2 + \frac{1}{T} \cdot 1 = 4.1 \text{ (good)} \cdot 20 / 100 \quad \boxed{3}$$

The expected value of die rolls:
lets examine this iterative more deeply

$$R = \int_{\Omega} \frac{1}{I} \cdot S^2(x) dx = R$$

$$I = \exp \left(\int_{\Omega} \frac{1}{I} \cdot S^2(x) dx \right)$$

A lesson in
approximation
rules of 03

$$\exp \left(\int_{\Omega} \frac{1}{I} \cdot f(x) dx \right) = \exp \left(\int_{\Omega} I(x) \cdot f(x) dx \right)$$

$$(1.0) \text{ no weighting is required } \frac{1}{I} = f(x) \quad \boxed{P}$$

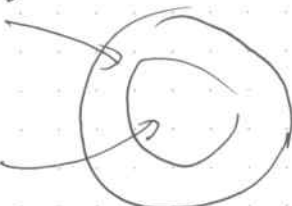
What we have done:

$$\overbrace{(6x^2 + 2x + 1)}^S \cdot \overbrace{(6 - a(x, x_0))}^{I(x)} \cdot \overbrace{c(x, x_0)}^{f(x)}$$

$$\int_{\Omega} \frac{1}{I} \cdot \frac{2}{x} = \exp \int_{\Omega} \frac{2}{x}$$

start by doing
Monte-Carlo integration

• Light rays randomly emitted from a point
 → can be traced forward
 to two other rays {
 ↳ forward tracing
 at 13 nm $\times 10^9$
 yields 1000
 unphysically long paths
 → the longer the sum the higher the probability
 • converge in expectation
 so far always the same
 sampling in uniform way
 the rays should be
 distributed uniformly



If it does not sample a circle
 the sampling is not uniform.
 The sum is in expectation of the work where

$$\begin{aligned}
 & \text{choose } p_i \text{ such that } \\
 & \text{lower values have lower } p_i \\
 & \text{higher values have higher } p_i \\
 & \text{so } p_i = \frac{1}{\text{length}(x_i)} + 1 \\
 & \text{length}(x_i) = L(x_i)
 \end{aligned}$$

working further suggests by trial and error some
 choice of middle seems best
 length of path to be sampled

choose a random variable $\xi \in (0,1)$

if $\xi < p_i$, continue the light path, but multiply
 the collected with something?

if $\xi \geq p_i$ terminate light path, aka multiply it with
 something else (\emptyset)

What this means in terms of expected values:

$$E[L_i] = p_i \cdot ? + (1-p_i) \cdot \emptyset = L_i$$

If we stop we multiply this term with zero

$$\begin{aligned}
 E[L_i] &= \underbrace{p_i \cdot ?}_{\text{continue}} + \underbrace{(1-p_i) \cdot \emptyset}_{\text{stop}} = L_i
 \end{aligned}$$

$$\text{we want } L_i \text{ so } (?) = \frac{L_i}{p_i}$$

$$\Rightarrow E[L_i] = \underbrace{p_i \cdot \frac{L_i}{p_i}}_{\text{continue}} + \underbrace{(1-p_i) \cdot 0}_{\text{stop}} = L_i$$

We can send out one ray and add it with 800 instead of adding 800 rays.
 We won't get same result, but some expected value.

What choice for p_i ?

$p_i = 0 \rightarrow$ always stop, incorrect

$p_i = 1 \rightarrow$ never continue, impossible, never stop.

Anything in between is fine, but the only difference is the convergence speed.

The most promising choice samples brighter path longer than darker ones.

This is some importance sampling.

$$\int f(x) dx = \frac{f(x) \text{ Input} + 1}{f(x) \text{ Input}} = f(x) \text{ Output}$$

o computes high dynamic range

$$\log \exp(f(x,y)) = \frac{\log(f(x,y))}{\alpha}$$

What we're after is to make it middle-grey given a

$$(f(x) \text{ Input}) \prod_{i=1}^N = \left(\log(f(x,y)) \right) \sum_{i=1}^N \frac{1}{N} dx_i = \log \exp$$

note: this is not the same as the global mean
 o compute log average (luminance space)
 processing steps (global region)

from here we'll move to local mean

o global and local mean
 - well it's not really that good.
 o developed by Reinhard et al., photogeaphy from perspective
 Reinhard Tone mapping

+ local contrast enhanced.
 - less of detail
 + focus
 hope is uniform on image
 Global

o local
 - Merging function is uniform on whole image.
 - merging pixels in the neighborhood of the current pixel

Assignment 3: - Integrate a function of choice with monte carlo

- Integration with this code
- Prove calculations are correct by analytically solving.
- Attach latex code and the image for your calculations.

Modify code for higher dimension integrals

o Evaluate speed of convergence with uniform sampling
 vs. different importance sampling.
 you can also try low discrepancy sampling.

Plot error or different approaches
 against sample numbers.

http://cg.tuwien.ac.at/~zsolnai/rendering/rendering-assignments/monte_carlo_integration_and_small_point_3.pdf

Path Tracing Implementation & Code Walkthrough

Smallprint

- Implementation in 250 lines of code.
- Multi-threaded rendering thanks to the `openMP` library.
- C++11 wizardry.
- Quasi-Monte Carlo sampling using low-discrepancy Halton series
- cosine importance sampling
- soft shadows, antialiasing by integrating over screen pixels (Path Tracing)
- refractions, color bleeding, caustics
- Compiled into a binary with less than 4096 bytes.

Vector class

struct Vec {

double x,y,z;

Vec(double x=0, double y=0, double z=0) {x=x,y=y,z=z;}

Vec

struct Vec {

double x,y,z;

Vec(double x=0, double y=0, double z=0) {x=x,y=y,z=z;}

Vec operator + (const Vec &b) const {return Vec(x+b.x, y+b.y, z+b.z);}

Vec operator - (const Vec &b) const {return Vec(x-b.x, y-b.y, z-b.z);}

Vec operator * (double b) const {return Vec(x*b, y*b, z*b);}

Vec operator / (double b) const {return Vec(x/b, y/b, z/b);}

Vec mult (const Vec &b) const {return Vec(x*b.x, y*b.y, z*b.z);}

Vec& norm() {return *this = *this * (1/sqrt(x*x + y*y + z*z));}

double length() {return sqrt(x*x + y*y + z*z);}

double dot (const Vec &b) const {return x*b.x + y*b.y + z*b.z;}

Vec operator % (Vec &b) {return Vec(y*b.z - z*b.y, z*b.x - x*b.z, x*b.y - y*b.z);}

Classical 3D vector.

struct Ray {

Vec o,d;

Ray (Vec o=0, Vec d=0) {o=o,d=d,norm();}

love rendering is the motivation of writing the diffuser
in raytracing.
output of our simulation:
real world dynamic range -> high dynamic range (HDR)
input of convolutional display source:
low dynamic range -> output of our simulation:
two issues of rendering:
1. range conversion: convert HDR luminance of LDR luminance
2. color space conversion: convert srgb to linear
then we need to do the pixelwise luminance conversion
take multiple samples at separate exposure levels
here we have
clipping over all width pixels
exponentially mapping; clamp the luminance
distribution function, which has no exponent
for colors not mapped to zero; no of most common for
the colors not mapped to zero;
and then
rebinning; calculate the luminance
of each bin for each color channel
which has no exponent
for colors not mapped to zero; no of most common for
the colors not mapped to zero;
and then
rebinning; calculate the luminance
of each bin for each color channel
(NDC HRC)

256x1 8-bit image
 Display 1000x1
background
 Dynamic human body
 Need adaptation
 Ray tracing
 Photo realistic
 Human Vision
 Extended real world dynamics Ray
 Diffuse white light surface
 Surface luminance
 out complex display
 Dynamic scene
 Ray different between world and scene
 The random ray to be sampled by RGB.
 Output Raycast
 Input PBR
 PBR 0.2 ← 2 ← Ray casting → 3D scene ← Tone Mapping

11 10y 10y 10m 10m 1m 1m 10y 10y 11
 H181H S13VH
 our pixel row
 This leads to a quantized space after
 the maximum over all
 costs is expensive
 Correlation with minima

```

class Obj {
public:
  Vec cl;
  double emission;
  int type;
  void setMat (Vec cl_=0, double emission_=0, int type_=0)
  {
    cl=cl_; emission=emission_; type=type_;
  }
  virtual double intersect (const Ray& ray) const = 0;
  virtual Vec normal (const Vec& ray) const = 0;
};

class Sphere : public Obj {
public:
  Vec c;
  double r;
  Sphere (double r=0, Vec c=0, {c=c; r=r;})
  double intersect (const Ray& ray) const {
    double b=((ray.o-c)*2), dot(ray.d);
    double c=(ray.o-c).dot((ray.o-c))-(r*r);
    double disc=b*b-4*c;
    if(disc<0) return 0;
    else disc=sqrt(disc);
    double sol1=-b+disc;
    double sol2=b-disc;
    return (sol2>eps)? sol2/2 : ((sol1>eps)? sol1/2 : 0);
  }
  Vec normal (const Vec& p) const {
    return Vec ((p.x-c.x)/r,
               (p.y-c.y)/r,
               (p.z-c.z)/r);
  }
  Vec camcr (const double x, const double y) {
    double w=width;
    double h=height;
    float fovX=PI/4;
    float fovY=(h/w)*fovX;
    return Vec (((x-w)/w)*tan(fovX),
               ((2*y-h)/h)*tan(fovY),
               -1.0);
  }
}
  
```

in left of min to left of left

depth buffer together

A foot ← surface area of A foot

An ... Surface area of walls in

I ← inner nodes, L ... leaf nodes

$$SAH = \text{Chance} \sum \frac{A_m}{A_{foot}} + (\text{leaf}) \sum \frac{L}{A_{foot}}$$

Surface Area Hash (SAH)

~~object grouping can be done in many ways -~~
object grouping is usually done by bounding volume hierarchies

- spatial partitioning
+ easier to update
+ faster traversal on the GPU
o Bounding Volume Hierarchy (BVH)

+ faster traversal on CPU
- larger memory overhead

By creating tree structure we can quickly choose
the closest object which has a direct hit



o Bounding Volume Hierarchy (BVH)
in overlapping space and store all objects
divide space

Uniform sampling of hemisphere.

Vec hemisphere (double u1, double u2) {

const double r = sqrt(1.0 - u1*u1);

const double phi = 2 * PI * u2;

return Vec(cos(phi)*r, sin(phi)*r, u1);

}

The Trace function

if (depth >= 20) return;

double t;

int id = -1;

double mint = INF;

const unsigned int size = scene.size();

for (unsigned int x = 0; x < size; x++) {

t = scene[x] → intersect(ray);

if (t > eps && t < mint) { mint = t; id = x; }

}

if (id == -1) return;

Vec hp = ray.o + ray.d * mint;

Vec N = scene[id] → normal(hp);

ray.o = hp;

clr = clr + Vec (scene[id] → emission, scene[id] → emission,
scene[id] → emission) * 2;

,

Russian Roulette path termination

double rrFactor = 1;

if (depth >= 5)

const double rrStopProbability = std::min(1.0, 0.0625 * depth);

if (rnd2 < rrStopProbability)

{ return; }

rrFactor = 1.0 / ((1.0 - rrStopProbability));

Linear in. $O(n \log n)$

more of the parts of the scene
are visible if the objects have a smaller
bounding box.

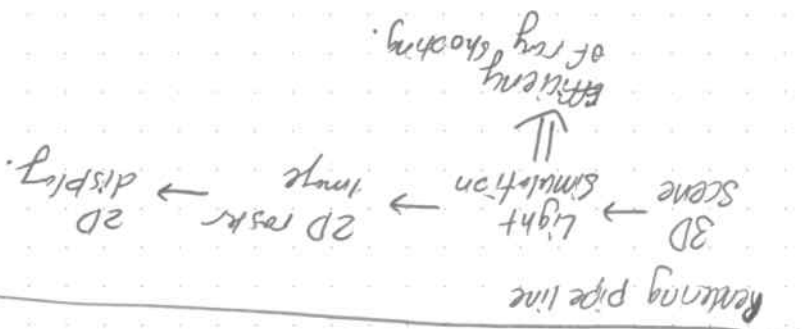
- Better approach:
 - (sort in $O(n \log n)$ for n objects)
 - the closest ray with all objects of determine
 - intersection
 - the intersection of computing the ray with the scene
 - is equivalent to summing the lengths of rays that pass through each object.

This is expensive for large scenes.

Computing the closest intersection with the scene
is equivalent to summing the lengths of rays that pass through each object.

Problem: many-to-many intersections

spatial acceleration makes ray tracing fast.



samples in a distribution are distributed

```

// Trace function
if (scene[id] → type == 1) {
    hal.next();
    hal2.next();
    ray.d = (N + hemisphere(hal.get(), hal2.get()));
    double cost = ray.d.dot(N);
    Vec tmp = Vec();
    trace(ray, scene, depth+1, tmp, Params, hal, hal2);
    clr.x += cost * (tmp.x * scene[id] → cl.x) * 0.1;
    clr.y += cost * (tmp.y * scene[id] → cl.y) * 0.1;
    clr.z += cost * (tmp.z * scene[id] → cl.z) * 0.1;
}
  
```

If the object hit is a type of one, this is a diffuse BRDF.

We compute the law discrepancy Halton sample. Then construct a random sample, on outgoing direction on the hemisphere with uniform hemisphere sampling. This random sample is added to the normal of the intersected point.

The dot product is used for light attenuation.

We then trace the out going ray, and add its contribution.

Specular BRDF.

```

if (scene[id] → type == 2) {
    double cost = ray.d.dot(N);
    ray.d = (ray.d - N * (cost * 2)).norm();
    Vec tmp = Vec(0, 0, 0);
    trace(ray, scene, depth+1, tmp, Params, hal, hal2);
    clr = cl + tmp;
}
  
```

We have discussed handling the outgoing direction specifically or it is descended by a delta distribution. It will be set automatically to perform the perfect reflection directions. We also have to compute attenuation of light, and add the contribution of the outgoing ray.

costs us and shadows are volumetric
 ray can also do this
 for each ray media
 with shading with super sampling is expensive.
 we often only do this and other effects first,
 but if we integrate all the surfaces of the pixel
 a pixel, we could send them all through the same path
 If we: with global illumination, we shoot lots of rays through
 with time perspective
 we have to consider bounces in the color space
 with 4-5 iterations
 we will be able to compute million objects
 due to logarithmic time.
 we can use kd trees and n-body optimization

All's trade off stochastic convergence

since for the scene is less than less than less
 the more iterations and more samples

sample off function of multiple rays and the
 $\int_a^b f(x) dx$

$$(f(0), f(15), f(30), f(45))$$

Instead of hits, we get information from the function.

Sample mean monte carlo integration

refractive BSDF

We invert the index of refraction upon medium change, and compute refraction direction with vector form of snell's law:

```

if(Scene[id]→type == 3){
  double n = params["refr-index"];
  if(N.dot(ray.d) > 0)
    {N = N*-1;
     n = 1/n;
    }
  n = 1/n;
  double cosin = (N.dot(ray.d))*-1;
  double cost2 = 1.0 - n*n*(1.0 - cosin*cosin);
  if(cost2 > 0)
    {
      ray.d = (ray.d*n) + (N*(n*cosin - sqrt(cost2)));
      ray.d = ray.d.normalize();
      Vec tmp = Vec(0,0,0);
      trace(ray, scene, depth+1, tmp, params, h1, h2);
      clr = clr + tmp;
    }
  else return;
}
  
```

Vector version of snell's law

$$\cos\theta_1 = n \cdot (-1)$$

$$\cos\theta_2 = \sqrt{1 - \left(\frac{n_1}{n_2}\right)^2} / \sqrt{1 - (\cos\theta_1)^2}$$

$$Vreflct = \left(\frac{n_1}{n_2}\right) I + \left(\frac{n_1}{n_2} \cos\theta_1 - \cos\theta_2\right) n$$

- $\int f(x) dx \approx A / \lambda \int_0^A f(x) dx$
 - for every point, determine if it's a spec or a refl
 - Throw random points on paper
 - Close it in a box of size A
 - Draw a function on paper
HMC3
 - sample mean
 - μ/σ
 Samples are either taken into consideration or
 The goal is to compute $\int_0^A f(x) dx$
 If it is one of the most parallel distributed
 second world war, dummy munition project.
 Monte Carlo integration
 Simple method of approximate integrals.

The solution is to handle this EOF explicitly: we
 get all reflection directions (and only that).
 get all input directions (and only that).
 all reflection directions (and only that).
 sample

$f(\vec{x}, \vec{w}) = \int_0^{\pi} \int_0^{\pi} \int_0^{\pi} \int_0^{\pi}$ spherical
 - spherical BEM

$L(\vec{x}, \vec{w}) = L_c(\vec{x}, \vec{w}) + \int_{\Omega} L(\vec{x}, \vec{w}) \cdot \vec{n}(\vec{y}, \vec{w}) \cos d \vec{s}$
 What is the dimensionality of global illumination?

```

if (scene[Cd] > type == 3) {
    double n = params["refr_index"];
    double R0 = (1.0 - n) / (1.0 + n);
    R0 = R0 * R0;
    if (N.dot(ray.d) > 0) {
        N = N * -1;
        n = 1 / n;
    } n = 1 / n;
    double cosin = (N.dot(ray.d)) * -1;
    double Rprob = R0 + (1.0 - R0) * Pow((1.0 - cosin), 5.0);
    double cost2 = 1.0 - n * n * ((1.0 - cosin) * cosin);
    if (cost2 > 0 && RND2 > Rprob) { // refraction
        ray.d = (ray.d * n) + (N * (n * cosin - sqrt(cost2))).norm();
    } else { // reflection
        ray.d = (ray.d + N * cosin * 2).normalize();
    }
    Vec tmp = Vec(0, 0, 0);
    trace(ray, scene, depth + 1, tmp, params, hal1, hal2);
    clr = clr + tmp * 1.15;
}
    
```

$$R_o = \left(\frac{n_1 - n_2}{n_1 + n_2} \right)^2$$

$$L(\theta) = R_o + (1 - R_o)(1 - \cos \theta)^5$$

```

int main() {
    srand(time(NULL));
    PI params;
    vector<Obj*> scene;
    auto add=[&scene](Obj* s, Vec cl, double emission, int type) {
        s->setMat(cl, emission, type);
        scene.push_back(s);
    };
}

```

// Radias, position, color, emission, type (1=dif, 2=spec, 3=refr)
add(new Sphere(1.05, Vec(1.45, -2.75, -4.4)), Vec(4.84), 2, 2);
add(new Sphere(0.45, Vec(2.05, 0.8, -3.7)), Vec(10, 10, 1), 2, 3);
add(new Sphere(0.6, Vec(1.95, -1.75, -3.1)), Vec(4.4, 12), 0, 1);
//

```

add(new Plane(2.5, Vec(-1, 0, 0)), Vec(6, 6, 6), 0, 1); // bottom
add(new Plane(5.5, Vec(0, 0, 1)), Vec(6, 6, 6), 0, 1); // back
add(new Plane(2.75, Vec(0, 1, 0)), Vec(12, 2, 2), 0, 1); // left
add(new Plane(2.75, Vec(0, -1, 0)), Vec(12, 12, 2), 0, 1); // right
add(new Plane(3.0, Vec(1, 0, 0)), Vec(6, 6, 6), 0, 1); // ceiling
add(new Plane(0.5, Vec(0, 0, 1)), Vec(6, 6, 6), 0, 1); // front
const Vec LD = (Vec(-1, 0, 0, -3));
add(new Sphere(eps, LD), Vec(0, 0, 0) / 120, 1); // light
params["refr_index"] = 1.9;
params["SPP"] = 8.0; // samples per pixel

```

```

#pragma omp parallel for schedule(dynamic) firstprivate(hal, hal2)
for(int j=0; j<width; j++) {

```

```

    fprintf(stderr, "VR Rendering: %d of spp %d.%d\n",
            SPP, (double)j / width * 100);

```

```

    for(int i=0; i<height; i++) {
        for(int s=0; s<SPP; s++) {

```

```

            Vec c;

```

```

            Ray ray;

```

```

            ray.o = (Vec(0, 0, 0));

```

```

            Vec com = com[i][j];

```

```

            com.x = com.x + RND / 700;

```

```

            com.y = com.y + RND / 700;

```

```

            ray.d = (com - ray.o).norm();

```

```

            trace(ray, scene, 9, c, params, hal, hal2);

```

```

            Ray r[10];
            r[0].ix += c.x * (1 / SPP);

```

```

            r[0].iy += c.y * (1 / SPP);

```

```

            r[0].t += c.z * (1 / SPP);

```

$DE(0)$

$$\frac{11}{f} = (1.2 \times 1.2) f$$

but does not take into account all the light coming in if it is reflected off the surface.

$$\frac{11}{f} = (1.2 \times 1.2) f$$

If we add the surface reflection, we can calculate the overall BRDF.
 If we add the surface reflection, we can calculate the overall BRDF.
 BRDF (The total reflection)

reflecting from
no cycles occurs



reflecting from
intercepted bounces

$$L_o(x, f) = L_e(x, f) + \int L_i(x, f) f(x, l) \cos(\theta) d\Omega$$

surface of object is illuminated!

$$I = k_s I_o + \int k_d L_i(x, f) f(x, l) \cos(\theta) d\Omega$$

used for rendering
the scene



reflective

In general, we have to consider all incoming light from off the illumination
BRDF locally, which is useful in real-life since we would have to

Output

```
FILE *f = fopen("ray.ppm", "w");
fprintf(f, "%d\n%d %d\n%d %d\n", width, height, 255);
for (int i=0; i<width; i++) {
    for (int j=0; j<height; j++) {
        fprintf(f, "%d %d %d\n" min((int)pix[i][j].x, 255),
                min((int)pix[i][j].y, 255), min((int)pix[i][j].z, 255));
    }
}
f.close();
clock_t end = clock();
double t = (double)(end - start) / Clocks_per_sec;
printf("|\nRender time: %fs.\n", t);
return 0;
```

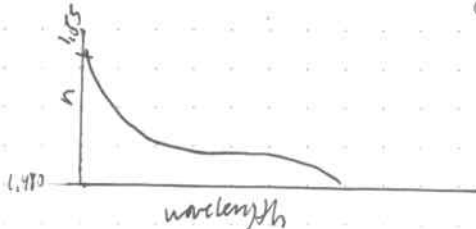
Spectral Rendering - Dispersion.

We have discussed the meaning of the index of refraction for different materials. We have treated it as a constant.

In reality, the index of refraction is not necessarily a constant value. It can depend on the wavelength of light incoming.

This means that different colors would be taken into consideration with different indices of refraction—different colors would be refracted in different directions. This is what we call effect dispersion.

Is the Index of Refraction of glass constant?

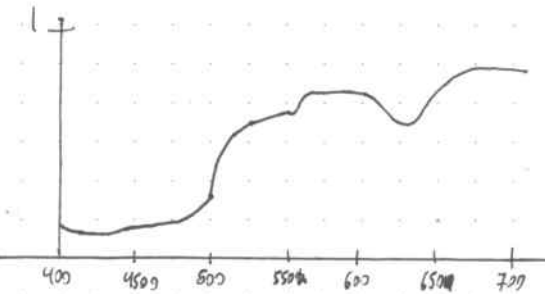


No it varies in
wavelength.

How to carry out a simulation for the whole visible wavelength spectrum?

First we introduce a function that describes how much light is carried at different wavelengths.

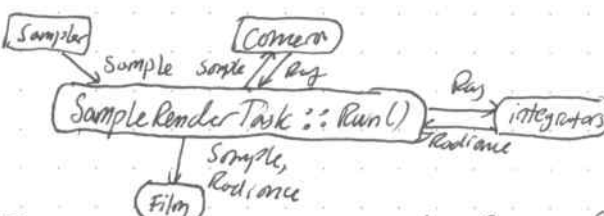
Spectral Power Distribution (SPD)



Naive Solution! We sample a randomly chosen wavelength, and take into account the corresponding TPRs when tracing the ray of light.

More on this in PBRT Chapter 5 - Color and Radiometry.

pbrt architecture
Lux render based on pbrt



- the SampleRender Task asks Sampler to provide random samples for BRDF sampling, outgoing ray directions on a hemisphere, etc.

- The Sampler-Render Task asks the Camera for the location of the next pixel. The Camera constructs a ray toward it and sends it back.
- The integrator receives a ray as input, and computes the radiance carried along the ray.
- The SampleRender Task writes this information on film. We can separate indirect vs. direct rendering.

($\text{LSD}[\text{E}]$)
of cameras to
different illumination:
num 20 ($\text{ELDS}[1]$) carry key information
about illumination

multiple bounces further for the ones
ones on the stuff we want to get in
the way to do things like
bounce to camera off of
one other one

LSD E S244W

we get indirect illumination.

The rendering will be a response to carrying the

$$\text{LSD}[\text{E}] = \text{LSD}[\text{E}] + \text{LSD}[\text{E}] \cdot \text{LSD}[\text{E}]^2 + (\text{LSD}[\text{E}])^2$$

51

$$I = K_a I_a + I_i (K_d (L \cdot N) + K_t F_t + K_r R_r) + \left(K_s (V \cdot N) + K_g (L \cdot N) \right) R_g$$

We have received information about the environment.

What kind of rendering algorithms are we interested in?

Global Illumination Algorithm Classes

Consistent

$$\lim_{N \rightarrow \infty} E_N[F] = \int f(x) dx$$

Intuition: A consistent algorithm will converge to the right solution after an infinite amount of samples. Sooner or later it will converge.

Unbiased

$$E_N[F - \int f(x) dx] = 0$$

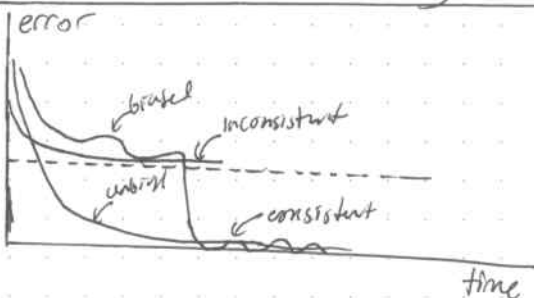
Intuition: The expectation error is zero, regardless of the samples.

With an unbiased algorithm, if we had two noisy images, combining them would give a more accurate solution.

The algorithm has the same chance of over and underestimating the integrand.

There is no systematic error in the algorithm, the deviation is caused by variance only.

Corollary: If mathematics are correct, it should be possible to do network rendering without a network!



State of the art Algorithms.

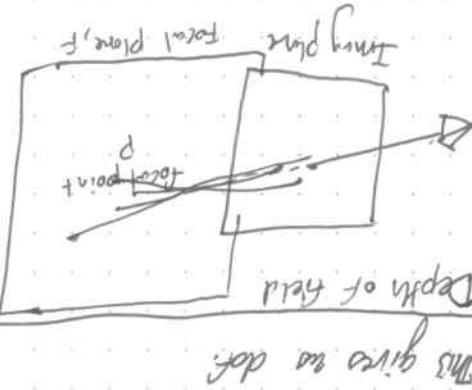
If I create a new algorithm, it will have to be proven better than these.

Always hold drafts and look for drawbacks.

- Motivation, key idea, advantages, disadvantages, results, implementations, additional literature.

and also the nearby.

we have
the local
samples
as the
local
point



the higher the F-stop, the smaller the aperture
the higher the F-stop, more light let in, more samples are
needed to get the same result, more noise

F-stop On hand-held cameras, we can set
the size of the aperture

BRDF explorer by Disney

Ashikhmin-Shirley model: this is soft-shade, specular cases

Gooch-Torrasen Model: Phong-Blinn + microscopes

$$\frac{\|V+L\|}{\|V\|} = H \quad \text{where } H = k \sqrt{N \cdot H^*}$$

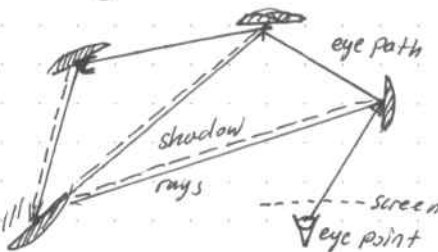
An alternative specular model is Phong-Blinn model

Dreher-Nayar model takes into consideration microscopes

Zamborlin Model

11.5

Path Tracing [1986] We have discussed this one before.



Schematic overview of the Path tracing algorithm. With next event estimation. Direct illumination is now computed explicitly at each point on the random walk by sampling the light sources.

Unbiased, consistent. It explores every light path and makes no simplifications on integrand.

* There are corner cases, but its out of scope for now.

- + Easy to implement
- + Parallelizes well
- Caustics converge slowly,

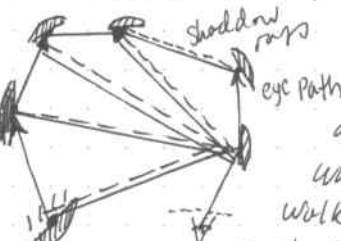
Bidirectional Path Tracing [1993]



A difficult case for Path Tracing Starting from Camera: A light source is illuminating a small area on the ceiling such that only path with a second-to-last vertex in the area indicated will be able to find illumination from the light. Bidirectional methods, where a path is started from the light and is connected with a path from the camera, can handle situations like these more robustly.

The camera is not too likely to hit the light source, possible, but improbable. Even with next event destination, most connections are obstructed.

Solution: Start rays from both the light source and camera, and connect the end points of these paths.



Light tracing. Schematic overview of eye path Bidirectional path trace. The flux through a pixel is estimated by tracing a random walk from the eye point and by then doing a shadow ray from each point and by tracing a random walk between points on respective paths.

A note: Light tracing is a bidirectional path trace, but it's not a full bidirectional path trace because it only traces the eye path.

$E[SDL]:$ bounces from surfaces

$E[SDL]:$

: 1990/5
: 1990/5 illumination

$E[O]:$ reflection

$E[DL]:$ Ray tracing

$[SID] \leftarrow$ specular or diffuse

(and amount of diffuse bounces (or 300))

$[O] \leftarrow$ any amount of diffuse bounces (or 300)

$E \leftarrow$ eye/camera

$S \leftarrow$ Specular light path

$D \leftarrow$ diffuse light path

$L \leftarrow$ light source

check for reflection for light path

intensity of light \leftarrow
from diffusion coefficient

It \leftarrow intensity from path direction.
It \leftarrow present transmission coefficient

Intensity \leftarrow It

ambient is a hole, or we can do block shading

$$I = K_a I_a + K_s (L \cdot R)_n + K_d (U \cdot R)_n + K_f f + K_r r$$

+ reflection
+ refraction
+ scattering

The illumination from environment

reflects to light source pixels
down to a simple reflection. If it's a mirror, then it's a simple reflection. If it's a glass, then it's a reflection.

Bi-directional Path Tracing [1993]

What is difficult about bi-directional path tracing is there are two light paths and we connect them in all possible different ways.

- This is actually two Monte Carlo processes.
 - The light source samples the distribution of the light source itself.
 - When we start from eye and hit diffuse or glossy object, then we start importance sampling the BRDF.
 - Take likely path more often.

We have two different sampling strategies (BRDF and light source sampling) for the same integrand - We need to combine them for best result.

It is a non-trivial matter, because the separate path methods converge at different rates.

The ~~noise~~ variance is additive, therefore averaging will not give better result.

There are techniques that are provably good both in a theoretical and practical sense.

We call this technique Multiple Importance Sampling (MIS)

Eric Veach's Thesis, Chapter 9

Look for Multiple Importance Sampling, and Balance Heuristics
PBRT Chapter 14.4

Convergence speed improvements with proper multiple importance sampling.

+ Better convergence speed, especially in indoor scenes

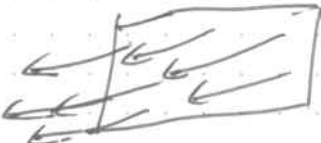
+ Quicker convergence for caustics.

- Getting the path weighting and MIS perfectly requires quite a bit of effort.

This is still a brute force method that is doing an exhaustive search therefore...

Unbiased ✓

Applications of Bidi
Light
The Camera



Raytracing Camera

Winding order of a polygon
of a plane reflecting angle

$$1 = z$$

$$(x \text{ ref. } m/h) / w = \frac{y}{y - dh} = h \quad x \text{ ref. } m/h = \frac{y \text{ ref. }}{w}$$

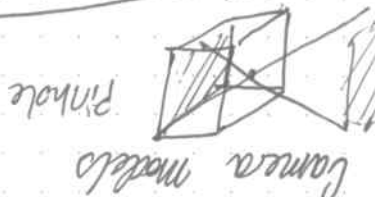
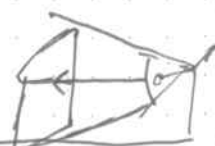
$$\frac{m}{m - dh} \tan(\text{fov}x) \leftarrow$$

$$\begin{aligned} (1/h) &\equiv dh \\ (y/h) &\equiv dh \\ (m/h) &\equiv dx \end{aligned}$$

spread over 2D given and the derived pixel positions
from pixels red (hx) to ray pixel being

Perspective

in the edge of the view.
ray as fixed height



Camera model
Pinhole

Metropolis Light Transport [1997]

Key idea: "Seek the light" - try to sample brighter paths more often than darker regions.

This sounds like classical importance sampling, but it is not!

Traditional importance sampling is unable to determine whether the bright path it is on will be terminated.

It is "multibounce" importance sampling. It need initially make suboptimal decisions if it knows it will be a bright light path.

Key Idea: Imagine a dark room with a door ajar, and light is in the other room.

We finally randomly found a light path that enters the room... and it would be a crime to just forget about this fact and start randomly sampling again.

It tries to remember the successful paths.

Once found, it adds small perturbations to light path.

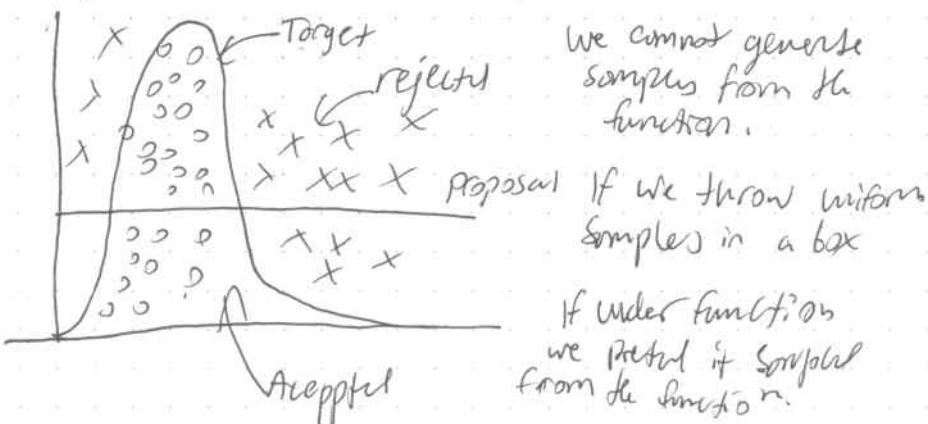
$$E\left[\frac{f(x)}{p(x)}\right] = \int_a^b \frac{f(x)}{p(x)} p(x) dx \approx \frac{1}{N} \sum_{i=1}^N \frac{f(X_i)}{p(X_i)}$$

Importance Sampling

$$p(X_i) \propto f(X_i)$$

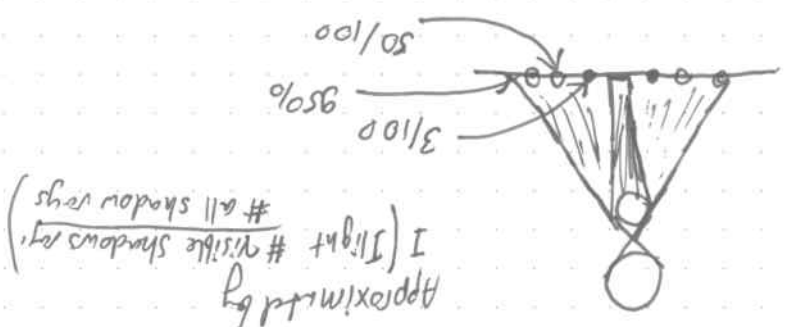
How to find $p(x)$?

We construct a function very similar to $f(x)$, and we try draw samples of it with rejection sampling.



$$I \cdot \left(\frac{\text{Area of light that is visible}}{\text{Area of light that is visible}} \right) \rightarrow I$$

The brightness of the point would be



We construct a function similar to $f(x)$, and we draw samples of it by rejection sampling — This is inefficient, since depending on the shape of function, we may encounter a lot of rejections.

Or it is done through a technique called Inverse Transform sampling or Smirnov Transform — This takes quite a bit of work, even for simple cases, and it's not always possible to use.

$$L_0(w_0, x) = \int_{\Omega} L(w_i, x) \cos^n \theta_i \cos \phi_i dw$$

$$P(\theta_s, \phi_s) = \frac{\cos^n \theta_s \sin \theta_s}{\int_{-\pi}^{\pi} \int_0^{\pi/2} \cos^n \theta_s \sin \theta_s d\theta_s} = \frac{n+1}{2\pi} \cos^n \theta_s \sin \theta_s$$

$$P(\theta_s) = \int_0^{2\pi} P(\theta_s, \phi_s) d\phi_s = (n+1) \cos^n \theta_s \sin \theta_s$$

$$P(\phi_s | \theta_s) = P(\theta_s, \phi_s) = \frac{1}{P(\theta_s)}$$

$$\theta_s = \arccos\left(\xi_1^{\frac{1}{n+1}}\right), \quad \phi_s = 2\pi \xi_2$$

$\xi_{1,2} \rightarrow$ uniform random variables

we do transformations to the variables, and integrate.

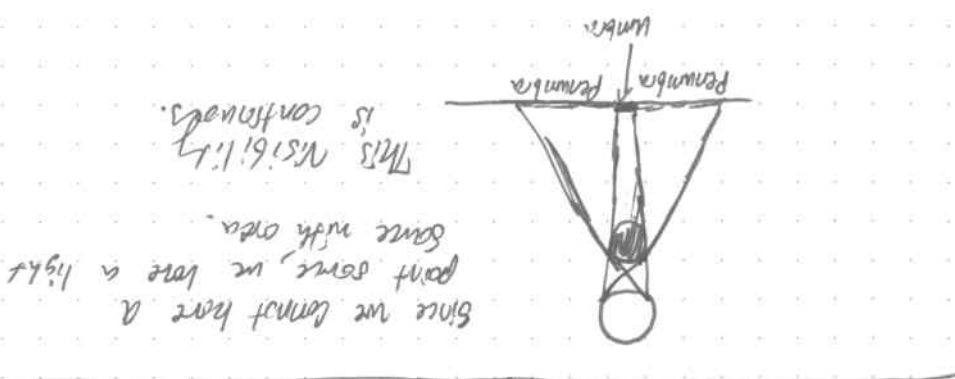
Solution: It works as a Markov chain process, which, in its steady state distribution, provides us with optimal importance sampling automatically!

over multiple bounces

Variants of MCT: There are two main variants

- Reach-type Metropolis works in path-space, which means it behaves differently based on type of sampled paths (caustics, etc.)

It is incredibly difficult to implement, Published in 1997 wrote in 2010!



To solve this, first do the direct source

complete path

we get $I \rightarrow 0$ when there is a

ambiguity out there

number



occluded ray normal path source
simple path source
occluded ray normal path source
Dynamical

Each style incredibly difficult. A simpler version returns the robustness of the algorithm.
We call it Primary Sample Space Metropolis Light Transport.

It is still path tracing, just with better sampling. Therefore,
unbiased ✓
consistent ✓

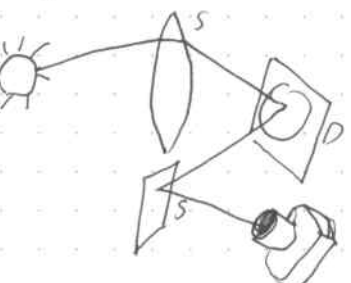
It is tailored for different scenes.

It is a very robust algorithm able to handle a variety of light transport situations.

For easy scenes, it is not helpful, a bidirectional Path Tracer will outperform it as it is able to compute more samples per pixel in unit time.

MLT is unbiased, but it starts biased.

MLT is very useful for SDS (specular-diffuse-specular) transport



It is very unlikely that starting from the diffuse surface, sampling the BRDF and moving to the Specular surface would hit the camera.

Note that this point on the diffuse surface is chosen explicitly.



Next are biased algorithms that try to fix this problem.

We want to sample a surface with a small footprint across all the objects in the scene.

$$\text{Can we sample } f \cdot \phi \cdot p$$

If we only pick the smallest possible positions we have a lot of time constraints.

If the depth of field is large enough, the camera will only see the nearest far is good enough.

Intersection Routine
Intersect the ray of all objects in scene.

$$\left(1 - \frac{h^2 d^2}{2} \times \frac{x^2 p}{2}\right) = (S h(x) f \Delta)$$

$$1 - \frac{Sc}{fP} \frac{h^2 d^2}{2} = \frac{he}{fC} \times \frac{x^2 p}{2} = \frac{xp}{fP}$$

$$\left(\frac{Sc}{fP} \frac{he}{fC} \frac{xp}{2}\right) = (S h(x) f \Delta)$$

Normal engine off surface stops

opposed ray
of no samples are of

$$E = \frac{2S}{R} + \frac{2d}{X} : (S h(x) f \cdot \text{samples})$$



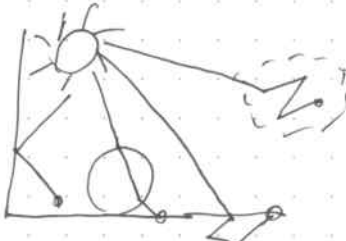
Photon Mapping [1996]

Key idea:

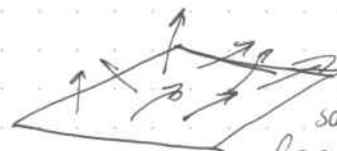
Let's not evaluate all possible light path, but make an approximation by shooting photons out of light sources, record them into a photon map, and compute the final image by interpolating results.

$$\left(\frac{\partial c}{\partial C}, \frac{\partial c}{\partial R}, \frac{\partial c}{\partial G} \right) = (\rho_c(x,y)) f \Delta$$

$(\rho_c(x,y)) f \Delta$ surface normal is the gradient
For no highlights emission $f(x,y) = 0$, the
surface becomes



indirect light map is actually low frequency information, lends itself well to interpolation.



incident directions of 50 photons around a point on the floor in the example scene. Many photons are coming from a cluster of nearby directions. These directions can be used to derive a distribution of importance sampling that approximates the direction distribution of indirect illumination at the point.

+ Caustics, indirect illumination converges quickly.

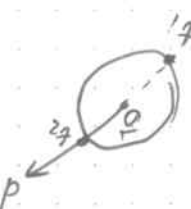
+ High frequency noise cleans up rapidly

- Storing detailed photon maps are memory-intensive.

- interpolation causes artifacts to appear.

Biased

consistent position infinite amount of photons.



a raytrace will if we are inside object.
However, if we have two softshadows, it can be

ΔA

$$t_{i,2}^2 = -B \pm \sqrt{-4AC}$$

two solutions:

$$C = (\vec{r}_i - \vec{r}_j) \cdot (\vec{r}_i - \vec{r}_k) - r^2$$

$$B = 2 \vec{d} \cdot (\vec{r}_i - \vec{r}_j)$$

$$\vec{p} \cdot \vec{p} = A$$

$$A^2 + B^2 + C = 0$$

$$0 < h_i + h_k \quad B^2 - 4AC > 0$$

$$Two hits if \quad B^2 - 4AC > 0$$

$$0 = r_i - (\vec{r}_i - \vec{r}_j) \cdot (\vec{r}_i - \vec{r}_k) + r_j^2 (\vec{r}_i - \vec{r}_j)^2 + r_k^2 (\vec{r}_i - \vec{r}_k)^2$$

Photon Mapping Mikhail Kharlamov

2019-09-29

K

(Stochastic) Progressive Photon Mapping [2008]

Frequently used Symbols and their meaning.

Symbol	Description
x	Position
\hat{x}'	Position of incoming light
\vec{n}	Normal at x (always normalized: $ \vec{n} =1$)
\vec{w}	Direction (away from Surface.)
\vec{w}'	Direction of incoming radiance (away from Surface)
$d\omega$	Differential solid angle ($d\omega = \sin \theta d\theta d\phi$)
(θ, ϕ)	Direction in spherical coordinates
L	Radiance
$L(x, \vec{w})$	Radiance at x in \vec{w} direction
$L(x, \vec{w}')$	Incident radiance at x from direction \vec{w}'
$L(x' \rightarrow x)$	Radiance leaving x' in the direction of x .
L_e	Emitted radiance
L_r	Reflected radiance
L_i	Incident radiance
Φ	Flux
E	Irradiance
f_r	BRDF
f_d	Diffuse BRDF
f_s	Specular BRDF
ρ	Reflectance
Ω	Hemisphere of directions
$\Omega_{4\pi}$	Sphere of directions
η	Index of refraction
Λ	Albedo
σ_a	Absorption Coefficient
σ_s	Scattering Coefficient
σ_t	Extinction Coefficient
τ	Optical depth
Δx	Small step
ξ	Uniformly distributed random number between 0 and 1.
ξ_1, \dots, ξ_n	n uniform numbers between 0 and 1.

Current physics light transport models consist of the following.

- Ray optics: models light as independent rays that travel in different optical media according to a set of geometrical rules. Ray optics can be used to describe most effects we see, such as reflection, refraction, and image formation.
- Wave optics: Models light as electromagnetic waves and can be used to model all the phenomena that ray optics can model and, in addition, interference and diffraction.
- Electromagnetic optics: Includes wave optics and, in addition, exploring polarization and dispersion.
- Photon optics provides the foundation for understanding the interaction of light and matter.

In Computer graphics there is an almost exclusive use of Ray Optics. Despite the name photon mapping uses ray optics as the foundational model of light scattering.

The interaction of light with matter is based on high-level models that abstract away actual scattering of photons by molecules and atoms. This means we ignore effects such as diffraction and interference. We typically ignore polarization even though ray optics can be extended to include light polarization quite easily.

Another assumption is light has infinite speed. This means when the light source is turned on, the illumination immediately reaches a steady state.

Despite these being approximations we can simulate almost all of the lighting phenomena around us.

Radiometry and Photometry, the only difference is photometry takes into account our optical response.

Radiometry

The basic quantity in lighting is the photon. The energy, e_λ , of a photon of wavelength λ is:

$$(2.1) \quad e_\lambda = \frac{hc}{\lambda}$$

$h \approx 6.63 \cdot 10^{-34} \text{ J} \cdot \text{s}$ is Planck's constant
 $c = c_0 = 299\,792\,458 \text{ m/s}$.

The spectral radiant energy, Q_λ , in n_λ photons with wavelength λ is:

$$(2.2) \quad Q_\lambda = n_\lambda e_\lambda = n_\lambda \frac{hc}{\lambda}$$

The Radiant energy, Q , is the energy of a collection of photons and is computed by integrating the spectral energy over all wavelength:

$$(2.3) \quad Q = \int_0^\infty Q_\lambda d\lambda \\ \Rightarrow Q = \int_0^\infty Q_\lambda d\lambda = \int_0^\infty n_\lambda \frac{hc}{\lambda} d\lambda = hc \int_0^\infty \frac{n_\lambda}{\lambda} d\lambda$$

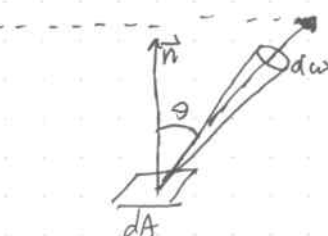


Figure 2.1. Radiance, L , is defined as the radiant flux per solid angle, $d\omega$, per unit projected area, dA .

Radiant flux, Φ , is the time rate flow of radiant energy:

$$(2.4) \quad \Phi = \frac{dQ}{dt}$$

$$\Phi = \frac{dQ}{dt} = \frac{d}{dt} \int_0^\infty Q_\lambda d\lambda = \frac{d}{dt} \int_0^\infty n_\lambda \frac{hc}{\lambda} d\lambda = hc \frac{d}{dt} \int n_\lambda \frac{1}{\lambda} d\lambda$$

$$\Phi = \frac{dhc}{dt} \int \frac{n_\lambda}{\lambda} d\lambda$$

Radiant flux Φ is often called the flux. For wavelength dependence there is the spectral radiant flux, Φ_λ , which is the time rate flow of spectral radiant energy.

The radiant flux area density is defined as the differential flux per differential area (at a surface), $\frac{d\Phi}{dA}$. Radiant flux area density is often separated into $\frac{dA}{dA}$, the radiant excitation M , which is the flux leaving a source (this quantity is known as the radiosity, B) and the irradiance, E , which is the flux arriving at location, x :

$$E(x) = \frac{d\Phi}{dA}. \quad (2.5)$$

The radiant intensity, I , is the radiant flux per unit solid angle, $d\omega$:

$$I(\vec{\omega}) = \frac{d\Phi}{d\omega} \quad (2.6)$$

Radiance, L , is the radiant flux per unit solid angle per unit projected area

$$L(x, \vec{\omega}) \propto E(x) \cdot I(\vec{\omega}) \\ L(x, \vec{\omega}) = \frac{d\Phi}{\cos \theta dA d\omega} = \int_0^\infty \frac{d^4 n \lambda}{\cos \theta d\omega dA dt d\lambda} \frac{hc}{\lambda} d\lambda \quad (2.7)$$

where the last term represents radiance expressed as the integral over wavelength of the flow of energy in n_λ photons per differential area per differential solid angle per unit time.

Radiance is a 5-dimensional quantity. (Three position, two direction) is often written as $L(x, \vec{\omega})$ where x is the position and $\vec{\omega}$ is the direction.

Radiance is the most important quantity in global illumination, since it closely represents the colour in the object.
— This applies to any device that detects light, such as a human observer.

Radiance can be thought of photons hitting per unit time in a given direction on a point.

In a vacuum Radiance is constant along a line of sight

Equation 2.7 computes Radiance vs flux. If the radiance field on a surface is available then the flux can be computed by integrating the radiance field over all directions ω and area A :

$$\Phi = \int_A \int_{S2} L(x, \vec{\omega}) (\vec{\omega} \cdot \vec{n}) d\omega dA \quad (2.8)$$

where \vec{n} is the surface normal of the surface. The Radiometric terms are summarized in Table 2.1.

Symbol	Quantity	Unit
Q_λ	Spectral radiant energy	$J \text{ m}^{-1}$
Q	Radiant energy	J
Φ	Radiant Flux	
I	Radiant Intensity	W
E	Irradiance (incident)	$W \text{ sr}^{-1}$
M	Radiant excitation (outgoing)	$W \text{ m}^{-2}$
B	Radiosity (outgoing)	$W \text{ m}^{-2}$
L	Radiance	$W \text{ m}^{-2}$
L_λ	Spectral Radiance	$W \text{ m}^{-2} \text{ sr}^{-1}$ $W \text{ m}^{-2} \text{ sr}^{-1} \text{ nm}^{-1}$

Table 2.1 Radiometric symbols, names, and units.

2.2.2 Photometry

The important difference between radiometry and photometry is that the photometric values include the visual response of a standard observer. Luminous flux, Φ_V , is the visual response to radiant flux.

It is computed as:

$$\Phi_V = \int_A \Phi_\lambda V(\lambda) d\lambda \quad (2.9)$$

where $V(\lambda)$ is the visual response of a standard observer and A is the wavelength for the visible spectrum (380nm–780nm).

The luminous flux area density, $\frac{d\Phi_V}{cos \theta dA d\omega}$, is called the illuminance, E_V , if incident, and $\frac{d\Phi_V}{cos \theta dA}$, if outgoing. Luminous intensity, I_V , is the flux per solid angle $\frac{d\Phi_V}{d\omega}$, and the luminance l_V is:
$$I_V(x, \vec{\omega}) = \frac{d^2 \Phi_V}{cos \theta dA d\omega} \quad (2.10)$$

Luminance is the photometric equivalent of radiance and is often used for global illumination.

In this book we only deal with physical quantities of light and not with

2.2.3 The Solid Angle.

The differential solid angle, $d\omega$, is used extensively in the description of light.

It relates the raw stream of photons (the flux) to the intensity of light.

and it is almost exclusively the integration variable of choice in Monte-Carlo ray tracing when the incoming radiance is integrated.

The solid angle represents the angular "size" of a beam as well as the direction. We can think of the solid angle as representing both a direction and an infinitesimal area on the unit sphere. We can express this direction and size in spherical coordinates (θ, ϕ) . This requires a base coordinate system. (e.g. A surface normal, and two orthogonal vectors, \vec{t}_x and \vec{t}_y , in the surface tangent plane). The size of a differential solid angle in spherical coordinates is given by:

$$d\omega = \sin\theta d\theta d\phi \quad (2.11)$$

Here, θ is the angle between the direction and \vec{n} , and ϕ is the angle between the direction projected onto the surface tangent plane and \vec{t}_x . The right-hand side of the equation expresses the infinitesimal area on the unit sphere as a product of the length of the longitude arc ($d\phi$) and the length of the latitude arc ($\sin\theta d\theta$).

Given the spherical coordinates we can compute the direction, $\vec{\omega}$, of the solid angle. $\vec{\omega} = \sin\theta \cos\phi \vec{t}_x + \sin\theta \sin\phi \vec{t}_y + \cos\theta \vec{n}$. $\quad (2.12)$

A frequently encountered expression is the integral over the incoming directions on the hemisphere, Ω . When evaluating this integral it is convenient to write it as an integral in spherical coordinates:

$$\int_{\Omega} f(\theta, \phi) d\omega = \int_0^{2\pi} \int_0^{\pi/2} f(\theta, \phi) \sin\theta d\theta d\phi \quad (2.13)$$

2.3 Light Emission

Light in the form of photons is generated at light sources. Sources of light include light bulbs and natural sources such as the sun, fire, and biochemical processes.

The intensity of a given light source is often given as the power or the wattage of the source. For a small (point) light source with power Φ_s that emits light uniformly in all directions, we can compute the irradiance, E , at a surface as:

$$E(x) = \frac{\Phi_s}{4\pi r^2 \cos\theta} \quad (2.14)$$

where r is the distance from x to the light source, and θ is the angle between the surface normal and the direction to the light source.

This equation is intuitive: imagine a small source sending photons in all directions, where the density of the photons decreases with the distance to the source. The rate at which the photon density decreases is proportional to the surface area of a sphere at the same distance. One can think of each batch of emitted photons as sitting on an expanded sphere.

The surface area of the sphere is $4\pi r^2$. The cosine factor in the denominator is due to the surface orientation. A surface facing the source will receive more photons per area than a surface oriented differently.

It is common to refer to color temperature of a light source. This quantity has an exact physical meaning since it is related to the blackbody radiation. For a blackbody at a given temperature the spectral radiant flux can be computed using Planck's formula:

$$\Phi_s = \frac{2\pi C_1}{\lambda^5 (e^{C_2/\lambda T} - 1)} \quad (2.15)$$

Here T is the temperature of the object, $C_1 = \pi C_0^2 \approx 3.7418 \cdot 10^{-16}$, and $C_2 = \frac{hc}{k} \approx 1.4388 \cdot 10^{-2}$, where $k \approx 1.38 \cdot 10^{-23} \text{ J/K}$ is Boltzmann's constant. As an example the color temperature of the Sun is approximately 5900K.

2.4 Light Scattering.

When light encounters an obstacle it is scattered or absorbed. The obstacle can be the surface of a different material or medium. It can also be a very small particle or molecule, but this case requires special scattering techniques which will be covered later.

In this section we will introduce tools for modeling the local light scattering at surfaces, i.e. what happens when a beam of light strikes a given surface.

In graphics this is known as local illumination.

First we present the theoretical framework used to describe light scattering, and then we present a few reflection models commonly used in computer graphics. Unless stated we assume that the wavelength of light does not change as a result of scattering. (i.e. fluorescence, scintillation), we therefore omit the wavelength parameter as part of our description.

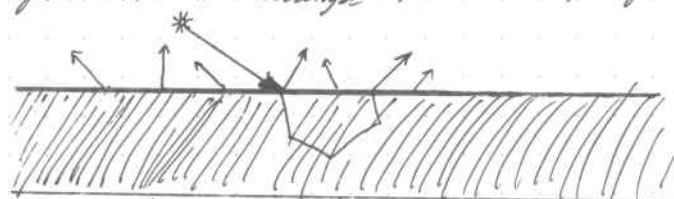


Figure 2.2. When a beam of light hits a material it is often scattered inside the material before being "reflected" at a different location.

This general concept can be described using a BSSRDF.

2.4.1 The BSSRDF

When a beam of light is scattered by a material it normally enters the material and then scatters around before the surface at a different location.

This is particularly noticeable for translucent materials such as marble and skin, but it happens to some degree for all non-metallic materials.

We can describe this scattering using the Bidirectional Scattering Surface Reflectance Distribution Function or (BSSRDF)

The BSSRDF relates the differential reflected radiance, dL_r , ~~at a direction~~ at x in a direction $\vec{\omega}$, to the differential incident flux, $d\Phi_i$ at x' from direction $\vec{\omega}'$:

$$S(x, \vec{\omega}, x', \vec{\omega}') = \frac{dL_r(x, \vec{\omega})}{d\Phi_i(x, \vec{\omega}')} \quad (2.16)$$

Notice that S is a function of both the incoming position and direction as well as the outgoing position and direction. This is the most general description of light transport. The only assumption is that there is some interaction at some point in space and that some flux incident at some location is scattered to some other location as a result of this interaction.

Unfortunately, the BSSRDF is eight dimensional and costly to evaluate, and has only been used in a few papers in computer graphics. These papers all deal with subsurface scattering, where light enters the material and scatters before leaving the material. Even though subsurface scattering is the most common case, the BSSRDF can be used to describe scattering between the elements of a rough metallic surface as well. But this case is typically dealt with in the rendering ~~program~~ algorithm.



Figure 2.3 The BRDF models the local reflection of light by assuming that all light is reflected at the same location where it hits the surface.

This approximation works well for most materials.

2.4.2 The BRDF. The Bidirectional Reflectance distribution function

was introduced by McAdams et al. as a tool for describing reflection of light at a surface. The BRDF is an approximation of the BSSRDF. For the BRDF it is assumed that light striking a surface location is reflected at the same surface location. This reduces the BRDF to a six-dimensional function.

[1.] The vectors $\vec{\omega}$ and $\vec{\omega}'$ always point away from the surface. For incident illumination such as $d\Phi_i(x, \vec{\omega}')$ we will assume $\vec{\omega}'$ points to the illumination.

This may not seem like a big win, but it enables a series of simplifications that will be described in the following:

The BRDF, ~~was introduced~~ for, defines the relationship between reflected radiance and irradiance:

$$f_r(x, \vec{\omega}, \vec{\omega}') = \frac{dL_r(x, \vec{\omega})}{dE_i(x, \vec{\omega}')} = \frac{dL_r(x, \vec{\omega})}{dI_i(x, \vec{\omega}')(\vec{\omega} \cdot \vec{n}) d\omega'} \quad (2.17)$$

where \vec{n} is the normal at x . At first it may seem strange that the BRDF is defined as the ratio of reflected radiance and irradiance instead of as the ratio between incident and reflected radiance. The reason for this is that the change in the reflected radiance is proportional to the solid angle and $\cos \theta'$ for I_i . By including these values in the denominator we avoid having to include this fundamental factor in the BRDF.

The BRDF describes the local illumination model. If we know the incident radiance field at the a surface location, then we can compute the reflected radiance in all directions. This is done by integrating the incident radiance, I_i :

$$L_r(x, \vec{\omega}) = \int_{\Omega} f_r(x, \vec{\omega}, \vec{\omega}') dE_i(x, \vec{\omega}') = \int_{\Omega} f_r(x, \vec{\omega}, \vec{\omega}') I_i(x, \vec{\omega}') (\vec{\omega} \cdot \vec{n}) d\omega' \quad (2.18)$$

Here \vec{n} is the normal at the surface location x . (note that $(\vec{\omega} \cdot \vec{n}) = \cos \theta'$), and Ω is the hemisphere of all incoming directions at x .

An important property of the BRDF is Helmholtz's law of Reciprocity, which states the BRDF is independent of the direction in which light flows: $f_r(x, \vec{\omega}', \vec{\omega}) = f_r(x, \vec{\omega}, \vec{\omega}')$

This is a fundamental property that is used by most global illumination algorithms, since it makes it possible to trace light in both directions, as the following chapters will demonstrate. It is also a simple procedure for checking if a BRDF is valid by making sure it is reciprocal.

Another important physical property of the BRDF is energy conservation. A surface cannot reflect more than it receives, so eq. 2.20 must be satisfied.

$$\int_{\Omega} f_r(x, \vec{\omega}, \vec{\omega}') (\vec{\omega} \cdot \vec{n}) d\omega' \leq 1, \forall \vec{\omega} \quad (2.20)$$

2.4.3 The Reflectance.

To quantify the amount of lux reflected by the surface we can use the ratio of the reflected to incident flux.

This quantity is known as the reflectance, ρ_s , of the surface, and it is given by:

$$\rho_s(x) = \frac{d\Phi_r(x)}{d\Phi_i(x)} = \frac{\int_{\Omega} f_r(x, \vec{\omega}', \vec{\omega}) L_i(x, \vec{\omega}') d\vec{\omega}' d\vec{\omega}}{\int_{\Omega} L_i(x, \vec{\omega}') d\vec{\omega}'} \quad (2.21)$$

$\rho_s(x)$ is the fraction of the incident light that is reflected by the surface; the remaining part is either transmitted or absorbed. For physically-based rendering it must be a vary from zero to one.

2.4.4 Diffuse Reflection.

A surface with diffuse reflection is characterized by light being reflected in all directions when it strikes the surface. This type of reflection typically occurs at rough surfaces or for materials with subsurface scattering, where light is reflected in some random direction, as shown in Figure 2.4(a).

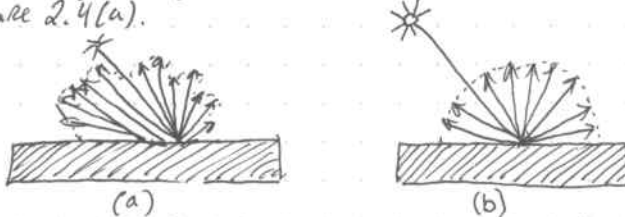


Figure 2.4. A Diffuse material reflects light in all directions
(a) general diffuse reflection (b) shows lambertian ideal diffusion.

A special case of diffuse reflection is Lambertian or ideal diffuse reflection, in which the reflected direction is perfectly random. As a result the reflected radiance is constant in all directions regardless of irradiance. This gives the constant BRDF,

$$L_r(x, \vec{\omega}) = f_{r,d}(x) \int_{\Omega} dE_i(x, \vec{\omega}') = f_{r,d}(x) E_i(x) \quad (2.22)$$

Using this relationship we can find the diffuse reflectance, ρ_d , for a Lambertian surface:

$$\rho_d(x) = \frac{d\Phi_r(x)}{d\Phi_i(x)} = \frac{\int_{\Omega} L_r(x) dA \int_{\Omega} d\vec{\omega}'}{E_i(x) dA} = \pi f_{r,d}(x) \quad (2.23)$$

The reflected direction of the light is, as mentioned, perfectly random for a Lambertian surface. Given two uniformly distributed random numbers:

$\xi_1 \in [0, 1]$ and $\xi_2 \in [0, 1]$ we find that this randomly reflected direction, $\vec{\omega}_d$, is distributed as:

$$\vec{\omega}_d = (\theta, \phi) = (\cos^{-1}(\sqrt{\xi_1}), 2\pi \xi_2) \quad (2.24)$$

where we have used spherical coordinates (θ, ϕ) for the direction: θ is the angle with the surface normal, and ϕ is rotation around the ~~the~~ normal.

2.4.5 Specular Reflection

Specular reflections happen when light strikes a smooth surface - typically a metallic surface or a smooth dielectric surface (such as glass or water). Most surfaces have some imperfection and as a result light is reflected only in the mirror direction we have perfect specular reflection. (Figure 2.5(b)).

The reflected radiance due to specular reflection is

$$L_r(x, \vec{\omega}_s) = \rho_s(x) L_i(x, \vec{\omega}') \quad (2.25)$$

For perfect specular reflection the mirror direction, $\vec{\omega}_s$, is:

$$\vec{\omega}_s = 2(\vec{\omega} \cdot \vec{n})\vec{n} - \vec{\omega}' \quad (2.26)$$

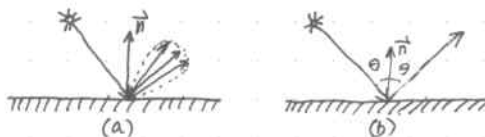


Figure 2.5 A specular surface reflects the incoming light in the mirror direction.
(a) shows glossy specular reflection (i.e., a rough mirror surface), and
(b) shows perfect specular reflection.

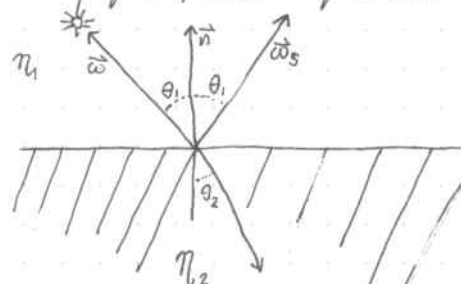


Figure 2.6. The geometry of refraction and reflection.

Notice that $\vec{\omega}_s$ and $\vec{\omega}'$ both point away from the surface in figure 2.6. We can express the perfect mirror reflection as a BRDF by using spherical coordinates for the direction.

$$f_{r,s}(x, \vec{\omega}', \vec{\omega}) = 2\rho_s \delta(\sin^2\theta' - \sin^2\theta) \delta(\phi' - \phi \pm \pi) \quad (2.27)$$

where Dirac's delta function, $\delta(x)$, is used to limit the direction in which the BRDF is nonzero (Recall that $\delta(x)$ is nonzero only when $x=0$)

Note $\vec{w} = (\theta, \phi)$ and $\vec{w}' = (\theta', \phi')$.

The Fresnel Equations

For smooth homogeneous metals and dielectrics the amount of light reflected can be derived from Maxwell's equations, and the result is the Fresnel equations. Given a ray of light in a medium with index of refraction n_1 (See figure 2.6) that strikes a material with index of refraction n_2 , we can compute the amount of light reflected as:

$$P_{II} = \frac{n_2 \cos \theta_1 - n_1 \cos \theta_2}{n_2 \cos \theta_1 + n_1 \cos \theta_2}, \quad P_I = \frac{n_1 \cos \theta_1 - n_2 \cos \theta_2}{n_2 \cos \theta_1 + n_1 \cos \theta_2} \quad (2.28)$$

These coefficients take into account polarization: P_{II} is the reflection coefficient for light with the electric field being parallel to the plane of incidence, and P_I is the reflection coefficient for light with the electric field being orthogonal to the plane of incidence. The value of the index of refraction can be found in most optical textbooks.

Air ($\eta \approx 1.0$), water ($\eta \approx 1.33$), and glass ($\eta \approx 1.5-1.7$) depending on the type of glass. Note the index of refraction can be complex. This is the case for metals where imaginary component specifies the absorption of light by the metal (i.e. the fact that metals are not transparent).

For unpolarized light the specular reflectance (also known as the Fresnel reflection coefficient F_r) becomes:

$$F_r(\theta) = \frac{1}{2} (P_{II}^2 + P_I^2) = \frac{d\Phi_r}{d\Phi_i}. \quad (2.29)$$

For unpolarized light a good approximation to the Fresnel reflection coefficient was derived by Schlick:

$$F_r(\theta) \approx F_0 + (1-F_0)(1-\cos \theta)^5 \quad (2.30)$$

where F_0 is the value of the real Fresnel reflection coefficient at normal incidence

Refraction

The Fresnel Equation (2.28) contains factor $\cos \theta_2$, where θ_2 is the angle of the refracted ray. It is computed from Snell's law:

$$\eta_1 \sin \theta_1 = \eta_2 \sin \theta_2 \quad (2.31)$$

The geometry for refraction is shown in Fig 2.6. Using Snell's law, the direction, \vec{w}_r , of the refracted ray (for a perfectly smooth surface with normal \vec{n}) is computed as:

$$\vec{w}_r = \frac{\eta_1}{\eta_2} (\vec{w} - (\vec{w} \cdot \vec{n}) \vec{n}) - \left(\sqrt{1 - \left(\frac{\eta_1}{\eta_2} \right)^2 (1 - \vec{w} \cdot \vec{n})^2} \right) \vec{n} \quad (2.32)$$

For the refracted ray the amount of transmitted light can be computed as $1-F_r$.

2.4.6 Reflection Models

Most materials reflect light in a way that is too complicated to be described by the simple Lambertian and perfect specular reflection models.

To address this problem several reflection models have been developed for computer graphics.

The early early models such as the phong model were phenomenological models with no physical basis. The phong model is used to simulate highlights due to either area lights or glossy reflections of a point source. This is done by adding a simple blur to the reflection of the light sources. With the rise of physically based simulations it was noticed that the phong model results in a surface that reflects more lights than received. This problem was addressed by Lewis who derived a normalizing factor for the Phong model.

The first physically based reflection models were derived outside the field of computer graphics. One of the best known is the Torrance-Sparrow model, introduced to the computer graphics field by Blinn.

The Torrance-Sparrow model uses the concept of microfacets to explain several observed phenomena of light reflection – in particular the off-specular peaks where light is reflected mostly to a location slightly away from the mirror direction.

The microfacet theory assumes that the surface is made of many tiny facets where each facet has some perfect specular reflection. The facets are distributed according to some known distribution – for example, one can assume that the average slope angle can be modeled using a Gaussian distribution. This knowledge can be used to compute the local self-shadowing of light by the microfacets, as well as the distribution of the reflected light based on the orientation of the facets.

The Torrance-Sparrow model explains Specular-related phenomena (in particular off-specular peaks). It is still necessary to add some diffuse term. For rough diffuse surfaces the model by Oren and Nayar is better.

It builds upon a V-groove theory similar to the microfacet theory; however it uses facets with Lambertian diffuse reflection.

The Oren-Nayar model can simulate reflection of rough, diffuse surfaces such as clay, where local indirect illumination and self-shadowing is important.

Another special class of materials is brushed metals. Brushed metals often exhibit anisotropic reflection, where the amount of light depends on the rotation of the surface around the normal. This can be modeled by assigning two roughness parameters that control the slope of the microfacets for different directions. Commonly used is the model by Boulin and Fourier.

Some other reflection models include the model by Laforetne et al supports importance sampling, which is useful, but the model parameters are not intuitive and are most easily obtained by fitting the model to measured data.

The Schlick model

A simple, intuitive, and empirical reflection model for physically plausible rendering has been proposed by Schlick. In addition this model is computationally efficient and it supports importance sampling, which is useful for Monte Carlo methods. The model is not derived from a physical theory of surface reflection. Instead it is a mix of approximations to existing theoretical models and some intuition of light reflection behavior.

The model has three parameters:

- F_0 , the specular reflection at normal incidence.
- σ , a roughness factor ($\sigma=0$ for perfectly smooth and specular, $\sigma=1$ is rough and Lamberian)
- ψ , an isotropic factor ($\psi=1$ is perfect anisotropy and $\psi=0$ is isotropic)

The σ parameter is particularly useful since it provides a simple way to continuously adjust the surface properties from perfect specular to Lamberian.

Schlick's BRDF is a combination of a specular factor $S(u)$ and a term controlling the amount of diffuse (d), glossy (g), specular (s) reflection:

$$f(x, \vec{w}, \vec{w}') = S(u) \left\{ \frac{d}{\pi} + g D(t, v, v', w) + S_{fs}(x, \vec{w}, \vec{w}') \right\}. \quad (2.33)$$

where f_{fs} is the BRDF for perfect specular reflection as given in equation 2.27 and $D(t, v, v', w)$ is a directional term controlling the glossy reflection.

The parameters u, t, v, v' , and w are computed from the surface orientation and the incoming and outgoing directions:

$$\begin{aligned} \vec{H} &= \frac{\vec{w} + \vec{w}'}{\|\vec{w} + \vec{w}'\|}, \quad u = \vec{w} \cdot \vec{H}, \quad t = \vec{n} \cdot \vec{H} \\ v &= \vec{w} \cdot \vec{n}, \quad v' = \vec{w}' \cdot \vec{n}, \quad w = \vec{T} \cdot \frac{\vec{H} - \vec{n} \cdot \vec{H}}{\|\vec{H} - \vec{n} \cdot \vec{H}\|} \end{aligned}$$

\vec{H} is the half vector between the incoming and outgoing radiance, and \vec{T} is a surface tangent vector in the direction of the scratches on an anisotropic material.

The specular factor $S(u)$ is given by the Fresnel approximation.

Equation (2.33):

$$S(u) = F_0 + (1-F_0)(1-u)^5 \quad (2.34)$$

The directional factor $D(t, v, v', w)$ accounts for the microfacet orientation via the two terms $Z(t)$ and $A(w)$, as well as the geometrical constraints of the microfacets via a geometrical term $G(v)$. These terms are given by:

$$Z(t) = \frac{\sigma}{(1+\sigma-t^2)^2} \quad \text{and} \quad A(w) = \sqrt{\frac{\psi}{\psi^2 - \psi^2 w^2 + w^2}} \quad (2.35)$$

and

$$G(v) = \frac{v}{\sigma - \sigma v + v}. \quad (2.36)$$

The directional factor D then becomes:

$$D(t, v, v', w) = \frac{G(v)G(v')Z(t)A(w) + 1 - G(v)G(v')}{4\pi vv'} \quad (2.37)$$

Equation 2.33 contains the three factors d, g , and s controlling the amount of diffuse, glossy, and specular reflection respectively.

Schlick suggested automatically setting these based on the roughness factor:

$$g = 4\sigma(1-\sigma) \quad (2.38)$$

$$d = \begin{cases} 0 & \text{for } \sigma < 0.5 \\ 1-\sigma & \text{otherwise} \end{cases}$$

$$s = \begin{cases} 1-\sigma & \text{for } \sigma < 0.5 \\ 0 & \text{otherwise} \end{cases} \quad (2.40)$$

To compute a direction for light reflected due to Schlick's BRDF we need to pick one of the modes (Lambertian, glossy, specular).

This can be done randomly based on the importance of each term. We already described the methods for computing a reflected direction for a Lamberian and a Specular BRDF.

For the glossy component of Schlick's BRDF it is possible to construct a function based on $Z(t) A(w)$ to compute a glossy reflected direction.

The expression for this spherical coordinates around the half-vector H is:

$$t = \sqrt{\xi_1} \sigma - \xi_1 \sigma + \xi_1, \quad \text{and} \quad w = \cos \frac{\pi}{2} \sqrt{\frac{\psi^2 \xi_2^2}{1 - \xi_2^2 + \xi_2^2 \psi^2}} \quad \text{eq (2.41)}$$

where ξ_1 and ξ_2 are uniform random numbers between 0 and 1. Note this expression does not account for the geometry factor, and the amount of reflected light needs to be scaled by G as in equation 2.37.

2.5 The Rendering Equation

The rendering equation forms the mathematical basis for all global illumination algorithms. It states the necessary conditions for equilibrium of light transport in models without participating media.

The rendering equation can be used to compute outgoing radiance at any surface location in a model. The outgoing radiance, L_o , is the sum of the emitted radiance, L_e and the reflected radiance, L_r :

$$L_o(x, \vec{\omega}) = L_e(x, \vec{\omega}) + L_r(x, \vec{\omega}) \quad (2.42)$$

By using eq. 2.18 to compute the reflected radiance we find that:

$$L_r(x, \vec{\omega}) = \int_S f_r(x, \vec{\omega}', \vec{\omega}) dE(x, \vec{\omega}') = \int_S f_r(x, \vec{\omega}', \vec{\omega}) Li(x, \vec{\omega}')(\vec{\omega}' \cdot \vec{n}) d\vec{\omega}' \quad (2.43)$$

This rendering algorithm

This is the rendering equation as it is often used in Monte Carlo ray-tracing algorithms including photon mapping.

For finite element algorithms, the rendering equation is normally expressed as an integral over surface locations. This can be done by using the following formula for the differential solid angle:

$$d\vec{\omega}'(x) = \frac{(\vec{\omega}' \cdot \vec{n}') dA'}{\|x' - x\|^2} \quad (2.44)$$

Here x' is another surface location, and \vec{n}' is the normal at x' . By introducing a geometry term G where

$$G(x, x') = \frac{(\vec{\omega} \cdot \vec{n})(\vec{\omega}' \cdot \vec{n}')}{\|x' - x\|^2} \quad (2.45)$$

we can rewrite the rendering equation as:

$$L_o(x, \vec{\omega}) = L_e(x, \vec{\omega}) + \int_S f_r(x, x' \rightarrow x, \vec{\omega}) Li(x' \rightarrow x) V(x, x') G(x, x') dA' \quad (2.46)$$

Here we have used the notation $Li(x' \rightarrow x)$ to denote the radiance leaving x' in the direction towards x , S is the set of all surface points, and $V(x, x')$ is the visibility function.

$$V(x, x') = \begin{cases} 1 & x \text{ and } x' \text{ are mutually visible} \\ 0 & \text{otherwise.} \end{cases} \quad (2.47)$$

We can formulate the rendering equation entirely in terms of surface locations x, x' , and x'' :

$$L_o(x \rightarrow x) = L_e(x \rightarrow x) + \int_S f_r(x'' \rightarrow x' \rightarrow x) Li(x'' \rightarrow x') V(x', x'') G(x', x'') dA'' \quad (2.48)$$

This is very similar to the original rendering equation as presented by Walter Karfagiya in his seminal paper, where he showed how both finite element methods (Radiosity) and Monte Carlo methods are solving the same equation. Finite element methods use a discretized approximation of the radiosity equation, and most Monte Carlo ray-tracing methods use a continuous Markov chain random walk, based on the Neumann series expansion or the path integral version of the rendering equation.

2.5.1 The Radiosity Equation

One strategy for solving the rendering equation is to simplify the problem.

One simplification is to assume that every surface in the model is Lambertian, so that the reflected radiance is constant in all directions.

This means that we can replace the computation of radiance with the simpler radiant exitance term, also known as the radiosity, B . This simplification reduces equation 2.46 to:

$$\begin{aligned} B(x) &= B_e(x) + \int_S f_{r,d}(x) B(x') V(x, x') G(x, x') dA' \\ &= B_e(x) + \frac{P_d(x)}{\pi} \int_S B(x') V(x, x') G(x, x') dA' \end{aligned} \quad (2.49)$$

where B_e is the emitted radiosity.

The finite element radiosity algorithm solves the integral by discretizing it into a system of linear equations.

This is done by picking an appropriate basis; a common choice is N elements with constant radiosity which results in:

$$B_i = B_{e,i} + \rho_i \sum_{j=1}^N B_j F_{ij} \quad (2.50)$$

where B_i is the radiosity for patch i and ρ_i is the diffuse reflectance for this patch. The form factor, F_{ij} , is computed as:

$$F_{ij} = \frac{1}{A_i} \int_{A_i} \int_{A_j} \frac{V(x, x') G(x, x')}{\pi} dA_j dA_i \quad (2.51)$$

The form factor, F_{ij} , represents the fraction of the power leaving patch i that arrives at patch j .

A significant amount of research has been devoted to solving the radiosity equation efficiently. These techniques have been described in several books.

Michael F. Cohen and John R. Wallace. Radiosity and Realistic Image Synthesis. San Diego, CA : Academic Press, 1993.

2.5.2 Neumann Series Expansion

The rendering equation cannot be directly evaluated since the radiance value is on both sides of the equation. One way to get around this problem is to recursively replace the radiance on the right side of the equation with the expression for Radiance.

For this purpose it is more convenient to use integral operator notation in which the rendering equation can be represented using the following compact form:

$$L = L_e + TL \quad (2.52)$$

Here the integral operator T is:

$$\langle Tg \rangle(x, \vec{w}) = \int_L f_r(x, \vec{w}, \vec{w}') g(x, \vec{w}') / (\vec{w} \cdot \vec{n}) d\vec{w}' \quad (2.53)$$

Recursive evaluation of Equation 2.52 gives:

This is the Neumann series expansion of the rendering equation, and it forms the basis for several Monte Carlo ray-Tracing algorithms (most notable the path-tracing algorithm introduced by Kajiya). An intuitive interpretation of the Neumann Series is that it sums terms representing light reflected 0, 1, 2, 3, ... times. This can be formulated slightly differently using the path integral formulation.

James T. Kajiya. "The Rendering equation." Computer Graphics (Proc. SIGGRAPH '86) 20(4): 143-150 (August 1986)

2.5.3 Path Integral Formulation

Using the concept in the Neumann Series we can rewrite the rendering equation as the sum over all paths of length k. This gives

$$L_o(x, \vec{w}) = \sum_{k=0}^{\infty} \iiint \dots \int_S H(x_k, x_{k-1}, x_{k-2}) \dots H(x_1, x_0, x_i) \times L_e(x_k \rightarrow x_{k-1}) dA_k dA_{k-1} \dots dA_0$$

where $\vec{w} = x_1 - x_0$ (i.e., x_1 is the location of the observer), and H is:

$$H(x'', x', x) = f_r(x'' \rightarrow x' \rightarrow x) V(x'', x') G(x', x).$$

To evaluate this path integral we need an algorithm that can compute the radiance from any path of length k.

Recursive evaluation of equation 2.52 gives:

$$L = L_e + T L_e + T^2 L_e + T^3 L_e + T^4 L_e + T^5 L_e \dots = \sum_{m=0}^{\infty} T^m L_e \quad (2.54)$$

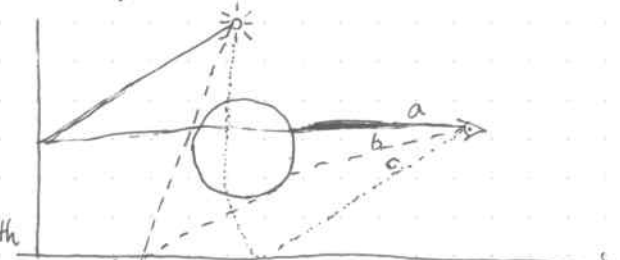
This is the Neumann series expansion of the Rendering equation, and it ...

2.6 Light Transport Notation

When describing a light path it is often necessary to distinguish between different types of surface reflection on the path.

Hackerbert has introduced a compact notation for exactly this purpose. In Hackerbert's notation the "Vertices" of the light path can be:

- L → light source
- E → eye
- S → Specular Reflection
- D → a diffuse reflection



For example, LDSSE means a path starting at the light source.

Having two diffuse reflections makes it easy to classify different paths. In this Scene, with a glossy ball and two diffuse walls, the paths are shown as:

Note: we assume that a BRDF can be composed into a Specular-like component and a diffuse-like component. For some applications it may be useful to introduce a glossy G_s reflection as well.

(a) LDSSE (b) LDSE (c) LSSDE

To describe combinations of paths it is common to use regex:

- $(k)^+$ one or more k events
- $(k)^*$ zero or more k events
- $(k)^?$ zero or one k events
- $(k|k')$ k or a k' event.



As an example $L(SID) + DE$ means a path starting at the light source having one or more diffuse or specular reflections before being reflected at a diffuse surface toward the eye.

Chapter 3 Monte Carlo Ray Tracing.

Monte Carlo Ray Tracing techniques are the most general class of global illumination. All of them methods use point sampling to estimate the illumination in a model. A point sample consists of tracing a ray through the model and computing the radiance in the direction of this ray. This concept has several advantages over finite element rendering techniques:

- Geometry can be procedural, no tessellation necessary.
- It is not necessary to precompute a representation for the solution.
- Geometry can be duplicated using instancing.
- Any type of BRDF can be handled.
- Specular reflections (on any shape) are easy, easy.
- Low memory consumption
- Accuracy controlled at the pixel/image level.
- Complexity has empirically been found to be $O(\log N)$ where N is the number of scene elements.

Compare this with the fastest $O(N \log N)$ for the fastest finite element methods.

In addition the Monte Carlo ray tracing algorithms that we describe here have the property that they are unbiased. In practice this means the only error in the result is seen as variance (noise).

3.1 Classical Ray Tracing.

Ray tracing was popularized for computer graphics by Shaded in 1980 with the introduction of the recursive ray tracing algorithm. Ray Tracing is an elegant and simple algorithm that makes it easy to render shadows and specular surfaces.

An example

The key idea in Ray Tracing is that light can be traced backwards from the observer to the light sources. In nature the light sources emit photons that scatter through the scene. Only a very tiny amount of these photons reach the eye, and a naive simulation of this process is not practical. However, we can use the fact photons move in straight lines through empty space — that radiance is constant along a line of sight (See Section 2.2.1). In addition, we can use the fact that light scattering at surfaces is symmetric (See Section 2.4.2). These two properties enable us to trace light backwards from the observer to the light sources.

The input to a ray tracer is the position of the observer, an image plane (viewing direction and field of view), and a scene description of the geometry and the materials as well as the light sources (as shown in figure 3.2). The goal is to compute the color (the average radiance) of each pixel in the image plane. This can be done by tracing one or more rays through each pixel in the image and averaging the radiance. The rays from the observer through the pixels are called primary rays.

A Ray, r , has the form:

$$r(x, \omega) = x + d \cdot \omega \quad (3.1)$$

where x is the origin of the ray, ω is the direction of the ray, and d is the distance moved along the ray.

To compute the radiance of a primary ray, we must find the nearest (small d) object intersected by a ray (this is the object that is seen through the pixel). For the example ray in Figure 3.2,

the sphere is the first object intersected.

Given an intersection point, x , we need to find the outgoing radiance in the direction of the ray. For this purpose we need to know the surface normal n , at x as well as the BRDF, f_r . With this information we can compute the illumination from each light source by estimating the radiance at x . As an example the reflected radiance, L_r , due to a point light source with power P_1 at position p can be computed as

$$L_R(x, \vec{\omega}) = f_r(x, \vec{\omega}, \vec{\omega}') \underbrace{\frac{\vec{\omega}' \cdot \vec{n}}{\|\vec{P} - \vec{x}\|^2}}_{\text{BRDF unit}} \underbrace{V(x, p)}_{\text{visibility}} \underbrace{\frac{d\sigma}{4\pi}}_{\text{area accumulation.}} \quad (3.2)$$

where $\vec{\omega}' = (\vec{p} - \vec{x}) / \|\vec{p} - \vec{x}\|$ is a unit vector in the direction of the light source. The visibility function, V , is evaluated by tracing a shadow ray from x to the light. If the shadow ray intersects an object between x and the light then $V=0$ (x is in shadow); otherwise $V=1$.

For specular surfaces, ray tracing can evaluate the specular reflection by tracing a ray in the mirror direction, $\vec{\omega}'$ (computed using equation 2.26). The radiance computation for this reflected/refracted ray proceeds exactly in the same way as for the primary ray. This is the reason why this method is called Recursive Ray Tracing.

The recursive nature of the algorithm can be seen in Fig 3.3

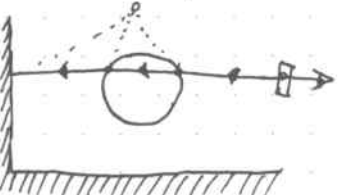


Figure 3.2. The ray-tracing algorithm traces rays (backwards) from the observer to the light. At each intersection point the direct illumination is computed, the visibility of the light source is evaluated using shadow rays (dotted lines). If the surface is specular, then a specular ray is traced in the reflected or transmitted direction. Ray tracing is not a full global illumination algorithm. It cannot compute indirect illumination on diffuse surfaces. Only for perfect specular materials can the incoming light be computed by tracing the a ray in the reflected or the mirror direction. In the light transport notation, we find that Ray tracing can compute light paths of the form:

2D PS*E

In addition, the basic ray-tracing algorithm does not compute soft shadows, following effects due to camera lenses, and motion blur. To simulate these phenomena it is necessary to use Monte Carlo Sampling as exploited for the path-tracing algorithm.

render image using ray tracing

for each pixel
pick \vec{p} ray from the eye through this pixel

Pixel color = trace (ray)

trace (ray)

find nearest intersection with scene
compute intersection point to normal
color = shade (Point, normal)

return color

shade (Point, normal)

color =

for each light source

trace shadow ray intersects light source

color = color + direct illumination

if specular

color = color + trace (reflected / refracted ray)

return color

Figure 3.3. The Ray Tracing Algorithm.

3.1.1. Algorithm.

The ray-tracing algorithm is shown in Figure 3.3. There are two functions found in every recursive ray tracer. The trace function traces rays through the scene, and finds the first intersection point with the scene objects. When an intersection is found, shade() calls shade() function which is responsible for computing the reflected radiance (color). This is done by adding the contribution (if any) from each light source, as well as tracing reflected or transmitted rays for specular surfaces.

~~A practical implementation of ray tracing can be quite complex. For each scene, for scenes with many objects, it is wasteful to check for the intersection with each object for every ray. In this situation, it is better to partition the model into smaller regions, and only test the objects in regions that a ray passes through. The most common accelerators include grids, hierarchical grids, octrees, bsp-trees, and bounding volume hierarchies. [55, 26, 39, 53, 107, 104]. An example implementation~~ In addition it can be costly to trace rays through every pixel of the image. Often an image with the same view is seen through several pixels. For these regions it is faster to interpolate the pixel values from nearby pixels. The decision to interpolate the values between two pixels can be decided based on the contrast [67] between two pixels or the local

3.2 Path tracing.

Path tracing is an extension of the Ray-tracing algorithm that makes it possible to compute a complete global illumination solution. Path tracing can simulate all possible light bounces in the model. L(CID)AE Figure 3.4 shows an example of a path tracing rendering of the simple box scene.

Figure 3.4. The box scene rendered using path tracing. Path tracing simulates all light bounces. Unlike the Ray-tracing algorithm (Figure 2.1), this image was rendered using 1k pixels/pixel. Notice the illumination on the ceiling and the caustic below the sphere.

The path-tracing technique was introduced by Hajyna in 1986 [32] as a solution to the rendering equation. The path-tracing algorithm is based on ideas introduced by Cook et al. in 1984 [21] in the distribution ray-tracing algorithm. Distribution ray-tracing uses stochastic sampling to compute effects such as soft shadows, motion blur and depth of field. The path-tracing algorithm extends this idea by stochastically sampling all light paths.

Path tracing is a straightforward extension of Ray Tracing that makes it possible to compute lighting effects that requires evaluating integration problems such as area lights and indirect light reflected by a diffuse surface. These integration problems are handled by tracing a "random" ray within the intersection domain to estimate the value of the integral. For example, if a ray intersects a diffuse material then the indirect illumination is computed by tracing a diffusely reflected ray. In the case of a Lambertian surface the direction of the ray is computed using Eq. 2.24.

To understand why this strategy works it is necessary to understand the concept of Monte Carlo integration. In path tracing the unknown function (the lighting distribution) is sampled by tracing rays stochastically along all possible light paths. By averaging a large number of sample rays for a pixel we get an estimate of the integral over all possible light paths.

By averaging over a large number of sample rays for a pixel we get an estimate of the integral over all light paths through

that pixel. Mathematically, path tracing is a continuous Markov chain random walk technique for solving the rendering equation.

The solution technique can be seen as Monte Carlo Sampling of the Neumann series outlined in 2.5.2.

Figure 3.5 The main problem with path tracing is noise. If too few samples are used the rendered image will have noisy pixels. The two images show the same box scene rendered with

(a) 10 paths/pixel and (b) 100 paths/pixel. 100 paths/pixel is not enough to eliminate noise for this simple scene.

An important aspect of the path-tracing algorithm is that it uses only one reflected ray to estimate the indirect illumination (in addition one or more rays may be used to sample the light sources). As an alternative it would have been possible to use several rays per scattering event. However, since path tracing is a recursive algorithm this would result in an exponential growth in the number of rays as the number of reflections increase.

For example, if ten rays are used to compute irradiance, and each of these ten rays intersect another diffuse surface, again use ten rays to compute the irradiance then the result is 100 rays used to compute diffuse light reflected twice.

Hajyna noticed that it is better to focus the computations on events that more undergo few reflections. By tracing only one ray per bounce, the path-tracing algorithm ensures that at least the same effort is invested in surfaces seen directly by the observer.

To compute an accurate estimate for the pixel it is necessary to average the result of several primary rays (often thousands).

The only problem with path tracing is variance in the estimates. Seen as noise in the final image. The noise is a result of using too few paths per pixel (too few samples to accurately integrate the illumination)

Figure 3.5 shows two images of the box rendered at 10 paths/pixel - 100 paths/pixel.

Such a small number of rays is usually not sufficient to render an image.

The rendering of the box scene in figure 3.4 used 1000 paths/pixel, and the noise, while still visible, does not distract from the rendering.

1,000-10,000 paths/pixel seems to be typical for most "noise-free" path-tracing images. However, if the complexity of the image is high then it may be necessary to use a higher number of samples. Figure 3.6 shows an architectural model with complex indirect illumination rendered with 1,000 paths/pixel (approximately one billion rays for the entire image).

Even with the substantial number of rays and a very long rendering time the image is quite noisy.

If the indirect illumination varies slowly, for example, for an outdoor model with a constant-colored skylight, then the path-tracing algorithm can be relatively efficient. The Jaguar model rendered in Figure 3.7 is an example of such a scene. The illumination of the car is due to a constant white hemispherical light source covering the model. In this case 100 paths/pixel is enough to get an image with little noise. The reason why path tracing works well in this case is that the function (the light) that we are trying to integrate is slowly varying.

Therefore even a few samples can give a good estimate of the integral.

Figure 3.6. Path tracing can handle complex geometry, but in a complex lighting situation such as this architectural model it is necessary to use a very high number of samples. This image was created using 1000 paths/pixel and it still contains a significant amount of noise. Even at 10,000 paths/pixel the noise is visible in this model.

Figure 3.7 Path tracing works well if the indirect illumination varies slowly. This example shows a Jaguar model illuminated by a constant colored hemispherical light source covering the entire model. The rendered image has little noise even though it was rendered at just 100 paths/pixel.

All of the images that we have shown that were rendered with path tracing contain visible noise. Unfortunately it is very costly to eliminate this noise. As explained in Appendix A this is due to the basic property of Monte Carlo integration that states the standard error is proportional to $1/\sqrt{N}$, where N is the number of samples!

$$S.E \propto \frac{1}{\sqrt{N}}$$

3.1. MK1

This means that to halve the error (the noise, the variance) it is necessary to use four times as many samples! Figure 3.8 illustrates this for the center pixel in the image of the box scene.

The noise and the cost of eliminating it is clearly a problem for path tracing and Monte Carlo ray tracing in general. Fortunately, there are several variance reduction techniques available. If the shape of the function being integrated is known, then it is possible to use importance sampling to concentrate the samples toward them. This has been done using photon mapping [41] and also dynamically building a representation of the radiance in the model [53]. Other useful optimizations include stratified sampling in which samples are placed in cells on a grid.

This ensures that the samples are properly spaced, which reduces variance. Properly stratifying the samples is an important optimization since it improves the convergence to $\frac{1}{n}$. For all the optimization techniques, the key idea is that all knowledge about the problem should be included in the sampling strategy.

More discussion on this topic found in Chapter 13.

Another very important optimization for path tracing is Russian Roulette.

Russian Roulette makes it possible to trace only through a finite number of bounces, and still get the same result as an infinite number of bounces had been performed. This is done described in a statistical technique in section 5.2.4.

For a good general overview of Monte Carlo sampling techniques in Computer graphics see [87, 56, 24, 107].

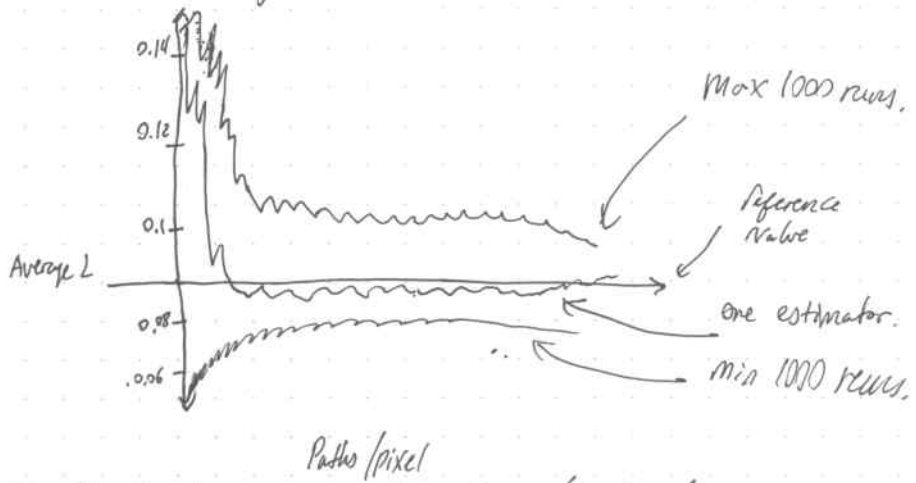


Figure 3.8. Example of convergence for one pixel (center pixel of Cornell box scene). The estimator curve shows a representative value of one estimator, this estimator is the average on N paths/pixel as indicated on the x-axis.

The min and max curves represent the minimum and maximum average value observed out of 1000 estimators.

Note: The jaggies on the example estimator curve.

This appearance is typical. Here the jaggies occur when a sample ray hits the light source via one of the specular surfaces in the model. This gives a significant contribution to the estimate and causes a jump in the average value.

(Smirnov transform) render later.

3.2.1 Algorithm.

The path-tracing algorithm is illustrated in Figure 3.9. Notice the similarity with basic ray-tracing algorithm in Fig 3.3. The main difference here is that all rays (not just Specular reflections) are traced in the shade() function, and that elements of each ray (such as time and pixel position) additional can be sampled stochastically.

render image using path tracing
for each pixel

Color = \emptyset

for each sample

Pick ray from observer through random pixel position

Pick random time and lens position for the ray

Color = Color + trace(ray)

Pixel-color = Color / # Samples

trace(ray)

Find nearest intersection with scene

Compute intersection point and normal

Color = Shade(point, normal)

return Color.

Shade(point, normal)

Color = \emptyset

for each light source

Test visibility of random position on light source
if visible

Color = Color + direct illumination

Color = Color + trace (a randomly reflected ray)

return Color.

Figure 3.9 The path-tracing algorithm.

3.3 Bidirectional Path Tracing.

Bidirectional path tracing was introduced by Lafortune and Guibas [57] in 1998 and independently in 1991 by Veach. Bidirectional path tracing traces paths starting from both the eyes as well as the light sources.

The idea behind bidirectional path tracing is to exploit the fact that certain paths are most easily sampled from the eye whereas other paths can be sampled better by starting at light.

A particular example is caustics (IS+DE paths). To sample caustics using traditional path tracing, it is necessary to trace a random diffusely reflected ray such that it goes through a series of Specular bounces before hitting the light sources.

This is often an event with a small probability but a significant contribution, and caustics are indeed a major source of noise in path tracing. Starting the path from the light source makes the problem easier, since the light has to reflect off the Specular surface, hit the diffuse surface, and then be projected onto the image plane. The concept was first introduced by Arvo [2] when he demonstrated how tracing rays from light sources could be used to render caustics.

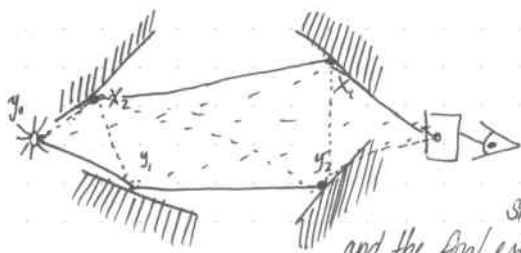


Figure 3.10 Bidirectional path tracing traces path starting from both the eye and light sources. The path vertices are connected via shadow rays (dashed lines).

and the final estimate is computed as a sum of weighted averages of the different path combinations.

Bidirectional path tracing begins by tracing two paths through the scene: one path, y_j , starting at the light source, and one path x_i , starting at the eye. The next step is combining the information in the two paths. This is done by connecting all the path vertices, where a path vertex is an intersection point along a path including the endpoints (the light and eye).

For each vertex pair, x_i and y_j , the visibility function, $V(x_i, y_j)$, is evaluated with a shadow ray (shown as dashed lines in Fig 3.10).

The next step is computing the individual contributions from the light path vertices to the eye.

Here it is important to pay attention to the fact that the light propagates flux, not radiance. We cannot simply connect the two paths and take the value from the light vertex. Instead the reflected radiance at x_i due to y_j is computed as:

$$L_{i,j}(x_i \rightarrow x_{i-1}) = f_r(y_j \rightarrow x_i \rightarrow x_{i-1}) V(x_i, y_j) \frac{|(y_j \rightarrow x_i) \vec{n}_{x_i}|}{\|x_i - y_j\|^2} I(y_j \rightarrow x_i) \quad \text{eq. (3.3)}$$

Here we have used the path notation introduced in Section 2.5.

x_{i-1} refers to the previous vertex on the eye path, and \vec{n}_{x_i} is the normal at x_i . $I(y_j \rightarrow x_i)$ is the radiant intensity leaving y_j in the direction of x_i .

NOTE: Special care needs to be taken when $i=0$: $i=j$ & the light source is directly visible, $i=0, j>0$ is a light ray reaching the eye, and the flux must be accumulated at the appropriate pixel. See [57, 107] for details on this case.

The radiant Intensity $I(y_j \rightarrow x_i)$, for a vertex on the light paths is computed as:

$$I(y_j \rightarrow x_i) = \Phi_i(y_j) / (y_j \rightarrow x_i) \cdot \vec{n}_{y_j} / f_r(y_{j-1} \rightarrow y_j \rightarrow x_i) \quad (3.4)$$

Here $\Phi_i(y_j)$ is the flux of the incoming photon at y_j . The origin of this photon is vertex y_{j-1} . \vec{n}_{y_j} is the normal at y_j .

Given Equation 3.3 (and taking into Special case $i=0$) we can compute the weighted sum of contributions from all paths:

$$Z_p = \sum_{i=0}^m \sum_{j=0}^{n_i} w_{i,j} L_{i,j} \quad (3.5)$$

where Z_p is an estimate for the pixel. This equation assumes that we have used perfect importance sampling for all BRDFs (otherwise we would have to scale $\Phi_i(y_j)$ on the eye that do not contain x_0). Note that $i=0$ will be estimates for other pixels in the image. The weights $w_{i,j}$ must be normalized:

$$\sum_{i=0}^N \sum_{j=0}^N w_{i,N-i} = 1 \quad \text{for } N=0, 1, 2, 3, \dots \quad (3.6)$$

This ensures that the weights for paths of length 0, 1, 2, 3, ... which add up to 1.

$$It is easy to see that: \quad w_{i,j} = \begin{cases} 1 & \text{for } i=0 \\ 0 & \text{otherwise} \end{cases} \quad (3.7)$$

is the standard path tracing algorithm.

The choice of weights has a substantial influence on the variation of the combined estimate. Veerh and Guibos [109] introduced a technique for combining estimators based on different sampling techniques (or different paths). They argued that the power heuristic gives good results for bidirectional path tracing. With the power heuristic the weights are computed as:

$$w_{i,j} = \frac{p_i^8}{\sum_{k=0}^{i-1} p_k^8} \quad (3.8)$$

where the power $\beta=2$. p_{ij} is the probability density for generating the path $x_0, \dots, x_i, y_j, \dots, y_s$. This path probability can be computed by multiplying the probability of generating each of the vertices in the paths:

$$p(x_i \rightarrow x_{i+1}) = p_{fr}(x_i \rightarrow x_{i+1}) \frac{[(x_i \rightarrow x_{i+1}) \cdot \vec{n}_{x_{i+1}}]}{\|x_i - x_{i+1}\|^2} \quad (3.9)$$

Here $p_{fr}(x_i \rightarrow x_{i+1})$ is the probability $\|x_i - x_{i+1}\|^2$

density for sampling the direction $x_i \rightarrow x_{i+1}$ with respect to the solid angle that is projected. For a Lambertian surface using equation 2.29 to generate a sample direction, we find that $p_{fr} = p_d$, where p_d

$p_d = \rho_d$, where ρ_d is the diffuse reflectance.

Note: probabilities for the paths starting points are different; they depend on the sampling technique used for the light source and for the pixel (See [110] for details).

The final image is computed as in path tracing by averaging a large amount of estimates per pixel. Bidirectional path tracing uses fewer samples per pixel than paths tracing. This is easy to see. Since a bidirectional path-tracing sample is a superset of a path-tracing sample. However, path tracing may still be faster since the cost of each sample in bidirectional path tracing is higher as it is the combination of two paths.

The only problem with Bidirectional path tracing is noise.

Exactly as with paths tracing the final image will be noisy unless enough samples are used. For problems with small sources of strong indirect illumination (such as caustics) bidirectional paths tracing is much better than paths tracing. For outdoor scenes where the observer is seeing only a small part of the model it is often preferable to use path tracing (for example, sending light rays from the sun toward the earth is not useful). As mentioned caustics are a good case for bidirectional paths tracing due to the light paths.

However, mirror reflections of caustics still represent a problem that is very hard to sample for bidirectional path tracing is no better than path tracing. In general path tracing is best when the light sources are "easiest" to reach the eye. otherwise bidirectional is preferable.

Another problem with Bidirectional path tracing arises when the distance between the eye vertex and the light vertex is short (such as in corners). The square of this distance is in the denominator of Equation 3.3 and the estimate can become arbitrarily large. This problem can fortunately be eliminated by using the power heuristic (eq. 3.8) since the weights associated

render image using bidirectional Path tracing

for each pixel

for each Sample

Pos = random position in pixel

tracePaths(Pos)

tracePaths (Pixel Pos)

trace primary ray from observer through pixel pos

Generate an eye path of Scattering events from the primary ray
emit random photon from the light source

generate a light paths of Scattering events from the photon
combine (eye path, light Path)

Combine (eye path, light path)

for each vertex y_j on the light path

for each vertex x_i on the eye path

if $V(x_i, y_j) == 1$ # Vertices are mutually visible

compute weight for $x_i - y_j$ path

add weighted contribution to the corresponding pixel.

Figure 3.11 The bidirectional Path tracing algorithm

3.3.1 Algorithm

The pseudocode for bidirectional paths tracing is shown in Figure 3.11.

Here the shade() function of the path tracing algorithm has been replaced with the computation of scattering probabilities for the path vertices. The combine() function resolves the weighting issue and the visibility issue for the path vertex pairs.

3.4 Metropolis Light Transport

The Metropolis Light Transport technique, MLT was introduced by Veach and Guibas [110] in 1997 as a method for exploiting the knowledge of the path space more efficiently.

The concept in the Metropolis Sampling algorithm is quite different from path tracing and bidirectional path tracing. Instead of randomly sampling a function to compute the values of an integral, the Metropolis method generates a distribution of samples proportional to the rendering function. This concept was first introduced by Metropolis et al. in 1953 [64].

For rendering this means that the MLT algorithm samples the image with rays proportional to the radiance. This is a useful feature since it automatically concentrates work in the bright regions of the image.

To achieve this sampling distribution the MLT algorithm starts with a Random Sampling (using bidirectional path tracing) of the space of all light paths in the model. These paths are then randomly cloned and modified (mutated). If the newly mutated path y is invalid (for example it goes through a wall) then it is thrown away, and the current path x is used again for an image contribution as well as for a new mutation. If the new path y is valid then it may be accepted as a new candidate path based on an acceptance probability $a(y/x)$:

$$a(y/x) = \min \left\{ 1, \frac{f(y) T(x/y)}{f(x) T(y/x)} \right\} \quad (3.10)$$

Here $a(y/x)$ is the acceptance probability of the path y given path x . $f(y)$, and $T(y/x)$ is the probability of obtaining path y , given path x .

By using this acceptance probability the mutated paths will be distributed according to the radiance. This is the basic Metropolis Sampling Scheme.

The Metropolis light transport algorithm uses several strategies for mutating paths:

- **Bidirectional Mutations:** Randomly replace segments of a path with new segments. This mutation strategy ensures the entire path space will be visited (necessary to ensure convergence).
- **Perturbations:** These include lens perturbations, Caustic perturbations, and multichain perturbations. Each of these mutation strategies are targeted towards specific important effects such as caustics. If a caustic path (LSTDE) is encountered then the caustic perturbation strategy might be used. This strategy works by making a small change to the ray connecting the Specular and diffuse surface. This makes it possible to sample small localized caustic effects.

These mutation strategies are described in more detail in [110, 107]. For each mutation strategy the acceptance probability must be evaluated.

This involves evaluating the radiance returned by the newly mutated path (done using the same techniques as bidirectional path tracing.) In addition, the transition probabilities $T(y/x)$ and $T(x/y)$ must be evaluated (i.e. the probability of changing $x \rightarrow y$ and vice versa) — notice that these probabilities are normally not symmetric.

The MLT algorithm is quite sophisticated and it is particularly good at simulating lighting situations that are normally considered difficult. These are cases where a concentrated region of space is responsible for

most of the illumination of the scene. This can be a small hole in a wall next to a room with a bright light. Once the MLT algorithm finds a path through the hole it will mutate and explore this path to capture the illumination. This is much more efficient than path tracing and bidirectional path tracing, where new random paths are used for each sample.

The MLT algorithm is quite sophisticated and is particularly good at simulating lighting situations that are normally considered difficult. These are cases where a concentrated region of space is responsible for most of the illumination in the scene. This can be a small hole in a wall next to a room with a bright light. Once the MLT algorithm finds a path through the hole it will mutate and explore this path in order to capture the illumination. This is much more efficient than path tracing and bi-directional path tracing, where new random paths are used for each sample.

For scenes with normal illumination such as the box scene that we have used in this chapter it does not seem likely that MLT will be very helpful. The specialized mutation strategies will not help much (except for the caustics) since the entire space is important for the indirect illumination. Since mutations are cheaper than sampling a complete path it may be MLT is faster. For scenes that don't have coherence — an example would be the box scene with a grid full of holes in the middle — MLT can converge more slowly since it will be "caught" in a hole and not properly investigate the illumination from other holes.

Caustics due to mirror reflections are still difficult with MLT. Even though the multi-chain perturbation was introduced to handle this case, its efficiency gets worse as the light source gets smaller, and for point sources it does not work. Neither MLT or bidirectional path tracing can render mirror reflections of caustics due to a point source. An example where this type of illumination can occur is the illuminated area of a table as seen through the base of a wine glass.

Another difficulty with MLT is that it has several parameters that significantly influence the variance of the final image.

Of particular importance are the probabilities of picking the different mutation strategies. The right choice of parameters is highly scene dependent.

3.4.1. The Algorithm

The Metropolis light transport algorithm is outlined in Figure 3.12. The choices of when to stop (if any) can be made by comparing the changes to the image as more paths are explored, or by using a fixed number of paths.

```

render image using MLT
clear image
generate N random paths
for each path x
    MLT(x)
MLT(Path x)
    add contributions from x to the image
    if done
        return
    Select mutation strategy
    y = Mutate path x
    if y is valid
        compute T(x/y) and T(y/x)
        compute L(x) and L(y)
        compute a(y/x)
        if  $\xi < a(y/x)$   $\xi \in [0, 1]$  is a random number.
            MLT(y)
        else
            MLT(x)
    else
        MLT(x)

```

Figure 3.12. The Metropolis light Transport Algorithm.

Chapter 4: The Photon mapping concept.

The purpose of this chapter is to give an overview of photon mapping approach and give some insight into the learning that motivated the development of the method. The presentation here is designed to provide an intuitive understanding; the details will be presented in following chapters.

4.1 Motivation.

Our goal is an algorithm that is capable of efficiently rendering high-quality images of complex models with global illumination. We want an algorithm capable of handling any type of geometry and use any BRDF.

Pure finite element radiosity techniques do not satisfy our requirements. Radiosity methods suffer from mesh artifacts, face problems with general BRDF representations (in particular specular materials), and are too costly for complex geometry.

An alternate to pure finite element radiosity is multi-pass techniques that use finite element techniques to compute an initial coarse solution.

The final image is then rendered with a Monte Carlo technique ray-tracing algorithm such as path tracing. (See for example [37].) These ~~two methods~~ two-pass methods are faster than pure monte carlo ray tracing and generate images of better quality than pure finite element methods, but they suffer from the limitations of the finite element techniques. In particular they cannot deal with complex geometry since the finite element pre-processing becomes ~~too~~ too costly. One paper [82] has addressed the issue using geometry simplification, where the finite element algorithm is performed on a coarse representation of the model. This reduces the complexity of the two pass methods.

However, the geometry simplification is hard and not an automatic procedure. Furthermore, the errors resulting from using simplified geometry are not understood.

Illumination maps are an alternative to the mesh-based finite element representations, where a texture map with illumination values is used to represent the irradiance of the model. This approach does, however, suffer from the same problems as the finite element methods. For illumination maps, the problem is computing the resolution of the map. It is also too costly to use illumination maps on arbitrary surfaces even if they can be parameterized. [19].

The only methods that can simulate global illumination in complex models with arbitrary BRDF's are Monte Carlo ray-tracing based techniques such as those described in the previous chapter. These techniques have several advantages:

- All global illumination effects can be simulated
- arbitrary geometry (no meshing required)
- Low memory consumption
- Result is correct except for variance. (seen as noise).

The main problem with these methods is noise (variance), and, as discussed in the previous chapter, it is very costly to eliminate this noise.

Photon Mapping was developed as an efficient alternative to the pure Monte Carlo ray tracing techniques. The goal was to have the same advantages, but at the same time obtain a more efficient method which does not suffer from the higher frequency noise.

4.2 Developing the Model.

To achieve the same general properties as Monte Carlo ray tracing it seems natural to use the same fundamental ray-tracing-based sampling technique.

In addition it seems clear that an efficient light transport algorithm must perform a sampling of both the scene both from the light sources as well as from the objects. Both the objects and the lights are the important elements in the model.

We see the scene from the point of view of the observer, but the lighting comes from the lights. Furthermore, we have already seen how certain effects are most efficient to simulate with sampling from the lights (such as caustics) or the eye (such as mirror reflections).

We want to utilize the Monte Carlo ray-tracing technique, we saw in the previous chapter, but we also want an efficient model. As such, we want to exploit the fact that the radiance field in most models is often smooth over large regions.

For these regions it makes sense to store and reuse information about the illumination. However, we do not want to generate the model or use illumination maps, since this limits the complexity of the types of models we can handle.

The primary idea is that illumination can be stored as points in a global data structure. The photon map. Several alternatives to points were considered, but they all failed to satisfy three conditions: the ability to represent highly varying illumination, being decoupled from geometry, and being compact.

In addition, points are an extremely flexible representation that makes it possible to handle non-Lambertian surfaces, (by including information about the incoming light direction of the light.) and other information to make the computations more efficient.

The photon map can be seen as a cache of the light paths in Bidirectional Path Tracing, and it would indeed be possible to use it as such. However, it also enables a different method for estimating illumination based on density estimation. Density estimation using the photon map has the advantage that the error is of low frequency rather than high frequency.

Noise seen with traditional Monte Carlo ray tracing. This is a very desirable property from a perceptual point of view since the noise is much more distracting than slow varying illumination. Finally, the density estimation method is much faster than pure Monte Carlo Ray Tracing (even if it uses many rays per pixel).

The price we pay for using density estimation to compute illumination statistics is that the method is no longer unbiased. This means the average expected value of the method may not be the correct value.

However, the technique is consistent, which means it will converge to the correct result as more points/photon are used.

We use the name photon mapping for the algorithm that generates, stores, and uses illumination as points, and the photon map is the data structure used to process these points.

Photon tracing is the technique used to generate the points representing the illumination in a model. Since this algorithm is ray-tracing based and since the photon map uses points as the fundamental primitive, we get the advantages of the ray-tracing algorithm: complex geometry, no missing, specular reflections and more.

4.3 Overview

The photon-mapping method is a two-pass method where the two passes are:

Photon Tracing: Building the photon map structure by tracing photons from the lights through the model.

Rendering: Rendering the model using the information in the photon map to make the rendering more efficient.

There are various ways that the two steps can be designed and these are discussed in the following chapters.

Chapter 5 Photon Tracing

Photon tracing is the process of emitting photons from the light sources and tracing them through a model. It is the technique used to build the Photon map (Figure 5.1 illustrates the concept). This chapter contains the details of photon tracing. We describe how photons are generated at light sources and how they are traced efficiently through the model. The techniques in this chapter form a fundamental basis for building a good photon map.

5.1 Photon Emission

Photons are created at the light sources in the model. These lights can be typical computer graphics light sources such as point lights, directional lights, and area light sources, or they can be physically based sources with arbitrary geometry and distributions. Any type of light source can be used.

Just as in nature, a large number of photons is typically emitted from each light source. The power ("wattage") of the light source is divided among all the emitted photons, and each photon therefore transports a fraction of the light source power. It is important to note that the power of the photons is proportional only to the number of emitted photons and not to the number of photons stored in the model (more detail later). The following sections contain more detail on how to emit photons from different types of light sources. Some examples shown in Figure (Fig 5.2)

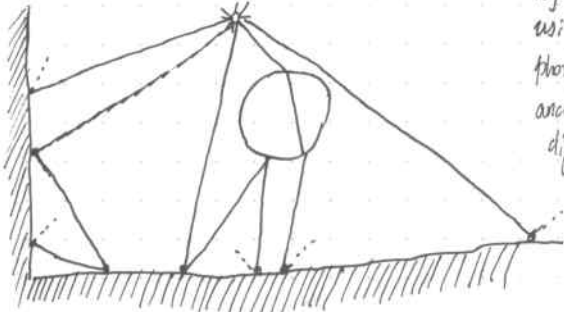


Figure 5.1 The photon map is built using the Photon tracing in which photons are emitted from the light sources and stored as they interact with the diffuse surfaces on the model.

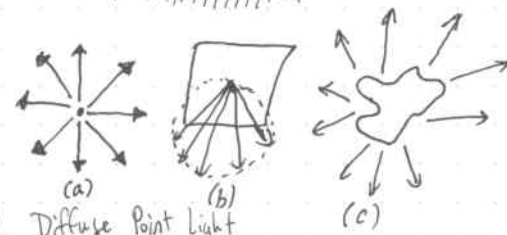


Figure 5.2 Photon emission from different light sources:
(a) point light (b) square light, and (c) complex light.

5.1.1. Diffuse Point Light

The diffuse point light is one of the simplest types of light sources. Photons from a diffuse point light are emitted uniformly in all directions.

To generate photons at a diffuse point light we use Monte Carlo Sampling. There are two major techniques for sampling a sphere uniformly: explicit Sampling or rejection Sampling. Explicit Sampling maps the random numbers

to the surface of the sphere, typically by random Sampling technique (the angles of a spherical mapping (see [90] for details)). The rejection Sampling technique uses repeated evaluation of random numbers until a certain property is present.

In the case of the diffuse point light, rejection Sampling works by generating inside the unit cube. If a point inside the unit cube is also inside the unit sphere, then it is accepted as a direction to emit a photon. Pseudocode for rejection Sampling is shown in Figure 5.3.

```

emit_photons_from_diffuse_point_light() {
    Ne = 0 # Number of emitted photons
    while (not enough photons) {
        do { # use Rejection Sampling to find new photon direction
            x = ξ₁ # ξ₁ ∈ [0,1] is a random number
            y = ξ₂ # ξ₂ ∈ [0,1] is a Random number
            z = ξ₃ # ξ₃ ∈ [0,1] is a Random number
        } while (x² + y² + z² > 1)
        d̂ = ⟨x, y, z⟩
        P̂ = light source position
        trace photon from P̂ in direction d̂
        Ne = Ne + 1
    }
    Scale power of stored photons with  $\frac{1}{N_0}$ 
}

```

Figure 5.3 Pseudocode for emission of photons from a diffuse point light using rejection Sampling

5.1.2. Spherical Light

To emit photons from a spherical light source with a given radius we can first pick a random position on the surface (using, for example, a rejection Sampling technique similar to the one used for picking directions from the point light) and next a random direction in the hemisphere above this position. For a diffuse spherical light the probability of selecting a given outgoing direction should be proportional to the cosine of the outgoing angle. This is necessary to take into account the fact that the receiver sees the projected surface area of the light source. See Section 2.4.4 for information on how to generate this direction.

5.1.3 Square light

Emission of photons from a square light source is similar to the procedure for the spherical light. First a Random position on the square is Selected, then a Random position direction is selected. Similarly for a diffuse square light the probability of selecting a given outgoing direction should be proportional to the cosine of the outgoing angle. (eq. 2.24)

5.1.4 Directional light: is a non-physical light: no such concept exists in nature.

Nonetheless it can be a useful approximation for very distant lights such as the sun.

For directional lights we need to know the bounding volume (for example a sphere around the entire model. A photon direction is found by selecting a random position within the projected bounding volume.

The origin of this photon should be outside the bounding volume. Note that in the case of directional lights, the power of the light source should be given as radiant emittance, so that it is independent of the size of the scene. Each photon still transports flux, but the projected area of the scene also needs to be taken into account.

5.1.5 Complex Light.

For a complex light with arbitrary shape and emission profile, the photons should be emitted with a density proportional to the distribution of the light source. Generating photons with a density that matches the emission profile ensures that the power of the emitted photons is the same. This is a good property that gives us better photon map statistics. (In particular the radiance of the next chapter.)

The simplest way to handle a complex light source is to choose some random position and direction on the light and then simply scale the power of the photon according to the emissive profile of the light. This may result in photons that have highly varying power levels, and thus reduce the final quality of the statistics of the photon map.

Another simple technique for handling complex lights is rejection sampling. This works by picking a random photon (position and direction), and computing a probability p_i of generating this photon (the intensity of the light source in that direction divided by the total power of light source). Another random number, ξ , is then compared with p_i , and only if $(\xi < p_i)$ is the photon emitted; otherwise another random location and direction is selected. This technique may be slow for light sources with varying intensity distributions, but it has the advantage that the emitted photons have the same power.

5.1.6 Multiple Lights.

If the scene contains multiple light sources, photons should be emitted from each light source. More photons should be emitted from bright lights than from dim lights, to make the power of all emitted photons approximately even. One might worry that scenes with many light sources would require many more photons to be emitted than scenes with a single light source.

Fortunately, it is not so. In a scene with many light sources, each light contributes less to the overall illumination, and typically fewer photons can be emitted from each light. If, however, only a few light sources are important one might use visual importance [76, 105] to concentrate the photons in the areas that are of importance to the scene.

5.1.7 Projection Maps

In scenes with sparse geometry, many emitted photons will not hit any objects. Emitting these photons is a waste of time. To optimize the emission, projection maps may be used [40, 42]. A projection map is a map of the geometry as seen from the light source. This map is made of many little cells. A cell is "on" if there is geometry in that direction, and "off" if not.

For example, a projection map is a spherical projection of the scene for a point light, and it is a planar projection of the scene for a directional light. To simplify the projection it is convenient to project the bounding sphere around each object or around a cluster of objects [42]. This also significantly speeds up the computation of the projection map since we do not have to examine every geometric object in the scene. The most important aspect of the projection map is that it gives a conservative estimate of the directions in which it is necessary to emit photons from the light source. A conservative estimate of this is essential to ensure that we capture all important effects such as caustics, which can be very localized.

The emission of photons using a projection map is very simple. One can loop over the cells that contain objects and emit a random photon into the directions represented by the cell. This method can, however, lead to a biased result since the photon map can be "full" before all cells have been visited.

An alternative approach is to generate random directions and check if the cell corresponding in that direction has any objects (if not a new random direction should be tried). This approach works well usually work, but for sparse scenes it may be costly. For sparse scenes it is better to generate photons randomly for the cells which have objects. A simple approach is to pick a random cell with objects and then pick a random direction for the emitted photon for that cell. [40] In all circumstances it is necessary to scale the power of the emitted photons based on the solid angle of the active cells in the projection map [42].

Another important optimization for the projection map is to identify objects with specular properties (i.e. objects that can generate caustics) [92]. As will be described later, caustics are generated separately, and since specular objects often are distributed sparsely, it is very beneficial to use the projection map for caustics.

5.2 Photon Scattering

When a photon is emitted, it is traced through the scene using photon tracing.

Photon tracing works exactly in the same way as ray tracing, except for the fact that photons propagate flux whereas rays gather radiance. This is an important distinction since the interaction of a photon with a material can be different than the interaction of a ray.

A notable example is refraction, where radiance is changed based off the relative index of refraction [3]—this does not occur with photons.

When a photon hits an object, it can either be reflected, transmitted or absorbed. Whether it is reflected, transmitted, or absorbed is decided probabilistically based on the material parameters of the surface. The technique used to decide the type of interaction is known as *Russian Roulette*.

In the following we will describe how to reflect a photon off different types of materials and how to utilize the photons more efficiently by using Russian Roulette.

5.2.1. Specular Reflection

If a photon hits a mirror surface a new photon is reflected in the mirror direction given a normal \vec{n} , and an incoming direction, \vec{w} , the reflected direction, \vec{w}' , is found as:

$$\vec{w}' = 2(\vec{n} \cdot \vec{w}')\vec{n} - \vec{w}' \quad (5.1)$$

where the incoming direction is assumed to point away from the intersection point. This equation is the same that is used in ray tracing to trace specularly reflected rays. The power of the reflected photon should be scaled by the reflectivity of the mirror (unless Russian Roulette Sampling is used).

5.2.2 Diffuse Reflection

When a photon hits a diffuse surface it is stored in the photon map. The direction of the diffusely reflected photon (from a Lambertian surface) is found by picking a random direction in the hemisphere above the intersection point with a probability proportional to the cosine of the angle with the normal. The expression for this is given in Eq 2.24.

The power of the reflected photon is found by scaling the power of the incoming photon with the diffuse reflectance (unless Russian Roulette is used.)

5.2.3 Arbitrary BRDF Reflection

Given an arbitrary BRDF the new photon direction should be computed by importance sampling the BRDF. For several reflection models the importance sampling function can be found analytically. Examples include Ward's anisotropic model [115] and Lafortunes reflection model [53].

If importance-sampling function is unavailable, then a random direction can be selected. The power of the reflected photon should then be scaled according to the BRDF as well as the reflectivity of the material. Alternatively, it may be better to use rejection sampling similar to the approach described for complex lights.

Photon Scattering with the Schlick's Model

For Schlick's model presented in chapter 2 we need to pick the type of reflection (Lambertian, glossy, specular). This can be done using Russian roulette as described in the next section. For the glossy reflection we do not have the a perfect importance sampling function (only for $Z(+A(w))$ terms), so this factor has to be scaled with the geometrical factor G as explained in Section 2.4.6.

5.2.4 Russian Roulette

A very important technique in photon tracing is Russian Roulette. It is a stochastic technique used to remove unimportant photons so that the effort can be concentrated on the important photons. It is also used to ensure that the stored photons have approximately the scene power. This is important for good quality of the radiance estimate that will be presented in chapter 7.

Russian roulette is a standard monte carlo technique introduced to speed up computation in particle physics [101]. Russian roulette was introduced to graphics by Arvo and Kirk [3].

The basic idea in Russian roulette is that we can use probabilistic sampling to eliminate work and still get the correct result. It can be thought of as an importance-sampling technique where the probability distribution function is used to eliminate unimportant parts of the domain. Given a probability, p , that another radiance estimate, L_n , is evaluated we find that:

$$L_n = \begin{cases} \frac{E\{P\}}{p} & \\ \text{otherwise} & \end{cases} \quad (5.2)$$

Here L is computed typically by tracing another ray. To see why this works we can compute the expected value of the estimator for L :

$$E\{L\} = (1-p) \cdot 0 + p \cdot \frac{E\{Z\}}{p} = E\{L\} \quad (5.3)$$

Here we see that the Russian roulette scheme does give us the right unbiased estimate of L . The fact that we get the *important* correct result even though we do not evaluate all of the problem is important. It means that we can trace a ray through a finite number of bounces and still obtain the correct result as if we had an infinite number of bounces!

In the following we give some examples of the use of Russian Roulette. It is often used to decide whether a photon should be reflected, absorbed, or transmitted, and to decide whether a reflected photon should be reflected differently or specularly.

Reflection or absorption?

Given a material with reflectivity ρ , and an incoming photon with power Φ_p , we can use Russian roulette to decide if the photon should be reflected or absorbed. This is illustrated in the following pseudocode:

```

p=d
ξ=random
if (ξ < p)
    reflect photon with power Φp
else
    Photon is absorbed
  
```

The intuition behind this algorithm is very simple. Imagine shooting 1000 photons at a surface with reflectivity 0.5. We can either reflect 1000 with half power, or we can reflect 500 photons with full power. Russian Roulette enables us to select more SM photons. As shown by this example, Russian roulette can be a powerful technique for reducing the computational requirements for photon tracing.

Specular or Diffuse Reflection

Another simple example is in the case of a surface with both specular and diffuse reflection. The diffuse reflectance is ρ_d and the specular reflectance coefficient is ρ_s ($\rho_d + \rho_s \leq 1$). Again we choose a uniformly distributed random variable $\xi \in [0, 1]$ and make the following decision:

```

ξ ∈ [0, ρd] → diffuse reflection
ξ ∈ [ρd, ρd+ρs] → Specular reflection
ξ ∈ [ρs+ρd, 1] → absorption
  
```

If the photon is reflected, the power should not be modified - correctness is ensured by averaging several photon interactions over time.

Specular or Diffuse Reflection (RGB)

With more color bands (for example RGB colors), the decision gets slightly more complicated. Consider again a surface with some diffuse reflection and some specular reflection, but this time with different reflection coefficients in the three color bands.

To select the type of reflection we can use the same approach as described in the previous section. For the reflectance we can use the average diffuse reflectance, $\rho_{d, avg}$, and the average specular reflectance, $\rho_{s, avg}$:

$$\rho_{d, avg} = \frac{\rho_{d,r} + \rho_{d,g} + \rho_{d,b}}{3} \quad (5.4)$$

$$\rho_{s, avg} = \frac{\rho_{s,r} + \rho_{s,g} + \rho_{s,b}}{3} \quad (5.5)$$

Here the subscripts r,g,b denote³ reflectance in the red, green, blue band respectively. Using the average reflectance values we find that:

- $\xi \in [0, \rho_{d, avg}] \rightarrow$ diffuse reflection
- $\xi \in [\rho_{d, avg}, \rho_{s, avg} + \rho_{d, avg}] \rightarrow$ specular reflection
- $\xi \in [\rho_{s, avg} + \rho_{d, avg}, 1] \rightarrow$ absorption

To account for the fact that the reflection should have used a spectral reflectance value, we need to scale the power of the reflected photon. If specular reflection is chosen we get:

$$\begin{aligned}\bar{\Phi}_{s,R} &= \bar{\Phi}_{i,R} \rho_{s,R} / \rho_{s, avg} \\ \bar{\Phi}_{s,g} &= \bar{\Phi}_{i,g} \rho_{s,g} / \rho_{s, avg} \\ \bar{\Phi}_{s,b} &= \bar{\Phi}_{i,b} \rho_{s,b} / \rho_{s, avg}\end{aligned}$$

where $(\bar{\Phi}_{i,R}, \bar{\Phi}_{i,g}, \bar{\Phi}_{i,b})$ is the spectral reflectance value, we need to scale the power of the reflected photon and $(\rho_{s,R}, \rho_{s,g}, \rho_{s,b})$ is the spectral power of the reflected photon.

It is simple to extend the selection scheme also to handle transmission, to handle more than three color bands, and to handle combinations of multiple BRDFs.

Why use Russian Roulette?

Why do we go through this effort to decide what to do with a photon? Why not just trace new photons in the diffuse and specular directions and scale the photon energy accordingly? There are two main reasons why the use of Russian Roulette is a good idea. Firstly, we prefer photons with similar power in the photon map. This makes the statistics of the photon map much better. Secondly, if we generate, say, two photons per surface interaction then we will have 2^8 photons after 8 interactions.

This means 256 photons after eight interactions compared to one photon coming directly from the light source! Clearly this is no good.

We want at least as many photons that have only 1-2 bounces as photons that have made 5-8 bounces. The use of Russian Roulette is therefore very important in photon tracing.

There is one caveat with Russian Roulette: it increases variance on the solution. Instead of using the exact values for reflection and transmission to scale photon energy, we now rely on sampling of these values that will converge to the correct result as enough photons are used.

More details on Russian Roulette [101, 88, 74, 28].

5.3 Photon Storing

As already mentioned photons are stored only when they hit diffuse surfaces. (or more precisely, non-specular surfaces). The reason is that storing photons on specular surfaces does not give any useful information: the probability of having a matching incoming photon from a specular direction is small (and zero for perfect Specular materials); So, if we want to render accurate Specular reflections, the best way is to trace a ray in the mirror direction using standard Ray Tracing. For all other photon-surface interactions, data is stored in a global data structure, the photon map. Note

that each emitted photon can be stored several times along its path.

Also, information about a photon is stored at the surface, where it is absorbed if that surface is diffuse.

It is important to realize that photons represent incoming illumination (flux) at the surface. This is a valuable optimization that enables us to use a photon to approximate the reflected illumination at several points on a surface even if the surface is textured (more details in chapter 7.)

Figure 5.4 shows the stored photons (estimated flux density) in the box scene. Notice how the photons estimate the incoming illumination and how the density is higher in regions with strong incoming illumination, such as in the caustic glass sphere.

Figure 5.4 The photons stored in the box scene. The top picture shows the box scene, and the lower image shows the photon hits. We used 100,000 photons in this image. The photon fat represents incoming flux in the model. Each photon shows the incoming flux density - the power of the photons multiplied by the local photon density.

Chapter 6 The Photon Map Data Structure : The photon map is a representation (a map) of all the stored photons in the model. A fundamental aspect of the photon map is that it is decoupled from the geometry in the model. This means that we do not associate photons with certain geometry, but instead keep them in a separate structure. This chapter describes the actual data structure used and efficient techniques for representing and using it.

6.1 The Data Structure : Photons are only generated during the photon tracing pass. When the image is rendered, the photon map is a static data structure that is used to compute statistics of the illumination in the model. The statistics are based on the nearest photons at any given point, and can be computed at all locations in the model.

In order for the Photon-Mapping algorithm to be practical, the data structure has to be fast when it comes to locating nearest neighbors in a three dimensional data set. At the same time it should be compact since we intend to use millions of photons.

We can immediately discard simple structures such as arrays and lists. Since searching these for nearest neighbors is costly, far too costly.

A simple data structure for maintaining proximity within a set of points is the three-dimensional grid in which a cube containing the photons is divided uniformly along x, y, and z into a number of subcubes, each containing photons. A search for the nearest neighbors is simply a matter of finding the right subcube and examining the photons in the cube and perhaps the neighboring cubes. This strategy is near optimal if data is uniformly distributed in three-dimensional space. This however is not the case with photons. Since the photons are stored at surfaces they will be distributed highly non-uniformly for most models. Furthermore certain important light effects such as caustics can focus light and thus generate a very high concentrations of photons in a small volume. This non-uniform nature of the photons makes the three dimensional grid impractical.

A data structure that is much better at handling the non-uniform distribution of photons is the k-d-tree [5, 6, 7] (See Figure 6.1(a)). The k-d-tree [5, 6, 7] is a multidimensional binary search tree in which each node is used to partition one dimension. (A one dimensional k-d-tree is simply a binary tree). The photon map is a three-dimensional point set and we need a three dimensional tree quite similar to the B+-tree [104] to store the photons.

Each node in the tree contains one photon and pointers to the left and right subtrees. All nodes except for the leaf nodes have one axis-orthogonal plane that cuts one of the dimensions, (x, y, z) nodes except into two pieces. All photons in the left subtree are below this plane and all photons in the right subtree are above the plane. This structure makes it possible to locate one photon in the k-d-tree with n photons in $O(\log n)$ time on average, but $O(n)$ worst time if the tree is very skewed. If the tree is balanced, the worst case time becomes $O(\log n)$. It has been shown that on average the time it takes to locate the k nearest neighbors is on the order of $O(k \log n)$ [6] which, combined with the fact that k-d-trees can be represented efficiently, makes the k-d tree a good candidate for storing the photon map.

Another efficient structure for solving Nearest-Neighbor-based queries is the Voronoi Diagram [4,87] (see Figure 6.1(b)) — the dual of the Delaunay Triangulation. In the Voronoi diagram each node is linked to its nearest neighbors (the natural neighbors).

Locating the nearest points can be done by starting at a random node (point) and then performing a directed walk toward the node (point) of interest by recursively selecting the next node as the one nearest to its point of interest.

Having found the node, it is trivial to make a recursive examination of the nearest neighbors. The directed walk ~~toward the~~ can be rather complex in three dimensions and to optimize it one can construct a Natural tree [119] (which is good for locating a specific node) upon the Voronoi diagram. Voronoi diagrams support queries for the nearest neighbors in $O(k \log n)$ time [4].

Furthermore the Voronoi diagram can provide information on the density of points — this information is used when radiance is estimated (Chapter 7).

Unfortunately the Voronoi diagram requires $O(n^2)$ storage in three dimensions [4] which is too costly for use with the photon map.

Given our requirements for efficiency, the kd-tree seems a natural choice for the Photon Map. In addition to being a reasonably fast structure for locating nearest neighbor, the kd-tree provides a very compact representation. In the following sections we will give the details of how to manage the kd-tree, including how to balance the kd-tree and how to efficiently locate the nearest photons in this balanced tree.

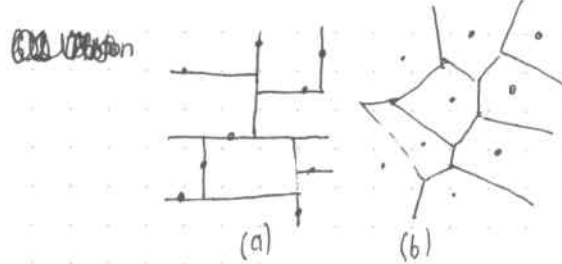


Figure 6.1 A two dimensional point set classified using
(a) kd-tree and (b)
a Voronoi diagram

6.2 Photon Representation

For each photon-surface interaction, the position, incoming photon power, and incident direction are stored. Expressed in C the following structure is used for each photon [42]:

struct Photon {

float X,Y,Z; //Position (3x32bit floats)

char Pwr; //Power packed as 4 chars

char Phi,Theta; //Compressed incident direction

short flag; //Flag used in kd-tree

The power of the photon is represented compactly as four bytes using Ward's shared-exponent RGB format [114]. If memory is not of concern, one can use three floats to store the power in the red, green, and blue color band (or, in general, one float per color band if a spectral simulation is performed).

The incident direction is a mapping of the spherical coordinates of the photon direction to 65536 possible directions. They are computed as:

$$\text{Phi} = 256 * \text{atan2}(dy, dx) / (2 \cdot \pi)$$

$$\text{Theta} = 256 * \text{acos}(dx) / \pi$$

where atan2 is from the standard C Library. Recall that atan2(y,x) returns the absolute angle ($0 - 2\pi$) of the vector (x,y) with the positive x-axis. The direction is used to compute the contribution for non-Lambertian surfaces [44], and for Lambertian surfaces it is used to check if a photon arrived at the front of the surface. Since the photon direction is used often during rendering, it pays to have a lookup table that maps the theta, phi direction to three floats directly instead of using the formula for spherical coordinates, which involve the costly cos() and sin functions.

A minor note is that the flag in the structure is a short. Only two bits of this flag is used (this is for the splitting plane axis in the kd-tree), and it would be possible to use just one byte for the flag. However for alignment reasons it would be preferable to have a 20 byte photon rather than a 19 byte photon — on some architectures it is a necessity, since the float value in subsequent photons must be aligned on a four-byte address.

We might be able to compress the information more by the fact that we know the cube in which the photon is located. The position is however, used very often when the photons are processed and, by using standard float, we avoid the overhead involved in extracting the true position from a specialized format.

During the photon-tracing pass, the photon map is arranged as a flat array of photons. For efficiency reasons this array is reorganized into a balanced kd-tree before rendering, as explained in Section 6.3.2.

6.3 The Balanced Kd-Tree

The complexity for locating one photon in a balanced kd-tree is $O(\log N)$, where N is the number of photons in the tree. Once the photon map is created by tracing photons randomly through a model, one might think that a dynamically built kd-tree would be quite well-balanced already. However, the fact that the generation of the photons at the light source is based on the projection map combined with the fact that models often contain highly directional reflectance models easily results in a skewed tree. Since the tree is created only

It is quite natural to consider balancing the tree. Examples of using a balanced versus an unbalanced kd-tree can be found in [94].

6.3.1. Memory Layout

The balanced kd-tree can be represented very compactly by using heap-like data structures [86]. In this structure it is not necessary to store pointers to the sub-trees explicitly. In the heap data structure it is not necessary to store pointers to the sub-trees explicitly. In the heap structure the array element at index 1 is the root, and element i has element $2i$ as left child and element $2i+1$ as the right child. Left-balancing the tree ensures that the heap does not contain empty slots. Not storing pointers saves eight bytes (on a 32-bit architecture), which is 40% in the case of the compact 20-byte photon representation. This can lead to substantial savings when a large number of photons are used.

6.3.2. Balancing Algorithm.

Balancing a kd-tree is similar to balancing a binary tree. The main difference is the choice at each node of a splitting dimension. When a splitting dimension of a set is selected, the median of the points in that dimension is chosen as the root node of the tree representing the set, and the left and right subtrees are constructed from the two sets separated by the median point. The choice of a splitting dimension is based on the distribution of points within the set. One might use either the variance or the maximum distance between the points as a criterion. We prefer a choice based upon maximum distance since it can be computed very efficiently (even though a choice based upon variance might be slightly better). The splitting distance dimension is thus chosen as the one which the largest maximum distance between points.

Figure 6.2 contains a pseudocode outline for the balancing algorithm [43].

To speed up the balancing process, it is convenient to use an array of pointers to the photons. In this way only pointers need to be shuffled during the median search. An efficient median search algorithm can be found in most textbooks on algorithms — see for example [86] or [22].

The complexity of the balancing algorithm is $O(N \log N)$, where N is the number of photons in the photon map. In practice, this step only takes a few seconds even for several million photons.

KdTree *balance (Points) {

 Find the cube surrounding the points

 Select dimension dim in which the cube is largest

 Find median of the points in dim

 S1 = all points below median

 S2 = all points above median

 Node = median

 node.left = balance (S1)

 node.right = balance (S2)

 return node

}

Figure 6.2. Pseudocode for balancing the photon map.

6.4 Locating The Nearest Photons Efficiently

Efficiently locating the nearest photons is critical for good performance of the photon mapping algorithm. In scenes with caustics, multiple diffuse reflections, and/or participating media, there can be a large number of photon map queries.

6.4.1. Algorithm.

Fortunately the simplicity of the kd-tree permits us to implement a simple but quite efficient search algorithm. This search algorithm is a straightforward extension of the standard search algorithms for binary trees [22, 26, 36].

It is also related to range searching, where kd-trees are commonly used as they have optimal storage and good performance [80]. The nearest-neighbors query for kd-trees has been described extensively in several publications by Bentley et al., including [5, 6, 7, 8]. More recent publications include [80, 26].

Some of these papers go beyond our description of a nearest-neighbors query by adding modifications and extensions to the kd-tree to further reduce the cost of searching. We do not implement these extensions because we want to maintain a low storage overhead of the kd-tree, as this is an important aspect of the photon map.

Locating the nearest neighbors in a kd-tree is similar to range searching [82] in the sense that we want to locate photons within a volume. For the photon map it makes sense to restrict the size of the initial search range, since the contribution from a fixed number of photons becomes small for large ranges. This simple observation is particularly important for caustics as they often are concentrated in small regions. A search algorithm that does not limit the search range will be slow in such situations. Since a large part of the kd-tree will be visited for regions with a sparse amount of photons.

Given the photon map, a position x and a max search distance d^2 this recursive function returns a heap H with the nearest photons. Call with `locate_photons(1)` to initiate search at the root of the kd-tree.

```

locate_photons(p) {
    if ( $2p+1 < \text{number of photons}$ ) {
        examine child nodes
        // Compute distance to plane (just a subtract.)
         $s = \text{Signed distance to splitting plane of node } n$ 
        if ( $s < 0$ ) {
            // We are left of the plane - Search left subtree first
            locate_photons( $2p$ )
            if ( $s^2 < d^2$ )
                locate_photons( $2p+1$ ) # check right subtree
        } else {
            // We are right of the plane - Search right subtree first
            locate_photons( $2p+1$ )
            if ( $s^2 < d^2$ )
                locate_photons( $2p$ ) # check left subtree
        }
    }
}

 $s^2 = \text{Squared distance from photon } p \text{ to } x$ 
if ( $s^2 < d^2$ ) { // check if the photon is close enough?
    insert photon into max heap  $H$ 
    # Adjust maximum distance to pruned search
     $d^2 = \text{squared distance to photon in root node of } H$ 
}

```

Figure 6.3 Pseudocode for locating nearest photons in the photon map.

A generic nearest-neighbors search algorithm begins at the root of the kd-tree and adds photons to a list if they are within a certain distance. For the n nearest neighbors, the list is sorted such that the photon that is furthest away can be deleted if the list contains n photons and a newer closer photon is found. Instead of naive sorting of the full list it is better to use a max heap [80, 86, 86]. A max heap (Also known as a priority queue) is a very efficient way of keeping track of the element that is furthest away from the point of interest. When the max heap is full, we can use the distance of to the root element (i.e. the photon that is furthest away) to adjust the range of the query. Thus we skip parts of the kd-tree further away than d .

Another simple observation is that we can use squared distances — we do not need the real distance. This removes the need for the costly square root calculation per distance check.

The pseudocode for the search algorithm is given in Figure 6.3. Appendix B has the source code of an implementation of this routine.

For this search algorithm it is necessary to provide an initial maximum search radius. A well-chosen radius allows for good pruning of the search, reducing the number of photons tested. A maximum radius that is too low will on the other hand, introduce noise in the photon map estimates.

The radius can be chosen based on an error metric or the size of the scene. The error metric could, for example, take the average power of the stored photons into account and compute a maximum radius from that, assuming some allowed error in the radiance estimate.

A few extra optimizations can be added to the search routine: for example, a delayed construction of the max heap to the time when the number of photons needed has been found. This is particularly useful when the requested number of photons is large.

Chapter 7 The Radiance Estimate.

Given a photon map we can begin to compute various types of statistics of the illumination of the model. We have already seen how the density of the photons indicate how much light a given region receives. In this chapter we demonstrate how the photon map can be used to estimate the reflected radiance at any surface location in the model.

7.1 Density Estimation

The photon map represents incoming flux in the model. Each photon transports a fraction of the light source power, and a photon hit in a region indicates that this region is receiving some illumination from the light source either directly or indirectly. However, based on a single photon say how much light the region receives. This is given by the photon density, $d\Phi/dA$, and to estimate the irradiance for a given region we therefore need to compute the density of the photons.

 The first methods using the photon tracing [2, 87] used illumination maps (similar to texture maps, but storing illumination instead of color.) to bin the photons. Later approaches used a tessellated version of the geometry to store the photons [74]. In all of these approaches the individual photons are not stored explicitly. Instead the power carried by the photons is accumulated for some local region. Knowing the area of this region immediately gives an estimate of the photon density. This approach can be seen as a histogram approach to density estimation.

Density estimation is a research area in statistics, and several books have been written about density estimation functions [96, 97]. It is well known that the histogram-based density based estimation approach is inferior to another class of density estimation approaches: the kernel density estimation techniques. Kernel Density estimation techniques speak directly on the individual elements, in our case the Photon Bits, and use a local Kernel operator to smooth the estimate.

Storing the individual photon Bits makes it possible to use kernel density estimation, but it also has several other advantages. The histogram approach is only practical as long as the number of elements is not too large. In addition all histogram approaches so far have been restricted to Lambertian surfaces, where the incoming direction of photons can be ignored. This reduces the dimensionality of the density estimation problem and makes it possible to use fewer photons. Unfortunately, it limits the simulation to only consider illumination on Lambertian surfaces. We remove the Lambertian Surfaces restriction of the previous approaches by storing the incoming direction of the photons in the photon map.

The photon map is decoupled from the geometry. A similar geometry decoupling has not been demonstrated for this histogram approach. Storing illumination in illumination maps or with geometry represents a tight coupling with the geometry that puts a limitation on the complexity of the models that the histograms can handle. In particular the histogram methods rely on a "good" optimal bin size to get good statistics, for complex models the size of the individual geometric elements can vary significantly. For example, in a room the door handle might be modeled very accurately with many tiny polygons. Getting good local statistics for these polygons requires tracing enough photons through the model such as these polygons each receive some photons. In most cases a histogram-based approach will risk getting zero photons in small polygons, resulting in no illumination at any point which can result in block pixels in the rendered image — for high quality image synthesis this is not acceptable. As a contrast, the use of individual photons makes it possible to get a reasonable estimate of the illumination at any point in the model regardless of the geometry. For the door handle case, this means that we do not need a photon for every polygon, but instead just a few photons to estimate the incoming flux in the region around the door handle. The radiance estimate that is derived in the next section is capable of providing an estimate of the illumination even in situations where the geometry is highly complex.

7.2 Derivation.

To compute reflected Radiance at a surface location we need to evaluate the expression for reflected Radiance (from Section 2.5):

$$L_r(x, \vec{\omega}) = \int_{\Omega_x} f_r(x, \vec{\omega}, \vec{\omega}') L_i(x, \vec{\omega}') (\vec{n}_x \cdot \vec{\omega}') d\omega' \quad (7.1)$$

where L_r is the reflected radiance at point x in direction $\vec{\omega}$. Ω_x is the hemisphere of incoming directions, f_r is the BRDF (See Section 2.4.2) at x , and L_i is the incoming radiance. For this integral we need information about the incoming radiance. Since the photon map provides information about the incoming flux, we have to rewrite this term. This can be done using the relationship between radiance and flux:

$$L_r(x, \vec{\omega}) = \int_{\Omega_x} \frac{d^2 \Phi_i(x, \vec{\omega}')}{(\vec{n}_x \cdot \vec{\omega}') d\vec{\omega}' dA_i} \quad (7.2)$$

We can rewrite the integral as

$$\begin{aligned} L_r(x, \vec{\omega}) &= \int_{\Omega_x} f_r(x, \vec{\omega}', \vec{\omega}) \frac{d^2 \Phi_i(x, \vec{\omega}')}{(\vec{n}_x \cdot \vec{\omega}') d\vec{\omega}' dA_i} (\vec{n}_x \cdot \vec{\omega}) d\vec{\omega}' \\ \Rightarrow L_r(x, \vec{\omega}) &= \int_{\Omega_x} f_r(x, \vec{\omega}', \vec{\omega}) \frac{d^2 \bar{\Phi}_i(x, \vec{\omega}')}{dA_i} \end{aligned} \quad (7.3)$$

The incoming flux $\bar{\Phi}_i$ is approximated using the photon map by locating the n photons that have the shortest distance to x . Each photon p has the power $\Delta \bar{\Phi}_p(\vec{\omega}_p)$ and, by assuming that the photon intersects the surface at x , we obtain

$$L_r(x, \vec{\omega}) \approx \sum_{p=1}^n f_r(x, \vec{\omega}_p, \vec{\omega}) \frac{\Delta \bar{\Phi}_p(x, \vec{\omega}_p)}{\Delta A} \quad (7.4)$$

The procedure can be imagined as expanding a sphere around x until it contains n photons (see figure 7.1) and then using these n photons to estimate Radiance.

Equation 7.4 still contains ΔA , which is related to the density of the photons around x . By assuming that the surface is locally flat around x , we can compute this area by projecting the sphere onto the surface and use this area of the resulting circle. This is indicated by the grey area in Figure 7.1 and equals:

$$\Delta A = \pi r^2 \quad (7.5)$$

where r is the radius of the sphere — i.e. the largest distance between x and each of the photons. This is equivalent to using a nearest-neighbor density estimation technique [98].



Figure 7.1. Reflected radiance is evaluated by locating the nearest photons in the photon map in order to estimate the local photon density. This approach can be seen as expanding a sphere around the intersection point until it contains enough photons. The photon density is estimated based on the surface area covered by the sphere. The result is an equation that makes it possible to compute an estimate of the reflected radiance at any surface using the photon map:

$$L(x, \vec{\omega}) \approx \frac{1}{\pi r^2} \sum_{p=1}^N f(x, \vec{\omega}_p, \vec{\omega}) \Delta \Phi_p(x, \vec{\omega}_p) \quad (7.6)$$

The radiance estimate is based on many assumptions and the accuracy depends on the number of photons used in the photon map and in the formula. Since a sphere is used to locate the photons, one might easily include wrong photons in the estimate, in particular in corners and at sharp edges of objects. Edges and corners also cause the area estimate to be wrong. The size of those regions in which these errors occur depends largely on the number of photons in the photon map and in the estimate. As more photons are used in the estimate and in the photon map, Eq 7.6 becomes more accurate. If we ignore the error due to limited accuracy of the representation of the position, direction, and flux, then we can go to the limit and integrate the photons to infinity or near infinity. This gives the following interesting result where N is the number of photons in the photon map: $L \propto [N]$

$$\lim_{N \rightarrow \infty} \frac{1}{\pi r^2} \sum_{p=1}^N f_r(x, \vec{\omega}_p, \vec{\omega}) \Delta \Phi_p(x, \vec{\omega}_p) = L_r(x, \vec{\omega}) \quad \forall \vec{\omega} \in [0, 1]. \quad (7.7)$$

- Plate I. Path tracing can simulate full global illumination, but often results in noisy images as seen in the box scene. (See figure 3.5)
- Plate II. Finite element radiosity algorithms are good at simulating diffuse interreflections as seen in this replica of the widely used Cornell box. (Fig 1.4)
- Plate III. Photon mapping can simulate full global illumination in complex models as seen in this rendering of an architectural model (Fig 1.2)
- Plate IV. Acoustic through a glass of cognac. (Fig 8.9)
- Plate V. Closeup of the caustic in plate IV. (See Fig 8.10)
- Plate VI. The box scene ray-traced (Fig 9.10)
- Plate VII. The box scene with full global illumination. (Fig 9.9)
- Plate VIII. A rendering of a geometrical model of little Matterhorn, with a camera in the foreground.

at sunset. We use 10^6 photons for this model to simulate the illumination from the Sun as well as the sky. (Fig 9.16)

Plate IX. Sequence of rendered images from a simulation of smoke flowing past a sphere. (From [25]). (See Fig 10.11)
Plate X. A simulation of the "lighting in the unbuilt "Courtyard House with Curved Elements" by Ludwig Mies van der Rohe (See Figure 9.17)

Plate XI. A weathering simulation of a granite sphinx. (a) is the fresh granite, (b) shows salt erosion, (c) shows reddening due to dissolved iron, and (d) shows combined weathering from salt + iron erosion. (Fig 10.11)

Plate XII. A translucent marble bust. Plate XIII. A diffuse rendering of a marble bust. (Fig 10.17)



Figure 7.2. In corners the sphere location technique can include photons from the wall that do not belong to the radiance estimate as shown on the left. To avoid this problem, the sphere can be squashed into a disc in the direction of the normal.

This formulation applies to all points x located on a locally flat part of a surface for which the BRDF does not contain the dirac delta function (this excludes perfect specular reflection). The principle in Eq 7.7 is that not only will an infinite number be used to represent the flux in the model, but an infinite amount of photons used to estimate radiance, and the photons in the estimate will be located on infinitesimal spheres.

The degrees of infinity are controlled by the term N^α where $\alpha \in]0, 1[$ (the open brackets mean $0 < \alpha < 1$ non-inclusive ends). This ensures that the number of photons in the estimate will be infinitely fewer than the number of photons in the photon map.

Equation 7.7 says that we can obtain arbitrarily good radiance estimates by just using enough photons! In finite element-based approaches, it is more complicated to obtain arbitrary accuracy, since the error depends on the resolution of the mesh, the resolution of the directional representation of radiance, and the accuracy of the light simulation.

Figure 7.3. If the radiance estimate is computed close to a wall, then the projected area of the disc may not be correctly representing the true area covered by the photons. This problem can be eliminated by computing the convex hull of the photons or, alternatively, via filtering.

Figure 7.1 shows how locating the nearest photons is equivalent to expanding a sphere around x and using the photons within this sphere. It is possible to use other volumes than the sphere in this process. One might use a cube instead, a soft cylinder, or a disc. This could be useful to obtain an algorithm that is either faster at locating the nearest photons or perhaps more accurate in the selection of photons. If a different volume is used, then ΔA in Equation 7.4 should be replaced by the area of the intersection between the volume and the tangent plane touching the surface at x .

The sphere has the obvious advantage that the projected area of the intersection and the distance computations are simple and thus efficiently computed. A more accurate volume can be obtained by modifying the sphere into an ellipsoid by compressing the sphere along the surface normal at x (shown in Fig 7.2) [43].

The advantage of using a disc would be that fewer "false photons" are used in the estimate at edges and in corners. This modification works pretty well at the edges and corners. In a room, for instance, since it prevents photons on the walls to leak down on the floor. One issue that still occurs, however, is that the area estimate might be wrong or photons might leak to areas they do not belong. As illustrated in Figure 7.3, this is the case where a large part of the disc is inside the wall. The projected area does not fully reflect the photon density in this case. One way to eliminate this problem is to compute the convex hull of the photons (there are several standard algorithms for this purpose [86]). A simpler strategy is with filtering, which will be described later in this chapter.

7.3 Algorithm The pseudocode for computing the radiance estimate is shown in Figure 7.4. It is a straightforward implementation of Equation 7.6. For Lambertian surfaces the code can be simplified further. The BRDF evaluation $f_r(x, \vec{\omega}, \vec{p}_d)$ can then be replaced with a simple dot product comparison to exclude photons hitting the backside of the surface.

7.4 Filtering If the number of photons in the photon map is too low, the radiance estimates become blurry at the edges of sharp features in the illumination. This artifact can be pleasing when the photon map is used to estimate indirect illumination for a distribution ray tracer (see chapter 9 and Figure 9.7) but it is unwanted in situations where the radiance estimate represents caustics. Caustics often have sharp edges and it would be nice if the radiance estimate had

radiance estimate $(x, \vec{\omega}, \vec{n}) \Sigma$

Locate n nearest photons

$r =$ distance to the n^{th} nearest photon

$\sum \text{flux} = \Phi$

for each photon p do Σ

$\vec{p}_d = \text{photon direction}$

$\Phi_p = \text{photon power}$

$\Sigma \text{flux} += f_r(x, \vec{\omega}, \vec{p}_d) * \Phi_p$

$\Sigma L_e = \Sigma \text{flux} / (2\pi r^2)$

return L_e

Figure 7.4 Pseudocode for computing a radiance estimate for an incoming ray with direction $\vec{\omega}$, hitting the surface location x with normal \vec{n} . The n nearest photons are located and evaluated using equation 7.6.

To reduce the amount of blur at edges, the radiance estimate can be filtered. The idea behind filtering is to increase the weight of photons that are close to the point of interest, x . Since we use a sphere to locate photons the photons it would be natural to assume that the filter should be three dimensional. However, photons are stored at surfaces which are two dimensional. The area estimate is also based on the assumption that photons are located at the surface. We therefore need a two dimensional filter (similar to image filters) which is normalized over the region defined by the photons.

The idea of filtering caustics is not new. Collins [18] has examined several filters in combination with illumination maps. The filters described in the following are two radially symmetric filters: the cone filter, and the gaussian filter [43], and the specialized differential filter introduced in [67]. For examples of more advanced filters see [68].

7.4.1 The Cone Filter

The cone filter [43] assigns a weight, w_{pc} , to each photon based on the distance, d_p , between x and the photon p . This weight is:

$$w_{pc} = 1 - \frac{d_p}{kr} \quad (7.8)$$

where $kr \geq 1$ is a filter constant characterizing the filter and r is the maximum distance. The normalization of the filter based on a two-dimensional distribution of the photons is $1 - 2/3kr$ and the filtered radiance estimate becomes:

$$L(x, \vec{\omega}) \approx \frac{\sum_{p=1}^n f_r(x, \vec{\omega}_p, \vec{p}_d) \Phi_p(x, \vec{\omega}_p) w_{pc}}{(1 - \frac{2}{3kr}) \pi r^2} \quad (7.9)$$

The effect of the cone filter is shown in Figure 7.5

Fig 7.5 The caustic from a lens on a cube using 10e3 photons. The left is unfiltered radiance estimate and has some blur at the edges. The right image shows the result of using the cone filter with $K=1.1$. Note how the edges are much sharper and more well defined.

7.4.2 The Gaussian Filter

The Gaussian filter [63] has previously been reported to give good results when filtering caustics in illumination maps [18]. It is easy to use the Gaussian filter with the photon map since we do not need to warp the filter to some surface function. Instead we use the assumption about the locally flat surfaces, and we can use the assumption about the locally flat surfaces, and we can use a simple Gaussian filter [75]; the weight w_{pg} of each photon becomes

$$w_{pg} = \alpha \left[1 - \frac{1 - e^{-\frac{d_p^2}{2r^2}}}{1 - e^{-\beta}} \right] \quad (7.10)$$

where d_p is the distance between the photon p and x and $\alpha = 0.918$ and $\beta = 1.953$ (See [75] for detail). The filter is normalized, and the only change to Equation 7.6 is that each photon contribution is multiplied by w_{pg} :

$$\mathcal{L}_r(x, \vec{\omega}) \approx \sum_{p=1}^N f_r(x, \vec{\omega}_p, \vec{\omega}) \Delta \Phi_p(x, \vec{\omega}_p) w_{pg} \quad (7.11)$$

7.4.3 Differential checking

The differential checking approach is a technique for deciding how many photons to include in the radiance estimate [47]. The idea is to detect regions near edges in the estimation process and use fewer photons in these regions. This may result in noise near the edges, but is often preferable to blurry edges.

The radiance estimate is modified based on the following observation: when adding the photons to an estimate process, near the edge, the changes will be monotonic. For example, if we are just outside a caustic and we begin to add photons to the estimate, near an edge the changes in the estimate will be monotonic. For example, if we are just outside a caustic and we begin to add photons to the estimate (by increasing the size of the sphere centered at x that contains photons), then it can be observed that the value of the estimate is increasing as we add more photons, and vice versa when we are in the caustic. Based on this observation, differential checking can be added to the estimate — we stop adding photons and use the estimate available if we observe the estimate to either constantly increasing or decreasing as more photons are added. In practice this can be a little tricky to control, and in general the cone filter or the gaussian filter are better to use.

7.5 Photon Gathering

The radiance estimate derived in this chapter uses density estimation to compute reflected radiance from the photon map. This is not the only method by which radiance can be estimated from the photon map.

Another approach which does not use density estimation is to consider each photon as a light source (it is necessary to include the BRDF at the position where the photon is stored.) Photons that have been reflected n times before being stored represent $n+1$ bounces of indirect light illumination.

To compute reflected radiance at a given point the photon map is simply used as a collection of lights in addition to the real light sources in the model. Each light source and photon is sampled to compute the contribution to the reflected radiance. Since the photon map typically stores more than 1000³ photons, this approach is very costly. It can be optimized by randomly selecting photons instead of sampling them. This could also be done using importance sampling by finding the most important photons.

This photon gathering technique can be seen as a special case of bidirectional path tracing where light rays are traced through multiple bounces. The intersection locations of these light rays are cached and re-used multiple times.

Chapter 8 Visualizing the Photon Map

The radiance estimate derived in the previous chapter allows us to begin rendering images. The first step is building a photon map using photon tracing as described in chapter 5. This photon map can then be visualized directly (via the Radiance estimate) by using a simplified Ray tracer. This Ray Tracer uses the radiance estimate to compute the reflected radiance from all diffuse materials and standard recursive ray tracing for Specular Materials. This is illustrated in Figure 8.1. ↗ Is this simple visualization a full solution to the rendering equation? To answer this question we can look at all the paths traced by the photons and the rays and see if they cover the space of all paths.

$L(S|D)*D$ are all the paths represented by the photon map. $(S*E)/(D*S)$ are all paths traced by the ray tracer. The combination of these paths shows that the method does indeed trace all paths between the eye and the light source. Pure Ray tracing handles the case where the light is directly visible or seen through one or more Specular reflections. The photon map combined with the Ray Tracer handles all the cases where there is at least one diffuse reflection between the eye and the light source. In particular, this approach can render all caustics efficiently.

8.1 Rendering Caustics

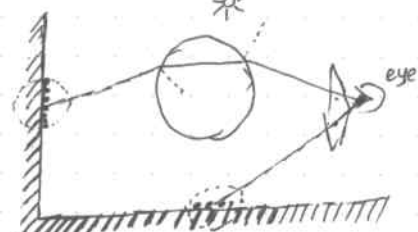


Figure 8.2 A caustic is formed as light is focused through a glass ball onto a wood table. (a) was rendered using photon mapping. (b) was rendered using path tracing.

8.1 Rendering Caustics. Caustics ARE formed when light reflected from or transmitted through one or more Specular Surfaces strikes a diffuse surface. As discussed in Chapter 3, Caustics and reflections of caustics are particularly difficult to handle with standard Monte Carlo ray-tracing techniques. In contrast caustics are very easy to compute using photon mapping.

In Figure 8.2 we can see a simple example of a caustic. It is a glass ball on a wood table. When the light illuminates the glass ball, it is focused through the ball and it forms a caustic, a concentrated spot of light, on the table.

We can simulate just the caustics by storing only the photons that have been reflected or transmitted by the glass ball. The result of this caustics simulation is shown in Figure 8.2(a). This example uses just 10⁵ photons in the photon map. Note that even this relatively small number of photons results in a nice focused caustic, and it's very fast to render.

In comparison, Figure 8.2 (b) shows the same glass ball scene rendered using path tracing with 1000 paths/pixel. Even with this large numbers of rays and a rendering time that is several hundred times longer than for the photon mapping example, we still get a noisy caustic. This illustrates the assertion in chapter 3 that monte carlo ray-tracing has problems simulating caustics and their mirror reflections (as seen in the glass ball).

8.2 Rendering Color Bleeding

Caustics are Having seen the success by which we could render caustics it seems natural to try using the same approach to render other types of illumination, such as color bleeding. Color bleeding is a result of the light exchange between diffuse surfaces — an example is the red glow on a white wall due to light reflected off an adjacent carpet. This type of illumination is

visualized directly using a single Ray tracer. For all diffuse surfaces the Ray tracer uses the radiance estimate from the Photon Map, whereas

Standard recursive Ray tracing is used for Specular Surfaces.

with photon mappings we can use the exact same approach as for caustics the result of such a simulation on the simple box scene is shown in Fig 8.3.

Figure 8.3 (a) shows a simulation using just 10³ photons in the photon map and 100 photons in the radiance estimate. Even this small number of photons gives a reasonable estimate of the overall illumination in the box (compared with the reference image in Figure 9.9). However, using only 10,000 photons does give a number of unwanted artifacts, such as the lack of detail as well as a bumpy appearance due to variance in the radiance estimate. Compared to the 100000 pixels in the rendered image, 10000 is a low number, and it is sufficiently low that the assumption about the surface being locally flat is no longer valid.

A workaround could be to remove this assumption and try estimating the photon density using more accurate techniques. Another approach could be simply using photons.

A simulation with 500,000 photons in the photon map and 500 in the radiance estimate is shown in Figure 8.3(b). This image is clearly better than the previous image with 10,000 photons. There is better detail, and the artifacts along the edges have been reduced significantly.

Figure 8.3. The box scene simulated using a direct visualization of the photon map. Image (a) was 10,000 photons in the photon map and 100 in the radiance estimate, and image (b) was 500,000 in the photon map and 500 in the radiance estimate.

To improve the results further one can use more photons. This strategy has been advocated in a number of papers [93, 113] under the name density estimation. To obtain good quality these techniques often use more than 100 million photons and more than 10000 photons in the estimate.

Due to this extreme number of photons, the underlying structures are different from those used in a photon map. Density estimation uses a large file on a local hard disk to store all the photons. Each photon is stored with just a 2D position within a given triangle. This data can be represented with just six bytes, and this makes it possible to store more than 100 million photons. The photons are later processed per triangle in order to estimate irradiance (only for Lombertian surfaces since the incoming direction of photon is not stored). The density estimation algorithm can be used to capture fine detail in caustics and indirect illumination, but the processing time is very high. Tracing and processing several hundred million photons takes several hours or even days for complex scenes. Furthermore, it would be even more costly to include non-diffuse surfaces in the algorithm. But for complex scenes with diffuse surfaces, density estimations can be used to compute accurate walk-through solutions [111], and for this reason it is a little easier to implement a photon map if

8.2.1 Excluding Direct Illumination

Another technique for improving the accuracy of the rendered image is to use the photon map only for indirect illumination, and then use ray tracing to compute the direct illumination. This is similar to strategies used for radiosity [87] to improve the accuracy of the shadow boundaries. For scenes that are dominated by indirect illumination this approach is less useful, and a large number of photons may still be necessary for accurate simulations. But for simple scenes it does give a relatively practical approach that is very robust. See Figure 8.4 for an example of this approach.

Fig 8.4. A simulation of global illumination in the box using 10000 photons in the photon map and 50 photons in the radiance estimate. For the image we used only the photon map to compute the indirect illumination. This direct lighting is computed using standard ray-tracing techniques. Even though the indirect lighting is blurry (in particular the caustic below the glass sphere) the overall quality of the illumination is reasonable.

8.3 Fast Approximations

In the previous section it was shown how increasing the number of photons in the photon map can be used to simulate color bleeding accurately. Increasing the number of photons does, however, increase both the time it takes to build the photon map and the time it takes to render the image. What if we are just interested in an approximate representation of indirect illumination? Can we do in the other direction using fewer photons to get fast results? One technique for obtaining a fast approximation is to use very few photons. This results in a blurry estimate, which for some applications may be acceptable.

Fig 8.5. A fast simulation of the box scene. This example was rendered faster than using ray tracing. A trick is to use 200 photons in the photon map and 50 in the radiance estimate. A consequence of this simple approximation is that the illumination is very blurry (even the shadows are missing.)

Figure 8.5 shows the illumination is blurry, and as a result the caustics and shadows are missing, but the overall illumination is approximately correct, and this visualization is representative of the final rendering in Figure 8.3. This image was rendered faster than the ray-tracing image, and the main reason is that we are using ray tracing only to compute the first intersection and the mirror reflections and transmissions. The cost of the photon map is negligible in this example.

Another fast visualization technique [68, 111] for walkthroughs computes interaction from the photons only at the vertices of the mesh. The photons can also be used to refine the mesh if necessary.

Fig 8.6 Cordioid-Shaped caustic due to reflection inside a metal Ring.

8.4 Caustics Examples As shown in this chapter, directly visualizing the photon map works best for caustics, and the examples for this chapter are all related to caustics.

8.4.1 Reflection Inside a Ring

Figure 8.6 shows a caustic formed on a Table due to light reflected inside a metal ring. This cordioid-shaped caustic can be observed very often among real objects—for example, on the bottom of a coffee cup or by placing a metal ring. The caustic was simulated using 50,000 photons.

The reason why we can use this relatively small number of photons is that they are stored where the caustic is most intense.

8.4.2 Prism with Dispersion

The classic example of dispersion with a glass prism is shown in Figure 8.7. Here dispersion is simulated by using a different index of refraction for each of the three "wavelengths" corresponding to red, green, and blue. Even though only three separate wavelength have been sampled, the color variations in the caustics are smooth. An accurate color representation would require more wavelength samples; such an extension to the photon map is easy to implement. 50,000 photons were used in the caustics and 80 photons were used in the radiance estimate.

Figure 8.7 Caustics through a prism with dispersion.

8.4.3 Caustics on a Non-Lambertian Surface

Figure 8.8 shows one of the standard models used to illustrate caustics. The cordioid caustic is formed by placing a light source on the edge of a cylinder which has a reflective curved side. The incoming direction of the light at the edge of a cordioid equals the tangent to the cordioid. This information is useful for analyzing the changes as we change the reflective properties of the receiving surface. It allows us to predict how the caustic should look as the surface becomes more glossy. The figure contains four rendered images showing how the caustic looks as we change the roughness (using Schlick's reflection model) of the surface from 1. to 0.01.

As expected the intensity of the caustic is reduced most greatly in those parts where the incoming direction of light differs most from the incoming direction of the viewing ray. We used approximately 340,000 photons in this example.

8.9.4. A Glass of Cognac on a Rough Surface

Figure 8.9 demonstrates the caustic from a glass of cognac onto a sand surface. The sand is a procedural surface (with 2²¹ triangles) with a synthetic sand texture. We used Schlick's reflection model with $\sigma=0.6$ for the sand — using a Lamberian approximation makes the sand look more unnatural and flat.

Figure 8.8 Fair image demonstrating the looks of the cordiod caustic created as light is reflected inside a cylinder ring. The receiving surface is changed from Lamberian (top left) to glossy specular (lower right). For this purpose we used Schlick's reflection model with $\sigma=1.0, 0.5, 0.1$, and 0.01 (from top left to lower right.)

Figure 8.9 A glass of cognac on a sand surface. The sand is a sandal surface with a synthetic sand texture. Schlick's reflection model with a roughness $\sigma=0.6$ was used for the sand. (See Color Plate III.) Figure 8.10 Close-up of the caustic in Figure 8.9. Notice that all of the illuminated area below the glass is part of the caustic. The shadow boundary below the cognac glass is simulated with a photon map, whereas the shadow outside the glass is computed using standard ray-tracing techniques (See Color Plate V.)

The Caustic in this image was rendered using approximately 350,000 photons. Notice how the red-looking caustic is formed as light is transmitted through several layers of glass and cognac. The intensity of each photon is modified based on the distance it moves through the glass and cognac media (using Beer's law). Fig 8.10 is a closeup of the caustic in Fig 8.9.

Chapter 9 A Practical Two-Pass algorithm

In the previous chapters a number of tools and techniques were developed for building and using a photon map. In this chapter we show how to combine these techniques into an efficient and practical two-pass algorithm [42]. In this chapter we will ignore the presence of participating media (techniques for handling participating media are presented in Chapter 10).

9.1 Overview The two steps in the algorithm are:

Pass 1: Building the photon maps using photon tracing.

Pass 2: Rendering using these photon maps.

Unlike the previous chapter, the rendering method here is a distribution ray tracer that computes both the direct and indirect illumination (except for caustics). This makes it possible to render accurate images using a small amount of photons.

We first show mathematically how to split the rendering equation into several components that can be computed separately. In the following sections, we describe how each of these components can be evaluated efficiently.

9.2 Solving the Rendering equation

As shown in Section 2.5 the outgoing radiance, L_o , at a surface location, x , can be computed as: $L_o(x, \vec{\omega}) = L_e(x, \vec{\omega}) + L_r(x, \vec{\omega})$ (9.1)

where the reflected radiance, L_r , is computed by the following integral:

$$L_r(x, \vec{\omega}) = \int_{\Omega} f_r(x, \vec{\omega}, \vec{\omega}') L_i(x, \vec{\omega}') (\vec{\omega} \cdot \vec{n}) d\vec{\omega}' \quad (9.2)$$

To evaluate this integral efficiently it is worth considering the properties of the BRDF, f_r , and the incoming radiance, L_i .

The BRDF is often a combination of two components: a smooth (diffuse) and a sharp (specular) component. This information is very useful when evaluating the BRDF, and therefore we split the BRDF into the sum of these terms: a Specular/glossy term, $f_{r,s}$, and a diffuse term, $f_{r,d}$ (note that these do not have to be Lamberian $f_{r,l}$ or perfect specular $f_{r,p}$):

$$f_r(x, \vec{\omega}', \vec{\omega}) = f_{r,s}(x, \vec{\omega}, \vec{\omega}') + f_{r,d}(x, \vec{\omega}, \vec{\omega}') \quad (9.3)$$

Similarly the incoming radiance is the sum of the three components:

$$L_i(x, \vec{\omega}') = L_{i,l}(x, \vec{\omega}') + L_{i,c}(x, \vec{\omega}') + L_{i,d}(x, \vec{\omega}') \quad (9.4)$$

where

- $L_{i,l}(x, \vec{\omega}')$ is the direct illumination from the light sources.
- $L_{i,c}(x, \vec{\omega}')$ is caustics — indirect illumination from the light sources via Specular reflection or transmission.
- $L_{i,d}(x, \vec{\omega}')$ is indirect illumination from the light sources that have been reflected diffusely at least once.

We can combine our classifications of the BRDF and the incoming radiance and split the expression for reflected radiance into the sum of four integrals:

$$\begin{aligned} L_r(x, \vec{\omega}) &= \int_{\Omega} f_r(x, \vec{\omega}, \vec{\omega}') L_i(x, \vec{\omega}') (\vec{\omega} \cdot \vec{n}) d\vec{\omega}' = \int_{\Omega} f_{r,s}(x, \vec{\omega}, \vec{\omega}') L_{i,s}(x, \vec{\omega}') (\vec{\omega} \cdot \vec{n}) d\vec{\omega}' + \\ &\quad \int_{\Omega} f_{r,s}(x, \vec{\omega}, \vec{\omega}') [L_{i,c}(x, \vec{\omega}') + L_{i,d}(x, \vec{\omega}') (\vec{\omega} \cdot \vec{n})] d\vec{\omega}' + \\ &\quad \int_{\Omega} f_{r,d}(x, \vec{\omega}, \vec{\omega}') L_{i,c}(x, \vec{\omega}') (\vec{\omega} \cdot \vec{n}) d\vec{\omega}' + \\ &\quad \int_{\Omega} f_{r,d}(x, \vec{\omega}, \vec{\omega}') L_{i,d}(x, \vec{\omega}') (\vec{\omega} \cdot \vec{n}) d\vec{\omega}'. \end{aligned} \quad (9.5)$$

This is the equation used whenever we need to compute the reflected radiance from a surface. In the following sections we discuss the evaluation of each of the integrals in the equation in more detail.

9.3 Pass 1: Photon Tracing As shown in the previous section the incoming radiance is split into a sum of several components. In particular there are caustics and an indirect illumination component.

We have already seen how caustics are difficult to compute using standard Monte Carlo ray-tracing techniques, whereas the photon map is very efficient for caustics. For efficiency reasons it is therefore desirable to have a caustics photon map that only represents caustics. For efficiency reasons it is therefore desirable to have a caustics photon map that only represents caustics. In addition we can use a global photon map to represent all illumination including caustics and direct illumination. It will become clear in the rendering section (Section 9.4) why this is useful.

9.3.1 The Caustics Photon Map

The caustics photon map contains photons that have been reflected or transmitted via one specular surface before hitting a diffuse surface. In the path notation these are L^{S+D} .

Figure 9.1 illustrates the computation of the caustics photon map. Photons are emitted toward the glass sphere and stored as they hit the diffuse floor in the model. Once a caustic photon hits a diffuse material, it is terminated. Diffuse materials do not generate caustics. For scenes with strong indirect illumination it may be useful to render caustics due to indirect illumination more efficiently. Here, these types of "caustics" are rendered using Monte Carlo Ray Tracing.

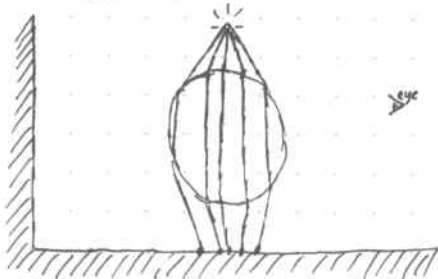


Figure 9.1. The caustics photon map is built by tracing photons toward the specular surfaces in the model. All photons that are reflected or transmitted by a specular surface will be stored if hit by a diffuse surface. Once the photon hits a diffuse surface it will be terminated.

The caustics photon map *directly* is used to render caustics that are seen by the eye and it therefore be of high quality. This means collecting enough photons such that the amount of blur and other potential artifacts are reduced to an acceptable minimum. Fortunately, caustics are often focusing phenomena, in which case even every few photons can give good results.

To build the caustics photon map quickly it pays off to concentrate the emitted photons in the direction toward the specular surfaces. These can either be identified by, or for more control, explicitly (meaning that a person specifies exactly which objects generate caustics).

For artistic control this concept can be extended such that the renderer only allows such objects to actually generate caustics. Similarly, it may be useful to place constraints on which objects can receive a caustic.

This would allow an animator to specify, for example, that a glass of cognac should create a caustic only on the table. This information gives more control to the animator, but it also makes it possible to make the render faster by computing only a limited number of caustics.

The projection map is particularly useful for computing caustics. It is often the case that the model contains a small object (such as a glass) that creates a caustic. The projection map makes it possible to concentrate the emitted photons toward this small object. This is better than the stochastic approach, which might miss important caustic generators. Caustics in particular can be very intense even for small objects, and the projection map can give very good speedups while ensuring that these important caustics are simulated.

9.3.2 The Global Photon Map

The global photon map contains all photons that hit diffuse surfaces in the model. The photons in the global photon map represent direct illumination, indirect illumination, and caustics (in path notation: $L^{(S+D)+D}$). ~~This global photon map is built by tracing photons toward all objects~~. This obviously means that we obviously cannot just add the caustics photon map and the global photon map to get a full solution. This rendering step must be careful not to add terms twice.

The global photon map is built by tracing photons toward all objects in the model and storing these as they hit diffuse surfaces.

Diffuse surfaces also reflect photons, unlike the caustics photon map. This is shown in Figure 9.2.

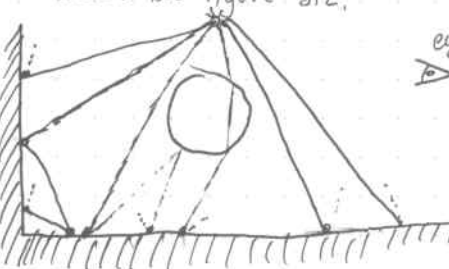


Fig 9.2 The global photon map is created by tracing photons toward all objects in the model. During photon tracing all surfaces can reflect and transmit photons. All photons that hit a diffuse surface are stored in the global photon map.

The ideas and optimizations that apply to the caustics photon map also work for the global photon map. The renderer does not have to identify specular surfaces, but it might still be useful to build in tools to allow the technical director to control which surfaces should generate indirect illumination and which surfaces should clip away indirect illumination.

The projection map is still useful for the global photon map in order to concentrate emitted photons toward the geometry (for example, in a model where light sources are far away from the geometry).

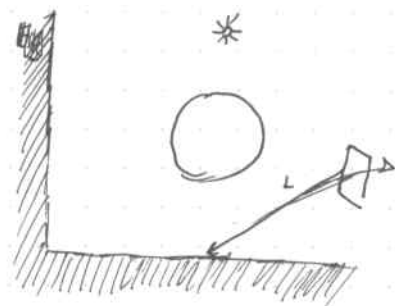


Figure 9.3 The Radiance through a Pixel is estimated by Ray Tracing a Ray from the eye through the Pixel and computing the reflected Radiance at the first surface intersected by the Ray.

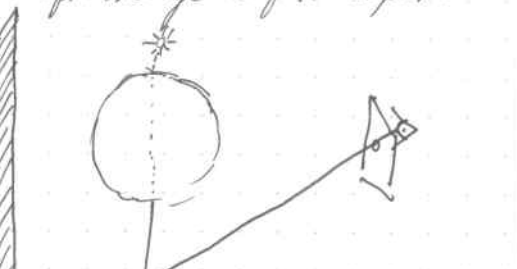
9.4 Pass 2 Rendering The final image is rendered using distribution Ray Tracing, in which the Radiance of each pixel is evaluated by averaging a number of sample estimates. Each sample estimate is computed by Ray Tracing a Ray from the eye through a pixel into the scene (See Figure 9.3). At the first surface intersected by the ray we evaluate Equation 9.5.

In the following it will be explained how each component of equation 9.5 is computed. We distinguish between two different types of computations: An accurate and an approximate.

The accurate computation is used if the surface is seen directly by the eye or perhaps via a few Specular Reflections. It is also used if the distance between the ray origin and the intersection point is below a small threshold value — to eliminate potential inaccurate color bleeding effects in corners.

The approximate evaluation is used if the ray intersecting the surface has been reflected diffusely since it left the eye or if it contributes little to the pixel Radiance.

Figure 9.4. Direct illumination is evaluated accurately using Ray Tracing between the light source and the point of interest to determine the point is illuminated or in shadow.



9.4.1 Direct Illumination

Direct illumination is given by the term $\int_{\Omega^2} f_r(x, \vec{\omega}', \vec{\omega}) \mathcal{L}_{i,c}(x, \vec{\omega})(\vec{\omega}' \cdot \vec{n}) d\vec{\omega}'$ and it represents the contribution to the reflected radiance due to direct illumination. This term is often the most important part of the reflected radiance and it has to be computed accurately, since it determines lighting effects to which the eye is highly sensitive, such as shadow edges. The accurate computation of the direct illumination is quite simple in ray tracing based methods. At the points of interest, shadow

edges are easily determined by tracing a ray from the eye through the pixel to the light source. If the ray intersects the light source, the contribution to the reflected radiance is included in the integral; otherwise it is neglected. For large area light sources, several shadow rays are used to properly integrate the effect of illumination.

It is also possible to use an extension to the Photon Mapping algorithm in which shadow photons are used to classify regions with full illumination, penumbra, and shadow [48]. Shadow photons are photons with negative power created by tracing photons from the light source through objects and storing them on diffuse surfaces. By examining the local distribution of shadow photons and photons coming directly from the light source, it is possible to quickly estimate the shadow properties of a given region. This approach can lead to considerable speedups in scenes with large area light sources that are normally very costly to render using standard ray tracing. The approach is stochastic though, so it might miss shadows from small objects in case these aren't intersected by any photons. This is a problem with all techniques that use stochastic evaluation for visibility. See Section 11.5 for more detail on the shadow photon approach. The approximate evaluation of the direct illumination is the Radiance estimate obtained from the global photon map (no shadow rays or light source evaluations are used.). This is seen in Figure 9.7 where the global photon map is used in evaluation of the incoming light for the secondary diffuse reflection.

9.4.2 Specular and Glossy Reflection

Specular and glossy reflection is computed by evaluation of the term

$$\int_{\Omega^2} f_{r,s}(x, \vec{\omega}, \vec{\omega}') [\mathcal{L}_{i,c}(x, \vec{\omega}') + \mathcal{L}_{i,d}(x, \vec{\omega}')] (\vec{\omega}' \cdot \vec{n}) d\vec{\omega}' \quad (9.7)$$

The photon map is not used in the evaluation of this integral since it is strongly dominated by $f_{r,s}$, which has a narrow peak around the mirror direction. Using the photon map to optimize the integral would require a large number of photons in order to make a useful classification of the different directions within the peak of $f_{r,s}$ (we have shown that this can be done in Figure 8.8). To save memory this strategy is not used, and the integral is evaluated using standard Monte Carlo Ray Tracing optimized with importance sampling based on $f_{r,s}$. This is still quite efficient for glossy surfaces and the integral can in most cases be computed using a smaller amount of sample rays. This is illustrated in Figure 9.5.

9.4.3 Caustics

Caustics are represented by the integral

$$\int_{\Omega^2} f_{r,o}(x, \vec{\omega}', \vec{\omega}) \mathcal{L}_{i,c}(x, \vec{\omega}') (\vec{\omega}' \cdot \vec{n}) d\vec{\omega}' \quad (9.8)$$

The evaluation of this term is dependent on whether an accurate or an approximate computation is required.

For an accurate computation, the term is evaluated using a radiance estimate from the caustics photon map (See Fig 9.6). The number of photons in the caustics photon map is large, and we can expect a good quality of the estimate. Caustics are never computed using Monte Carlo ray tracing, since this is a very inefficient method when it comes to rendering Caustics.

The approximate evaluation of the caustics term is included in the radiance estimate from the global photon map.

9.4.4 Multiple Diffuse Reflections

The last term in equation 9.5 is

$$\int_{\Omega^2} f_r(\mathbf{x}, \vec{\omega}', \vec{\omega}) L_{id}(\mathbf{x}, \vec{\omega}) (\vec{\omega} \cdot \mathbf{n}) d\omega' \quad (9.9)$$

This term represents incoming light that has been reflected diffusely at least once since it left the light source. The light is then reflected diffusely by the surface (using $f_r(\mathbf{x})$). Consequently the resulting illumination is very "soft."

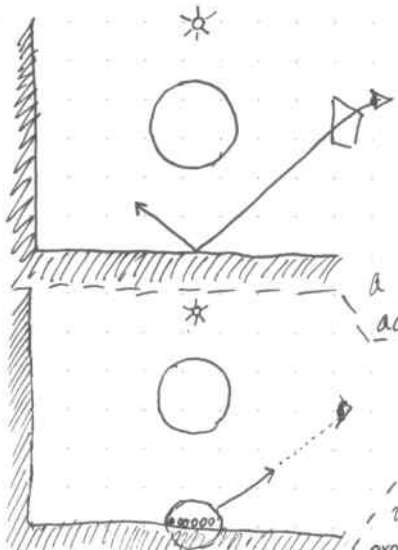


Figure 9.5. Specular and glossy reflections or transmissions are evaluated using recursive Ray Tracing. Ray Tracing is good at integrating the contribution from the narrow peaks in the BRDF. For glossy reflections it is possible to use a photon map, but this would require a large number of photons to get an accurate directional estimate.

Figure 9.6 Caustics seen directly by the eye are rendered using the radiance estimate from the caustics photon map.

The accurate evaluation of the integral is calculated using Monte Carlo Ray Tracing. Monte Carlo ray tracing is rarely expansive for computing diffuse indirect illumination, but this integral has several properties that make it simpler.

The indirect illumination is very smooth, since we have separated out caustics (computed using the Caustics photon map). Caustics are often the main source of noise in Monte Carlo Ray Tracing. Furthermore, we can use information in the photon map about the incoming flux at \mathbf{x} . This allows us to importance-sample not only according to the BRDF, but also according to the incoming light [9]. The details of this approach are described later in Chapter 11. Another very important optimization for Lambertian Surfaces is the use of irradiance caching. Irradiance Caching is a method that enables sparse evaluations of the irradiance by interpolating from previously cached values [18]. This method is also described more detail in Chapter 11.

The approximate evaluation of indirect illumination is computed using the radiance estimate from the global Photon Map. Notice that this radiance estimate can be combined for Caustics, direct illumination, and indirect illumination - this is the reason why the global Photon Map contains all the types of illumination. The computation of indirect diffuse illumination is illustrated in Figure 9.7.

9.5 Examples

The following pages contain several images and examples demonstrating the two-pass photon mapping technique.

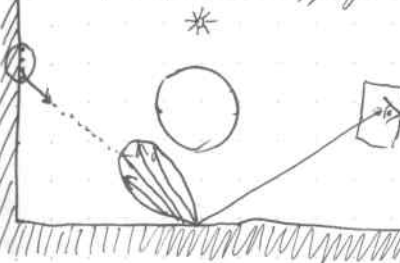


Figure 9.7 Indirect diffuse illumination is evaluated accurately by distribution ray tracing, where a number of sample rays are used to estimate the incoming light. For approximate evaluations (when these sample rays intersect another diffuse surface), the radiance estimate from the global Photon Map is used.

9.5.1 The Four Rendering Components

The four components (direct, specular, caustics, and indirect illumination) as shown in Figure 9.8 for the box scene (with a mirror ball to the left and a gloss ball to the right). The sum of these four components (images) is the full global illumination solution shown in Figure 9.9.

For comparison the image in Figure 9.10 is a classic Ray-Tracing Solution. Figure 9.11 includes soft shadows (distribution ray tracing), and Figure 9.12 includes caustics. Note that only the full global illumination solution in Fig. 9.9 is capable of capturing the indirect illumination of the ceiling in the box.

9.5.2 Fractal Box

An example of a more complex scene is shown in Fig 9.13. The walls have been replaced with displacement-mapped surfaces (generated using a fractal midpoint subdivision algorithm) and the model contains more than 1.6 million elements. Notice that each wall segment is an instanced copy of the same fractal surface. With photon maps it is easy to take advantage of instancing, and the geometry does not have to be explicitly represented. We used 200,000 photons in the global Photon Map and 50,000 in the Caustics Photon Map. This is the same number of photons as in the simple box scene, and our reasoning for choosing the same values is that the complexity of the illumination is more or less the same as in the simple box scene.

is that the complexity of the illumination is more or less the same of the simple box scene. We want to capture the color bleeding from the colored walls and the indirect illumination of the ceiling. All in all we used the same parameters for the photon map as in the simple box model.

9.5.3 Box with model

In the box scene in Figure 9.14 we have inserted a displacement-mapped water surface. To render this scene we used 5000 photons in both the caustics and the global photon map, and up to 100 photons in the radiance estimate. We used a higher number of caustic photons due to the water surface, which causes the entire floor to be illuminated by the photons in the caustics photon map. Also the number of photons in the global photon map has increased to account for the more complex indirect illumination in the scene. The water surface is made up of 20,000 triangles.

Figure 9.9. The box scene with soft global illumination. (See Color plate VI)

Figure 9.10 The box Scene Ray-traced (see Color plate VII)

Fig 9.11 The box Scene with Soft Shadows. Fig 9.12 The box scene with caustics

Fig 9.13 Fractal box. Fig 9.14 Box with water

Fig 9.15 Two bunnies represented using points. The shape of each bunny is represented using less than 35,000 points. Using a technique for ray tracing points (introduced in [84]) we can store photons on this geometry. This allows us to simulate caustics on the point-sampled wood bunny due to light scattered through the point-sampled glass bunny.

Figure 9.16 A rendering of a geometric model of Little Matterhorn with trees (200 million polygons) in the middle of the day and at sunset. We used just 100,000 photons for this model to simulate the illumination from the Sun as well as the sky. (See Color plate VIII).

9.5.4 Global Illumination on a point Cloud

Figure 9.15 demonstrates a simulation of global illumination in a model with point-sampled geometry. Each bunny is represented using less than 35,000 points. Using a technique for ray tracing points, (introduced in [84]), we can store photons on this geometry. This allows us to simulate caustics on the point-sampled wood bunny due to light scattered through the point-sampled glass bunny.

9.5.5 A Mountain Landscape

Figure 9.16 demonstrates a mountain landscape (Little Matterhorn) illuminated with Sky and Sunlight. To represent the illumination of the landscape, we approximately used 10¹³ photons emitted both from the Sun as well as the Sky.

The low number of photons - compared with the high number of polygons (200 million) is possible due to the relatively simple illumination configuration.

9.5.6 The Courtyard House by Mies van der Rohe

Photon mapping makes it possible to simulate global illumination in complex models, such as the architectural model shown in Fig. 9.17. The images are from an animation [79] that demonstrate how the natural lighting (Skylight and Sunlight) of a model changes during the day.

Figure 9.17 A Simulation of the lighting in the unbuilt "Courtyard House with curved elements" by Ludwig Mies van der Rohe. (See Color Plate X.)

Chapter 10 Participating Media In the previous chapters it was assumed that all photons interactions happen at the surfaces. This is the only only the case in vacuum. Even clean air scatters photons - this is the reason why the sky is blue. Often, we can ignore the presence of the Leon ever in a model, but this is no longer the case for large (outdoor) models or when the air is filled with dust and other particles.

Dusty air, clouds, and salty water are all examples of participating media, and the presence of these phenomena requires new light transport techniques.

Another class of participating media is translucent materials such as marble, skin, and plants. To perform a full simulation of the subsurface scattering in graphics [23, 60], and the first method to efficiently simulate volume caustics [48]. Before going into the details of how to use photon mapping in participating media this chapter begins by reviewing the light transport properties of participating media.

10.1 Light Scattering in Participating Media

When a photon enters a participating medium, it can either continue unaffected through the medium or it can interact with the medium at a given location. When a photon interacts with a medium at a given location one of two things can happen: It is either absorbed or scattered. The probability of a photon being either scattered or absorbed as it moves through a medium is given by the scattering coefficient, σ_s , and the absorption coefficient, σ_a . For a light ray moving through a medium, this can be seen as a continuing change in the radiance of the ray.

The change in radiance, ΔL , in the direction, $\vec{\omega}$, due to Direct scattering is given by the following equation:

$$(\vec{\omega} \cdot \nabla) L(x, \vec{\omega}) = -\sigma_s(x) L(x, \vec{\omega}) \quad (10.1)$$

and the change due to absorption is:

$$(\vec{\omega} \cdot \nabla) L(x, \vec{\omega}) = -\sigma_a(x) L(x, \vec{\omega}) \quad (10.2)$$

As it can be seen from these equations the radiance is reduced due to light being either scattered or absorbed. The combined loss in Radiance is given by: $(\vec{\omega} \cdot \nabla) L(x, \vec{\omega}) = -\sigma_t(x) L(x, \vec{\omega})$ where $\sigma_t = \sigma_s + \sigma_a$ is the extinction coefficient.

As we move through the media there will also be a gain in Radiance due to in-scattering of light. The change of Radiance due to in-scattering is given by:

$$\begin{aligned} (\vec{\omega} \cdot \nabla) L(x, \vec{\omega}) &= -\sigma_t(x) L(x, \vec{\omega}) \\ (\vec{\omega} \cdot \nabla) L(x, \vec{\omega}) &= \sigma_i(x) \int_{2\pi} p(x, \vec{\omega}', \vec{\omega}) L_i(x, \vec{\omega}') d\omega' \end{aligned} \quad (10.4)$$

where the incident radiance, L_i , is integrated over all directions on the sphere, $\Omega_{4\pi}$. $p(x, \vec{\omega}', \vec{\omega})$ is the phase function describing the distribution of the scattered light.

Finally, there can be a gain in Radiance due to emission, L_e , from the medium (i.e., a flame), and it is given by:

$$(\vec{\omega} \cdot \nabla) L(x, \vec{\omega}) = \sigma_a(x) L_e(x, \vec{\omega}) \quad (10.5)$$

By combining Equations 10.3, 10.4, and 10.5 we find the total change in Radiance per unit distance:

$$(\vec{\omega} \cdot \nabla) L(x, \vec{\omega}) = \sigma_a(x) L_e(x, \vec{\omega}) - \sigma_t(x) L(x, \vec{\omega}) + \sigma_s(x) \int_{2\pi} p(x, \vec{\omega}', \vec{\omega}) L_i(x, \vec{\omega}') d\omega' \quad (10.6)$$

10.2 The Volume Rendering equation

By integrating equation 10.6 on both sides for a segment of length S , and adding the contribution of incoming Radiance from the other side of the medium we find that:

$$\begin{aligned} L(x, \vec{\omega}) &= \int_0^x e^{-\tau(x, x')} \sigma_a(x') L_e(x') dx' + \\ &\quad \int_0^x e^{-\tau(x, x')} \sigma_a(x') \int_{2\pi} p(x, \vec{\omega}, \vec{\omega}') L_i(x', \vec{\omega}') d\omega' dx' + \\ &\quad e^{-\tau(x, x+S)} L(x+S, \vec{\omega}) \end{aligned} \quad (10.7)$$

$$\text{where the optical depth } \tau(x, x') = \int_x^{x'} \sigma_t(t) dt \quad (10.8)$$

Equation 10.7 is the volume rendering equation, and it is the equation that MUST be solved to render participating media. The equation is more complex than the rendering equation.

It is describing Radiance in a five dimensional space instead of a four dimensional one (surface and direction) for the rendering equation (Section 2.5). This is due to the fact that light is influenced by light of every facet in space, not just the points on other surfaces. This is one of the reasons why the participating media is costly to simulate.

10.3 The Phase Function

The phase function describes the distribution of scattered light in participating media. Unlike the BRDF for surfaces, the phase function is unitless and normalized (the amount of scattering and adsorption is controlled by the scattering and absorption coefficients).

The phase function often depends only on the angle, θ , between the incoming Ray and the scattered Ray, and it can be written as $p(\theta)$ where $\theta=0$ is the forward direction and $\theta=\pi$ is the backward direction.

To specify the preferred direction of the phase function (forward or backward) one can compute the average cosine of the scattered direction g , as:

$$g(x) = \int_{2\pi} p(x, \vec{\omega}', \vec{\omega}) \cos\theta d\omega' \quad (10.10)$$

The value of $g \in [-1, 1]$ will be positive for forward scattering and negative for backward scattering. It is also the parameter for the commonly used Henyey-Greenstein phase function. (described later)

The shape of the phase function is also used to classify the participating medium. The scattering is either isotropic or anisotropic. That is any phase function with a preferential scattering direction is anisotropic. (this is the most common case); otherwise the scattering is isotropic. If the phase function further depends on the orientation of the medium, then the medium is anisotropic; otherwise it is isotropic. Notice that, unlike surfaces, we have two components that are either isotropic or anisotropic.

10.3.1 Isotropic Scattering The phase function for isotropic scattering is constant: $p(\theta) = \frac{1}{4\pi}$ (10.11)

This means that a photon that is scattered will be scattered in any random direction without history. Where it come from. (Figure 10.1(a)).

10.3.2 The Henyey-Greenstein Phase Function

The most commonly used phase function is the empirical Henyey-Greenstein phase function [35]. It was introduced to explain scattering by intergalactic dust, but it has since been used to describe scattering in oceans, clouds, skin, stone, and more. The function is:

$$P(\theta) = \frac{1-g^2}{4\pi(1+g^2-2g\cos\theta)^{1.5}} \quad (10.12)$$

where $g \in [-1, 1]$ is a symmetry parameter equal to the average cosine of the scattered directions (See equation 10.10). Positive g gives forward scattering and negative g gives backward scattering ($g=0$ for isotropic scattering). Higher values of g makes the scattering more preferential ($g=1$ gives pure forward scattering in the same direction).

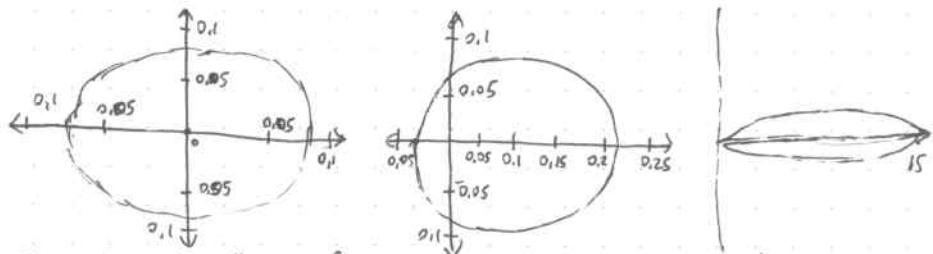


Figure 10.1. The Henyey-Greenstein phase function with different g . From left to right $g=0.0$, $g=0.3$, and $g=0.09$

This illustration in Figure 10.1. The function is essentially giving ellipsoid-shaped scattering distributions where the shape of the ellipsoid is controlled by g .

For more complex types of scattering one can use a combination of several Henyey-Greenstein functions.

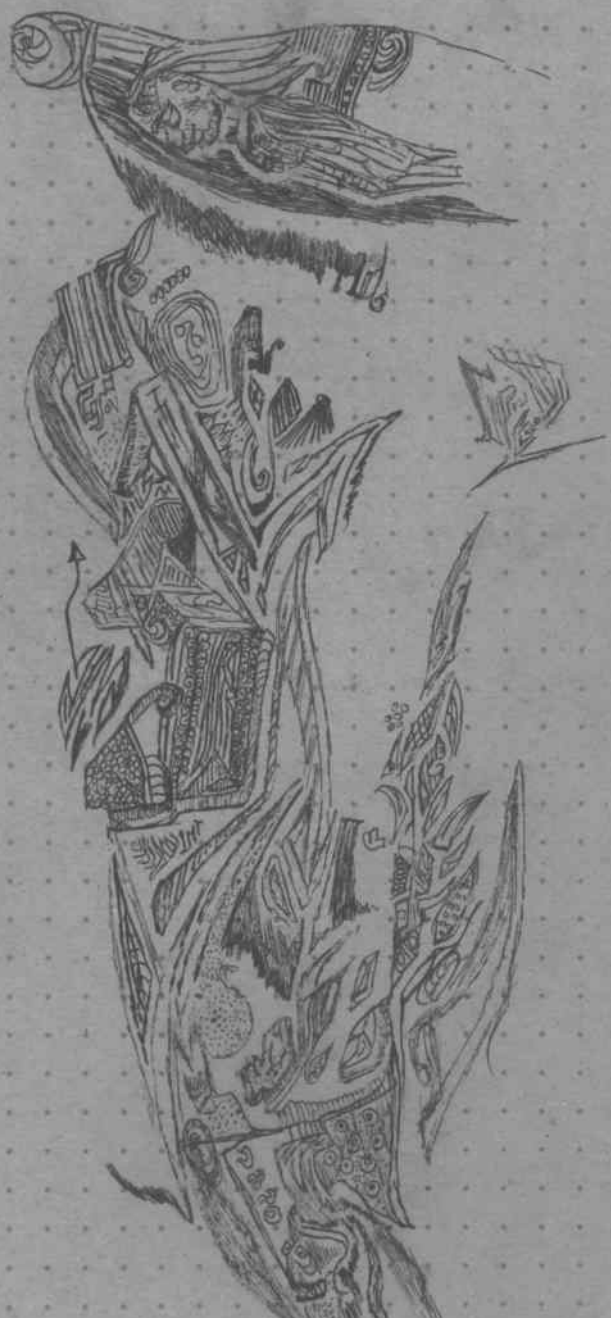
$$P(\theta) = \sum_{i=1}^N w_i \frac{1-g_i^2}{4\pi(1+g_i^2-2g_i\cos\theta)^{1.5}} \text{ where } \sum_{i=1}^N w_i = 1 \quad (10.13)$$

Here g_i controls the shape of each lobe and w_i the weight. Such a multilobed function can be used to model more complex scattering, and it can give very realistic results. Commonly used is a sum of a forward scattering and backward scattering lobe. Another advantage of the Henyey-Greenstein function is that it can be importance sampled very easily.

Given an incoming direction, $\vec{\omega}$, of a photon, the angle, θ , of the new scattered direction is given by:

$$\cos\theta = \frac{1}{2g} \left(1 + g^2 - \left(\frac{1-g^2}{1+g+2g\xi} \right)^2 \right) \quad (10.14)$$

where ξ is a uniform random number between zero and one, θ is the same angle of the phase function. The rotation ϕ is uniformly distributed.



Frequently Used Symbols and Their Meaning

Symbol	Description
x	Position
x'	Position of the incoming light
\vec{n}	Normal at x (always Normalized: $ \vec{n} =1$)
$\vec{\omega}'$	Direction (away from surface.)
$\vec{\omega}$	Direction of incoming Radiance (away from surface)
$d\Omega$	Differential Solid angle ($d\Omega = \sin\theta d\theta d\phi$)
(θ, ϕ)	Direction in Spherical coordinates
\mathcal{L}	Radiance
$\mathcal{L}(x, \vec{\omega})$	Radiance at x in $\vec{\omega}$ direction.
$\mathcal{L}(x, \vec{\omega}')$	Incident Radiance at x from direction $\vec{\omega}'$.
$\mathcal{L}(x' \rightarrow x)$	Radiance at x in $\vec{\omega}$ direction
\mathcal{L}_e	Emitted Radiance
\mathcal{L}_r	Reflected Radiance
\mathcal{L}_i	Incident Radiance
Φ	flux
E	Irradiance
f_r	BRDF
f_d	Diffuse BRDF
f_s	Specular BRDF
P	Reflectance
Ω	Hemisphere of directions
$\Omega_{4\pi}$	Sphere of directions
n	Index of refraction
A	Albedo
σ_a	Absorption Coefficient
σ_s	Scattering Coefficient
σ_t	Extinction Coefficient
τ	Optical depth
Δx	Small step
ξ	Uniformly distributed random variable between 0 and 1.
ξ_1, \dots, ξ_N	N uniform numbers between 0 and 1.

Radiometry and Photometry, the only difference is photometry takes into account an optical response [32]

④ Radiometry: The basic quantity in lighting is the photon. The energy, e_λ , of a photon of wavelength λ is:

$$e_\lambda = \frac{hc}{\lambda} \quad (2.1)$$

\rightarrow Planck's Constant: $\hbar \approx 6.63 \cdot 10^{-34} \text{ Js}$, $C \rightarrow$ Speed of light in a vacuum: $C = C_0 = 299\,792\,458 \text{ m/s}$.

$Q_\lambda \rightarrow$ Spectral Radiant energy. Q_λ , is n_λ photons with wavelength λ :

$$Q_\lambda = n_\lambda e_\lambda = n_\lambda \frac{hc}{\lambda} \quad (2.2)$$

$Q \rightarrow$ Radiant Energy: The energy of a collection of photons. Computed by integrating the Spectral Radiant energy over all wavelength:

$$Q = \int_0^\infty Q_\lambda d\lambda \quad (2.3)$$

$$Q = \int_0^\infty Q_\lambda d\lambda = \int_0^\infty n_\lambda \frac{hc}{\lambda} d\lambda = hc \int_0^\infty \frac{n_\lambda}{\lambda} d\lambda$$

$\Phi \rightarrow$ Radiant flux: The time Rate flow of Radiant energy.

$$\Phi = \frac{dQ}{dt} \quad (2.4)$$

$$\Phi = \frac{dQ}{dt} = \frac{d}{dt} \int_0^\infty Q_\lambda d\lambda = \frac{d}{dt} \int_0^\infty n_\lambda \frac{hc}{\lambda} d\lambda = hc \frac{d}{dt} \int \frac{n_\lambda}{\lambda} d\lambda = \frac{d(hc)}{dt} \int \frac{n_\lambda}{\lambda} d\lambda$$

$\Phi_\lambda \rightarrow$ Spectral Radiant flux: The time Rate flow of Spectral Radiant energy.

$\frac{d\Phi}{dA} \rightarrow$ Radiant Flux area density: The differential flux per differential area (at a surface)
Radiant flux area density is often separated into the Radiant excitation (M) and the irradiance (E).

$M \rightarrow$ Radiant excitation: The flux leaving a surface. (also known as the Radiosity (B))

$B \rightarrow$ Radiosity: The flux leaving a Surface.

$E \rightarrow$ Irradiance: The flux arriving at a location x .

$$E(x) = \frac{d\Phi}{dA} \quad (2.5)$$

$I \rightarrow$ Radiant intensity: The Radiant flux per unit solid angle $d\omega$.

$$I(\vec{\omega}) = \frac{d\Phi}{d\omega} \quad (2.6)$$

[12, 83, 121, 38]

$\mathcal{L} \rightarrow$ Radiance: The Radiant flux per unit Solid angle $d\omega$ per unit projected area.

$$\mathcal{L}(x, \vec{\omega}) \propto E(x) \cdot I(\vec{\omega})$$

$$\mathcal{L}(x, \vec{\omega}) = \frac{d^2\Phi}{\cos\theta dAd\omega} = \int_0^\infty \frac{d^4n_\lambda}{\cos\theta d\omega d\Omega d\lambda} \frac{hc}{\lambda} d\lambda \quad (2.7)$$

The last term represents the Radiance expressed as an integral over wavelength of the flow of energy in n_λ Photons per differential area per differential Solid angle per unit time.

Radiance is a 5-dimensional quantity. (Three position, two direction)

It is often written as $\mathcal{L}(x, \vec{\omega})$ where x is the position and $\vec{\omega}$ is the direction.

Radiance is the most important quantity in global illumination, since it closely represents the colour in the effect. This applies to any device that detects light, including one such as a human observer.

Radiance can be thought of as photons hitting per unit time in a given direction on a point. In a vacuum Radiance is constant along a line of sight.

If the radiance field on a surface is available then the flux can be computed by integrating the Radiance field over all directions Ω and area A :

$$\Phi = \iint_A \mathcal{L}(x, \vec{\omega}) (\vec{\omega} \cdot \vec{n}) d\omega dx \quad (2.8)$$

where \vec{n} is the surface normal of the surface.

Symbol	Quantity	Unit
Q_λ	Spectral Radiant energy	Jm^{-1}
Q	Radiant energy	J
Φ	Radiant flux	W
I	Radiant Intensity	Wsr^{-1}
E	Irradiance (incident)	Wm^{-2}
M	Radiant excitation (outgoing)	Wm^{-2}
B	Radiosity (outgoing)	Wm^{-2}
L	Radiance	$\text{Wm}^{-2}\text{sr}^{-1}$
L_λ	Spectral Radiance	$\text{Wm}^{-2}\text{sc}^{-1}\text{nm}^{-1}$

Table 2.1 Radiometric symbols, names, and units.

2.2.2 Photometry

① The important difference between Radiometry and photometry is that the photometric values include the visual response of a standard observer.

$\Phi_v \rightarrow$ Luminous flux: The visual response to radiant flux.

$$\Phi_v = \int_{\lambda} Q(\lambda) V(\lambda) d\lambda \quad (2.9)$$

$V(\lambda) \rightarrow$ Visual Response: Response of a standard observer.

$\Lambda \rightarrow$ Albedo: The wavelength for the visual spectrum (380nm - 780nm)

$d\Phi_v \rightarrow$ illuminance, E_v : Luminous flux area density is illuminance if incident

$dA \rightarrow$ Luminous exittance, M_v : Luminous flux area density is Luminous exittance if outgoing.

$E_v \rightarrow$ illuminance,

$M_v \rightarrow$ Luminous exittance

$I_v \rightarrow$ Luminous Intensity: flux per solid angle $(d\Phi_v)$. $I_v = \frac{d\Phi_v}{dA}$.

$L_v \rightarrow$ Luminance: The photometric equivalent of Radiance

$$L_v(x, \vec{\omega}) = \frac{d^2\Phi_v}{\cos \theta dA d\omega} \quad (2.10)$$

2.2.3 The Solid Angle

$d\vec{\omega} \rightarrow$ The differential Solid angle: It relates the angular magnitude of a beam with its direction.

The differential solid angle relates the flux (a raw stream of photons) with the intensity of light. It is the almost exclusively the integration variable of choice in Monte-Carlo Ray-Tracing when the incoming radiance is integrated.

The size of a differential solid angle in spherical coordinates (θ, ϕ) is given by:

$$d\vec{\omega} = \sin \theta d\theta d\phi \quad (2.11)$$

Here, θ is the angle between the normal direction \vec{n} and the direction " $\vec{\omega}$ "?

ϕ is the angle between the directed projection onto the surface tangent and \vec{t}_x . (\vec{t}_x and \vec{t}_y are two independent vectors on a surface plane)

Given the spherical coordinates we can compute the direction $\vec{\omega}$ of the solid angle:

$$\vec{\omega} = \sin \theta \cos \phi \vec{t}_x + \sin \theta \sin \phi \vec{t}_y + \cos \theta \vec{n} \quad (2.12)$$

A frequently encountered expression is the integral over the incoming directions in the hemisphere Ω

$\Omega \rightarrow$ Domain of hemisphere integration:

$$\int_{\Omega} f(\theta, \phi) d\vec{\omega}' = \int_0^{2\pi} \int_0^{\pi/2} f(\theta, \phi) \sin \theta d\theta d\phi \quad (2.13)$$

2.3 Light Emission

The intensity of a given light source is often given as the power or the wattage of the source. For a small (Point) light source with power Φ_s that emits light uniformly in all directions, we can compute the irradiance, E , at a surface at point x as:

$$E(x) = \Phi_s \cdot \frac{1}{4\pi r^2 \cos \theta} \quad (2.14)$$

where r is the distance from x to the light source. θ is the angle between the surface normal and the direction to the light source.

The surface area of the sphere is $4\pi r^2$. The cosine factor in the denominator is due to surface orientation. A surface facing the source receives more photons per area than a different orientation. It is common to refer to the color temperature of a light source. This quantity has an exact physical meaning since it is related to the blackbody radiation.

$\Phi_\lambda \rightarrow$ Spectral Radiant Flux:

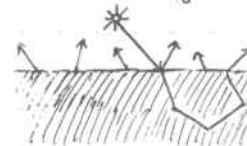
$$\Phi_\lambda = \frac{2\pi C_1}{\lambda^5 (e^{C_2/\lambda T}) - 1} \quad (2.15)$$

Here T is the Temperature of the object, $C_1 = h C_0^2 \approx 3.7418 \cdot 10^{-16}$, and $C_2 = \frac{h C_0}{k} \approx 1.4388 \cdot 10^{-2}$ where $k \approx 1.38 \cdot 10^{-23} \text{ J/K}$

$k \rightarrow$ Boltzmann's Constant. As an example

2.4 Light Scattering

When light encounters an obstacle it is scattered and absorbed.



2.4.1 The BSSRDF

When a beam of light is scattered by a material it normally enters a material and then scatters around the surface at a different location.

The BSSRDF relates the differential reflected radiance, dL_r , at x in a direction $\vec{\omega}'$ to the differential $d\Phi_i$ incident flux at x' from direction $\vec{\omega}$:

$$S(x, \vec{\omega}; x', \vec{\omega}') = \frac{dL_r(x, \vec{\omega}')}{d\Phi_i(x', \vec{\omega}')} \quad (2.16)$$

Notice that S is a function of both the incoming and outgoing directions and positions. This is the most general description of light transport. Unfortunately it is eight dimensional and costly to evaluate.



Figure 2.3 the BRDF models the local reflection of light assuming that all light is reflected at the same location taken if hits the surface

2.4.2 The BRDF The Bidirectional Reflectance distribution function, the BRDF, f_r , defines the relationship between reflected Radiance and irradiance

$$f_r \rightarrow \text{BRDF} : f_r(x, \vec{\omega}, \vec{\omega}) = \frac{dL_r(x, \vec{\omega})}{dE_i(x, \vec{\omega})} = \frac{dL_r(x, \vec{\omega})}{Li(x, \vec{\omega})'(\vec{\omega} \cdot \vec{n}) d\vec{\omega}'} \quad (2.17)$$

The BRDF describes the local illumination model. If we know the incident radiance field at a surface location, then we can compute the reflected radiance in all directions.

$\vec{L}_r \rightarrow \text{Reflected Radiance}$:

$$\vec{L}_r(x, \vec{\omega}) = \int_{\Omega} f_r(x, \vec{\omega}', \vec{\omega}) dE_i(x, \vec{\omega}) = \int_{\Omega} f_r(x, \vec{\omega}', \vec{\omega}) Li(x, \vec{\omega}')(\vec{\omega}' \cdot \vec{n}) d\vec{\omega}' \quad (2.18)$$

Note that $(\vec{\omega}' \cdot \vec{n}) = \cos\theta'$.

The surface is energy conservant. A surface cannot reflect more than it receives.

$$\int_{\Omega} f_r(x, \vec{\omega}', \vec{\omega}) (\vec{\omega}' \cdot \vec{n}) d\vec{\omega}' < 1, \text{ if } \vec{\omega}$$

2.4.3 The Reflectance

$P \rightarrow \text{Reflectance}$: To quantify the amount of flux reflected we use the ratio of the reflected and incident flux.

$$P(x) = \frac{d\Phi_r(x)}{d\Phi_i(x)} \frac{\int_{\Omega} \int_{\Omega} f_r(x, \vec{\omega}', \vec{\omega}) Li(x, \vec{\omega}') d\vec{\omega}' d\vec{\omega}}{\int_{\Omega} Li(x, \vec{\omega}') d\vec{\omega}'} \quad (2.21)$$

$P(x)$ is the percent of light reflected by the surface.
the remaining part is either transmitted or absorbed.

For physically based rendering $P(x)$ must be in the range $[0, 1]$.

2.4.4 Diffuse Reflection A surface with diffuse reflection is characterized by light being reflected in all directions when it strikes the surface.

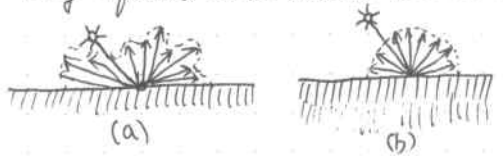


Fig 2.4 a diffuse material reflects light in all directions (a) general diffuse reflection (b) shows ideal Lambertian diffusion

A special case of diffuse reflection is Lambertian or ideal diffuse reflection, in which the reflected direction is perfectly random.

As a result the reflected Radiance is constant in all directions regardless of the incidence. This gives the constant BRDF, $f_{r,d}$:

$$L_r(x, \vec{\omega}) = f_{r,d}(x) \int_{\Omega} dE_i(x, \vec{\omega}') = f_{r,d}(x) E_i(x) \quad (2.22)$$

Using this relationship we can find the diffuse reflectance, ρ_d , for a Lambertian surface:

$$\rho_d(x) = \frac{d\Phi_r(x)}{d\Phi_i(x)} = \frac{\int_{\Omega} L_r(x) dA \int_{\Omega} d\vec{\omega}'}{E_i(x) dA} = \pi f_{r,d}(x) \quad (2.23)$$

The reflected direction of the light is as mentioned, perfectly random for a Lambertian surface. Given two uniformly distributed random numbers, $\xi_1 \in [0, 1]$ and $\xi_2 \in [0, 1]$ we find that the randomly reflected direction, $\vec{\omega}_d$, is distributed as:

$$\vec{\omega}_d = (\theta, \phi) = (\cos^{-1}(\sqrt{\xi_1}), 2\pi\xi_2) \quad (2.24)$$

We have used spherical coordinates (θ, ϕ) for the direction:

(θ) theta is the angle with the surface normal.

(φ) phi is the rotation around the normal.

2.4.5 Specular Reflection

Specular Reflections happen when light strikes a smooth surface - typically a metallic surface or a smooth dielectric surface (such as glass or water). Most surfaces have some imperfection, and as a result light is reflected only in the mirror direction, of which we have a perfect specular reflection.

The Reflected Radiance due to Specular reflection is:

$$L_r(x, \vec{\omega}_s) = \rho_s(x) Li(x, \vec{\omega}_s) \quad (2.25)$$

For perfect Specular reflection the mirror direction, $\vec{\omega}_s$, is:

$$\vec{\omega}_s = 2(\vec{\omega} \cdot \vec{n})\vec{n} - \vec{\omega} \quad (2.26)$$

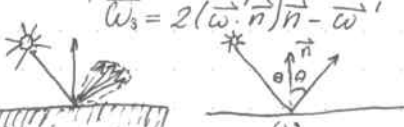
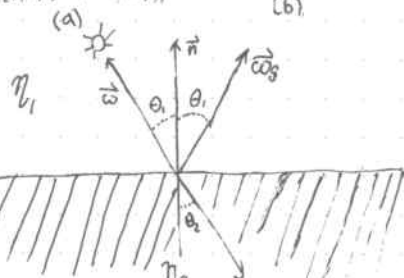


Fig 2.5 A Specular Surface Reflects the incoming light in the mirror direction

(a) Shows glassy Specular reflection (i.e. a rough mirror surface)

(b) Shows perfect specular reflection.

Fig 2.6 The geometry of Refraction and reflection.
(Notice that $\vec{\omega}_s$ and $\vec{\omega}'$ both point away from the surface)



We can express the perfect mirror reflection as a BRDF by using spherical coordinates for the direction.

$$f_{rs}(x, \vec{\omega}, \vec{\omega}) = 2P_s \delta(\sin^2\theta - \sin^2\phi) \delta(\phi - \phi \pm \pi) \quad (2.27)$$

$\delta(x) \rightarrow$ Dirac Delta function : Limits the direction in which the BRDF is nonzero.
 $(\delta(x))$ is nonzero only when $x=0$.

The Fresnel Equations / For smooth homogeneous metals and dielectrics the amount of light reflected can be derived from Maxwell's equations.

Given a ray of light in a medium with index of refraction we can compute the amount of light reflected as:

$$P_{||} = \frac{\eta_2 \cos\theta_i - \eta_1 \cos\theta_r}{\eta_2 \cos\theta_i + \eta_1 \cos\theta_r}, \quad P_{\perp} = \frac{\eta_1 \cos\theta_i - \eta_2 \cos\theta_r}{\eta_1 \cos\theta_i + \eta_2 \cos\theta_r} \quad (2.28)$$

$P_{||}$: Reflection Coefficient for light with the electric field parallel to the incident plane.

P_{\perp} : Reflection Coefficient for light with the electric field orthogonal to the plane incident.

$\eta_{\text{air}} \approx 1.0$, $\eta_{\text{water}} \approx 1.33$, $\eta_{\text{glass}} \approx 1.5-1.7$

For unpolarized light the Specular Reflectance (Also known as the Fresnel reflection coefficient) becomes:

$$F_r(\theta) = \frac{1}{2} (P_{||}^2 + P_{\perp}^2) = \frac{d\Phi_r}{d\Phi_i} \quad (2.29)$$

For unpolarized light, a good approximation to the Fresnel reflection coefficient was derived by Schlick.

$$F_r(\theta) \approx F_0 + (1 - F_0)(1 - \cos\theta)^5 \quad (2.30)$$

where F_0 is the value of the Real fresnel reflection coefficient at normal incidence.

Refraction: The Fresnel Equation (2.28) contains factor $\cos\theta_r$, where θ_r is the angle of the refracted ray. It can be computed from Snell's law:

$$\eta_i \sin\theta_i = \eta_r \sin\theta_r \quad (2.31)$$

The geometry for Refraction is shown in Fig 2.6. Using Snell's law, the direction, $\vec{\omega}_r$, of the refracted Ray (for a perfectly smooth surface with normal \vec{n}) is computed as:

$$\vec{\omega}_r = \frac{\eta_i}{\eta_r} (\vec{\omega} - (\vec{\omega} \cdot \vec{n}) \vec{n}) - \left(\sqrt{1 - \left(\frac{\eta_i}{\eta_r} \right)^2 (1 - (\vec{\omega} \cdot \vec{n})^2)} \right) \cdot \vec{n} \quad (2.32)$$

For the Refracted ray the amount of Transmitted light can be computed as $1 - F_r$.

10.3. The Phase Function

The phase function describes the distribution of the scattered light in participating media. Unlike most BRDF functions for surfaces, the phase function must integrate to one over the sphere.

$$\int_{\Omega_{4\pi}} p(x, \vec{\omega}, \vec{\omega}') d\vec{\omega}' = 1 \quad (10.9)$$

Even though it seems similar to the BRDF used for surfaces, there are two important differences: the phase function is unitless and normalized (the amount of scattering and absorption is controlled by the scattering and absorption coefficients).

The phase function often depends only on the angle, (θ) between the incoming ray and the scattered ray. And it can be written as $p(\theta)$, where $\theta=0$ is the forward direction and $\theta=\pi$ is the backward direction.

To Specify the preferred scattering direction of the phase function (forward or backward) one can compute the average cosine of the scattered direction, g , as:

$$g(x) = \int_{\Omega_{4\pi}} p(x, \vec{\omega}, \vec{\omega}') \cos\theta' d\vec{\omega}' \quad (10.10)$$

The value of $g \in [-1, 1]$ will be positive for forward scattering and negative for backward scattering. It is also a parameter for the commonly used Henyey-Greenstein phase function (described later).

The shape of the phase function is also used to classify the participating medium. The scattering is either isotropic or anisotropic. That is any phase function with a preferential scattering direction is anisotropic (this is the most common case). otherwise the scattering is isotropic. If the phase function further depends on the orientation of the medium, then the medium is ~~anisotropic~~ anisotropic, otherwise it is isotropic. Notice that unlike surfaces, we have two components that are either isotropic or anisotropic.

10.3.1 Isotropic Scattering: The phase function for isotropic scattering is a constant: $p(\theta) = \frac{1}{4\pi}$ (10.11)

This means that a photon that is scattered will be scattered in any random direction without memory of its origin (Fig 10.16)

10.3.2 The Henyey-Greenstein phase function.

The most commonly used phase function is the empirical Henyey-Greenstein phase function. [5] It was introduced to explain scattering by intergalactic dust, but it has since been used to describe scattering in atoms, clouds, skin, stone, and more. The function is:

$$P(\theta) = \frac{1-g^2}{4\pi(1+g^2-2g\cos\theta)^{1.5}} \quad (10.12)$$

where $g \in [-1, 1]$ is an asymmetry parameter equal to the average cosine of the scattered directions (See equation 10.10). Positive g gives forward scattering and negative g gives backward scattering (no preference ($g=1$) gives pure forward scattering in the same direction). This is illustrated in figure 10.1. The function is essentially giving ellipsoid scattering distributions where the shape of the ellipsoid is controlled by g .

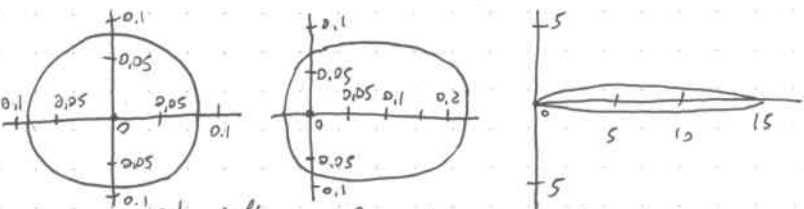


Figure 10.1 The Henyey-Greenstein phase function with different g .

From left to right $g=0.0$, $g=0.3$, and $g=0.9$

→ For more complex types of scattering, one can use a combination of several Henyey-Greenstein functions.

$$P(\theta) = \sum_{i=1}^N w_i \frac{1-g_i^2}{4\pi(1+g_i^2-2g_i\cos\theta)^{1.5}} \quad \text{where } \sum_{i=1}^N w_i = 1 \quad (10.13)$$

Here g_i controls the shape of each lobe and w_i the weight. Such a multiflobed function can be used to model more complex scattering, and it can give very realistic results. Commonly used is a sum of a forward scattering and backward scattering lobe.

→ Another advantage of the Henyey-Greenstein function is that it can be importance-sampled very easily. Given an incoming direction, ω_i of a photon, the angle, θ , of the new scattered direction is given by:

$$\cos\theta = \frac{1}{|2g|} \left(1 + g^2 - \left(\frac{1-g^2}{1-g+2g\xi} \right)^2 \right) \quad (10.14)$$

Where ξ is a uniform random number between zero and one. ϵ is the same angle ω in the phase function. The rotation ϕ is uniformly distributed.

10.3.3 The Schlick phase function

For most applications the accurate shape of the empirical Henyey-Greenstein phase function is less important.

Since the shape of the function is close to an ellipsoid, one might approximate it by an ellipsoid and thereby eliminate the relatively costly 1.5 exponent in the denominator. This observation was made by Schlick [9] who used the following phase function:

$$P(\theta) = \frac{1-k^2}{4\pi(1+k\cos\theta)^2} \quad (10.15)$$

where $k \in [-1, 1]$ is used to control the preferred direction of the scattering (similar to g in the Henyey-Greenstein function).

$k=0$ gives isotropic scattering, $k>0$ is forward scattering, $k<0$ is backward scattering. → The Schlick phase function is also very simple to importance-sample. The angle, θ , of the new scattered direction is given by:

$$\cos\theta = \frac{2k\xi + k - 1}{2k\xi - k + 1} \quad (10.16)$$

where ξ is a uniformly distributed random number between zero and one. The rotation is uniformly distributed.

10.3.4 Other Phase Functions.

There are many other phase functions available to describe scattering of light. In particular a number of analytical phase functions have been derived for the scattering of electromagnetic waves for specific geometries.

The type of geometry most frequently used is the homogeneous spheres. This makes the medium isotropic, and the scattering can be explained with a phase function that takes only the scattered angle as a parameter. Phase functions have been derived for the case when the medium contains many small spheres that each reflect light diffusely according to Lambert's law. Most interesting those functions have been derived for dielectric and metal spherical particles.

→ Scattering from very small spheres (smaller than the wavelength of light) is explained by Rayleigh Scattering [11]. The phase function is almost uniform, but the scattering coefficients include a dependency on the wavelength raised to the fourth power. This makes the scattering slightly wavelength-dependent, with blue light being scattered more than the other wavelength of light. Rayleigh Scattering can be used to scatter model scattering of light from molecules in the atmosphere and to model the diffuse sky and sunsets.

For homogeneous spheres of arbitrary size the scattering pattern becomes more complex. It is necessary to use Mie Theory [85] to compute the sphere function. These formulas are quite complex and difficult to use, and it makes sense to use them only when accurate scattering of a homogeneous sphere is needed. An interesting observation is that Mie scattering often is characterized by a strong forward scattering component and a smaller backward scattering component. This scatter pattern can, for most graphics simulation, be adequately modeled with a multi-lobed Henyey-Greenstein phase function.

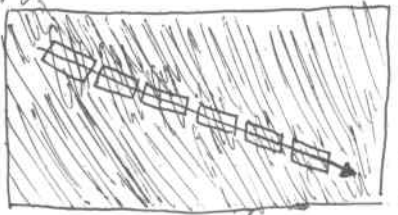


Figure 10.2 The Ray marching algorithm computes the contribution from the medium by dividing the ray into smaller segments. For each segment the medium is assumed to be homogeneous.

10.4 Ray Marching

The volume rendering equation (eq 10.7) can, except for the simplest cases, only be solved using numerical integration. A numerical integration can be done by taking small steps through the medium and making some local simplifying assumptions within the segment considered. This approach is called Ray Marching.

→ In Ray marching the ray is divided into little segments of length Δx . For each segment it is assumed that the incoming light is constant and that the properties of the medium are constant. With these simplifications the Radiance from a small segment due to direct illumination can be computed as:

$$L(x, \vec{\omega}) = \sum_i L_i(x, \vec{\omega}_i) p(x, \vec{\omega}_i, \vec{\omega}) \sigma_s(x) \Delta x + e^{-\tau(x) \Delta x} L(x + \Delta x, \vec{\omega}) \quad (10.17)$$

Where N is the number of light sources in the scene, and L_i is the radiance from each light source. The first term sums the contribution from the segment due to direct illumination and the last term is the radiance entering the segment at the backside.

→ For a medium of a finite size, Ray Marching can be used to compute the radiance due to direct illumination (single scattering) by recursively calling the formula to move backwards through the medium. (See Fig 10.2) (10.18)

$$L_{n+1}(x, \vec{\omega}) = \sum_i L_i(x, \vec{\omega}_i) p(x, \vec{\omega}_i, \vec{\omega}) \sigma_s(x) \Delta x + e^{-\tau(x) \Delta x} L_n(x + \Delta x, \vec{\omega})$$

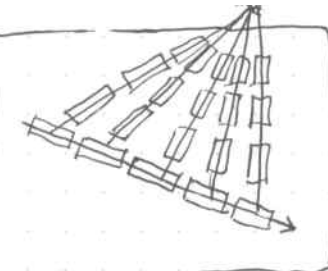


Figure 10.3. The Contribution From the Light Source Must Be Attenuated Based on the Medium Along the Shadow Ray. In non-homogeneous media this requires a Ray-Marching Integration for each Shadow Ray.

Notice that direct illumination must be attenuated properly based on the distance that the shadow ray moves through the medium (for non-homogeneous media it is often necessary to integrate this using another Ray marching evaluation). This is shown in Figure 10.3.

To improve visual appearance and reduce aliasing artifacts it is often useful to randomly pick the sample position at which the direct illumination is computed. This can be done either locally within each segment, or globally by adding a small random offset to the entry point of the ray.

Equation 10.18 includes only single scattering. For a multiple scattering simulation, it is necessary to integrate all of the in-scattered radiance at every segment. This can be done by sampling the sphere of directions around the segment (point) of interest, which leads to the following formulation:

$$L_{n+1}(x, \vec{\omega}) = \sum_i^N L_i(x, \vec{\omega}_i) p(x, \vec{\omega}_i, \vec{\omega}) \sigma_s(x) \Delta x + \left\{ \frac{1}{S} \sum_{i=1}^S L_i(x, \vec{\omega}_s) p(x, \vec{\omega}_s, \vec{\omega}) \right\} \sigma_s(x) \Delta x + e^{-\tau(x) \Delta x} L_n(x + \Delta x, \vec{\omega}) \quad (10.19)$$

Here S sample rays are used to estimate the in-scattered light. The contribution from each sample ray is found by recursively evaluating this formula, which is already recursive! As such this formula is very costly to evaluate, and one of the reasons why most simulations of participating media have excluded multiple scattering. In many cases, however, multiple scattering is essential to get the correct appearance. For example, a cloud will look flat and dark grey without multiple scattering. In general it is necessary to simulate multiple scattering in media with a high albedo i.e. scattering dominates over absorption. Fortunately, the photon map provides an efficient solution to the problem.

10.4.1 Adaptive Ray Marching

The ray marcher in equation 10.19 is based on a uniform step size through the medium. For non-homogeneous media and media with local variations in the lighting (such as shadows), it is better to use adaptive Ray Marching. Adaptive Ray marching uses segments of varying length to capture local changes more efficiently. This is usually done by adjusting the step size on the fly, based on the observed local illumination and scattering properties.

If a contrast in the illumination is seen or if the scattering properties (albedo or extinction coefficient) changes significantly in one step, then the segment can be subdivided into a sequence of smaller segments. The simplest method for doing this is a recursive ray marcher, where the midpoint of the segment is sampled recursively until the length of the segment is below a certain threshold, or until the contrast between the endpoints of the segment is sufficiently low.

Another simple method for non-homogeneous media is to adjust the step size based on the observed extinction coefficient. For media with unknown properties this can be efficient. One possibility is to use a random step size computed as:

$$\Delta x = -\log \xi / \sigma_t(x) \quad (10.20)$$

where $\xi \in [0, 1]$ is a uniform random number. In this way the average step size will be the same as the average distance that a photon moves through the medium before an interaction.

10.5 Photon Tracing

When tracing photons in a scene with participating media, the photons interact with the media and are scattered and/or absorbed. If a photon hits a surface we can use the techniques described in chapter 5, and the photon is either absorbed, reflected, or transmitted. When a photon enters a participating medium, it does not scatter at the boundary of the medium.

Instead it moves through the medium until it is either scattered or absorbed. The probability that such an interaction happens is determined from the extinction coefficient.

The average distance, d , that a photon moves through a medium before the next interaction happens is determined from the extinction coefficient. Happens is given by:

$$d = \frac{1}{\sigma_t} \quad (10.21)$$

A beam of light passing through a medium will have its intensity reduced by $e^{-\sigma_t s}$ where s is the distance through the medium. So non-homogeneous media σ_t is replaced by $\sigma_t(x)$, which is evaluated using Ray marching. When tracing photons, we can importance-sample according to this formula by using the following expression for the distance, d , to the next interaction:

$$d = -\log \xi / \sigma_t \quad (10.22)$$

where $\xi \in [0, 1]$ is a nonuniformly distributed random number. If we use this formula to determine the distance to the next event, then we do not have to trace the power of the photon as it moves through the medium.

10.5.1 Photon Scattering

At the point of interaction the photon is either absorbed or scattered. The probability of scattering is given by the scattering albedo, Λ :

$$\Lambda = \frac{\sigma_s}{\sigma_t} \quad (10.23)$$

Based on the value of Λ , a new scattered photon can be generated by scaling the power of the incoming photon with Λ . This approach will work, but it will in many cases lead to a large number of photons in the media with a very low power. This is wasteful. A better approach is to use Russian Roulette to decide if a photon is scattered or absorbed. This is done by computing a random number $\xi \in [0, 1]$ to 1.

$$\text{Given } \xi \in [0, 1] \rightarrow \begin{cases} \xi \leq \Lambda & \text{Photon Scattered} \\ \xi > \Lambda & \text{Photon absorbed} \end{cases} \quad (10.24)$$

If the photon is scattered it will continue with the same power (no scaling by Λ is necessary). For colored photons it may be necessary to use an average albedo, $\bar{\Lambda}$, and then scale the individual components of the scattered photon (similar to Parallax Removal).

The direction of a scattered photon should be computed by importance Sampling the phase function. The phase functions for participating media are often highly anisotropic, and a uniform sampling is therefore very inefficient. It is much better to use the importance-sampling formula presented in Section 10.3.

10.5.2 Photon Storing

When a photon interacts with a medium it is stored (independent of the fact of whether the event is scattering or absorption). For participating media we use a separate volume photon map. This is due to the fact that the radiance estimate in a participating medium is different than the estimate for surfaces (see Section 10.6).

A useful optimization for participating media is to store only photons that have been scattered at least once before (as shown in Figure 10.4). In this way the contribution due to the direct illumination is omitted — this component can be computed very easily using traditional techniques. See Section 10.7 for more detail!

10.5.3 Photon emission

Photons can also be emitted from the participating media. An accurate model of a candle flame might simulate the motion and temperature of the hot gas, and based on these parameters, photons can be emitted from locations in the media with a spectrum based on the local conditions. This would be more accurate than approaches that try to approximate the flame with a point light source.

④ 10.6 The Volume Radiance Estimate

How can we estimate the out-scattered radiance at a given point inside the medium, based on the stored photons? The two-dimensional approximation for surfaces cannot be used. To compute the out-scattered radiance, \mathcal{L}_o , we need to evaluate Equation 10.4:

$$(\vec{\omega} \cdot \nabla) \mathcal{L}_o(x, \vec{\omega}) = \sigma_s(x) \int_{\Omega 4\pi} p(x, \vec{\omega}, \vec{\omega}') L(x, \vec{\omega}') d\vec{\omega}' \quad (10.25)$$

The stored photons represent incoming flux, so this equation should be converted to an integral over incoming flux. This is done using the relationship between flux and radiance in the participating medium:

$$\mathcal{L}(x, \vec{\omega}) = \frac{d^2\Phi(x, \vec{\omega})}{\sigma_s(x) d\vec{\omega} dV} \quad (10.26)$$

$$\begin{aligned} \text{Combining Equations 10.25 and 10.26 we get [48]:} \\ (\vec{\omega} \cdot \nabla) \mathcal{L}_o(x, \vec{\omega}) &= \sigma_s(x) \int_{\Omega 4\pi} p(x, \vec{\omega}', \vec{\omega}) \frac{d^2\Phi(x, \vec{\omega}')}{\sigma_s(x) d\vec{\omega}' dV} d\vec{\omega}' \\ &= \sigma_s(x) \int_{\Omega 4\pi} p(x, \vec{\omega}', \vec{\omega}) \frac{d^2\Phi(x, \vec{\omega}')}{\sigma_s(x) d\vec{\omega}' dV} d\vec{\omega}' \\ &= \int_{\Omega 4\pi} p(x, \vec{\omega}', \vec{\omega}) \frac{d^2\Phi(x, \vec{\omega}')}{dV} \end{aligned} \quad (10.27)$$

Notice the similarity with the surface radiance estimate (Equation 7.6). Again we have an equation where we need to estimate the local photon density. However, for participating media, the density should be measured over the entire volume instead of the surface.

Using the same strategy as for the surface radiance estimate we can locate the n nearest photons, and using the same assumptions for the estimate we get:

$$\begin{aligned} (\vec{\omega} \cdot \nabla) \mathcal{L}_o(x, \vec{\omega}) &= \int_{\Omega 4\pi} p(x, \vec{\omega}, \vec{\omega}') \frac{d^2\Phi(x, \vec{\omega}')}{dV} \\ &\approx \sum_{p=1}^n f(x, \vec{\omega}_p, \vec{\omega}) \frac{\Delta \Phi_p(x, \vec{\omega}_p)}{\Delta V} \\ &\approx \sum_{p=1}^n f(x, \vec{\omega}_p, \vec{\omega}) \frac{\Delta \Phi_p(x, \vec{\omega}_p)}{\frac{4}{3}\pi r^3} \end{aligned} \quad (10.28)$$

Here we have substituted the small volume ΔV with the volume of the sphere ($\frac{4}{3}\pi r^3$) containing all the photons.

Similar to the surface estimate, this can be seen as expanding a sphere around the intersection point until it contains the n nearest photons. This is shown in Figure 10.5.



Figure 10.4. Photon Tracing in a Scene with a Participating Medium. The photons that enter the medium can be either scattered or absorbed. These photons are stored at the location of the interaction in a separate photon map. Photons that hit surfaces are scattered using standard techniques with the photon map.

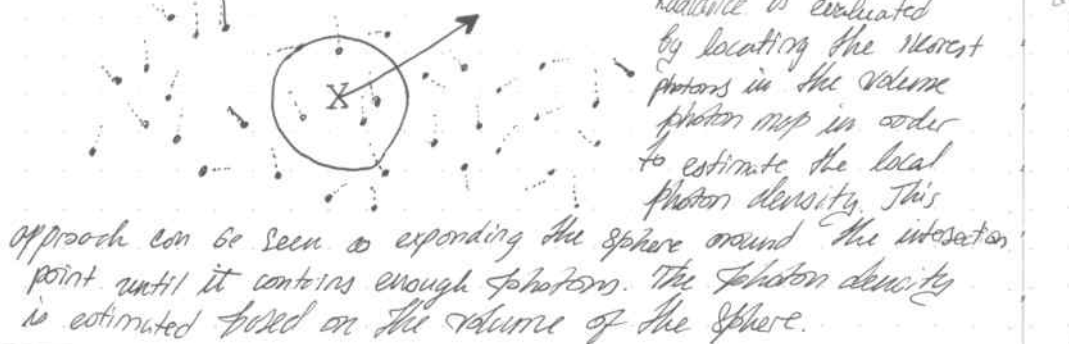


Figure 10.5 Out-scattered radiance is evaluated by locating the nearest photons in the volume photon map in order to estimate the local photon density. This approach can be seen as expanding the sphere around the intersection point until it contains enough photons. The photon density is estimated based on the volume of the sphere.

10.7 Rendering Participating Media

With the volume photon map and the ability to compute a Radiance estimate, we have the necessary tools to render scenes with participating media. The rendering technique is an extension of the two-pass algorithm presented in Chapter 9.

The first pass is emitting photons from the light sources and storing them as they hit the surfaces or the media in the model; the second pass uses ray tracing to render the image. If a ray hits a surface, we use the approach described in chapter 9. If the ray enters a participating medium, we use ray marching to integrate the illumination. We split the in-scattered Radiance into Single Scattering, I_s , and Multiple Scattering, I_m :

$$L(x, \vec{\omega}) = L_s(x, \vec{\omega}) + L_m(x, \vec{\omega}) \quad (10.29)$$

The single scattering term is evaluated using Ray Tracing, and the multiple scattering term is computed using the Volume Radiance estimate.

This is shown in Figure 10.6.

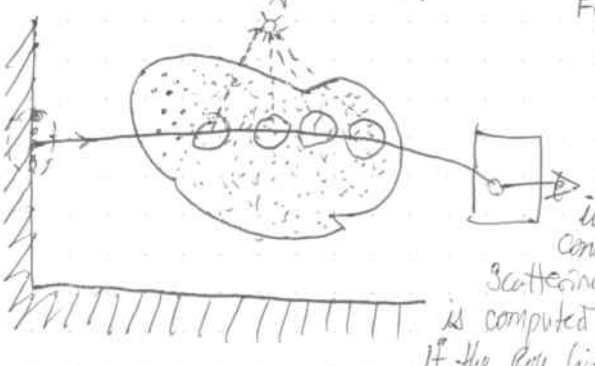


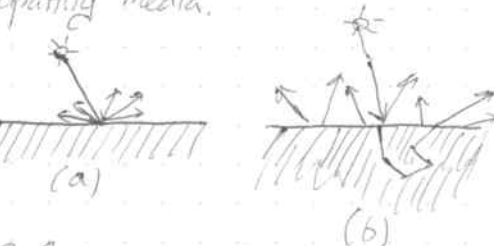
Fig 10.6. Participating media is rendered using Ray marching. When a ray enters the medium a ray marching algorithm integrates the contribution from multiple scattering to direct illumination.

is computed using Ray Tracing.

By inserting the Volume Radiance estimate in the Ray Marching algorithm (Eq. 10.19) we get:

$$\begin{aligned} L_{out}(x, \vec{\omega}) = & \sum_i^N L_i(x, \vec{\omega}_i) p(x, \vec{\omega}_i, \vec{\omega}) \Delta s(x) \Delta x + \\ & \left\{ \sum_{p=1}^n f(x, \vec{\omega}_p, \vec{\omega}) \frac{\Delta \phi_p(x, \vec{\omega}_p)}{4\pi r^3} \right\} \Delta x + \\ & e^{-\tau(x) \Delta x} L_n(x + \Delta x, \vec{\omega}) \end{aligned} \quad (10.30)$$

This equation is used to integrate the contribution from participating media.



(a)



(b)

10.8 Subsurface Scattering

Subsurface Scattering happens in all non-metallic materials. In computer graphics it is often approximated by a diffuse reflection term where the assumption is that light scattering the material leaves the material at the same location in a random direction (shown in Figure 10.7(a)). For translucent materials such as marble, skin, and milk, this is a bad approximation. Translucent materials often have a soft appearance and light will travel through thin slabs of the material. An example is a piece of paper illuminated from behind. To accurately render translucent materials it is necessary to take into account the fact that light entering the material can leave the material at a different location, as shown in figure 10.7(b). The first method that fully simulated this phenomena was based on Photon Mapping and presented in [23,52]. It uses the photon-mapping algorithm for participating media with some improvements specific to subsurface scattering.

To simulate Subsurface Scattering with Photon mapping, we first build a photon map using Photon Tracing as shown in Figure 10.8. Here the photons are reflected at the same material interface and forced through the material of medium using the same techniques described earlier in this chapter. Each time a photon interacts with the material it is stored in the volume photon map. We exclude photons coming directly from the light source, as is the case for participating media.

Since this contribution can be computed (with some approximations) using standard Ray-tracing Techniques.

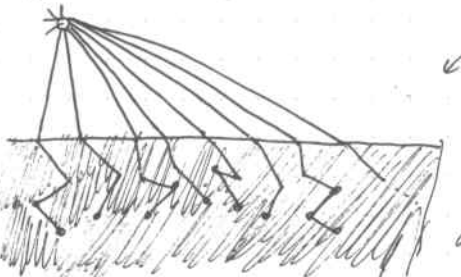


Fig 10.8. Photon Tracing for Subsurface Scattering.

10.8.2 Rendering

Rendering of materials with Subsurface scattering proceeds in a similar way as rendering of Participating Media.

When a Ray intersects a Subsurface scattering material, it is reflected into the medium. Ray tracing is used to evaluate the contribution from the medium along the reflected Ray. For efficiency reasons the step size for the Ray Marcher is varied locally, based on the extinction coefficient.

A good value is $\Delta x(x) = -\log \xi / \sigma_t(x)$, where $\xi \in [0, 1]$ is a uniform random number. For dense materials this ensures a small step size. Furthermore, the Ray Marcher should be stopped using Russian Roulette sampling once the optical depth reaches a certain value.

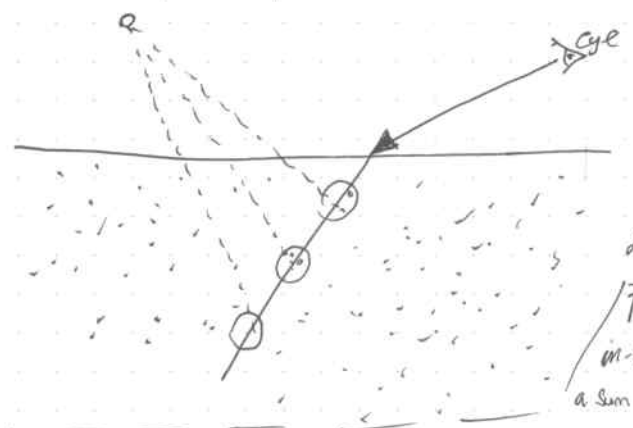


Figure 10.9
Rendering Materials with Subsurface scattering using the Photon Map.

The contribution due to in-scattered radiance is computed as a sum of two terms: A direct

single-scattering term and an indirect multiple-scattering term. The indirect multiple-scattering term is computed using the volume radiance estimate described earlier, and the direct illumination is computed using Ray Tracing. The Ray-tracing technique traces a shadow ray to the light source to check for visibility. This shadow ray goes straight through the material boundary. This is an approximation since the shadow ray should be refracted, but the configuration for the refraction is difficult to compute exactly. The only way to avoid this approximation is to use the Photon map for all types of illumination.

We can move the computation of direct illumination more easily by estimating the true distance that the Reflected Ray would have moved through the medium.

$$d_i' = d_i \frac{|\vec{w} \cdot \vec{n}|}{\sqrt{1 - \left(\frac{1}{n}\right)^2 (1 - |\vec{w} \cdot \vec{n}|^2)}} \quad (10.31)$$

Here d_i is the absorbed distance and d_i' is the estimate of the true distance \vec{n} is the normal at the surface location intersected by the shadow Ray. The attenuation of the light from the light source should be modified using this equation.

10.9 Examples The following pages of the book contain several examples illustrating the simulation of participating media and subsurface scattering with the Photon mapping.

10.9.1 Rising Smoke.

Figure 10.10 shows a multiple-scattering simulation in turbulent smoke. The smoke simulation is due to techniques described in Fedkiw in [25]. To render the smoke we used roughly two million photons. Multiple scattering is important for the realism of the smoke. A single-scattering simulation looks flat in comparison.

10.9.2 Smoke Flowing Past a Sphere.

Figure 10.11 is another smoke simulation from DSI [Ronald Fedkiw, Jis Stam, and Henrik Wann Jensen. "Visual Simulation of Smoke." In Proceedings of SIGGRAPH 2003, Computer Graphics Proceedings, Annual Conference Series, to appear] To render the smoke we used roughly two million photons.

Multiple Scattering

It illustrates a multiple scattering simulation for an animation showing smoke flowing past a sphere. Roughly 1-2 million photons were used per frame in the animation.

Fig 10.10 A simulation of multiple scattering in turbulent smoke rising due to buoyancy (from [25])

Fig 10.11 Sequence of rendering images from a simulation of smoke flowing past a sphere (from [25]. (See Color Plate IX)

10.9.3 A Volume Caustic. Figure 10.12 shows a volume caustic. The volume caustic is a result of light passing through the glass sphere and illuminating the fog medium. Here the volume caustic is simulated using 1500,000 photons. For this simulation the adaptive Ray-Marching algorithm significantly reduces the rendering time by concentrating the effort on the focused beam rather than the less interesting parts of the smoke.

10.9.4 Michelangelo's David

Figure 10.13 shows a rendering of Michelangelo's David (from [61]). The model has approximately 8 million triangles. We used one million photons to capture the multiple scattering component of the subsurface scattering simulation.

Figure 10.12. A volume caustic created as light focused through a glass ball illuminates the fog medium.

Figure 10.13. The David represented using approximately 8 million triangles. This image was rendered with subsurface scattering using photon mapping with roughly one million photon points.

Figure 10.14. A weathering simulation of a granite sphinx from [23].

(a) is the fresh granite, (b) shows the erosion due to salt, (c) shows the reddening due to dissolved iron, and (d) shows the combined weathering effect due to salt and iron. (See Color Plate XI.)

Figure 10.15. A marble bust. Subsurface scattering is essential to capture the soft appearance of marble.

Figure 10.16. A translucent marble bust (See Color Plate XII.)

Figure 10.17. A diffuse rendering of the marble bust. Notice the substantial difference with the full subsurface scattering simulation. The diffuse material gives the impression of a hard material. (See Color Plate XIII.)

10.9.5 A Weathered Granite Sphinx

The four images in Figure 10.14 demonstrate how photon mapping and subsurface scattering can render the result of a complex weathering simulation. [23] Subsurface scattering is the only way to correctly render the effect of weathering, which is due to changes in the material structure. Dissolved iron, in particular, is often present below the surface. Even without the weathering simulation, the simulation of subsurface scattering is important to the appearance of granite.

10.9.6 A Translucent Marble Bust

Marble is a translucent material and subsurface scattering is essential to capture the appearance of marble. Figure 10.15 is a simulation of a marble bust. Only 200,000 photons were used in this simulation. Subsurface scattering is important for the smooth appearance of marble, but it is also critical for correctly simulating translucency. This is particularly noticeable in Figure 10.16, which shows a close-up of the marble statue now illuminated from behind.

Note how the light bleeds through the hair and the nose and still gives a soft appearance of the marble. Compare this with the diffuse rendering of the same model and the same lighting conditions in Fig 10.17. The diffuse rendering looks the smooth and soft appearance and looks hard and unattractive compared with the subsurface scattering simulation.

11 Optimization Strategies. This chapter contains several different techniques to make a photon-mapping implementation faster and more efficient. Some of these ideas are fairly general, some are very important (such as irradiance caching), and some are special tricks for the photon map.

11.1 Irradiance Caching.

The irradiance caching idea was introduced by Ward et al. in 1988 [118] as a method for speeding up the computation of indirect illumination (color bleeding) in a Monte Carlo ray tracer (Radiance first). It is a method for caching and re-using (via interpolation) irradiance values on Lambertian surfaces. As mentioned in Chapter 9 it can (and should!) be used in the rendering step of the two-pass photon-mapping algorithm to cache irradiance values at Lambertian surfaces.

Indirect illumination on diffuse surfaces is often the most costly component to compute in a Monte Carlo Ray Tracer, since it requires a large number of rays. This is the case even in the two-pass photon-mapping algorithm where only the first source of diffuse illumination is computed. Speeding up this computation is very important.

The irradiance at a location, x , on a diffuse surface is computed by sampling the incident radiance above x . This is equivalent to evaluating the integral in Equation 2.18. Instead of sampling the hemisphere uniformly, we can include the signed cosine from the diffuse BRDF, which gives the following equation for sampling the irradiance.

$$E(x) = \frac{\pi}{MN} \sum_{j=1}^M \sum_{i=1}^N L_{ij}(\theta_i, \phi_i) \quad (11.1)$$

where $\theta_i = \sin^{-1}\left(\sqrt{\frac{i-\xi_1}{M}}\right)$ and $\phi_i = 2\pi \frac{i-\xi_2}{N}$ (11.2)

Here $\xi_1 \in [0, 1]$ and $\xi_2 \in [0, 1]$ are uniformly distributed random numbers, and M and N are the subdivisions of the hemisphere. Note that we could have used $\theta_i = \sin^{-1}(\sqrt{\xi_1})$ and $\phi_i = 2\pi \xi_2$ instead. However, the formulation in Equation 11.2 includes the stratification of the hemisphere, which includes much better results than uniform random sampling.

The evaluation of Equation 11.1 requires tracing $M \times N$ rays to estimate the incident radiance from different directions. To get good estimates it is usually necessary to use $M \times N = 200-5000$ sample rays. This is very costly. An important observation made by Ward et al. [118] is that indirect illumination on diffuse surfaces often changes slowly in a small area.

As such it seems like a natural candidate for interpolation. The idea is to compute irradiance only at the set selected locations on the surfaces in the model and then interpolate irradiance for the remaining locations.

The decision whether to interpolate or compute irradiance at a location is based on the previously computed values. If we want to compute a new irradiance value at x we first look at the previously computed irradiance values. For each of these values we compute a weight, w_i . That tells us if we can use the value for interpolation. For an irradiance value at x_i the weight is computed as:

$$w_i(x, \vec{n}) = \frac{1}{E_i(x, \vec{n})} \quad (11.3)$$

where $E(x)$ is an estimate of the amount of change in the irradiance from x_i to x . This change is estimated based on a split-sphere model [118]. This model assumes a hemisphere above x_i which is black on one half of the hemisphere and white on the other. This type of hemisphere represents a sharp boundary in the incident illumination, and it can provide a good estimate of the most change in the irradiance that we can observe as we move away from x_i . The two possible changes are: a change to the surface location and a change in the surface orientation (the normal). From this model the change in irradiance can be estimated as [118]:

$$E(x, \vec{n}) = E_i(x_i) \left\{ \frac{4}{\pi} \frac{\|x_i - x\|}{R_0} + \sqrt{2 - 2\vec{n} \cdot \vec{n}_i} \right\}, \quad (11.4)$$

where \vec{n}_i is the surface normal at x_i . E_i is the irradiance at x_i and R_0 is the harmonic mean distance to the objects seen from x_i . This value is computed as the reciprocal of the sum of the reciprocal distances recorded for each ray when evaluating Equation 11.1.

For the weight w_i , we can use a slightly simplified version of Equation 11.4 and we find that:

$$w_i = \frac{1}{\frac{\|x_i - x\|}{R_0} + \sqrt{1 - \vec{n} \cdot \vec{n}_i}} \quad (11.5)$$

The value of this weight is an indication of how good an estimate the irradiance E_i is of the irradiance at x . The higher the weight the better the estimate. If it is too low then we cannot use it. Ward suggested only using weights where:

$$w_i(x, \vec{n}) > \frac{1}{\alpha} \quad (11.6)$$

where α is a user-controlled parameter that is proportional to the maximum allowed error on the estimate.

To compute an estimate of the irradiance at x , we compute a weight for all previously computed irradiance values. For the irradiance values where $w_i > 1/\alpha$ we get:

$$E(x, \vec{n}) \approx \sum_{i, w_i > 1/\alpha} \frac{w_i(x, \vec{n}) E_i(x_i)}{\sum_{i, w_i > 1/\alpha} w_i(x, \vec{n})} \quad (11.7)$$

If there is no previously computed irradiance value with a sufficiently high weight, then we compute a new one.

This is the basic principle in the irradiance caching algorithm. There are a number of techniques to make it practical. Firstly, it is very costly to compute the weight for all irradiance values over and over. It is clear that each irradiance value is useful only in a small region of the model. We can precompute the maximum size of this region by ignoring the change in surface normal and only looking at the value of the weight as a function of the distance. The distance at which the weight becomes too low is the maximum distance. It defines a sphere in which the irradiance value is useful. We can place this sphere in an octree structure. The structure is efficient when we want to query if a previously computed irradiance value can be re-used, since we can search down the octree based on our current location and check only those irradiance values that are placed on voxels of the octree.

Another check for making the irradiance computations practical is to automatically reject all previously computed samples that are above the tangent plane of the current surface location. This is necessary since we may see important objects that are not visible from the samples in front of us.

11.1.1 Irradiance Gradients

It is possible to further improve the quality of the irradiance estimate by including information about the gradient of the irradiance with each irradiance value.

The gradient can be estimated from the rays used in Equation 11.1. There is a gradient for both the orientation, $\nabla_p E$, and the position, $\nabla_p E$. Ward and Heckel [117] derived the formulae for the gradients.

They found that the position gradient could be estimated as:

$$\nabla_p E = \sum_{i=1}^N \left\{ \overrightarrow{T}_i \frac{2\pi}{N} \sum_{j=2}^M \frac{\sin \theta_{j-} (\cos^2 \theta_{j-})}{\min(d_{j,i}, d_{j-1,i})} (Z_{j,i} - Z_{j-1,i}) + \overrightarrow{T}_{i-} \sum_{j=1}^M \frac{\sin \theta_{j+} - \sin \theta_{j-}}{\min(d_{j,i}, d_{j-1,i})} (Z_{j,i} - Z_{j-1,i}) \right\} \quad (11.8)$$

where

$$Z_{j,i}$$

$$d_{j,i}$$

$$\overrightarrow{T}_i$$

$$\overrightarrow{T}_{i-}$$

$$\theta_{j-}$$

$$\theta_{j+}$$

$$\Phi_{k-}$$

is the radiance from direction j,i

is the distance to the object seen in direction j,i ($d_{j,i}$)

is a vector orthogonal to the normal in the direction ϕ_j

is a vector orthogonal to the normal in the direction $\phi_{i-} + \pi/2$

$$\sin^{-1} \sqrt{f_{j,i}}$$

$$\sin^{-1} (c_{iH}) / M$$

$$2\pi k/N$$

The rotational gradient is estimated as:

$$\nabla_r E = \frac{\pi}{MN} \sum_{i=1}^N \left\{ \overrightarrow{T}_i \sum_{j=1}^M Z_{j,i} \tan \theta_j \right\} \quad (11.9)$$

where \overrightarrow{T}_i is a vector orthogonal to the normal direction $\phi_i + \frac{\pi}{2}$.

Using these gradients, the irradiance estimate in Equation 11.7 can be extended as:

$$E(x, \vec{n}) \approx \sum_{i, w_i > 1/\alpha} \frac{w_i(x, \vec{n}) \{ E_i(x_i) + (x - x_i) \nabla_p E_i + (\vec{n} \cdot \vec{x} \vec{n}) \nabla_r E_i \}}{\sum_{i, w_i > 1/\alpha} w_i(x, \vec{n})} \quad (11.10)$$

Figure 11.1. The irradiance cache works very well in the box scene.

The bright dots superimposed on the darkened box image represent the position at which a new irradiance sample was computed. Notice how large parts of the model can use an interpolated irradiance value.

11.1.2 Irradiance Caching and Photon Mapping

Photon mapping and irradiance caching work very well together. In the two-pass photon-mapping algorithm, the indirect illumination is soft since the high-frequency caustics contribution is completely computed using the caustics photon map. This is very important since it eliminates the main cause for the error in the irradiance cache. Caustics break the assumptions of the interpolation scheme, and if they are included in the irradiance cache, the results will be suboptimal.

Furthermore, the photon map can provide additional information to the irradiance sampling. Instead of distributing the sample rays uniformly in all directions, it is possible to use the approximate representation of the flux in the photon map to importance sample in the direction of the bright indirect sources. This is described in the following section.

11.2 Importance Sampling

Besides providing a radiance estimate, the photon map can be used to sample the scene more efficiently. Most Monte approaches use first the BRDF to select the region to sample. This is fine for specular surfaces, but for diffuse surfaces it is better to use information about where the light is coming from. The photon map has this information and the approximate flux representation has been demonstrated to reduce noise in Monte Carlo ray tracing [47].

The optimal probability distribution function, $p(x, \vec{\omega})$, for importance sampling when integrating the reflected radiance at a surface location x , is:

$$p(x, \vec{\omega}) \propto f_r(x, \vec{\omega}, \vec{\omega}') Z_r(x, \vec{\omega}') / (\vec{\omega}' \cdot \vec{n})$$

$$= f_r(x, \vec{\omega}, \vec{\omega}') \frac{d\Phi^2(x, \vec{\omega}')} {dA d\vec{\omega}'} \quad (11.1)$$

We have already seen how the photon map can provide information about the distribution of the flux of Φ at x . We can get a sampling of the flux at x by locating the nearest photons around x . We assume that these photons all hit x and, such, are representative of the flux at x .

A simple way to importance-sample according to both the BRDF as well as the flux distribution from the photons was presented in [47]. The concept is simple. Consider first importance sampling of a BRDF. Given an outgoing (reflected) direction we have a function that, given two random numbers, provides a direction in which to sample the incident radiance. For a Lambertian surface this function is:

$$\vec{\omega}' = (\theta', \phi') = (\cos^{-1} \xi_1, 2\pi \xi_2) \quad (11.2)$$

where $\xi_1 \in [0,1]$ and $\xi_2 \in [0,1]$ are the two random numbers. This function maps two random numbers in the unit square to a direction on the hemisphere.

Instead of just uniformly sampling the square with ξ_1 and ξ_2 , we can include further information about the flux. This can be done by dividing the square into a number of cells. A cell represents a region on the hemisphere (a set of directions). For each cell we accumulate the power of the photons from the directions represented by the cell. We can find the cell that a photon maps to by inverting the importance-sampling

— probability distribution used for the BRDF. In case of a diffuse surface this function is: $(u, v) = \left(\cos^2 \theta, \frac{\phi}{2\pi} \right)$ (11.13)

Here u, v are the coordinates in the unit square. Based on the recorded power in the cells, we can build a histogram of the power accumulated by the cells. The modified importance sampling proceeds by picking cells in the histogram with a probability proportional to the power accumulated in each cell. A new random position is then selected within the cell and mapped to a direction. A sample ray is then traced in the selected direction to estimate the radiance. The returned estimate should be divided by the probability of picking the cell.

Figure 11.2 gives an example of path tracing using the photon-map-based importance sampling scheme. Note how the amount of noise in the Photon Map image is much lower.

It is easy to use this photon-map importance-sampling method with the irradiance-caching scheme. It is also faster since the histogram only has to be built once for a new irradiance sample.

11.3 Visual Importance

For large models of which only a small part is visible to the observer, it is wasteful to store photons all over the model. In this situation it would be better to inform the photon-tracing step about the position of the observer and the "important" regions of the model.

One technique for doing this is by initially emitting "photons" from the observer to identify the regions of the scene that are important for the final image. This approach was used by Peter and Patrik [76]. They introduced the term 'importers' for photons emitted from the observer. To build the photon map, they used the importance-sampling techniques from [47] as presented in the previous section: for each photon traced from a light source they queried the importon map to importance-sample the scattered direction of the photon. Their results demonstrated that they were able to get a higher density photon map in the visually important parts of the model. Unfortunately, their results also suffered from highly varying photon power in the generated photon map due to their unbiased importance sampling strategy. Intuitively, their method could generate an importance sampling strategy, important photon even by sampling a direction with low probability.

Since importance sampling requires dividing by the probability, it is possible to generate high-powered photons that can cause the radiance estimate to be poor.

Another approach to controlling the visual quality of the generated photons was introduced by Gijssens and Willems [105]. They introduced the concept of density control for the photon map. The idea in density control is to limit the density of photons in bright regions of the model. These bright regions may not be the visually important parts of the model, and they may even be so bright that the intensity is clipped before being displayed. Both these issues make it valuable to limit the photon density in order to reduce the

~~Memory Requirements of the Photon Map~~. Limiting the photon density locally in bright regions of the model. These bright regions may not be the visually important parts of the model, and leaves room for more photons in darker regions that have more visual importance.

Density control works by imposing an upper limit on the number of photons per area (for example, 80,000 photons /m²). Before storing a photon in the photon map, the current local density is first examined.

The new photon is only stored if this density is below the limit.

Otherwise, the power of the photon is distributed among the existing local photons in the photon map. This ensures that the power received locally will be correct.

Guyker and Williams demonstrated how density control could be used to generate images of similar quality as the standard photon map method, but with the number of photons being reduced by a factor of 2-4.

The exciting aspect about density control is that it may be used to answer the question : how many photons are necessary?

~~Guyker and Williams demonstrated how density control could be used to generate images of similar quality as the standard photon map method, but with the number of photons~~

Guyker and Williams did take the first steps in that direction by investigating the relationship between visual importance and photon density. They computed the local required density based on an importance map similar to Peter and Pietzak [76]. The next step is coupling this work with methods models from perception to tune the photon map density to the requirements of the observer.

Fig 11.2 The photon map can be used to importance-sample based on the incident flux as well as the BRDF. The left image shows standard importance sampling using only the BRDF, and the right image shows importance sampling using the Photon map. Both images have been rendered using path tracing with 50 paths/pixel.

11.3.1 A Three-Pass Technique

A simple three-pass technique [43] that includes visual importance can be made by a simple extension to the two-pass technique presented in Chapter 9.

- The first step is the creation of a visual importance map (or importants map) by emitting visual importance (or importants) from the observer into the model. These importants are traced through at most one direct reflection (similar to the rendering step in the two-pass method).

• The second step is buffering the photon map by tracing photons through the model. This step is enhanced using the visual importance map. Photons are only stored when there is a "sufficient" density of visual importance in the region; otherwise the photon is thrown away. This strategy is clearly biased, but we remember that we throw away power in regions classified as unimportant.

- The third step is rendered using the photon map. The step proceeds in the same way as described in Chapter 9.

11.4 Efficient Stratification of Photons

One important technique for improving the quality of the photon map is making sure that the photons are distributed evenly. This improves the radiance estimate and is a good alternative and is a good alternative to just using more photons.

It is well known that the accuracy of Monte Carlo integration is improved when clumping of the random samples is avoided. The classic way to reduce clumping is to stratify the samples [81]. This concept is directly applicable to photon mapping. One way to stratify photons is at the light sources.

This is easily done by using the projection map, which already is a stratification of the directions at the light source. By alternatively selecting projection map cells with "active" objects, there will be at least a minimal stratification of photons.

In [47] it was suggested refining each cell in the projection map further to obtain an even finer level of stratification. Extending this concept to several dimensions is more complicated since the number of photons that are emitted often is unknown.

One way to stratify photons in several dimensions is quasi-Monte-Carlo (QMC) Sampling [70]. QMC Sampling uses special quasi-random low-discrepancy sequences to distribute the samples. Here quasi-random sampling means that the sequence often can replace the random sequence used in Monte-Carlo integration and still give the same result. However, these quasi-random sequences are not random.

They are clever constructs used to distribute samples evenly over a domain such that clumping is avoided. The elimination of clumping is measured by the discrepancy of the sequence. Discrepancy is a measure of how well spaced the samples are. Low discrepancy means that we want to try to maximize the local distance between samples.

The great advantage about QMC sequences is that they converge as fast as stratified sampling [1]. Without requiring knowledge about how many samples will be used. Therefore if we use QMC to select the directions in which to emit photons, then we automatically get evenly spaced photons. No matter how many photons are emitted. In addition, QMC sequences can provide a stratification of several dimensions. For photon tracing this means that not only are the photons properly stratified, but the first reflection of photons will also be properly stratified. This property has been demonstrated to give better convergence than randomly emitted photons.

The problems with QMC Sampling is that it can result in aliasing in the solutions, to which the eyes are sensitive too. For caustics that are visualized directly, the quasi-random sequences can give very noticeable patterns. A way to avoid this is to add some randomness to the sequence, and this may be indeed a good way to emit photons.

11.5 Faster shadows with Shadow Photons.

In scenes with many lights or with large area light sources it can be very costly to compute the direct illumination. This is mainly due to the fact that the visibility of each light is evaluated using shadow rays. Tracing a shadow ray through the scene is costly. Most scenes have large regions that are either fully illuminated or completely in shadow, and it seems wasteful to trace shadow rays for each point to see if there is a shadow. The penumbra regions, for which the light source visibility can be complex, usually cover a much smaller fraction of the scene. Based on these observations it seems natural to try to identify the different regions (shadow, illuminated or penumbra) of a scene, since this can significantly reduce the number of shadow rays traced.

A simple extension to the photon map makes it possible to classify the different illuminated regions of a model by introducing the concept of shadow photons [46]. Shadow photons are created in regions that are in shadow. As in Figure 11.3, this is done by tracing photons from the light source through the objects in the model. On all the objects beyond the first one we store shadow photons. We store the shadow photons only on the side of the object facing the light source (i.e., the surface normal points to the light source). If the normal points away from a light source, we correctly conclude the point is in shadow. With each shadow photon we store the negative power carried by the photon — the reasons for this will be clear later.

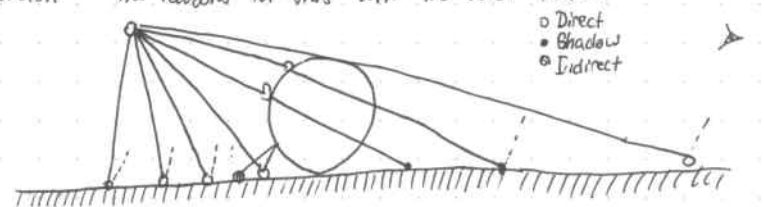


Figure 11.3. Shadow photons are created by tracing photons from the light sources through all objects in the scene and storing them all on all the objects beyond the first one. On the first object the stored photon is tagged as representing direct illumination. The remaining photons represent indirect illumination.

In addition to the shadow photons, a few minor modifications to the existing photon map is necessary. Each photon has a bit that is set to 1 if the photon comes directly from the light source and then add a radiance estimate based on the shadow photons (recall that they carry negative power). This is similar to splatting shadows based on the shadow photon density. Another simple approach is to estimate the visibility.

In addition to the shadow photons, a few minor modifications to the existing photon map is necessary. Each photon has a bit that is set to 1 if the photon comes directly from a light source. Furthermore, all photons are extended to include the light source number (for scenes with less than 2^{14} lights this number can be folded into the flag of the photon structure shown in Chapter 6).

There are several ways in which we can use this extended photon map to speed up the direct illumination computation. These include two fast approximations and one fairly accurate. For all of these methods,

we locate the nearest photons in the photon map that come directly from the light source and examine the distribution of shadow photons.

The two fast approximations do not use any shadow rays. One approach is to always compute the full direct illumination from the light source and then add a radiance estimate based on the shadow photons (recall that they carry negative power). This is similar to splatting shadows based on the shadow photon density. Another simple approach is to estimate the visibility of the light source based on the relative amount of direct illumination photons in the located photons:

$$V_{\text{fast}} = \frac{n_{d,s}}{n_{d,s} + n_{l,s}} \quad (11.14)$$

Here $n_{d,s}$ is the number of direct illumination photons, and $n_{l,s}$ is the number of shadow photons received from the light source, s .

V_{fast} is an estimate of the visibility of s (i.e. the fraction of the light source that is visible from the current location.) This fraction is multiplied by the irradiance from a fully visible light source to estimate the actual amount to received irradiance.

Figure 11.4 492 shadow photons have been used to identify the penumbra region in this camera glens model. Even with this low number of photons we are able to get a good estimate of where the shadow boundary is, and this enables a reduction of more than 77% in the number of shadow rays.

Both of the fast approximations can result in blurry shadows if too few photons are used, and for scenes with many light sources it can be costly to obtain good local shadow maps.

For more accurate results it is better to use a conservative approach that traces shadow rays in the penumbra regions.

The penumbra regions contain the shadow boundaries and can be identified. Since they have a mix of shadow photons and direct illumination photons. This means that if the nearest photons contain both shadow photons and direct illumination photons (even if it is just one of both), then we classify the region as a penumbra region and use shadow rays to evaluate the light source visibility. Tracing shadow rays in the penumbra regions makes sense since eyes are very sensitive to shadow boundaries.

In Figure 11.4 we show a model of a cognac glass that has been rendered with the identified penumbra region highlighted (the constant colored area around the glass) to illustrate the result of the light source visibility classification. All the other parts of the model have been classified as being either fully illuminated or in shadow. The global photon map uses just 33,994 of which only 492 are shadow photons. Even with this approximate representation, the number of shadow rays is reduced more than 90%.

11.6 Precomputed Irradiance

Another extension of the photon map was presented by Christensen [47]. The idea is to precompute the irradiance value for all photons in the global photon map. In the rendering step, the sampling of the indirect illumination results in many queries to the global query photon map, and by having precomputed irradiance values we can make this computation faster, since only the nearest photon is needed.

The precomputed irradiance values increase the size of the photon structure with 8 bytes (four bytes for a compressed representation of the irradiance and two bytes for the surface normal).

After the photon tracing step, the irradiance for all the photons is computed. This is done using the radiance estimate applied to each photon (by locating the nearest photons around it, etc.) The prepassing step can be quite costly, and therefore Christensen suggested only precomputing the irradiance for every fourth photon (and use only these photons in the global photon map to compute irradiance).

In the rendering step the queries to the global photon map are simplified since only the nearest photon is needed. To avoid artifacts it is necessary to locate the nearest photon at a surface with a similar normal (this is the reason why the surface normal is stored with the photons).

The precomputed irradiance optimization works well for Lambertian surfaces (for other materials it is still necessary to use the general photon map radiance estimate). Christensen reported very good speedups (4 factor of six) for some scenes. Even with a time-consuming precomputation of the irradiance values, the overall speedup was good.

11.7 Parallel Computations

The photon map is very easy to parallelize and very good results can be obtained (see for example [45]).

Since photons are independent they can be traced in parallel using multiple threads and/or machines. Photon tracing is usually pretty fast, so multiple threads on the same machine is usually preferable to multiple machines. In the case of multiple machines, it can be simpler to compute the full photon map locally - this may be faster since the photon map does not have to be transmitted over the network.

Rendering in parallel using the photon map can also be very efficient. As reported in [45] it is even possible to get super-linear speedups using a parallel rendering step. The rendering step is also straightforward to parallelize since rays are independent and can be traced in parallel.

The only slightly tricky element of a parallel implementation is the irradiance caching (if it is used), since it requires a locking mechanism to allow dynamic updates as new values are updated.

A Appendix A.

Basic Monte Carlo Integration

In rendering and in particular global illumination, we often encounter multi-dimensional integration problems of functions (light fields) with many discontinuities. Since these integrals cannot be evaluated efficiently using standard quadrature rules, it is better to use another class of techniques based on Monte Carlo integration.

A.1 The Sample Mean Method

Monte Carlo Integration uses random sampling of the function of interest to examine its properties. Given a function $f(x)$, that we wish to integrate over a one-dimensional domain from a to b :

$$I = \int_a^b f(x) dx \quad (A.1)$$

An intuitive way to evaluate this integral is by computing the mean value of $f(x)$ over the interval a to b , and then multiply this mean by the length of the interval $a \rightarrow b$. For this purpose we can average the values of $f(x)$ at N locations $\xi_1, \xi_2, \xi_3, \dots, \xi_N$ where ξ_1, \dots, N are uniformly distributed random numbers between a and b .

$$\text{This gives: } I_m = (b-a) \cdot \frac{1}{N} \sum_{i=1}^N f(\xi_i) \quad (A.2)$$

Here I_m is the Monte Carlo estimate becomes more accurate and in the limit we find that:

$$\lim_{N \rightarrow \infty} I_m = I \quad (A.3)$$

How fast does the estimate I_m converge to the correct result I ? To answer this question we can compute the variance σ^2 of our estimate I_m :

$$\sigma^2 = \frac{1}{N} \left(\int_a^b f^2(x) dx - I^2 \right) \quad (A.4)$$

Since the standard deviation σ is the square root of the variance, we find that:

$$\sigma \propto \frac{1}{\sqrt{N}} \quad (A.5)$$

In plain english: To halve the error we have to quadruple the amount of samples!

This is the cost of Monte-Carlo integration. It is simple, very easy to implement on most problems, but the convergence is slow. However, for high-dimensional integrals (such as those in rendering), the convergence is often better than any other method we can produce. [8].

We can also estimate the variance σ_s^2 of our sampling distribution:

$$\sigma_s^2 = \frac{1}{N-1} \sum_{i=1}^N (f(\xi_i) - I_m)^2 \quad (A.6)$$

This estimate contains the factor $\frac{1}{(N-1)}$, which we show that the variance (the noise, high noise \Rightarrow lots of information), which shows that the variance of our samples converges as slowly as the variance of our estimate.

Fortunately there are several variance reduction techniques available.

A.2 Variance Reduction Techniques

To improve the quality of our estimate we must reduce the variance. The basic strategy is to use as much knowledge as we have about the function we wish to integrate.

A technique that is very commonly used in rendering is importance sampling. The idea in importance sampling is to concentrate the samples of the function in the important parts of the function. For example, if the function has a high value in a small interval, then it pays to use more samples in this interval.

For this purpose we construct a probability density function, p, d, f , that "has the same shape" as $f(x)$. Given a stochastic variable X with p.d.f. $p(x)$, $X \in [a, b]$ such that $p(x) > 0$ when $f(x) \neq 0$ we find that:

$$I = \int_a^b \frac{f(x)}{p(x)} p(x) dx = E \left\{ \frac{f(X)}{P(X)} \right\} \quad (A.7)$$

At first glance this may not seem very useful. The power of this method relies on the ability to construct random samples $\gamma_1, \dots, \gamma_N$ from X . This gives the following estimator I_m for I :

$$I_m = \frac{1}{N} \sum_{i=1}^N \frac{f(\gamma_i)}{P(\gamma_i)} \quad (A.8)$$

The variance will still be proportional to $1/N$, but by picking a good p.d.f. we can make it arbitrarily low. The optimal p.d.f. $p_{opt}(x)$ is:

$$p_{opt} = \frac{f(x)}{I} \quad (A.9)$$

with this p.d.f. the variance is always zero! Unfortunately, it requires knowledge of I , which is the quantity that we are trying to compute. In general we can improve our estimate by adding small knowledge to the sampling distribution. In rendering it may be that we know that a certain object is brighter than the rest, and we can improve our sampling by sending more rays toward the subject.

Another powerful variance reduction technique is stratified sampling. The simplest form of stratified sampling divides the domain $[a, b]$ into N subdomains. In each subdomain we place one sample.

It can be shown [8] that this technique cannot result in higher variance than the random sampling approach, and if the function is smooth it often results in significantly better estimates. The variance is proportional to $1/N^2$, which is much better than naive random sampling. As such, stratified sampling should be used whenever possible! It is only when the number of samples to be taken is unknown that stratified sampling is problematic.

There are several other variance reduction techniques available for Monte Carlo integration. See the classic book by Rubinstein [5] for a good review.

Reuven Y. Rubinstein. Simulation and the Monte Carlo Method.
New York : John Wiley & Sons 1981.

Appendix B : A photon Map Implementation in C++

This appendix contains a full C++ implementation of a Photon map class. This class can be integrated into any ray tracer to provide the basic tool to add caustics and simple global illumination. The only additional code to add to such a ray tracer is photon tracing /emission of photons from the lights, and scattering and storing of photons by the materials). These photons can then be handled by the photon map implementation provided below. The usage of the implementation should be fairly easy to understand.

```
/* -----  
// photonmap.cc  
// An example implementation of the photon map data structure  
// -----
```

```
// Henrik Wann Jensen - February 2001  
// -----
```

```
#include <stdio.h>  
#include <stdlib.h>  
#include <string.h>  
#include <math.h>
```

```
/* This is the photon  
* The power is not compressed so the  
* size is 28 bytes  
*/
```

```
*****  
typedef struct Photon {  
    float Pos[3];
```

```
    short plane;  
    unsigned char theta, phi;  
    float power[3];  
} Photon;
```

```
    // Photon position  
    // splitting plane for kd-tree  
    // incoming direction  
    // Photon power (uncompressed)
```

```
/* This structure is used to locate the  
* nearest photons  
*/  
*****  
typedef struct Nearest Photons {  
    //*****  
    int max;  
    int found;  
    int got_heap;  
    float pos[3];  
    float *dist2;  
    const Photon **index;  
} Nearest Photons;  
/* This is the Photon-map class  
*/  
*****  
class Photon_map {  
    //*****  
public:  
    Photon_map (int max_phot);  
    ~Photon_map();  
    void store(  
        const float power[3],  
        const float pos[3],  
        const float dir[3]);  
        // photon power  
        // photon position  
        // photon direction  
    void scale_photon_power(  
        const float scale);  
        // 1/(number of emitted photons)  
    void balance(void);  
        // Balance the kd-tree (before use!)  
    void irradiance_estimate(  
        float irrad[3],  
        const float Pos[3],  
        const float dir[3]),  
        const float max_dist,  
        const int nphotons) const; // max distance to look for photons  
        // number of photons to use.  
    void locate_photons(  
        NearestPhotons *const np, // np is used to locate the photons  
        const int index) const; // call with index = 1.
```

```

void photon_dir {
    float *dir
    const Photon *p) const;
    // direction of photon (returned)
    // the photon.

private:
    void balance_segment(
        Photon **pball
        Photon ***porg,
        const int start,
        const int end);

    void median_split(
        Photon ***p,
        const int start,
        const int end,
        const int median,
        const int axis);

    Photon *photons;

    int stored_photons;
    int half_stored_photons;
    int max_photons;
    int prev_scale;

    float cosTheta[256];
    float sinTheta[256];
    float cosPhi[256];
    float sinPhi[256];

    float bbox_min[8];
    // use bbox_min;
    float bbox_max[3];
    // use bbox_max;
};

/* This is the constructor for the photon map.
 * To create the photon map it is necessary to specify the
 * maximum number of photons that will be stored
 */
//***** Photon_map::Photon_map (const int max_phot)
//***** Photon_map::~Photon_map()
//***** Photon-dir (float *dir, const Photon *p) const
//***** dir[0] = sinTheta[p->theta] * cosPhi[p->phi];
//***** dir[1] = sinTheta[p->theta] * sinPhi[p->phi];
//***** dir[2] = cosTheta[p->theta];
}

120
{
    stored_photons = 0;
    prev_scale = 1;
    max_photons = max_phot;

    Photon = (Photon *) malloc ( sizeof(Photon) * (max_photons + 1) );
    if (photons == NULL) {
        fprintf(stderr, "out of memory initializing photon map\n");
        exit(-1);
    }

130
    bbox_min[0] = bbox_min[1] = bbox_min[2] = 1e8f;
    bbox_max[0] = bbox_max[1] = bbox_max[2] = -1e8f;
    // -----
    // initialize direction conversion tables
    // -----
    for (int i=0, i<256, i++) {
        double angle = double(i)*(1.0/256.0)*M_PI;
        cosTheta[i] = cos(angle);
        sinTheta[i] = sin(angle);
        cosPhi[i] = cos(2.0*angle);
        sinPhi[i] = sin(2.0*angle);
    }

140
    //*****
    Photon_map::~Photon_map()
    //*****
    {
        free(photons);
    }

150
/* Photon_dir returns the direction of a photon
 */
//*****
void Photon_map::photon_dir (float *dir, const Photon *p) const
//*****
160
{
    dir[0] = sinTheta[p->theta] * cosPhi[p->phi];
    dir[1] = sinTheta[p->theta] * sinPhi[p->phi];
    dir[2] = cosTheta[p->theta];
}

```

```

/*
irradiance_estimate computes an irradiance estimate
* at a given surface position.
*/
170 //***** *****
Void Photon_map :: irradiance_estimate (
    float irrad[3], // returned irradiance
    const float pos[3], // Surface position
    const float normal[3], // Surface normal at pos
    const float max_dist, // Max distance to look for photons
    const int nPhotons) const // Number of photons to use
{
    irrad[0] = irrad[1] = irrad[2] = 0.0;
180

    Nearest Photons np;
    np.dist2 = (float*) alloca ( sizeof (float) * (nphotons+1) );
    np.index = (const Photon**) alloca ( sizeof (Photon*) * (nphotons+1) );

    np.Pos[0] = Pos[0]; np.Pos[1] = Pos[1]; np.Pos[2] = Pos[2];
    np.max = nphotons;
    np.found = 0;
    np.got_heap = 0;
    np.dist2[0] = max_dist * Max_dist;
190

    // locate the nearest photons
    locate_photons (&np, 1);

    // if less than 8 photons return
    if (np.found < 8)
        return;

    float pdir[3];

    200 // sum irradiance from all photons
    for (int i=1; i<=np.found; i++) {
        const Photon *p = np.index[i];
        // the Photon_dir call and following if can be omitted (for speed)
        // if the scene does not have any thin surfaces
        Photon_dir (Pdir, p);

```

if ((Pdir[0]*normal[0] + Pdir[1]*normal[1] + Pdir[2]*normal[2]) < 0.0f) {

 irrad[0] += P->Power[0];
 irrad[1] += P->Power[1];
 irrad[2] += P->Power[2];
}

}

220

/* locate_photons finds the nearest photons in the photons map
* given by the parameters in np
*/
//***** *****
void Photon_map :: locate_photons (
 Nearest_Photons *const np,
 const int index) const
//***** *****
{
 230 Const Photon *p = &photons[index];
 float dist1;

 if (index < half_stored_photons) {
 dist1 = np->pos[P->Plane] - P->Pos[P->Plane];
 if (dist1 > 0.0) { // if dist1 is positive search right plane.
 locate_photons (np, 2*index+1);
 if (dist1*dist1 < np->dist[0])
 locate_photons (np, 2*index);
 } else { // if dist1 is negative search left first
 locate_photons (np, 2*index);
 if (dist1*dist1 < np->dist2[0])
 locate_photons (np, 2*index+1);
 }
 }

 // compute squared distance between current photon and np->pos
 dist1 = P->Pos[0] - np->Pos[0];
250 float dist2 = dist1*dist1;
 dis_1 = P->Pos[1] - np->Pos[1];
 dist2 += dist1*dist1;
 dist1 = P->Pos[2] - np->Pos[2];
 dist2 += dist1*dist1;
}

```

if ( dist2 < np->dist2[0] ) {
    // we found a photon. Insert it in the candidate list.
    Parent=1;
    if ( np->found < np->max ) {
        // heap is not full; use array
        np->found++;
        np->dist2[np->found] = dist2;
        np->index[np->found] = p;
    } else {
        int j, parent;
        if ( np->got_heap == 0 ) { // Do we need to build the heap?
            // Build Heap
            float dst2;
            const Photon *phot;
            int half_found = np->found >> 1;
            for ( int k = half_found ; k >= 1 ; k-- ) {
                Parent=k;
                Phot = np->index[k];
                dst2 = np->dist2[k];
                while ( Parent <= half_found ) {
                    j = Parent + parent;
                    if ( j < np->found && np->dist2[i] < np->dist2[j+1] )
                        j++;
                    if ( dst2 >= np->dist2[1] )
                        break;
                    np->dist2[Parent] = np->dist2[0];
                    np->index[Parent] = np->index[1];
                    Parent=j;
                }
                np->dist2[Parent] = dst2;
                np->index[Parent] = phot;
            }
            np->got_heap = 1;
        }
        // insert new photon into max heap
        // delete largest element, insert new, and reorder the heap.
        Parent=1;
        if ( np->found < np->max ) {
            // heap is not full; use array
            np->found++;
            np->dist2[np->found] = dist2;
            np->index[np->found] = p;
        } else {
            int j, parent;
            if ( dist2 > np->dist2[0] )
                break;
            np->dist2[Parent] = np->dist2[0];
            np->index[Parent] = np->index[0];
            Parent=j;
            j+=j;
            }
            np->index[Parent] = p;
            np->dist2[Parent] = dist2;
        }
        np->dist2[0] = np->dist2[i];
    }
}
//***** *****
/* store put a photon into the flat array that will form
 * the final kid-tree.
 */
/* Call this function to store a photon.
 */
//***** *****
void Photon_map :: store(
    const float Power [3],
    const float Pos [3],
    const float dir [3])
{
    if ( stored_photons > max_photons )
        return;
    stored_photons++;
    Photon *const node = &photons [stored_photons];
}

```

```

for (int i=0; i<3; i++) {
    node->pos[i] = pos[i];
}

if (node->pos[i] < bbox_min[i])
    bbox_min[i] = node->pos[i];
if (node->pos[i] > bbox_max[i])
    bbox_max[i] = node->pos[i];
340
    node->power[i] = power[i];
}

int theta = int (acos (dir[2]) * (256.0/M_PI));
if (theta > 255)
    node->theta = 255;
else
    node->theta = (unsigned char) theta;
350
int phi = int (atan (dir[1], dir[0]) * (256.0 / (2.0*M_PI)));
if (phi > 255)
    node->phi = 255;
else if (phi < 0)
    node->phi = (unsigned char) (phi + 256);
else
    node->phi = (unsigned char) phi;
}

360
/* Scale_photon_power is used to scale the power of all
* photons once they have been emitted from the light
* source. scale = 1/(#emitted photons).
* Call this function after each light source is processed.
*/
// *****
Void Photon_map :: scale_photon_power (const float scale)
// *****
370
    for (int i=prev_scale; i<= stored_photons; i++) {
        Photon[i].Power[0] *= scale;
        Photon[i].Power[1] *= scale;
        Photon[i].Power[2] *= scale;
    }
    prev_scale = stored_photons;
}

/*
balance creates a left-balanced kd-tree from the flat photons
array. This function should be called before the photon map
is used for rendering.
*/
380
// *****
void Photon_map :: balance (void)
// *****
{
    if (stored_photons > 1) {
        // allocate two temporary arrays for the balancing procedure
        Photon **Pa1 = (Photon **) malloc (sizeof (Photon *)*(stored_photons+1));
        390
        for (int i=0, j=0; i<= stored_photons; i++)
            Pa1[j] = &photons[i];
        balance_segment (Pa1, Pa2, 1, stored_photons);
        free (Pa2);

        // recognize balanced kd-tree (make a heap)
        int d, j=1, foo=1;
        400
        Photon foo_photon = photons[j];
        for (int i=1; i<= stored_photons; i++) {
            d = pa1[i]-photons;
            Pa1[j] = NULL;
            if (d != foo)
                photons[d] = photons[i];
            else
                photons[j] = foo_photon;
        }
    }
    410
    if (i < stored_photons) {
        for (; foo <= stored_photons; foo++)
            if (Pa1[foo] != NULL)
                break;
            foo_photon = photons[foo];
    }
    continue;
}
j=d;
420
} free (Pa1);
} half_stored_photons = stored_photons/2 - 1;
}

```

```

#define swap(ph, a, b) { Photon *ph2=ph[a]; ph[a]=ph[b]; ph[b]=ph2}
430 // median_split splits the photon array into two separate
// pieces around the median, with all photons below the
// the median in the lower half and all photons above
// the median in the upper half. The comparison
// criteria is the axis (indicated by the axis parameter)
// (inspired by routine in "Algorithms in C++" by Sedgewick)
// *****
void Photon_map::median_split(
    Photon **p,
    const int start,
    const int end,
    const int median,
    const int axis) {
    // Start of photon block in array
    // end of photon block in array
    // desired median number
    // axis to split along
    // *****
}

440 int left = start;
int right = end;

while (right > left) {
    const float v = p[right]→pos[axis];
    int i = left - 1;
    int j = right;
    for (;;) {
        while (p[++i]→pos[axis] < v)
            ;
        while (p[--j]→pos[axis] > v && j > left)
            ;
        if (i >= j)
            break;
        swap(p, i, j);
    }
    swap(p, i, right);
    if (i >= median)
        right = i - 1;
    if (i <= median)
        left = i + 1;
}
450
460
470 // See "Realistic Image Synthesis using Photon Mapping" Chapter 6
// for an explanation of this function.
// *****
void Photon_map::balance_segment(
    Photon **pba,
    Photon **por,
    const int index,
    const int start,
    const int end)
480 // *****
{
    // -----
    // compute new median
    // -----
    int median = 1;
    while ((4 * median) <= (end - start + 1))
        median += median;
    490 if ((3 * median) <= (end - start + 1)) {
        Median += median;
        median += start - 1;
    } else
        median = end - median + 1;
    // -----
    // find axis to split along
    // -----
    500 int axis = 2;
    if ((bbox_max[0] - bbox_min[0]) > (bbox_max[1] - bbox_min[1]) &&
        (bbox_max[0] - bbox_min[0]) > (bbox_max[2] - bbox_min[2]))
        axis = 0;
    else if ((bbox_max[1] - bbox_min[1]) > (bbox_max[2] - bbox_min[2]))
        axis = 1;
    // -----
    // Partition Photon block around median
    // -----
}
510

```

```
median_split (Porg, start, end, median, axis);
```

```
Pbal [index] = Porg [median];
```

```
Pbal [index] → plane = axis;
```

```
//-----
```

```
// recursively balance the left and right block
```

```
//-----
```

```
if (median > Start) {
```

```
// balance left segment
```

```
if (start < median - 1) {
```

```
const float tmp = bbox_max [axis];
```

```
bbox_max [axis] = Pbal [index] → Pos [axis];
```

```
balance_segment (Pbal, Porg, 2 * index, start, median - 1);
```

```
bbox_max [axis] = tmp;
```

```
} else {
```

```
Pbal [2 * index] = Porg [start];
```

```
}
```

```
}
```

```
if (median < end) {
```

```
// balance right segment
```

```
if (median + 1 < end) {
```

```
const float tmp = bbox_min [axis];
```

```
bbox_min [axis] = Pbal [index] → Pos [axis];
```

```
balance_segment (Pbal, Porg, 2 * index + 1, median + 1, end);
```

```
bbox_min [axis] = tmp;
```

```
} else {
```

```
Pbal [2 * index + 1] = Porg [end];
```

```
}
```

```
}
```

```
}
```

Appendix C : A Cognac Glass Model

This appendix contains the data used for the cognac glass model which has appeared in several images in the book. It is a good model for simulating caustics.

The data is given as three contour curves. There is a contour for the cognac-air interface, the gloss-air interface, and the cognac-gloss interface.

The three interfaces are necessary to properly account for the fresnel effects.

Modeling a volume of cognac inside a glass with a tiny amount of air between the two would not be correct.

The contour curves can be typed into most modeling programs. The cognac glass is then created by rotating the curve around the center axis (Radius = 0).

The data for the cognac-air interface contour is:

Height	Radius
6.5	3.8
6.48	3.76
6.45	3.76
6.45	3.75

The data for the gloss-air interface contour is:

Height	Radius	Height	Radius
6.50	3.80	cont'd	cont'd
6.05	3.79	4.33	2.70
5.60	3.73	3.95	1.98
5.15	3.55	3.58	1.06
4.70	3.20	3.20	0.00

The data for the glass-cognac interface contour is:

Height	Radius	Height	Radius	Height	Radius
0.90000	0.000000	cont'd	cont'd	cont'd	cont'd
0.77500	0.087946	1.000000	0.500000	10.16250	2.807188
0.65000	0.167857	1.300000	0.500000	10.55000	2.700000
0.52500	0.338839	1.600000	0.500000	10.57250	2.695273
0.40000	0.700000	1.900000	0.500000	10.59500	2.692188
0.31250	1.178594	2.200000	0.500000	10.61750	2.690508
0.22500	1.821250	2.27500	0.515031 556750	10.64000	2.690000
0.18750	2.465781	2.350000	0.515031	10.65375	2.690469
0.15000	2.950000	2.42500	0.620094	10.66750	2.688750 2.688750
0.13750	2.981703	2.500000	0.700000	10.68125	2.680156
0.12500	2.993875	2.61250	1.149887	10.69500	2.660000
0.11375	3.009109	3.12500	1.710119	10.69825	2.650534
0.10000	3.050000	3.43750	2.277790	10.69750	2.633250
0.08750	3.062539	3.75000	2.750000	10.69875	2.616781
0.00050	3.088437	4.01250	3.048824	10.70000	2.610000
0.00025	3.113867	4.27500	3.294114	10.66250	2.592939
0.00000	3.125000	4.53750	3.492347	10.62500	2.595313
0.05000	3.218750	4.80000	3.650000	10.58750	2.475339
0.10000	3.250000	5.22500	3.831752	10.55000	2.620000
0.15000	3.218750	5.65000	3.937946	10.16250	2.724963
0.20000	3.125000	6.07500	3.987667	9.77500	2.840625
0.36250	2.497187	6.50000	4.000000	9.38750	2.966875
0.52500	1.642500	7.12500	3.916016	9.00000	3.100000
0.68750	0.885313	7.75000	3.709375	8.37500	3.332422
0.85000	0.550000	8.37500	3.498047	7.75000	3.559375
0.98750	0.540078	9.00000	3.200000	7.12500	3.701641
0.92500	0.523125	9.38750	3.063750	6.50000	3.890000
0.86250	0.507109	9.77500	2.930625		

Bibliography

- [1] Masaki Aono and Ryutarou Ohbuchi. "Quasi-Monte Carlo rendering with adaptive sampling." Technical Report RT067, IBM Tokyo Research Laboratory, 1996.
- [2] James Arvo. Backward Ray Tracing. In developments in Ray Tracing, SIGGRAPH '86 Seminar Notes, volume 12, August 1986.
- [3] James Arvo and David B. Kirk. "Particle Transport and Image Synthesis." Computer Graphics (Proc. SIGGRAPH '90) 24(4): 63-66 (August 1990).
- [4] Franz Aurenhammer. "Voronoi diagrams - a survey of a fundamental geometric data structure." ACM Computing Surveys 23(3): (September 1991).
- [5] Jon L. Bentley. "Multidimensional Binary Search trees used for associative searching." Communications of the ACM 18(9): 509-517 (1975).
- [6] Jon L Bentley. "Multidimensional binary search trees in database applications." IEEE Trans. on Soft. Eng. 5(4): 333-340 (July 1979).
- [7] Jon L Bentley, Bruce W. Weide, and Andrew C. Yao. "Optimal expected-time algorithm for closest point problems." ACM Trans. on Math. Soft. 6(4): 563-580 (1980).
- [8] Jon L Bentley and Jerome H. Friedman. "Data structures for Range Searching." Computing Surveys 11(4): 397-409 (1979).
- [9] Philippe Blasi, Bertrand Le Gaec, and Christopher Schlick. "A rendering algorithm for discrete volume photon density objects." Computer Graphics Forum (Eurographics '93) 12(3): 201-210 (1993).
- [10] James F. Blinn. "Models of light reflection for computer synthesized pictures." Computer Graphics (Proc. SigGraph '77) 11(2): 192-198 (July 1977).
- [11] Craig Bohren and Donald Huffman. *Absorption and Scattering of Light by Small Particles*. New York: John Wiley & Sons, 1983.
- [12] Ted Z. Buchwald. *The Rise of the Wave Theory of Light*. Chicago: The University of Chicago Press, 1989.
- [13] Shenchang Eric Chen, Holly E. Rushmeier, Gavin Miller, and Douglas Turner. "A progressive multipass method for global illumination." Computer Graphics (Proc. SigGraph '91) 25(4): 165-174 (July 1991).
- [14] Per H. Christensen. "Faster photon map global illumination." Journal of Graphics Tools 4(3): 1-10 (April 2000).
- [15] Per H. Christensen, Eric J. Stollnitz, David H. Salesin, and Tony D. DeRose. "Global illumination of glossy environments using wavelets and importance." ACM Transactions on Graphics 15(1): 37-71 (January 1996).
- [16] Michael F. Cohen and Donald P. Greenberg. "The Hemis-Cube: A radiosity solution for forward ray tracing in complex environments." Computer Graphics (Proc. SIGGRAPH '85) 19(3): 31-40 (August 1985).

- [17] Michael F. Cohen and John R. Wallace. *Radiosity and Realistic Image Synthesis*. San Diego, CA: Academic Press, 1993.
- [18] Steven Collins. "Adaptive splatting for specular to diffuse light transport." In *Fifth Eurographics Workshop on Rendering*, pp. 119-135, June 1994.
- [19] Steven Collins. *Volumefront Tracking for Global Illumination Solutions*. PhD thesis, Dept. Computer Science, Trinity College Dublin, 1996.
- [20] Robert L. Cook. "Stochastic sampling in computer graphics." *ACM Transactions on Graphics* 5(1): 51-72 (Jan 1986).
- [21] Robert L. Cook, Thomas Porter, and Loren Carpenter. "Distributed ray tracing." *Computer Graphics (Proc. SIGGRAPH '84)* 18(3): 137-151 (July 1984).
- [22] Thomas H. Cormen, Charles E. Leiserson, and Ronald L. Rivest. *Introduction to Algorithms*. Cambridge, MA: MIT Press, 1989.
- [23] Julie Dorsey, Alan Edelman, Henrik Wann Jensen, Justin Ziegakia, and Hans Koshling Pedersen. "Modeling and rendering of weathered stone." In *Proceedings of SIGGRAPH '99*, Computer Graphics Proceedings, Annual Conference Series, edited by Alyn Rockwood, pp. 225-234, Reading, MA: Addison-Wesley, 1999.
- [24] Philip Dutré. *Mathematical Frameworks and Monte Carlo Algorithms for Global Illumination in Computer Graphics*. PhD thesis, University of Leuven, 1998.
- [25] Ronald Fedkiw, Joe Stam, and Henrik Wann Jensen. "Visual simulation of smoke." In *Proceedings of SIGGRAPH 2001*, Computer Graphics Proceedings, Annual conference Series, to appear.
- [26] Andrew S. Glassner. "Space subdivision for fast Ray Tracing." *IEEE Computer Graphics and Applications* 4(10): 15-22 (October 1984).
- [27] Andrew S. Glassner. *An Introduction to Ray Tracing*. London Academic Press, 1989.
- [28] Andrew S. Glassner. *Principles of Digital Image Synthesis*. Los Altos: Morgan Kaufmann, 1995.
- [29] Cindy M. Goral, Kenneth E. Torrance, Donald P. Greenberg, and Bennett Battail. "Modelling the interaction of light between diffuse surfaces." *Computer Graphics (Proc. SIGGRAPH '84)* 18(3): 212-22 July 1984.
- [30] Steven J. Gortler, Peter Schröder, Michael F. Cohen, and Pat Hanrahan. "Wavelet Radiosity." In *Proceedings of SigGraph '93*, Computer Graphics Proceedings, Annual Conference Series, edited by James T. Kajiya, pp. 221-230, New York: ACM Press, 1993.
- [31] Roy Hall. *Illumination and color in computer generated Imagery*. New York: Springer-Verlag, 1989.
- [32] Pat Hanrahan, David Salesin, and Wolfgang Krueger. "Reflections from layered Surfaces due to Subsurface Scattering." In *Proceedings of SIGGRAPH '93*, Computer graphics proceedings, Annual Conference Series, edited by James T. Kajiya, pp. 165-174, New York: ACM Press, 1993.
- [33] Pat Hanrahan, David Salesin, and Larry Seppenre. "A rapid hierarchical radiosity algorithm." *Computer Graphics (Proc. Siggraph '91)* 25(4): 197-206 (July 1991).
- [34] Paul S. Heckbert. "Adaptive radiosity textures for bidirectional ray tracing." *Computer Graphics (Proc. SIGGRAPH '90)* 24(4): 145-154 (August 1990).
- [35] L. G. Heney and T.L. Greenstein. "Diffuse Radiation in the Galaxy." *Astrophysics Journal*, 93: 70-83, 1941.
- [36] Ellis Horowitz, Sartaj Sahni, and Susan Anderson-Freed. *Fundamentals of Data Structures in C*. New York: W.H. Freeman & Co., 1993.
- [37] David S. Immel, Michael F. Cohen, and Donald P. Greenberg. "A radiosity method for non-diffuse environments." *Computer Graphics (Proc. SIGGRAPH '88)* 20(4): 133-142 (August 1988).
- [38] American National Standard Institute. *Nomenclature and Definitions for Illumination Engineering*. ANSI report, ANSI/IES RP-16-1986, 1986.
- [39] Frederic W. Jensen. "Data structures for Ray Tracing." In *Data Structures for Raster Graphics*, edited by Z.R. A. Kessener, F.J. Peters, and M.I. P. van Zierop, pp. 57-73, Berlin: Springer-Verlag, 1985.
- [40] Henrik Wann Jensen. *Global illumination via Bidirectional Monte Carlo Ray Tracing*. Master's Thesis, Technical University of Denmark, 1993.
- [41] Henrik Wann Jensen. "Importance driven Path tracing using the photon map." In *Eurographics Rendering Workshop 1995*, edited by P. Hanrahan and W. Purcell, pp. 326-335, Eurographics, June 1995.
- [42] Henrik Wann Jensen. "The photon map in global illumination." PhD thesis, Technical University of Denmark, September 1996.
- [43] Henrik Wann Jensen. "Rendering caustics on non-Lambertian surfaces." In *Graphics Interface '96*, edited by Wayne A. Davis and Richard Bartels, pp. 116-121, Canadian Information Processing Society, Canadian Human-Computer Communications Society, May 1996.
- [44] Henrik Wann Jensen. Parallel global illumination using photon mapping. *SIGGRAPH 2001 Course Notes*, New York: ACM Press, July 2000.
- [45] Henrik Wann Jensen and Niels J. Christensen. "Efficient simulation rendering shadows using the photon map." In *Computgraphics '95* edited by Harold P. Soto, pp. 285-291, December 1995.
- [46] Henrik Wann Jensen and Niels Jørgen Christensen. "Photon maps in bidirectional Monte Carlo ray tracing of complex objects." *Computers & Graphics* 19(2): 215-224 (March '95).
- [47] Henrik Wann Jensen and Niels Jørgen Christensen. "Efficient simulation of light transport in scenes with participating media using photon maps." In *Proceedings of SIGGRAPH '98*, Computer Graphics Proceedings, Annual Conference Series, edited by Michael Cohen, pp. 311-320, Reading, MA: Addison Wesley, 1998.
- [48] Henrik Wann Jensen and Per H. Christensen. "The light of Mies von der Rohe, July 2000?" Animation in *SIGGRAPH '2000 Electronic Theater*.

- [50] Henrik Wann Jensen, Justin Zagorskis, and Jørgen Dalle Doreg. "Rendering of Wet materials." In *Rendering Techniques '99*, edited by P. D. Lischinski and G. W. Larson, Vienna: Springer-Verlag, 1999.
- [51] Henrik Wann Jensen, Steve Marschner, Marc Levoy, and Pat Hanrahan. "A practical model for subsurface light transport." In *Proceeding of SIGGRAPH 2001*, Computer Graphics Proceedings, Annual Conference Series.
- [52] James T. Kajiya. "The Rendering Equation." *Computer Graphics (Proc. SIGGRAPH '86)* 20(4): 143-150 (August 1986).
- [53] Timothy L. Shyu and James T. Kajiya. "Ray tracing complex scenes." *Computer Graphics (Proc. SIGGRAPH '86)* 20(4): 269-278 (August 1986).
- [54] Alexander Stoll. "Quasi-Monte Carlo radiosity." In *Eurographics Rendering Workshop 1996*, edited by Xavier Pueyo and Peter Shirley Schröder, pp. 101-110, Vienna: Springer-Verlag, 1996.
- [55] Krzysztof S. Klimanowicz and Thomas W. Sederberg. "Faster ray tracing using adaptive grids." *IEEE Computer Graphics & Applications* 17(1): 42-51 (January-February 1997).
- [56] Eric P. Zafortune. *Mathematical Models and Monte Carlo Algorithms for Physically Based Rendering*. PhD thesis, University of Leuven, 1996.
- [58] Eric P. Zafortune and Yves D. Willems. "A 5D tree to reduce the variance of Monte Carlo ray tracing." In *Eurographics Rendering Workshop 1995*, edited by Patrick Hanrahan and Werner Purgathofer, pp. 11-20, Eurographics, June 1995.
- [57] Eric P. Zafortune. *Mathematical Models and Monte Carlo Algorithms for Physically Based Rendering*.
- [59] Eric P. Zafortune and Yves D. Willems. "Bidirectional Path tracing." In *Computgraphics '93*, pp. 95-104, 1993.
- [60] Eric P. F. Zafortune, Sing-Choong Foo, Kenneth E. Torrance, and Donald P. Greenburg. "Non-linear approximation of reflectance functions." In *proceedings of SIGGRAPH '97*, Computer Graphics Proceedings, Annual Conference Series, edited by Kurt Akeley, pp. 131-144, Turner Whittier, pp. 117-126, Reading, MA: Addison Wesley, 1997 ISBN 0-89791-896-7.
- [61] Mark E. Lee, Richard A. Redner, and Samuel P. Uselman. "Statistically optimized Sampling for distributed ray tracing." *Computer Graphics (Proc. SIGGRAPH)* Marc Levoy, Horst Pfleiderer, Brian Curless, Seymour Pankiewicz, David Koller, Lucas Pereira, Matt Cline, Sean Anderson, James Davis, Jeremy Ginsburg, Jonathon Shade, and Duane Falk. "The digital michelangelo project: 3D Scanning of large statues." In *Proceedings of SIGGRAPH 2000*, Computer Graphics Proceedings, Annual Conference Series, edited by Kurt Akeley, pp. 131-144, Reading, MA: Addison Wesley, 2000.
- [62] Robert Lewis. "Making shaders more physically plausible." In *fourth Eurographics Workshop on Rendering*, edited by Michael F. Cohen, Claude Puech, and François Sillion, pp. 47-62, Eurographics, June 1993.
- [63] Daniel Lischinski, Filippo Tamplieri, and Donald P. Greenburg. "Discontinuity meshing for accurate Radiosity." *IEEE Computer Graphics and Applications* 12(6): 25-39 (November 1992).
- [64] Nicholas Metropolis, Arianna Lotte Rosenbluth, Marshall Rosenbluth, Augusta Teller, and Edward Teller. "Equation of State calculations by fast computing Machines." *The Journal of Chemical Physics* 21(6): 1087-1092 (1953).
- [65] Gustav Hie. "Beiträge zur Optik trüber Medien, speziell Holländaler Metallösungen." *Annalen der Physik* 25: 377-445 (1908.)
- [66] M. Minnaert. *Light and Color in the outdoors*. Berlin: Springer-Verlag, 1993.
- [67] Don P. Mitchell. "Generating anti-aliased images at low sampling densities." *Computer Graphics (Proc. SIGGRAPH '87)* 21(4): 65-72 (July 1987)
- [68] Paweł Myszkowski, "Lighting reconstruction using fast adaptive density estimation techniques." In *Eurographics Rendering Workshop 1997*, edited by Julie Dorsey and Philipp Slusallek, pp. 251-262, Vienna: Springer-Verlag, 1997.
- [69] F. E. Nicodemus, J. C. Richmond, J. T. Hsia, I. W. Ginsburg, and T. Imbens. *Geometric considerations and nomenclature for reflectance*. Monograph 161, National Bureau of Standards (US), October 1977.
- [70] Harald Niederreiter. *Random Number Generation and Quasi-Monte Carlo Methods*. Philadelphia: SIAM, 1992.
- [71] T. Nishita, I. Okamura, and E. Nakamae. "Shading models for point and linear sources." *ACM Transactions on Graphics* 4(2): 124-146 (April 1985).
- [72] Michael Oren and Shree K. Nayar. "Generalization of Lambert's reflectance model." In *Proceedings of SIGGRAPH '94*, Computer Graphics Proceedings, Annual Conference Series edited by Andrew Glassner, pp. 239-248, New York: ACM Press, July 1994.
- [73] James Painter and Kenneth Sauer. "Anti-aliased ray tracing by adaptive progressive refinement." *Computer Graphics (Proc. SIGGRAPH '89)* 23(3): 281-288 (July 1989)
- [74] Sumant N. Patnaik-Pattanaik. *Computational Methods for Global Illumination and Visualization of Complex 3D Environments*. PhD thesis, Birla Institute of Technology & Science, 1993.
- [75] Mark T. Pavlicic. "Convenient anti-aliasing filters that minimized bumping sampling." In *Graphics Gems I*, edited by Andrew S. Glassner, pp. 144-146, Cambridge, MA: Academic Press, 1990.
- [76] Ignjor Peter and Georg Preitler. "Importance driven Construction of photon maps." In *Rendering Techniques '98 Proceedings of the Ninth Eurographics Workshop on Rendering*, edited by G. Preitler and U. Max, pp. 269-280, Vienna: Springer-Verlag, 1998.
- [77] M. Pharr and P. Hanrahan. "Monte Carlo evaluation of non-linear scattering equations and for Subsurface reflection." In *Proceedings of SIGGRAPH 2001*, Computer Graphics Proceedings, Annual Conference Series, edited by S. J. Akeley, pp. 75-84, July 2001.

- [77] Bui-T. Phong and Alain Fournier. "A model for anisotropic reflection." *Computer Graphics* (Proc. SIGGRAPH)
- [78] Bui-T. Phong. "Illumination for computer generated pictures." *Communications of the ACM* 18(6) : 311-317 (June 1975)
- [79] Pierre Poulin and Alain Fournier. "A model for anisotropic reflection." *Computer Graphics* (Proc. SIGGRAPH '90), 24(4): 273-282 (August 1990)
- [80] Franco P. Preparata and Michael Ian Shamos. *Computational Geometry: An Introduction*. New York: Springer-Verlag, 1985.
- [81] Reuven Y. Rubinstein. *Simulation and the Monte Carlo Method*. New York: John Wiley & Sons, 1981.
- [82] Holly Rushmeier, Charles Patterson, and Aravindan Veerasamy. "Geometric simplification for indirect illumination calculations." In *Proceedings of Graphics Interface '93*, pp 227-236, Toronto: Canadian Information Processing Society, 1993.
- [83] B. Saleh and M. Teich. *Fundamentals of Photonics*. New York: John Wiley & Sons, 1991.
- [84] Bernhard Schaufler and Henrik Wann Jensen. "Ray Tracing point sampled geometry." In *Rendering Techniques 2000*, edited by B. Prechtel and H. Rushmeier, pp 319-328, Vienna: Springer-Verlag, 2000.
- [85] Christophe Scheliche. "A customizable reflectance model for everyday rendering." In *Fourth Eurographics Workshop on Rendering*, edited by Michael F. Cohen, Claude Puech, and François Sillion, pp. 73-84, Eurographics, June 1993.
- [86] Robert Sedgewick. *Algorithms in C++*. Reading, MA: Addison-Wesley, 1992.
- [87] Peter Shirley. *Physically Based Lighting Calculations for Computer Graphics*. Ph.D. thesis, Dept. of Computer Science, U. of Illinois, Urbana-Champaign, November 1990.
- [88] Peter Shirley. "A ray tracing method for illumination calculation in diffuse-specular scenes." In *Proceedings of Graphics Interface '90*, pp. 205-212, Toronto: Canadian Information Processing Society, May 1990.
- [89] Peter Shirley. "Non-uniform random point sets via warping." In *Graphics Gems III*, edited by David Kirk, pp. 80-83, San Diego: Academic Press, 1992.
- [90] Peter Shirley. "Discrepancy as a quality measure for sample distributions." In *Eurographics '91*, edited by Werner Purgathofer, pp. 183-194, Amsterdam: North-Holland, September 1991.
- [91] Peter Shirley. *Realistic ray tracing*. Natick, MA: A K Peters, 2002.
- [92] Peter Shirley and Kenneth Chin. Notes on adaptive quadrature on the $\frac{1}{4}$ sphere. Technical Report 911, Indiana University, 1995.
- [93] Peter Shirley, Bretton Wade, Phillip Hubbard, David Zorzan, Bruce Walter, and Donald P. Greenburg. "Global illumination via density estimation." In *Rendering Techniques '95*, edited by P. Hanrahan and W. Purgathofer, pp. 219-230, Vienna: Springer-Verlag, 1995.
- [94] Robert Siegel and John R. Howell. *Thermal Radiation Heat Transfer*. Washington, DC: Hemisphere Publishing Co., 1981.
- [95] François X. Sillion, James R. Arvo, Stephen H. Wester, and Ronald P. Greenburg. "A global illumination solution for general reflectance distributions." *Computer Graphics* (Proc. SIGGRAPH '91) 25(4): 187-198 (July 1991).
- [96] B.W. Silverman. *Density Estimation for statistics and Data Analysis*. Chapman & Hall.
- [97] Jeffrey S. Simonoff. *Smoothing methods in Statistics*. New York: Springer-Verlag, 1996.
- [98] Brion Smits, James Arvo, and Donald Greenburg. "A clustering algorithm for radiosity in complex environments." In *Proceedings of SIGGRAPH '94*, Computer Graphics Proceedings, Annual Conference Series, edited by Andrew Glassner, pp. 435-443, New York: ACM Press, July 1994.
- [99] Brion E. Smits, James R. Arvo, and David H. Salesin. "An importance-driven radiosity algorithm." *Computer Graphics* (Proc. SIGGRAPH '92) 26(2): 273-282 (July 1992).
- [100] John M. Snyder and Alan H. Barr. "Ray Tracing Complex Models containing Surface Tesselations." *Computer Graphics* (Proc. SIGGRAPH '87) 21(4): 119-128 (July 1987).
- [101] Jerome Sponer and Ely Gelfand. *Monte Carlo Principles and Newton Transport problems*. Reading, MA: Addison-Wesley 1989.
- [102] Jos Stam and Eric Lengyel. "Ray Tracing in non-constant media." In *Eurographics Rendering workshop 1996*, edited by Xavier Puech and Peter Schröder, pp. 225-234, Vienna: Springer-Verlag.
- [103] Marc Stamminger, Phillip Slusallek, and Hans-Peter Seidel. "Three pass clustering for radiance computations." In *Rendering Techniques '98*, edited by G. DeRose and N. Max, pp. 211-222, Vienna: Springer-Verlag, 1998.
- [104] Kelvin Sung and Peter Shirley. "Ray Tracing with the Oct-tree." In *Graphics Gems III*, edited by David Kirk, pp. 271-274, San Diego: Academic Press, 1992.
- [105] Frank Suykens and Yves D. Willems. "Density control for Photon maps." In *Rendering Techniques 2000*, edited by B. Prechtel and H. Rushmeier, pp. 23-34, Vienna: Springer-Verlag, 2000.
- [106] H.E. Torrance and E.M. Sparrow. "Theory for off-specular reflections from roughened surfaces." *Journal of Optical Society of America* 57(9): (1967).
- [107] Eric Veach. *Robust Monte Carlo Methods for Light Transport Simulation*. Ph.D. Thesis, Stanford University, 1997.
- [108] Eric Veach and Leonidas Guibas. "Directional estimation for light transport." In *Fifth Eurographics Workshop on Rendering*, pp. 147-162, Eurographics, 1994.
- [109] Eric Veach and Leonidas Guibas. "Optimally combining Sampling Techniques for Monte Carlo rendering." In *Proceedings of SIGGRAPH 95*, Computer Graphics Proceedings, Annual Conference Series, edited by Robert Cook, pp. 419-428, Reading, MA: Addison Wesley, August 1995.

- [110] Eric Rach and Leonidas T. Guibas. "Metropolis light transport." In proceedings of SIGGRAPH '97, Computer Graphics Proceedings, Annual Conference Series, edited by Turner Whitted, pp. 65-76, Reading, MA: Addison Wesley, August 1997.
- [111] Vladimir Veltrech, Karol Myszkowski, Andrei Khadilov, and Edward A. Kopylov. Perceptually-informed progressive global illumination solution. Technical Report 99-1-002, University of Arizona, 1999.
- [112] John R. Wallace, Michael F. Cohen, and Donald P. Greenberg. "A two-pass solution to the rendering equation: A synthesis of ray tracing and radiosity methods." Computer Graphics (Proc. SIGGRAPH '87) 21(4): pp. 311-320 (July 1987).
- [113] Bruce Walter, Phillip M. Phibbs, Peter Shirley, and Donald F. Greenberg. "Global illumination using local density estimation." ACM Transactions on Graphics 16(3): 217-259 (July 1997).
- [114] Greg Ward. "Real pixels." In Graphics Gems II, edited by Tomas Akeno, pp. 80-83, San Diego: Academic Press, 1991.
- [115] Gregory T. Ward. "The Radiance lighting simulation and rendering system: Measuring and modeling anisotropic reflection." Computer Graphics (Proc. SIGGRAPH '92) 26(2): 265-272.
- [116] Gregory T. Ward. "The Radiance lighting simulation and rendering system." In Proceedings of SIGGRAPH '94, Computer Graphics Proceedings, Annual Conference Series edited by Andrew Glassner, pp. 459-472, New York: ACM Press, July 1994.
- [117] Gregory T. Ward and Paul H. Heckbert. "Irradiance gradients." In Third Eurographics workshop on Rendering, pp. 85-98. Eurographics May 1992.
- [118] Gregory T. Ward, Francis M. Rubinstein, and Robert D. Clear. "A ray tracing solution for diffuse interreflection." Computer Graphics (Proc. SIGGRAPH '88) 22(4): 85-92 (August 1988).
- [119] David Watson and Alister Mees. "Natural trees - neighbourhood location in a nutshell." International Journal of Geographical Information Systems, 1996.
- [120] Turner Whitted. "An improvement illumination model for a shaded display." Communications of the ACM 23(6): 343-349 (June 1980).
- [121] Lawrence B. Wolff and David J. Kurlander. "Ray tracing with polarization parameters." IEEE Computer Graphics and Applications 10(6): 44-55 (November 1990).
- [122] G. Wyszecki and W.S. Stiles. Color Science: Concepts and Models Methods, Quantitative Data and Formulas. New York: John Wiley & Sons, 1982.
- [123] Kurt Zimmerman and Peter Shirley. "Two-pass Realistic image Synthesis Method for complex scenes." In Eurographics Rendering Workshop 1995, edited by Patrick Hanrahan and Werner Purgathofer pp. 284-295, Eurographics, July 1995.

Completed November 11, 2019 at 18:10
2019-11-11 18:10